The Geological Society of America Bulletin

Volume 72 May 1961 Number 5

CONTENTS

Geochronology of Proterozoic granites in Northern Territory, Australia. Part 1: K-Ar and Rb-Sr age determinations. . . . . *P. M. Hurley, N. H. Fisher, W. H. Pinson, Jr., and H. W. Fairbairn* 653–662

Geochronology of Proterozoic granites in Northern Territory, Australia. Part 2: Stratigraphy and structure. . . . . *B. P. Walpole and K. G. Smith* 663–668

Contact metasomatic iron deposits of California. . . . . *Carl A. Lamey* 669–678

Paleotemperature analysis of the Plio-Pleistocene section at Le Castella, Calabria, southern Italy. . . . . *C. Emiliani, T. Mayeda, and R. Selli* 679–688

Potassium-argon dates of biotites from Cordilleran granites. . . . . *H. Baadsgaard, R. E. Folinsbee, and J. Lipson* 689–702

Middle America Trench: Topography and structure. . . . . *Robert L. Fisher* 703–720

Middle America Trench: Seismic-refraction studies. . . . . *George G. Shor, Jr., and Robert L. Fisher* 721–730

Sediments of shallow portions of East China Sea and South China Sea. . . . . *Hiroshi Niino and K. O. Emery* 731–762

SHORT NOTES

Marine to nonmarine transition of sediments across Little Sycamore Beach, California. . . . . *Emanuel Azmon* 763–766

Unusual solution(?) cavities in the Manning Canyon shale near Fairfield, Utah. *J. A. Whelan* 767–768

Paleotemperature analyses of Mesozoic Belemnoidea from Australia and New Guinea. . . . . *Robert Bowen* 769–774

Geological significance of lead-alpha and isotopic age determinations of "alkalic" rocks of New England. . . . . *Priestley Toulmin, 3d* 775–780

Basal sedimentary section at Windy Gully, Taylor Glacier, Victoria Land, Antarctica . . . . . *E. J. Zeller, E. E. Angino, and M. D. Turner* 781–786

Marine-sediment thickness in the eastern Ross Sea area, Antarctica. . . . . *A. P. Crary* 787–790

Lava temperatures in the 1959 Kilauea eruption and cooling lake. . . . . *W. U. Ault, J. P. Eaton, and D. H. Richter* 791–794

Subscriptions $15.00 per year. Printing Office: Burlington, Vt. Second-class postage paid at Burlington, Vermont. Published monthly.

Communications regarding publications should be addressed to The Geological Society of America, Dr. Frederick Betz, Jr., Secretary, 419 West 117 Street, New York 27, N. Y.

Please give notice of change of address 4 weeks in advance. Claims for nonreceipt of the Bulletin of a given month must be sent to the Secretary of the Society before the end of the second succeeding month.

PAPERS IN PRESS FOR FORTHCOMING ISSUES

Exploration Geophysics: A Review. Frederick E. Romberg

Late Pleistocene Climate of Europe: A Review. H. E. Wright, Jr.

Factors Influencing Supply of Major Ions to Inland Waters, with Special Reference to the Atmosphere. Eville Gorham

Symmetry Concepts in the Structural Analysis of Deformed Rocks. M. S. Paterson and L. E. Weiss

Mohr Construction in the Analysis of Large Geologic Strain. W. F. Brace

Origin of Cyclothems of the Dunkard Group (Upper Pennsylvanian–Lower Permian) in Pennsylvania, West Virginia, and Ohio. James R. Beerbower

NEW MEMOIRS

82. Oligocene Plants from the Upper Ruby River Basin, Southwestern Montana. Herman F. Becker

Description of a well-preserved flora (37 families, 61 genera, and 82 identifiable species, 25 of which are new) from Tertiary fossiliferous shales of the Ruby River basin. The author uses the flora to interpret the paleoecology and paleoclimatology and suggests that the Ruby and Florissant assemblages represent a single botanical province.

128 pages, 4 figures, 32 photographic plates

Price, $4.25

Special price to Fellows and Members of GSA, $3.00

83. Biostratigraphic Studies in the Comanche (Cretaceous) Series of Northern Mexico and Texas. Bob F. Perkins

The author relates the biostratigraphy of the Aurora limestone of southwestern Coahuila to the type Aurora and to the type Lower Cretaceous of northern Texas and reports stratigraphic revisions of the Fredericksburg and Washita groups of north Texas. He describes a fauna of larger invertebrates from the upper member of the Aurora and on paleontological evidence correlates the member with the Fort Worth limestone and Grayson marl. He concludes that the Aurora limestone is of epineritic origin, deposited far from any source of terrigenous clastic material.

138 pages, 26 figures, 3 maps in color, 29 photographic plates

Price, $6.00

Special price to Fellows and Members of GSA, $4.50

P. M. HURLEY *Massachusetts Institute of Technology, Cambridge, Mass.*
N. H. FISHER *Bureau of Mineral Resources, Canberra, Australia*
W. H. PINSON, JR. *Massachusetts Institute of Technology, Cambridge, Mass.*
H. W. FAIRBAIRN *Massachusetts Institute of Technology, Cambridge, Mass.*

Geochronology of Proterozoic Granites in Northern Territory, Australia. Part 1: K-Ar and Rb-Sr Age Determinations

Abstract: K-Ar and Rb-Sr age measurements on granitic rocks intrusive into two subdivisions of the Lower Proterozoic in the Northern Territory of Australia show well-grouped ages averaging 1440 and 1630 million years. The writers present reasons for their belief that these are close to the true values for the times marking the end of two disturbances which produced intracratonic basins of sedimentation.

CONTENTS

Introduction 653
Acknowledgments 654
Samples 654
Analytical techniques and experimental errors . . 658
Analytical results and discussion 659
References cited 662

Figure
1. Distribution of age measurements in Australia . 655

Table
1. K-Ar age measurements on mica samples from the Katherine-Darwin region, Northern Territory, Australia 659
2. K-Ar age measurements on a central region in the Northern Territory, Australia 660
3. Rb-Sr age measurements on a sample of biotite from each group in Tables 1 and 2 661

INTRODUCTION

This paper and the accompanying paper by Walpole and Smith present the results of a collaboration between geologists of the Bureau of Mineral Resources of the Commonwealth of Australia and the geochronology laboratory at the Massachusetts Institute of Technology. Part 1 gives details of the age measurements, samples, and interpretations of the results in terms of known applicability of these methods elsewhere. Part 2 describes and discusses the geological field relationships in the region under study.

By agreement, the Commonwealth geologists collected the samples for the investigation (striving to obtain concentrates of the mica minerals known to be useful for age determinations by the K-Ar or Rb-Sr methods) and assumed the responsibility for (1) relating the samples to the geological history of the region and (2) studying the petrography of the rocks. Samples were prepared in Australia, and the mica concentrates only were sent to the geochronology laboratory for age study.

The M.I.T. group's effort was directed more to the global implications of the study, as a contribution to knowledge of the general Precambrian history of the earth and correlations of periods of orogeny between continents. Australia is particularly interesting as it is a relatively small, isolated continental mass which probably started from a single nucleus and was apparently unaffected by developments in neighboring nuclei. It is an ancient continent, as the few scattered age measurements reported previously indicated, and unusual in that it is dominantly Precambrian with only the eastern Tasman geosynclinal region representing younger major continental development.

Jeffery (1956) made Rb-Sr and K-Ar measurements on muscovite and microcline from pegmatites in Western Australia that indicated this Precambrian province is 2800 m.y.

Geological Society of America Bulletin, v. 72, p. 653–662, 1 fig., May 1961

old, suggesting that the continent started to develop at least as long ago as the other continents.

In Southern Australia, a superimposed later mineralization and anomalous lead deposition make dating of rocks difficult, but the original north-south-trending orogenic belt appears to have been developed 1500–1700 m.y. ago. Evidences for this are the model lead ages by Russell and Farquhar (1957) on the conformable type of lead ore at Broken Hill, which average 1500±150 m.y. old, and U-Pb ages by Greenhalgh and Jeffery (1959) on a sample of davidite from Crocker's Well, averaging 1660 m.y. In addition Collins, Russell, and Farquhar (1953) reported a Pb^{207}/Pb^{206} age for davidite from Radium Hill as 1510 m.y. Later mineralization gave rise to U-Pb ages ranging from 500 to 900 m.y. (Kulp, Bate, and Broecker, 1954; Greenhalgh and Jeffery, 1959) for uranium minerals from Crocker's Well, Radium Hill, and Myponga.

Greenhalgh and Jeffrey (1959) found that U-Pb ages from the Katherine-Darwin region in the Northern Territory ranged from 300 to 1450 m.y., mostly between 400 and 800 m.y., and they suggested two periods of uranium mineralization.

The significance of these determinations is discussed hereafter.

ACKNOWLEDGMENTS

The authors thank S. R. Hart for assistance in the argon measurements, S. M. Hasan and W. B. Dallwitz, petrologists with the Bureau of Mineral Resources of the Commonwealth of Australia, for the petrographic reports on the samples, and G. Faure for assistance in drafting. The authors gratefully acknowledge the continued support of the geochronology laboratory by the Division of Research of the U. S. Atomic Energy Commission.

SAMPLES

Figure 1 (*See also* Figure 1 of Part 2) and Tables 1 and 2 give the locations of the samples. S. M. Hasan and W. B. Dallwitz have provided the following petrographic details.

SPECIMEN B-3272, ALLIA CREEK GRANITE: Moderately coarse-grained granodiorite possessing slight lineation. Quartz forms completely anhedral grains and aggregates with markedly undulatory extinction. Feldspar, biotite, and iron oxide inclusions fairly common. Feldspar entirely plagioclase of labradoritic composition, ranging from An_{50} to An_{55}. Random and irregular alteration of feldspar has resulted in many places in more or less intense sericitization with associated development of very finely divided, white, powdery material (probably clay) and rare, coarser-grained muscovite. Rare epidote may be found in such places. Biotite (approximately 23 per cent), a deep red-brown variety, strongly pleochroic from deep red brown to straw brown, is presumably iron-rich with $(-)2V=0°$. Biotite generally fresh but commonly possesses marginal zones or mantles very rich in flaky or granular iron oxide. In a few places pale-green chlorite (probably penninite) or very fine, claylike material partly replaces biotite. Muscovite (approximately 5 per cent) occurs as colorless sheets and flakes which, from purely textural indications, seem to have crystallized before the biotite, as the colored mica is quite commonly molded on and around it, and occasional completely included muscovite sheets in totally different physical (and optical) orientation, In other cases, biotite cleavage planes clearly governed orientation of included muscovite. No clear evidence of recrystallization; no indication of shearing.

SPECIMEN B-3273, HERMIT HILL GRANITE: Coarse-grained, light-gray muscovite-biotite-granite (massive) having no foliation, lineation, or other internal directional features. All feldspars show slight alteration, but plagioclases show more than potassic types. Alteration mainly very fine sericitization, with flaky sericite in some places developing into distinct sheets of muscovite. Small sheets of primary biotite and muscovite commonly included in the feldspar. Pale-brownish, cloudy appearance of muscovite seems to result from tiny film-like inclusions along cleavage planes. Biotite brown and strongly pleochroic from pale yellow brown to deep gray brown. In most places biotite does not appear to be fresh because of abundant film-like inclusions along cleavage. No evidence of recrystallization or shearing in texture of rock; no detectable mineral orientation.

SPECIMEN B-3274, MT. LITCHFIELD GRANITE: Medium- to coarse-grained pale-gray garnetiferous adamellite showing moderate degree of foliation in hand specimen. Foliation arises from irregular, platy segregation of micas in some parts of the rock. Mica (muscovite and biotite) conspicuous in hand specimen. Generally, orthoclase and microperthite have been lightly kaolinized and finely sericitized. In some places the sericite is more coarsely crystalline and forms distinct flakes of muscovite in the feldspar, causing considerable difficulty in distinguishing between muscovite formed by alteration and that included in the feldspar during crystallization Plagioclase generally more heavily altered but in the same manner as the orthoclase. Sheets of muscovite (quite fresh) conspicuous in the rock. Biotite, in some places almost opaque, has a "dirty" appearance due to abundant included iron oxides. Small anhedral to subhedral crystals of clear, colorless garnet are found throughout the section, generally included in feldspar crystals.

SPECIMEN B-3275, BROCK'S CREEK GRANITE: Massive, even-grained, gray granite without apparent directional textures in hand specimen. Thin sections show typically granitoid texture, and the rock consists essentially of K feldspar (40 per cent), quartz (35 per cent), plagioclase (15 per cent), biotite (8 per cent), muscovite (2 per cent), and accessory zircon, apatite, and fluorite. K feldspar is mainly microperthite, microcline, and microcline microperthite. Microcline fresh, but albitic component of perthitic feldspar lightly kaolinized. Plagioclase an intermediate andesine (An 34) and in nearly all cases heavily sericitized. Biotite brown, strongly pleochroic, with occasional inclusions of zircon, fluorite, and grains of opaque material. It is generally fresh but in places shows some chloritization. Muscovite has formed mainly from alteration of plagioclase. Deep purple fluorite occurs in intergranular positions and in biotite; irregular patches of colorless fluorite are common among alteration products of plagioclase feldspars. Fluids responsible for alteration may have been rich in fluorine.

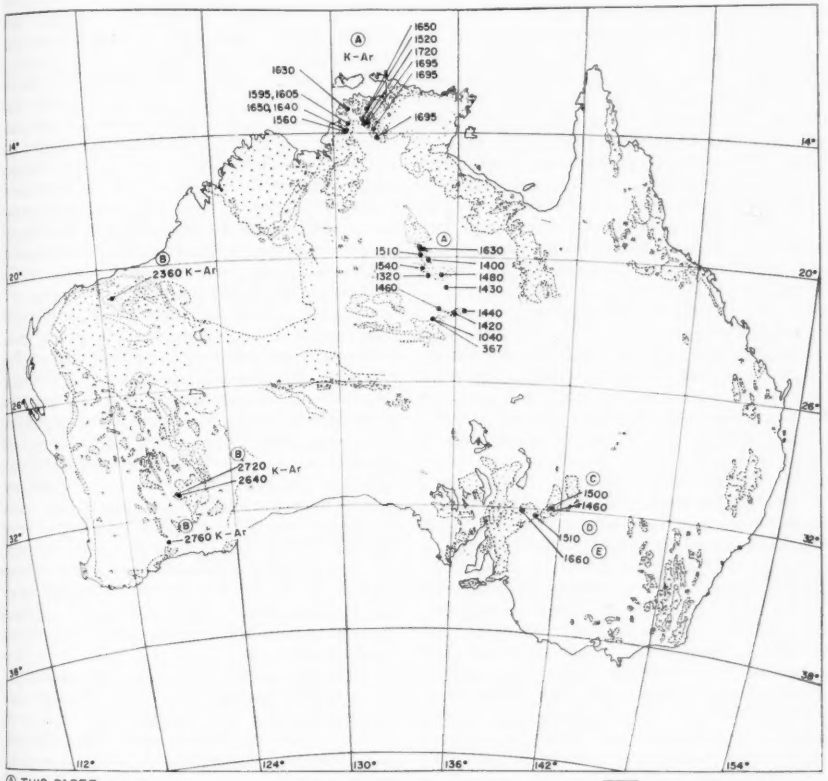

Figure 1. Distribution of age measurements in Australia

SPECIMEN B-3276, PRICE'S SPRINGS GRANITE: Coarse-grained, light-gray, massive granitic rock without any apparent directional structures in hand specimen. Thin sections show a sodipotassic biotite granite of typical granitoid texture that consists of quartz (30 per cent), microcline and orthoclase (50 per cent), altered plagioclase (15 per cent) and biotite (5 per cent), with accessory amounts of

apatite, zircon, and magnetite. Quartz has been highly strained and shows slight internal granulation. It contains "streams" of minute inclusions. K feldspars are fresh and show no deformation. Plagioclase generally deeply sericitized; calcite present amid fine alteration material. Biotite strongly pleochroic brown with abundant inclusions of apatite and rarer inclusions of zircon and magnetite, in general fresh, but in rare instances chloritized (in places completely so).

SPECIMEN B-3278, FENTON GRANITE: Very coarse-grained, pink granite with feldspar crystals up to 2 cm across. No indication of gneissic foliation or impressed tectonic features in hand specimen. Thin-section examination shows coarse granitoid texture. Rock composed of quartz (40 per cent), potassic feldspars (43 per cent), plagioclase (15 per cent), and biotite (2 per cent), with accessory amounts of chlorite, apatite, zircon, and fluorite. Quartz clear, only moderately strained. Biotite brown and strongly pleochroic, generally fresh, but shows marginal development of leucoxene and slight chloritization.

SPECIMEN B-3279, BURTON CREEK GRANITE: Medium-grained, gray, gneissic granite consisting essentially of quartz (30 per cent), potassic feldspar (50 per cent), plagioclase (15 per cent), biotite (4 per cent), and muscovite (1 per cent), with accessory chlorite, apatite, and epidote. Texture gneissic, average grain size about 2 mm, although feldspar crystals up to 7 mm across occur fairly commonly. Quartz strained and considerably recrystallized into fine mosaic texture in most places. Grain orientation in such recrystallized masses parallels over-all gneissic foliation of the rock. Plagioclase a calcic oligoclase (An_{30}) outwardly zoned to sodic oligoclase or rimmed by orthoclase. Alteration of the more calcic plagioclase has been intense and mainly involves deep kaolinization with subsidiary sericitization. Myrmekitic intergrowths are conspicuous. Biotite strongly pleochroic brown, occurs as elongated sheets parallel to gneissic foliation of the rock. Generally, it is fresh and contains minute zircon inclusions surrounded by pleochroic halos. In rare instances mica has been partly or completely chloritized. Apatite inclusion common.

SPECIMEN B-3283, CULLEN GRANITE: Coarse-grained, pale-brownish-gray granitic rock without indication of directional structure in hand specimen. Thin-section examination shows coarse sodipotassic biotite granite with typical granitoid texture and fairly even average grain size of about 5 mm. Constituent minerals are quartz (35 per cent), potassic feldspars (45 per cent), plagioclase (17 per cent), biotite (3 per cent), and accessory amounts of chlorite, apatite, iron oxide, zircon, and calcite. Quartz is coarse-grained and strained but shows no evidence of recrystallization. In nearly all places plagioclase has been deeply altered by kaolinization and subordinate sericitization, so that determination of composition is difficult. However, plagioclase appears to be an albite approaching An_5. Alteration of plagioclase appears to have taken place before final stage of crystallization of feldspar, for altered material is very commonly surrounded by a narrow zone of fresh, clear plagioclase of apparently the same composition. Some plagioclases also exhibit weak normal compositional zoning. Biotite a deep-brown, "dirty" variety containing much finely divided opaque material.

SPECIMEN B-3284, CULLEN GRANITE (EDITH RIVER): Coarse-grained porphyritic, dark-pink-gray gneissic granitic rock with large, euhedral, pink crystals of feldspar up to 3 cm long. Foliation fairly distinct owing to subparallel alignment of feldspar phenocrysts. Thin-section examination shows that the rock is a gneissic hornblende-biotite-adamellite consisting of quartz (10 per cent). K feldspar (35 per cent), plagioclase (35 per cent), biotite (10 per cent), and hornblende (10 per cent), with accessory amounts of sphene, zircon, apatite, and opaque oxides. Mafic minerals include brown biotite and green hornblende in approximately equal amounts. Both minerals are fresh, and no apparent reaction relationship exists between them.

SPECIMEN B-3286, MT. BUNDEY GRANITE: Very coarse-grained, pink hornblende-biotite granite. Texture typically granitoid, tending to be porphyritic in pink feldspar, but rock shows no clear evidence of directional features in hand specimen. Rock consists mainly of microperthite (approx. 60 per cent), quartz (15 per cent), plagioclase (15 per cent), hornblende (6 per cent), biotite (2 per cent), sphene (1 per cent), magnetite (1 per cent), and accessory apatite and zircon. Quartz clear, very slightly strained. Potassic feldspar lightly kaolinized and partly sericitized in most places. Biotite straw brown, strongly pleochroic to deep brown. In some cases it is considerably altered to strongly pleochroic green chloritic material in the same optical orientation; even the fresh mica has tiny inclusions along cleavage planes.

SPECIMEN F/53/2/1: Medium-grained light-gray granite. Hand specimen appears very much weathered. Slight traces of foliation can be seen. Essential constituents are quartz, K feldspars, plagioclase, and ferrophengite. Biotite, hematite, and magnetite are accessory minerals. Plagioclase feldspars very cloudy severely altered; alteration products are usually sericite and kaolin. Biotite flakes very rare; only two or three were noticed in the thin section studied.

SPECIMEN F/53/2/2: Moderately coarse-grained, pinkish biotite-muscovite granite. Hand specimen does not show any sign of foliation. Occasional xenolithic materials consist essentially of biotite. Under the microscope, typical hypidiomorphic texture is apparent. Rock has undergone a fair amount of deformation, evidenced by undulatory extinction in quartz and slightly bent muscovite flakes. Plagioclase has undergone a fair amount of alteration, appears cloudy in thin section. Alteration products are sericite and kaolin. Biotite is greenish and constitutes only 2 per cent of the

total. It is strongly pleochroic and has been partly altered to chlorite.

SPECIMEN F/53/2/3: Moderately coarse-grained massive light-gray quartz granite. Thin section shows a typically granitoid texture; rock consists essentially of quartz (47 per cent), K feldspars (24 per cent, plagioclase (18 per cent), biotite (4 per cent), white mica (4 per cent), and accessory fluorite and iron ores. Quartz occurs as medium to large anhedral grains and does not show undulatory extinction. Plagioclase is generally heavily altered andesine (An_{36}), showing distinct polysynthetic twinning. Alteration products are commonly sericite and kaolin. Biotite is strongly pleochroic from straw yellow to dark brown. Inclusions of fluorite, and feldspars are seen. In places biotite has been replaced by chlorite or iron oxide (ilmenite).

SPECIMEN F/53/2/4: Coarse-grained porphyritic muscovite-biotite adamellite. Average grain size about 1.3 mm. Larger grains (phenocrysts) are K feldspar (microcline-perthite) ranging from 2 mm to 5.5 mm. These are fresh; they commonly occur as subhedral crystals containing numerous inclusions of muscovite, biotite, chlorite, plagioclase, quartz, apatite, zircon, tourmaline, and iron ores. Under the microscope the rock shows hypidiomorphic texture. Undulatory extinction in quartz grains and bent biotite flakes suggest that the rock has undergone a fair amount of deformation. Biotite (19 per cent) occurs in long flakes and is strongly pleochroic from X=pale straw yellow; Y=brownish yellow; and Z=dirty greenish brown. Pleochroic halos surround rare zircon grains. Alteration to chlorite is slight.

SPECIMEN F/53/2/5: Medium-grained light-gray adamellite. Hand specimen does not show any directional structure. No xenolithic material noted in specimen provided. Under the microscope the typical granitoid texture is seen. Essential mineral constituents are quartz (34 per cent), K feldspars (36 per cent), plagioclase (22 per cent), and biotite (6 per cent). Nonopaque accessory minerals constitute 1.7 per cent, opaque accessory minerals 0.7 per cent. Plagioclase very clouded, has undergone a fair amount of alteration. Both green and brown biotite are present, occurring as small to medium flakes. They are strongly pleochroic from straw yellow to deep green and from pale yellowish brown to dark reddish brown. Some brown biotite has been replaced by chlorite.

SPECIMEN F/53/11/1: Coarse-grained pinkish rock, without foliation. Under the microscope the typical hypidiomorphic texture is seen. Essential mineral constituents are quartz (18 per cent), K feldspars (52 per cent), plagioclase (27 per cent), and biotite (1.2 per cent), with nonopaque accessory minerals (1.1 per cent) and opaque accessory minerals (1.0 per cent). Rock with its very low color index of 3.95 and high feldspar content, particularly its K feldspar, is unusual and can be named alaskite. Plagioclase is albite and occurs as medium to large anhedral to subhedral crystals which are very clouded and have undergone a fair amount of alteration. Common alteration products are sericite and kaolin. Biotite occurs as small to medium flakes and is pleochroic from pale yellowish brown to dark brown. Pleochroic halos are rare. Most biotite has been replaced by chlorite.

SPECIMEN F/53/11/2: Coarse-grained pink adamellite, without apparent directional structure in hand specimen. Adamellite consists of quartz (31 per cent), K feldspar (30 per cent), plagioclase (30 per cent), biotite (6.0 per cent), nonopaque accessory minerals (1.1 per cent), and opaque accessory minerals (2.5 per cent). Under the microscope the typical granitoid texture is seen. Undulatory extinction in quartz and bent muscovite flakes suggest moderate deformation. Plagioclase feldspar has been altered to sericite and kaolin. Severe alteration makes determination of the plagioclase difficult, but it seems to be andesine. Both green and brown biotite are present. The former is more common. Biotite flakes are strongly pleochroic, pleochroic halos have also been noticed. In some places biotite has been replaced by chlorite.

SPECIMEN F/53/11/3: Coarse-grained hornblende-biotite granite, without any apparent directional structure in hand specimen. Under the microscope the typical hypidiomorphic texture is seen. Granite consists of K feldspar, quartz, plagioclase, and biotite, with minor chlorite, hornblende, and magnetite and accessory zircon, apatite, and epidote. Quartz occurs as medium to large subhedral grains. These grains have been cracked, and undulatory extinction is common. Undulatory extinction in quartz and bent and twisted biotite flakes suggest that the rock has undergone moderate deformation. Plagioclase feldspar is andesine and is largely fresh. Biotite occurs in small to medium flakes strongly pleochroic from pale yellow to dark reddish brown. Basal sections are deep reddish brown. Pleochroic halos are present. Chlorite replaces biotite in places.

SPECIMEN E/53/14/1: Medium-grained light-gray gneissic granodiorite. In hand specimen the foliation, caused by parallelism of the biotite flakes, is marked. Xenolithic material, forming dark-gray clots up to 2½ inches by 1 inch are prominent. Plagioclase (43 per cent) is andesine (An_{36}) and is the most abundant mineral. It occurs as medium-sized subhedral grains, usually greatly altered. Alteration products are sericite, kaolin, and rarely epidote. Quartz (32 per cent) is next in abundance and occurs as small to medium anhedral grains. These grains show slight undulatory extinction. Biotite (18 per cent) occurs as small to medium flakes and is strongly pleochroic from pale yellow to dark greenish brown. Pleochroic halos are rare. Some replacement by chlorite and epidote has taken place.

SPECIMEN F/53/6/1: Medium-grained light-gray massive adamellite. In hand specimen the rock is homogeneous and free of xenolithic materials. In thin section the texture is typically granitoid. The

adamellite consists of quartz, K feldspars, plagioclase, biotite, muscovite, and damourite, with minor apatite and accessory fluorite, zircon, and iron oxide. Plagioclase feldspar (23 per cent) is oligoclase (An_{12}) and occurs as subhedral grains. It is cloudy and has undergone a fair amount of alteration. The alteration products are usually white mica and kaolin. Biotite (5.2 per cent) occurs as small to medium flakes strongly pleochroic from pale yellow to dark greenish brown. Pleochroic halos rare. Chlorite has replaced some biotite.

SPECIMEN F/53/7/1: Coarse-grained pinkish muscovite-biotite adamellite without any directional structure in hand specimen. Rock has undergone a fair amount of deformation as is evident from bent and twisted mica flakes and bent twin lamellae of plagioclase. Adamellite consists of quartz, K feldspars, plagioclase, muscovite, and biotite, with minor chlorite and accessory apatite, magnetite, and hematite. Plagioclase feldspars are much more cloudy than the K feldspars and have undergone some alteration. Common alteration products are sericite and kaolin. Muscovite occurs in small to medium flakes (usually bent or twisted). Biotite strongly pleochroic from pale yellowish brown to dark brown and occurs in small to medium flakes; some alteration to chlorite has taken place.

SPECIMEN F/53/14/4: Petrographic description of this rock is not given.

ANALYTICAL TECHNIQUES AND EXPERIMENTAL ERRORS

Argon was determined by isotope dilution using a spike gas containing 90 per cent Ar^{38} (Wetherill, Tilton, Davis, and Aldrich, 1956). Air contamination was measured by the relative abundance of Ar^{36}. The gas release system consisted of a 10-kw induction furnace in which the sample was held in an Alundum crucible inside a molybdenum casing, housed in a vacuum-tight, water-jacketed, pyrex bell jar. The sample was held in the crucible by a plug of pyrex glass wool and a molybdenum lid. Generally, about 3 gms of the mica sample was used in an analysis, without flux if it was biotite, with about 0.5 gm of sodium hydroxide if it was muscovite. The temperature was measured by optical pyrometer, and commonly the sample was heated to 1200° C. for about half an hour.

The gas was purified by hot titanium sponge, copper oxide, and liquid nitrogen traps after thorough mixing with the spike gas; the purity of the argon, particularly with respect to the amount of hydrogen left, was monitored by a cycloidal-focusing mass spectrometer. The spike release system was a simple gas pipette leading from a 3-l spike storage bulb; spike release calibrations have indicated both high precision and absolute accuracy when known quantities of pure argon, or argon in air, were being measured. The same original spike sample has been used for more than 2 years, providing spikes for more than 400 analyses. Limits of error in this procedure are discussed hereafter.

The gas-release, spike-release, and gas purification systems were connected together and also connected directly to three mass spectrometers. The first mass spectrometer, a cycloidal-focusing instrument, was used to monitor outgassing and purification; because of its speed, precision, and negligible background it was also used to measure the ratio Ar^{38}/Ar^{40}. The second was a standard Nier-type instrument, 60-degree sector 6-inch-radius copper tube, with ion current amplification by vibrating reed electrometer. It was used to measure the $Ar^{36}-Ar^{38}$ ratio for air contamination correction. The third was a high-sensitivity, low-background Reynolds-type instrument (Reynolds, 1954) with glass tube. This instrument was not used for routine measurements in this investigation but has given independent measurements of Ar^{36} with essentially zero background, thus confirming that there were not significant increases in background in the Nier-type instrument when sample gas was admitted. The limit of error in measurement of Ar^{36} has been evaluated by this means and is included in the over-all error given for the measurements.

Rubidium and strontium were measured by isotope dilution following an ion-exchange purification procedure in which the rubidium and strontium fractions from the columns were monitored respectively by flame test and by radioactive strontium 85 tracer. Isotopic analysis was made on a 6-inch radius, 60-degree sector, mass spectrometer with thermal ionization of the elements applied as nitrate and oxalate respectively to a tantalum ribbon filament in the source.

The potassium was measured by a Perkin-Elmer flame photometer using lithium internal standard and standard comparison solutions approximating the composition of those of the unknown. A single potassium analysis involves two solutions of separate portions of the sample, each with two separate photometric measurements.

The level of precision (reproducibility) in argon analyses was obtained by numerous duplicate analyses on different materials. On these

samples the average of all the measured values for air correction was 2.3 per cent, so that the error from this correction was low. The standard deviation of the argon analyses reported in Tables 1 and 2 is approximately 2 per cent. Systematic error of the mean is believed to be less than 1 per cent, based on measurement of the argon content of air and on interlaboratory agreement in the analysis of a standard sample of biotite (B-3203).

Reproducibility in potassium measurements is estimated to be 2–3 per cent standard deviation for a complete analysis, with an absolute error of the mean not exceeding 2 per cent. Thus, total K-Ar age values have an estimated analytical error of less than 5 per cent standard deviation, with a possible maximum systematic error of close to 2 per cent.

TABLE 1. K-AR AGE MEASUREMENTS ON MICA SAMPLES FROM THE KATHERINE-DARWIN REGION, NORTHERN TERRITORY, AUSTRALIA ($\lambda e = 0.585 \times 10^{-10}$ yr.$^{-1}$; $\lambda = 5.30 \times 10^{-10}$ yr.$^{-1}$)*

M.I.T. no.	Australian Survey no.; location	Mineral	K%	Ar^{40}†/K^{40}	K-Ar age, $\times 10^6$ years
3327	B-3278; Fenton 13°37′S., 131°24′E.	Biotite	4.31	.165	1720
3328	B-3273; Hermit Hill 14° 2′S., 130°33′E.	Biotite	6.33	.142	1560
3330	B-3272; Allia Creek 13°57′S., 130°40′E.	Biotite	3.56	.155	1650
3330	B-3272; Allia Creek 13°57′S., 130°40′E.	Muscovite	6.93	.153	1640
3331	B3279; Burton Creek 12°56′S., 130°40′E.	Biotite	6.31	.151	1630
3332	B-3274; Mt. Litchfield 13°30′S., 130°42′E.	Biotite	5.60	.147	1595
3332	B-3274; Mt. Litchfield 13°30′S., 130°42′E.	Muscovite	7.50	.148	1605
3334	B-3275; Brock's Creek 13°25′S., 131°24′E.	Biotite	5.11	.137	1520
3335	B-3284; Edith River 14°12′S., 132° 2′ E.	Biotite	6.43	.161	1695
3336	B-3286; Mt. Bundey 12°54′S., 131°34′E.	Biotite	4.68	.154	1650
3337	B-3276; Price's Springs 13°30′S., 131°37′E.	Biotite	5.61	.161	1695
3340	B-3283; Cullen 13°46′S., 131°51′E.	Biotite	4.95	.161	1695

* Aldrich and Wetherill (1958)
† Radiogenic argon 40

In Rb-Sr age measurements the error is so dependent upon the Rb-Sr ratio in the sample and on its age that errors are calculated separately for each determination. In Table 3 the errors quoted are precision errors only, based on known statistical variations in peak height measurements. Absolute errors of the mean are not yet established with certainty but from interlaboratory comparisons are believed to be less than 5 per cent.

ANALYTICAL RESULTS AND DISCUSSION

Tables 1 and 2 list K-Ar measurements; Table 3 lists Rb-Sr measurements. Each Rb-Sr age is slightly higher than the average of the K-Ar ages in the group represented by the sample. As there is some evidence that the value used for the half life of rubidium may be lowered by about 5 per cent, which would eliminate this discrepancy, the writers conclude that the observed difference in age be-

tween the two groups of K-Ar analyses is upheld by the Rb-Sr analyses, and that the age values by the two methods are essentially the same.

Concordance between Rb-Sr and K-Ar age measurements has been used in the past as an indication of reliability of the age values. The tionships between intrusions and host rocks, and between one part of the belt and another, have left no doubt that the ages reflect the later events. Such mixed-age areas have been observed in the Sudbury district, Ontario; the Quadrilatero Ferrifero area, Minas Gerais, Brazil; the southern part of the Quebec-

TABLE 2. K-AR MEASUREMENTS ON A CENTRAL REGION IN THE NORTHERN TERRITORY, AUSTRALIA
($\lambda e = 0.585 \times 10^{-10}$ yr.$^{-1}$; $\lambda = 5.30 \times 10^{-10}$ yr.$^{-1}$)

M.I.T. no.	Australian Survey no.; location	Mineral	K%	Ar^{40*}/K^{40}	K-Ar age, $\times 10^6$ years
3684	F/53/7/1 21° 25′S., 135° 30′ E.	Muscovite and biotite, some chlorite	3.74	.126	1430
3685	F/53/2/4 20° 10′S., 134° 35′E.	Slightly chloritized biotite	7.19	.122	1400
3686	F/53/2/3 20° 30′S., 134° 15′E.	Slightly chloritized biotite	5.18	.139	1540
3687	E/53/14/1 19° 44′S., 134° 17′E.	Slightly chloritized biotite	6.42	.152	1630
3688	F/53/6/1 21° 25′S., 133° 50′E.	Moderately chloritized biotite	6.14	.129	1460
3689	F/53/2/5 19° 54′S., 134° 40′E.	Green and brown biotite minor chlorite	3.86	.136	1510
3741	F/53/2/1 20° 55′S., 135° 15′E.	Biotite	7.05	.131	1480
3742	F/53/2/2 20° 55′S., 134° 40′E.	Mostly muscovite	4.48	.112	1320
3743	F/53/11/1 22° 40′S., 136° 30′E.	Much chloritized biotite	1.27	.127	1440
3744	F/53/11/2 22° 35′S., 135° 55′E.	Green and brown biotite, in some places much chloritized	3.55	.124	1420
3745	F/53/11/3 22° 28′S., 135° 7′E.	Yellow to brown biotite (hb.) minor chlorite	4.86	.129	1460
3747	F/53/14/4 23° 00′S., 135° 50′E.	From Arunta complex, biotite	7.22	.0237	367

* Radiogenic argon 40

authors are not inclined to place too much weight on this criterion alone, however, as many measurements of the age of known metamorphism of micas have shown concordant results by the two methods. The writers also place weight on widespread homogeneity and a study of the rock types, alterations, and other geological evidences in any decision regarding the meaning of the results.

In several unpublished studies of crystalline rocks in orogenic belts that have been metamorphosed and intruded subsequent to their original development, the measured age rela-

Labrador iron district; and other regions. The mixed-age areas are believed to represent hypabyssal, marginal, or relatively local tectonic and intrusive events.

An area showing homogeneous ages is conceived as one in which the entire belt, metamorphic and intrusive rocks alike, has risen from depths at which all the minerals were formed initially or metamorphosed, and which has remained unburied or unaffected by any significant thermal event since the time of the original uplift and erosion. This does not imply that the depth must be great, as the grade of

metamorphism is commonly of the greenschist facies. It implies that a stable shield area or crustal block was formed which has persisted without much further denudation or burial throughout the age measured. In these belts remnants of more ancient rocks unconformably underlying the rocks of the orogen will commonly show the same age as the belt because they rose from the same depth at the same time.

Alterations of the biotite to chlorite seem to have made little difference in the age, judging by the lack of correlation of lower age values with lower potassium values. The common alterations in the plagioclases of the rocks studied are probably largely deuteric, except for the kaolinization. Stress has produced much undulatory extinction in the quartz and has bent mica flakes, but this again does not seem to have modified the age of the rock relative to those samples which do not exhibit such effects. The fact that the K feldspars in most of the rocks have remained relatively unaltered, despite considerable sericitization of the plagioclases, suggests a late-stage K alteration in which the K feldspar and biotite remained in equilibrium. This is not typical of lower-temperature pervasive hydrothermal alterations, which commonly follow shearing and result in banded and foliated rocks. Most of the rock types show little or no preferred orientation or banding of the mica minerals.

As Walpole and Smith note in their report, the Lower Proterozoic sedimentary basins are intracratonic and fairly shallow, and although the sedimentary rocks are folded, there has been little regional metamorphism. Walpole and Smith do not consider these to be orogenic belts. The granite intrusions are a late-stage development and probably were intruded quite close to the existing surface. Many of them are relatively unstressed. The authors believe that the geological circumstances in these cases are ideal for obtaining dates very close to the time of intrusion of the granites. The movements responsible for the development of the basins and emplacement of the granites appear to be closely related in time; the sediments in the basins were probably derived from the uplifted basement blocks, which relate at least the later stages of sedimentation to the unroofing of the granites. The presence of volcanic rocks in the sections further supports this conclusion.

Table 3. Rb-Sr Age Measurements on a Sample of Biotite from Each Group in Tables 1 and 2 (λ for $Rb^{87} = 1.39 \times 10^{-11}$ yr.$^{-1}$)*

M.I.T. no.	Australian Survey no.	Total Sr, ppm by wt.	Total Rb, ppm by wt.	Sr^{87}† ppm by wt.	Sr^{87}†/Rb^{87}	Rb-Sr age, $\times 10^6$ years
B-3335	B-3284	32.6	532	3.74	.0248	1765 ± 90
B-3688	F/53/6/1	5.4	2240	13.8	.0218	1550 ± 75

*Aldrich and Wetherill (1958)
†Indicates radiogenic Sr

Argon diffuses out of mica structures at elevated temperatures, so that the cooling history of any rock mass must be known before conclusions can be drawn on the meaning of age measurements by K-Ar ratios. The writers believe that the granitic rocks of this study were relatively quickly cooled because they intruded rocks of low metamorphic grade in many cases, and once elevated remained close to the present surface. The agreement in age over wide areas and agreement with the Rb-Sr measurements would not be observed if the different granite masses had been emplaced at greatly different depths and had had different histories of cooling and uplift.

The lower age for the sample from the Arunta complex, near Alice Springs, shown in Table 2 (M.I.T. no. F/53/14/4), is an exception. This complex is considered as Archean basement and quite definitely underlies the Proterozoic sequence. South of this locality is the Amadeus Trough which contains folded Paleozoic rocks; the movement which deformed the Amadeus rocks probably resulted in some recrystallization of the basement or sufficient burial to cause diffusion loss of argon.

REFERENCES CITED

Aldrich, L. T., and Wetherill, G. W., 1958, Geochronology by radioactive decay: Ann. Review Nuclear Sci., v. 8, p. 257–298

Collins, C. B., Russell, R. D., and Farquhar, R. M., 1953, The maximum age of the elements and the age of the earth's crust: Canadian Jour. Physics, v. 31, p. 402

Greenhalgh, D., and Jeffery, P. M., 1959, A contribution to the pre-Cambrian chronology of Australia: Geochim. Cosmochim. Acta, v. 16, p. 39–57

Jeffery, P. M., 1956, The radioactive age of four Western Australian pegmatites by the potassium and rubidium methods: Geochim. Cosmochim. Acta, v. 10, p. 191–195

Kulp, J. L., Bate, G. L., and Broecker, W. S., 1954, Present status of the lead method of age determination: Am. Jour. Sci., v. 252, p. 345

Reynolds, J. H., 1954, A high sensitivity mass spectrometer: Phys. Rev., v. 98, p. 283

Russell, R. D., and Farquhar, R. M., 1957, Isotopic analyses of leads from Broken Hill, Australia: Am. Geophys. Union Trans., v. 38, p. 557–565

Wetherill, G. W., Tilton, G. R., Davis, G. L., and Aldrich, L. T., 1956, New determinations of the age of the Bob Ingersoll pegmatite, Keystone, South Dakota: Geochim Cosmochim. Acta, v. 9, p. 292–297

Manuscript Received by the Secretary of the Society, September 8, 1959
Massachusetts Institute of Technology Age Studies No. 18

B. P. WALPOLE
K. G. SMITH
Commonwealth Bureau of Mineral Resources, Canberra, Australia

Geochronology of Proterozoic Granites in Northern Territory, Australia. Part 2: Stratigraphy and Structure

Abstract: Potassium-argon and rubidium-strontium dating of 24 Proterozoic granites from the Northern Territory of Australia shows two main groups of ages averaging 1630 and 1440 million years. Both groups of granite were emplaced at the end of a period of folding. The regional structure connects the first period of folding with the lower, and the second with the upper, subdivision of what is regarded as Lower Proterozoic. The older group of granites (1630 million years) marks the top of the lower subdivision, and the younger group marks the top of the Lower Proterozoic. The base of the Proterozoic would naturally be much older than 1630 million years.

Major deviations from the average ages quoted are possibly due to recrystallization of mica or diffusion loss of argon resulting from local deformation or deeper burial of the rocks at the sample localities.

CONTENTS

Introduction 663
General geology 663
Archean rocks 664
Proterozoic rocks 665
General statement 665
Lower Proterozoic rocks 665
Comment 665
Agicondian series 665
Davenportian series 666
Structural environment 666
Discussion of age determinations 666
References cited 668

Figure
1. Generalized geological map of Northern Territory, Australia 664

Table
1. $K^{40}-Ar^{40}$ age determinations in Precambrian granites, Northern Territory, Australia . . 667

INTRODUCTION

This paper summarizes the stratigraphy and structure of the Precambrian rocks of the Northern Territory of Australia in the light of recent geochronological determinations carried out at the Massachusetts Institute of Technology, described in Part 1 of this report.

The Northern Territory of Australia covers about 500,000 square miles and includes rocks ranging from Archean to Tertiary. The Commonwealth Bureau of Mineral Resources began semidetailed and reconnaissance regional mapping of this area in 1949; previous work had been done by a number of different agencies and individuals. Although work is still in progress, the distribution and relationships of the major rock units have been determined. The work done has allowed definition, in broad terms, of the structural framework of the region and delineation of the main zones of tectonic and plutonic activity. These zones are being dated, and this paper attempts to relate the currently available K-Ar age determinations to subdivisions within the Precambrian.

GENERAL GEOLOGY

The Northern Territory forms part of the Australian Precambrian Shield and with the exception of the Paleozoic fold belts of the Amadeus Trough and the Ngalia Basin (Fig. 1) has remained comparatively stable since the end of Precambrian time. The sea has transgressed over the stable areas only four times

Geological Society of America Bulletin, v. 72, p. 663–668, 1 fig., May 1961

since the Precambrian. Veneers of Lower Paleozoic (mostly Cambrian) and Mesozoic rocks were laid down in broad and shallow basins which cover a large part of the area. Present information suggests that the Lower divisions referred to as Archean, Lower Proterozoic, and Upper Proterozoic. (Proterozoic is used herein to refer to structural form and metamorphic facies and not to an arbitrary time scale.)

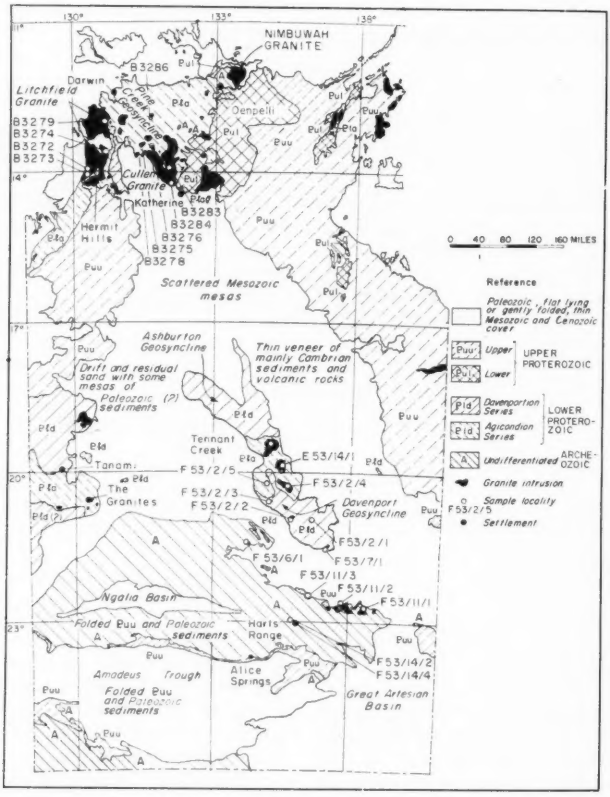

Figure 1. Generalized geological map of Northern Territory, Australia

Paleozoic is less than 3500 feet except in the Amadeus Trough. The Mesozoic rocks are probably less than 300 feet thick except in the little known southeastern corner of the territory. Two less extensive transgressions occurred in the Late Devonian which have not been definitely established as marine (K. G. Smith recently discovered Upper Devonian fish in the Dulcie Range area of central Australia), and the Permian. The Permian marine rocks occupy the extreme northwestern corner of the territory.

The Precambrian rocks include three major

ARCHEAN ROCKS

The Archean rocks are mostly crystalline. The high-grade metamorphic rocks from the Harts Range area described by Joklik (1955) may be considered as typical. The main area of outcrop is the Arunta block in central Australia. Small inliers have been mapped in the Hermit Hill, Oenpelli, and South Alligator areas of the Katherine-Darwin region.

The Archean rocks are separated from succeeding Precambrian sequences by a very prominent structural and metamorphic uncon-

formity and form the basement complex and source rocks for a large volume of the sediments deposited in later epochs. This unconformity is generally accepted in the Northern Territory as representing the dividing line between the Archean and Proterozoic eras.

PROTEROZOIC ROCKS

General Statement

The Proterozoic in the Northern Territory of Australia is represented by two main sequences recognizable in the field by their spatial relationships, by similarities in types of sediment, and by the degree of folding. The sequences are referred to as Lower Proterozoic and Upper Proterozoic; each has two main subdivisions. The Upper Proterozoic rocks have not yet been dated and will be considered only briefly here. In general they consist of sedimentary and volcanic rocks contained in fairly shallow intracratonic basins, commonly more or less modified by vertical movement along or near the margins of the basins. Except in the Amadeus and Ngalia structures, they are only gently folded. They are not metamorphosed and have not yet been shown to be intruded by granite. They contain numerous minor breaks in sedimentation, mostly local in character and probably resulting from instability of the basin margins during sedimentation. Glacial sediments occur in the Upper Proterozoic succession in central Australia.

The lower part of the Upper Proterozoic succession has a maximum known thickness of about 9000 feet and is separated from the upper part by a regional unconformity. The upper part has a maximum thickness of about 10,000 feet and contains at least two regional unconformities.

Lower Proterozoic Rocks

Comment. The Lower Proterozoic rocks include two subdivisions separated by a regional unconformity. Both consist of folded geosynclinal sediments which in each case, however, do not exceed 20,000 feet in thickness. The sedimentary rocks are intruded by granite.

We follow Hossfeld's (1954) nomenclature (Agicondi Series, Davenport Series), but apply the terms to wider areas, and in greater detail. Also, we regard the Davenportian as Lower rather than Middle Proterozoic. We prefer the adjectival form of the names.

Agicondian Series. The Agicondian is the lower subdivision. These rocks crop out in the Katherine-Darwin, Tennant Creek, and the Granites-Tanami areas.

In the Katherine-Darwin region Agicondian rocks occupy the Pine Creek geosyncline, a fairly shallow intracratonic structure, the development of which was largely controlled by vertical movements. The main axis of the geosyncline trends southeast; a subsidiary and late-stage trough branches to the southwest. The sedimentary record includes three main facies assemblages. The relationships between these indicate that the geosyncline developed in stages, punctuated by tectonic movements which caused shifts in the source and loci of sedimentation (Walpole, 1959, Ph.D. thesis, Australian National Univ.). The rocks are folded, but there has been little foreshortening and virtually no regional metamorphism except in broad sheared zones along the margins of the geosyncline.

The rocks are mineralized and intruded by a number of granite bodies. The largest outcropping intrusions are the Cullen and Litchfield granites. The Cullen granite lies roughly parallel to, and east of, the main trough of the geosyncline, but one arm crosses the trough farther east at right angles to the regional trend of the fold structures. The Litchfield mass lies along or near the western margin. The Nimbuwah granite intrudes basement rocks outside the confines of the geosyncline. Smaller granite stocks crop out at random.

The granite intrusions are a late-stage development in the evolution of the geosyncline. They do not occupy an orogenic belt and, in fact, no such belts can be identified within the geosyncline. In the main, they consist of massive rock with large feldspar phenocrysts. They are commonly unstressed, although two of the smaller intrusions show platey flow structures. S. M. Hasan and S. Baker (1958, unpub. ms., Bur. Min. Res. Australia Rec. 1956/68) consider the granites comagmatic.

Ivanac (1954) has described the Agicondian rocks of the Tennant Creek area as the Warramunga Group. They are similar to part of the sequence in the Pine Creek geosyncline in lithology and in the lack of regional metamorphism. They are intruded by granite and porphyry. These rocks are included in a structure named the Warramunga geosyncline by Noakes (1954), but the limits of this structure are not known, and no conclusions can be drawn as to the spatial distribution of the intrusive bodies.

We believe that the rocks in the Granite-

Tanami area belong to the Agicondian, but the intrusions have not been dated and the succession is not known in any detail.

Davenportian Series. A prominent unconformity separates the Davenportian rocks from the Agicondian at Tennant Creek. The Davenportian rocks crop out in the Ashburton and Davenport ranges in central Australia and in the Tanami-Winnecke area in the western part of the Northern Territory. They consist of rocks of geosynclinal origin, mainly graywacke, arenites, and rudites. Volcanic rocks are common in some areas. They are intruded by granite. The Davenport Range area has been studied in most detail (K. G. Smith, I. A. Stewart, and J. W. Smith, 1960, unpub. ms., Bur. Min. Res. Australia Rec. 1960/80). The sequence is about 20,000 feet thick, but granite intrusions penetrate only the base. As in the Pine Creek geosyncline, there is no well-defined orogen. The intrusions are distributed at random, both within the confines of the geosyncline and in the basement rocks of the Arunta complex on the southwestern margin.

This lack of spatial relationship between the granite intrusions and the geosynclinal structures indicates that the tectonic events which closed each geosynclinal stage—and, presumably, initiated a further episode of sedimentation—were effective over much wider areas than the geosynclinal zones.

STRUCTURAL ENVIRONMENT

The data now available on the structure and stratigraphy of the Proterozoic rocks of the Northern Territory show a different picture from that envisaged by earlier workers. Noakes (1954) considered that the Early Proterozoic geosynclines formed broad orogenic belts wrapped around Archean nuclei. He believed that these orogens were the source of sedimentary material for later sequences, shedding back onto the old nuclei. Walpole (1959, Ph.D. thesis, Australian National Univ.) suggests that much of the sedimentary material for succeeding sequences was derived from the Archean basement rocks. For example, the most probable source for the Davenportian is the Arunta complex, not the Agicondian. The same principles apply to the lower part of the Upper Proterozoic in the Katherine-Darwin region.

Walpole (1958, unpub. ms read before Section C, Australian and New Zealand Assoc. for Adv. of Science) has stated that

"... sedimentation in the Proterozoic era resulted from the break up of the crystalline basement complex. The break-up developed along a remarkably consistent fracture pattern following main trends of 320° and 90° magnetic with a minor direction at 360°. Succeeding episodes of sedimentation occurred in structures parallel or oblique to previous structures, but still in conformity with the fracture pattern which was maintained throughout the Proterozoic era. The movements were a result of strong tensional stress. This developed in the basement and is believed to have displaced the basement as well as, in some cases, the relatively thin veneers of sediments accumulated in Proterozoic troughs."

The regularity of the fracture pattern in succeeding time-rock units may indicate a periodicity in the tensional movements which caused the break-up. Such a periodicity should be reflected in the geochronology of the granite intrusions. Dating of the intrusions should give a minimum age for each of the sequences affected—and this age should be repeated from one area to another within sequences correlated on geological field evidence.

The sampling localities chosen as an initial test were: the Agicondian rocks of the Pine Creek geosyncline in the Katherine-Darwin region and in the Tennant Creek area; the Davenportian rocks of the Davenport geosyncline in central Australia; and a number of massive granites, thought to be Davenportian in age, which intrude the Arunta basement complex outside the known or suspected limits of Davenport sedimentation.

Determinations made to date must be considered preliminary. The results available support the suspected periodicity.

DISCUSSION OF AGE DETERMINATIONS

Samples listed in Table 1 are shown on Figure 1.

The determinations listed show two main groupings which illustrate the relative positions of each of the two main time-rock units. The spread of each group is about 200 m.y. Details of the analyses, and Rb-Sr check analyses, are given in Part 1 of this report.

The first group comprises nine determinations listed as Davenportian. Seven have an average of about 1440 m.y., the maximum variation from the mean being ± 40 m.y. Of the remaining two, one determination is 1320 m.y., the other 1540 m.y.

The second group comprises 14 determinations carried out on granites intrusive into the Agicondian rocks of the Warramunga and Pine Creek geosynclines. These show a mean value

of 1630 m.y., and 10 of them show a maximum variation of about ±55 m.y. Maxima and minima are 1720 m.y. and 1510 m.y. respectively.

Additional samples are necessary to confirm the maxima and minima in each case. It is not yet possible to determine whether these represent overlap between two periods of igneous intrusion. The average age of each of the two main groups is in accordance with the field evidence. Further work may show a greater spread of ages over a larger number of samples, but we believe that the present samples are fairly representative. There are, of course, other possibilities. Davenportian granites intruded the Arunta complex without relationship to the Davenportian depositional structures, and Davenportian granites could have intruded the Agicondian Series.

Part 1 of this report includes a discussion of the meaning of these age values in view of possible diffusion loss of argon or later recrystallization. We believe that geological circumstances are such that the measurements very probably indicate ages that closely follow the end of the periods of folding and intrusion. The granites were intruded into rocks at a fairly low temperature and probably cooled and were unroofed rather rapidly.

Sample F/53/14/4 is an exception. This sample was collected from the Irindina Gneiss on the Harts Range area (Joklik, 1955) and is dated at 367 m.y. This age agrees fairly well with a lead age from a samarskite-bearing pegmatite in the same general area which was dated at 420 m.y.[1] The 367 m.y. date must be viewed sceptically in the light of field evidence, which has definitely established the Arunta complex as basement to the Davenportian rocks. The Amadeus Trough (Fig. 1), south of the sample locality, is a folded belt containing rocks ranging from Late Proterozoic to Ordovician in age, neither metamorphosed nor intruded by granite. Stress in the basement, which caused the trough to form, and probably later caused its deformation, was perhaps of sufficient intensity to bring about recrystallization of the micas in the basement rocks. The Harts Range area contains a large number of

Table 1. $K^{40}-Ar^{40}$ Age Determinations in Precambrian Granites, Northern Territory, Australia

Sample no.	Davenportian	Agicondian	Remarks	K-Ar age (m.y.)
F/53/7/1	×		Intrudes Davenportian	1430
F/53/2/4	×		Intrudes Agicondian	1400
F/53/2/3	×		Intrudes Davenportian complex	1540
F/53/2/1	×		Intrudes Davenportian	1480
F/53/2/2	×		Intrudes Davenportian	1320
F/53/11/1	×		Intrudes basement complex	1440
F/53/11/2	×		Intrudes basement complex	1420
F/53/11/3	×		Intruded and metamorphosed basement complex	1460
F/53/6/1	×		Intrudes basement complex	1460
F/53/2/5		×	Intrudes Agicondian	1510
E/53/14/1		×	Intrudes Agicondian	1630
B-3278		×	Intrudes Agicondian	1720
B-3273		×	Intrudes Agicondian	1560
B-3272 (biotite)		×	Intrudes Agicondian	1650
B-3272 (muscovite)		×	Intrudes Agicondian	1640
B-3279		×	Intrudes Agicondian	1630
B-3274 (biotite)		×	Intrudes Agicondian	1595
B-3274 (muscovite)		×	Intrudes Agicondian	1605
B-3275		×	Intrudes Agicondian	1520
B-3284		×	Intrudes Agicondian	1695
B-3286		×	Intrudes Agicondian	1650
B-3276		×	Intrudes Agicondian	1695
B-3283		×	Intrudes Agicondian	1695
F/53/14/4			Arunta complex (Irindina Gneiss)	367

$\lambda_e = 0.585 \times 10^{-10}$ yr.$^{-1}$; $\lambda = 5.30 \times 10^{-10}$ yr.$^{-1}$

[1] Determination made by J. T. Wilson, University of Toronto.

sizable pegmatite bodies, and conceivably some mica in the Irindina Gneiss may have been recrystallized. The date may therefore represent the age of a tectonic movement and probably remobilized basement at depth. Joklik (1955, p. 180) notes that muscovite-rich pegmatites cut muscovite-bearing country rock, whereas pegmatites rich in biotite are confined to mafic country rock; this suggests that some of the constituents of pegmatites may have been derived locally. The date cannot represent the age of the Arunta complex.

Walpole (1959, Ph.D. thesis, Australian National Univ.) suggests that the break-up of the crystalline basement rocks into the remarkably consistent polygonal pattern of fractures which controlled later sedimentation represents the beginning of the Agicondian and therefore of the Proterozoic era. If so, it would appear that Proterozoic deposition in the Northern Territory commenced much earlier than the oldest granite age (1720 m.y.) so far determined in this area and may in fact extend back toward the 2000 m.y. mark.

The conclusions will necessarily be reviewed as further work is carried out, but the reasonably close groupings of most of the samples from each suite of intrusions cannot be ignored. These suggest that two intrusive episodes reached their peaks at roughly 1630 and 1440 m.y. respectively. Considering these dates together with the tectonic framework and the stratigraphy of the region, which clearly indicate that both episodes are younger than the folding of their respective successions and are of regional extent, the 1630 m.y. figure may represent approximately the close of the Agicondian and the start of the Davenportian. Similarly the 1440 m.y. date may indicate the development of tectonic activity which resulted in the Late Proterozoic sedimentation in the Northern Territory. The granite intrusions dated between 1440 and 1630 m.y. may represent a spread of Davenportian igneous activity, and those older than 1630 m.y. a spread of Agicondian intrusions.

REFERENCES CITED

Hossfeld, P. S., 1954, Stratigraphy and structure of the Northern Territory of Australia: Royal Soc. S. Australia Trans., v. 77, p. 103–161

Ivanac, J. F., 1954, The geology and mineral deposits of the Tennant Creek Goldfield, Northern Territory: Bur. Min. Res. Australia Bull. 22, 164 p.

Joklik, G. F., 1955, The geology and mica fields of the Harts Range, Central Australia: Bur. Min. Res. Australia Bull. 26, 226 p.

Noakes, L. C., 1954, The structure of the Northern Territory with relation to mineralization: 5th Empire Min. Metall. Cong. Pub., v. 1, p. 284–296

Manuscript Received by the Secretary of the Society, September 8, 1959
Publication Authorized by the Director, Bureau of Mineral Resources, Canberra, Australia

CARL A. LAMEY *The Ohio State University, Columbus, Ohio*

Contact Metasomatic Iron Deposits of California

Abstract: Iron deposits of California that cluster around small intrusive bodies and are localized in metamorphosed limestone or dolomite show varying degrees of mineralogic complexity. Minerals present along with those that more commonly occur in contact metasomatic deposits in the United States include chondrodite, humite, clinohumite, ludwigite, ilvaite, idocrase, spinel, and forsterite. One deposit is characterized by the very simple mineral assemblage calcite, antigorite, and magnetite except within a few feet of an intrusive body. Generally, pyroxene, garnet, chondrodite, humite, and clinohumite formed early; antigorite, magnetite, specularite, and goethite formed late. The writer suggests several sequences of mineral deposition and compares them with sequences determined by others.

Addition of material and replacement were prominent in the formation of these deposits. Iron was added during the formation of magnetite, hematite, and goethite and probably also during the formation of hedenbergite, andradite, ludwigite, ilvaite, and epidote; fluorine during the formation of chondrodite, humite, and clinohumite; boron during the formation of ludwigite; and probably magnesium during the formation of chondrodite, humite, clinohumite, and antigorite. Some recrystallized limestone was replaced by magnetite and antigorite; some antigorite was replaced by magnetite; some pyroxene, minerals of the humite group, and spinel were replaced by magnetite.

The writer classes the deposits as contact metasomatic but suggests that the mineralogy indicates a temperature range from high contact metamophic to moderate hydrothermal activity.

CONTENTS

Introduction 669
Acknowledgments 670
Deposits studied 670
  Location 670
  Geologic setting 670
  Mineralogy 671
  Sequence of mineral formation 673
    Criteria used 673
    Sequences indicated 673
    Comparison with sequences stated by others . 674
  Replacement 675
    Criteria used 675
    Replacements indicated 675
  Origin and classification of the deposits 676
References cited 676

Figure
1. Index map showing location of some iron deposits of California 670

Plate — Following
1. Garnet and ludwigite
2. Relationships of ore minerals and gangue minerals — 674
3. Replacement of limestone by magnetite
4. Replacement of limestone by antigorite and magnetite

Table
1. Compositions and relative abundances of minerals of the deposits 671
2. X-ray powder determination of garnets 672
3. Characteristics of ludwigite and ilvaite 673

INTRODUCTION

This paper presents the results of a laboratory study of some iron deposits of California (Lamey, 1948). The field work was done under the pressure of wartime conditions, and time was not available for very detailed study or thorough collecting; nor has the writer found time to return to the areas. This paper shows some interesting relationships and may add to our knowledge of contact metasomatic deposits. A study based on more thorough collecting might disclose additional information.

The following discussion is based on (1) field study during mapping, (2) laboratory study of several hundred hand specimens, and (3) microscopic study of 128 thin sections, 14 polished specimens, and powders of many minerals, supplemented by X-ray powder diffraction studies and chemical tests.

Geological Society of America Bulletin, v. 72, p. 669–678, 1 fig., 4 pls., May 1961

ACKNOWLEDGMENTS

The writer is indebted to Leslie C. Coleman, Department of Geology, University of Saskatchewan, formerly of the Department of Mineralogy, The Ohio State University, for X-ray powder diffraction studies of specimens of garnet, ludwigite, ilvaite, and magnetite and to Ernest G. Ehlers of the Department of Mineralogy, The Ohio State University, for chemical tests on specimens of ludwigite.

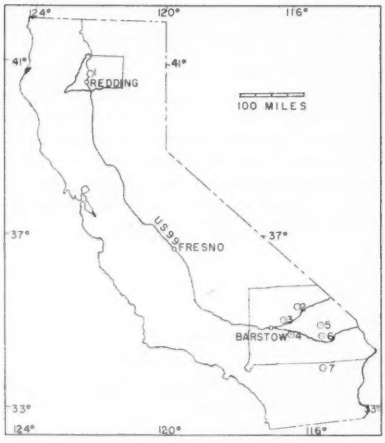

Figure 1. Index map showing location of some iron deposits of California. No. 1, Shasta, Shasta County; 2–6, Silver Lake, Cave Canyon, Lava Bed, Vulcan, Iron Hat, in San Bernardino County; 7, Eagle Mountains, Riverside County (not described)

DEPOSITS STUDIED

Location

The chief deposits studied are Iron Mountain, Lava Bed district (Bessemer); Cave Canyon; Iron Hat (Ironclad); and Vulcan, all in San Bernardino County; and Shasta, Shasta County. Brief reference is made to Iron Mountain and Iron King deposits, Silver Lake district, San Bernardino County. Figure 1 shows the location of these deposits.

Geologic Setting

The geologic setting is similar for all deposits discussed. The iron deposits are clustered about small intrusive masses that cut limestone or dolomite which locally is cherty or associated with quartzite. The sedimentary rocks were metamorphosed to varying degrees by the intrusive masses. The Vulcan deposit differs in respect to complexity of mineralogy and distribution of typical metamorphic minerals: its mineral assemblage is very simple, and typical metamorphic minerals occur only within a few feet of the intrusive contact. The Silver Lake deposits apparently were brought to their present position along great thrust faults but are similar to the other deposits in other respects.

The intrusions are composed of granitic rock (Iron Hat and Lava Bed), quartz monzonite (Vulcan and Silver Lake), and quartz diorite (Cave Canyon and Shasta). The granitic intrusions, although chiefly granite, include syenite and monzonite. The granites are composed of quartz, potassic feldspar, subordinate Na-Ca feldspar (chiefly oligoclase), minor biotite, accessory apatite, sphene, zircon and locally allanite, fluorite, or specularite. Two variants were noted: one contains a large amount of purple fluorite and sparse beryl, the other a large amount of specularite. The quartz monzonites consist of potassic feldspar, Na-Ca feldspar (andesine), quartz, and either hornblende or biotite or both, along with accessory sphene, magnetite, ilmenite, apatite, and zircon. The quartz diorite at Cave Canyon is composed of andesine, hornblende, biotite, quartz, oligoclase, and potassic feldspar, whereas the quartz diorite at Shasta is composed of andesine or andesine-oligoclase, diopsidic to augitic pyroxene, and quartz. Sphene is an accessory in both quartz diorites; in addition, apatite, magnetite, and possibly allanite are accessory minerals in the Cave Canyon quartz diorite.

The intrusive rocks have been altered to varying degrees; generally the granites are less altered than the quartz monzonites and quartz diorites. Epidote is the most abundant alteration mineral in all the intrusive masses; the quartz diorite of the Shasta deposit shows extensive epidotization. Actinolitic amphibole, chlorite, sericite, and calcite are present but usually subordinate.

The limestones and dolomites have been converted into marbles, calcareous hornfelses, and skarn rocks. The marbles are of three types: (1) those composed chiefly of recrystallized carbonate; (2) those composed of recrystallized carbonate and a few metamorphic minerals; and (3) those composed of recrystallized carbonate and a moderate to large amount of serpentine, usually antigorite. The calcareous hornfelses are composed of calcite and moderate amounts

of garnet, pyroxene, and amphibole, along with some less common minerals. The skarn rocks contain relatively small amounts of calcite and are composed chiefly of metamorphic minerals. The limestones and dolomites, marbles, calcareous hornfelses, and skarn rocks are the host rocks for the iron deposits.

Table 1. Compositions and Relative Abundances of Minerals of the Deposits

Mineral	Approximate composition	Relative abundance* Cave	Canyon Iron Hat	Lava Bed	Shasta	Vulcan
Gangue†						
Amphibole group						
Actinolite	$Ca_2(Mg,Fe)_5Si_8O_{22}(OH)_2$	3	..	..	2	3
Anthophyllite	$(Mg,Fe)_7Si_8O_{22}(OH)_2$	..	3?	..	2	..
Tremolite	$Ca_2Mg_5Si_8O_{22}(OH)_2$	2	3	3	3	..
Antigorite	$Mg_6Si_4O_{10}(OH)_8$	3	2	2	1	1
Chlorite	$(Mg,Fe,Al)_6(Al,Si)_4O_{10}(OH)_8$	..	..	..	2	..
Epidote group						
Chiefly pistacite	$Ca_2(Al,Fe)_3Si_3O_{12}(OH)$	3	2	3	2	3
Garnet group						
Grossularite-andradite	$Ca_3(Al,Fe)_2(SiO_4)_3$	2	3	3	1	..
Humite group						
Chondrodite	$Mg(F,OH)_2 \cdot 2\ Mg_2SiO_4$	..	..	1	..	..
Clinohumite	$Mg(F,OH)_2 \cdot 4\ Mg_2SiO_4$	..	..	2	..	..
Humite	$Mg(F,OH)_2 \cdot 3\ Mg_2SiO_4$	..	..	2	..	..
Idocrase	$Ca_{10}Mg_2Al_4(Si_2O_7)_2(SiO_4)_5(OH)_4$	..	3	3	..	..
Ilvaite	$CaFe_2Fe(OH)Si_2O_8$	..	..	..	3	..
Ludwigite	$(Mg,Fe)_2O_2FeBO_3(?)$	3	..	3	..	..
Mica group						
Biotite	$K(Mg,Fe)_3(AlSi_3O_{10})\ (OH)_2$	..	3	..	..	..
Muscovite	$KAl_2(AlSi_3O_{10})\ (OH)_2$	..	3	..	..	..
Phlogopite	$KMg_3(AlSi_3O_{10})\ (OH)_2$	2	3	2	..	..
Olivine group						
Forsterite	Mg_2SiO_4	..	3	2	..	..
Pyroxene group						
Diopside-hedenbergite	$Ca(Mg,Fe)Si_2O_6$	3	3	2	1	3
Sphene	$CaTiSiO_5$	3	3	3	3	..
Spinel	$MgAl_2O_4$	..	3	2	..	..
Talc	$Mg_3Si_4O_{10}(OH)_2$	..	2	..	..	..
Ore						
Goethite	$HFeO_2$	2	2	2	2	..
Hematite	Fe_2O_3	2	2	2	2	..
Magnetite	$FeFe_2O_4$	1	1	1	1	1
Specularite	Fe_2O_3	..	2	..	3	..

* Relative abundance is indicated as follows: 1, very abundant; 2, moderately abundant; 3, subordinate to rare.
† Except carbonates and quartz

Mineralogy

The chief ore mineral is magnetite, and the chief gangue minerals are calcite, garnet, pyroxene, amphibole, epidote, and antigorite. Other minerals, some of which are abundant locally, include humite, clinohumite, chondrodite, ilvaite, ludwigite, forsterite, spinel, idocrase, sphene, mica, talc, chlorite, hematite, and goethite. Minor minerals present locally are pyrite, chalcopyrite, and quartz. Table 1 lists the minerals, their compositions, and relative abundances.

A brief description of the characteristics of some of the minerals in or associated with the iron deposits follows.

GARNET: The garnets probably all are members of the grossularite-andradite series. The index of refraction of garnet from the Shasta, Iron Hat, and Cave Canyon deposits is near 1.89, indicating a very high content of andradite; the index of refraction of garnet from the Lava Bed deposit is 1.77, indicating a high percentage of grossularite. X-ray powder diffraction determinations appear in Table 2.

TABLE 2. X-RAY POWDER DETERMINATION OF GARNETS

Determinations made by Prof. Leslie C. Coleman, Department of Geology, University of Saskatchewan, using data from Skinner (1956).

Deposit	Minimum per cent of andradite	Unit Cell, Å, ±0.01
Shasta	Nearly 100	12.05
Iron Hat	92	12.03
Cave Canyon	83	12.01
Lava Bed	10	11.87

Individual garnets in hand specimen and outcrops range from 3 to 10 mm across, but some masses of fine-grained garnet more than 3–4 inches across show no individual crystals.

In thin section much of the garnet is colorless to brown and euhedral or anhedral. Some is zoned, some shows weak birefringence. Rarely, euhedral crystals are strongly anisotropic, zoned, and show triangular segments under crossed nichols (Pl. 1, fig. 2) as a result of twinning (Winchell and Winchell, 1951, p. 490). Most of the garnets are practically unaltered, but some show slight alteration to chlorite and local replacement by ilvaite.

PYROXENE: Pyroxene, present in most deposits, is conspicuous only at the Shasta deposit, where it forms masses up to 6 inches long. Some are almost completely altered to limonite.

In thin section much of the pyroxene is euhedral or subhedral, characteristically associated with magnetite and garnet, and relatively unaltered, although it is replaced by magnetite in places.

All pyroxene checked in thin section or with index liquids is in the diopside-hedenbergite series. Index determinations on material from the Iron Hat deposits gave 1.71 and 1.72 for the highest index and on material from the Shasta deposit gave between 1.72 and 1.73, indicating respectively 33 per cent and 50 per cent hedenbergite (Winchell and Winchell, 1951, p. 413, Fig. 302). Optical properties in thin section suggest a greater range of composition.

FORSTERITE: No forsterite was observed in hand specimens, but it is abundant in thin sections of specimens from the Iron Hat and the Lava Bed deposits in subhedral or euhedral crystals from 0.05 mm to 0.3 mm long. Some is practically unaltered, but characteristically it is surrounded by an alteration rim of antigorite. The forsterite is associated with spinel in most thin sections.

SPINEL: Spinel was observed only in thin section, chiefly from the Lava Bed deposit but also from the Iron Hat deposit. It occurs as grains and well-formed crystals ranging from minute specks to more than 0.2 mm across (Pl. 2, fig. 2). Much of it is bluish, but some is colorless. Some is slightly altered to antigorite, and some has been replaced by magnetite.

HUMITE GROUP: Members of the humite group were observed only at the Lava Bed deposit, but there this mineral group is abundant and, with magnetite, forms large masses that characteristically show black and yellowish-brown stripes (Pl. 2, fig. 1). Optical properties indicate that humite, clinohumite, and chondrodite are present, the last showing characteristic polysynthetic twinning. Chondrodite apparently is the most abundant. The crystals range from subhedral to strikingly euhedral; some are as long as 1 mm. Much of the material is unaltered, but some has been partly changed to antigorite. The characteristic alteration proceeded along fractures (Pl. 2, fig. 2) and thus differs from the characteristic alteration of forsterite, which was from the margins inward in these rocks. Locally members of the humite group are replaced by magnetite (Pl. 2, fig. 2).

ILVAITE AND LUDWIGITE: Ilvaite and ludwigite are similar in their general characteristics and optical properties, both weather to limonite, and hence are difficult to distinguish except by X-ray methods. Table 3 shows the results of X-ray powder diffraction identifications by Prof. Leslie C. Coleman, index of refraction determinations by the writer, and tests for boron by the writer and by Prof. Ernest G. Ehlers.

The indices of refraction were difficult to determine accurately because of the high value

and because these two minerals are nearly opaque in some positions.

The ilvaite of the Shasta deposit is associated with garnet or pyroxene. Much of it in hand specimens is black, submetallic, and massive but does show poor cleavage. Thin sections show that it has partially replaced garnet and pyroxene.

TABLE 3. CHARACTERISTICS OF LUDWIGITE AND ILVAITE

Deposit	Highest index of refraction	Flame test for boron	X-ray identification
Lava Bed	1.95	Positive	Ludwigite
Cave Canyon	1.92	One negative; one indicated boron but not decisively	Ludwigite
Shasta	1.93	Negative	Ilvaite

The ludwigite of the Cave Canyon and the Lava Bed deposits occurs as well-formed crystals in marble and greatly resembles hornblende. At Cave Canyon it is in thin, vertically striated black crystals, many of which are 5–10 mm long but rarely as much as 0.5 mm wide, whereas at Lava Bed some of the crystals are 20–30 mm long and nearly 3 mm wide (Pl. 1, fig. 5). These crystals also are black and vertically striated. In both places the ludwigite is altered in part to limonite. In thin sections the crystals are striking. The Cave Canyon ludwigite occurs in excellent euhedral crystals (Pl. 1, figs. 3, 4) that show pleochroism in dark green and brown to nearly or entirely black (opaque), whereas the Lava Bed ludwigite shows sieve structure (Pl. 1, fig. 6) and some pleochroism in green and brown but generally is nearly opaque.

TREMOLITE: Tremolite occurs rarely as crystals several inches long and a quarter to half an inch wide and somewhat more abundantly in places as thin crystals about a quarter of an inch long. It is not conspicuous in thin sections but is present as euhedral crystals a few millimeters long showing sieve structure. In some specimens the former presence of tremolite or anthophyllite is indicated by antigorite which formed by alteration of a mineral of tremolitic habit.

MAGNETITE: Magnetite, the most abundant iron ore mineral present, occurs as irregular grains, as subhedral to euhedral crystals, and as large masses showing mosaic fabric. All euhedral crystals observed, some of which are an inch across, are dodecahedrons rather than octahedrons. Much of the magnetite at the Shasta deposit is lodestone.

Some material at the Iron Hat deposit that had the properties of magnetite except for a brownish streak was examined to determine whether it was maghemite. X-ray powder diffraction determination by Prof. Leslie C. Coleman showed that the material is magnetite.

SPECULARITE: Specularite is most abundant at the Iron Hat deposit. It occurs as rosettes in masses of epidote and of quartz and as crystals in veins cutting masses of epidote, garnet, and quartz (Pl. 2, fig. 5). In some thin sections it occurs as striking skeletal to complete euhedral crystals that replace quartz (Pl. 2, fig. 6).

Sequence of Mineral Formation

Criteria used. The criteria used to determine the sequence of mineral formation were (1) veins and veinlike masses of one mineral cutting another; (2) fingerlike and tonguelike projections of one mineral into another, especially if such projections cut across crystallographic directions; (3) deposition of one mineral within and along crystallographic directions of another; (4) remnants of one mineral more or less surrounded by another; (5) skeletal and partial crystals of one mineral cutting across grain boundaries of another; (6) deposition along bedding, with partial preservation of bedding; (7) deposition of one mineral in the form of small, somewhat spherical masses scattered throughout another mineral or mineral aggregate.

Numerous specimens studied show these features. Veins and veinlike masses cutting a mineral are shown by Figures 2–5 of Plate 2; fingerlike and tonguelike projections by Figures 2 and 3 of Plate 2 and Figure 2 of Plate 3; deposition along cleavage and twinning directions by Figure 3 of Plate 2, Figure 2 of Plate 3, and Figure 4 of Plate 4; remnants of one mineral in another by Figures 3 and 6 of Plate 2 and Figure 2 of Plate 3; skeletal or partial crystals by Figure 6 of Plate 2; deposition along bedding by Figures 3–6 of Plate 3; and deposition as small, somewhat spherical masses by Figures 1–3 of Plate 4.

Sequences indicated. The criteria cited indicate that the sequences of mineral deposition differ somewhat from one deposit to another. Generally pyroxene, garnet, chondrodite,

humite, and clinohumite formed early; antigorite, magnetite, specularite, and goethite formed late. Specific sequences at the various deposits will be discussed briefly.

The Shasta deposit afforded the best opportunity for observing the sequence of mineral formation because of the availability of drill cores; there the usual sequence appears to have been (1) pyroxene, (2) garnet, (3) amphibole, (4) magnetite, (5) ilvaite, and (6) veins containing calcite, pyrite, and chalcopyrite either together or separately. No sequence among the three vein-forming minerals was indicated. Establishing the sequence cited raised some difficulties because not all the minerals were present in any thin section. However, where pyroxene and garnet occur together the pyroxene appears to have formed first; where magnetite is present with pyroxene, the pyroxene apparently formed first, since euhedral crystals of pyroxene have been partly converted into magnetite (Pl. 2, fig. 3); in all thin sections containing both magnetite and garnet, the garnet apparently formed first; the amphibole, an actinolitic variety, is an alteration of pyroxene. Locally garnet formed later than magnetite, as one vein containing calcite, pyrite, and some garnet was observed cutting masses of magnetite.

Sequences shown at other deposits usually involve only two or three minerals. At Lava Bed, pyroxene formed before garnet; chondrodite formed before antigorite, which fills fractures in and is an alteration of the chondrodite; both chondrodite and antigorite formed before magnetite, which cuts across stringers of antigorite and corrodes chondrodite (Pl. 2, fig. 2). At Iron Hat, both garnet and tremolite formed before magnetite; also, locally epidote formed earlier than specularite, since it is cut by veins of specularite (Pl. 2, fig. 5), but in some places epidote and specularite may have formed contemporaneously. At this same deposit specularite cuts across grain boundaries of quartz and thus formed later than the quartz (Pl. 2, fig. 6), but some may have formed contemporaneously with quartz, as both minerals are present together in veins in which no criteria indicate a difference in the order of formation.

The age relationships between magnetite and antigorite are unknown except at the Lava Bed deposit, where at least some antigorite formed first (Pl. 2, fig. 2, especially lower and upper left). Relationships similar to those at Lava Bed appear to exist at the Cave Canyon, the Vulcan, and the Iron Hat deposits, but the evidence is less definite and consists of antigorite surrounding magnetite, the contacts of the two minerals suggesting that the magnetite replaced the antigorite (Pl. 4, figs. 2, 5, 6). At the Shasta deposit, drill holes indicate a close relationship between serpentinization and ore formation; serpentinized zones commonly occur above ore zones (Lamey, 1948, p. 155–161, drill holes 2, 3, 4). Whether serpentinization there preceded, was essentially contemporaneous with, or followed ore deposition is not known, as none of the thin sections studied show the relationships between antigorite and magnetite.

A generalized order that seems to be likely for most of the deposits, omitting some of the minerals present in only a few deposits or about which relationships are too obscure, is (1) pyroxene; (2) most garnet; (3) some antigorite; (4) magnetite, some antigorite; and (5) veins containing calcite, pyrite, chalcopyrite, quartz all in the same vein, in combinations, or singly.

Comparison with sequences stated by others. Sequences among some of the minerals discussed have been noted by others at the Shasta deposits and at the Eagle Mountains deposits, Riverside County, California (Fig. 1). Prescott (1908, p. 475) stated that at the Shasta deposit the succession in one place was (1) magnetite accompanied by a small amount of pyrite and chalcopyrite, (2) garnet and hedenbergite, with interrelations not distinguishable, (3) quartz and ilvaite. He also stated that there was no evidence that the formation of garnet was limited to the stage cited. His generalization for the area (p. 475) was (1) skarn, with massive garnet and lenses of magnetite, (2) iron ore, (3) crystalline garnet or hedenbergite, (4) quartz and ilvaite. Harder (1912, p. 69, 70, 75) stated that at the Eagle Mountains deposits, marble and ophicalcite (serpentine marble) were locally replaced by iron ore, and that in places a serpentine-magnetite rock was formed, which he thought represented the replacement of ophicalcite by iron ore. Hadley (1948, p. 7) in a later description of the same deposits suggested that after the formation of various minerals during an earlier metamorphic stage, tremolite was formed and then altered to serpentine, and that magnetite and pyrite were deposited along with the tremolite and serpentine.

Investigators in various other places have suggested sequences among pyroxene, garnet, and magnetite. Loughlin and Koschmann (1942, p. 100) and Terrones (1958, p. 366) noted pyroxene formed earlier than garnet,

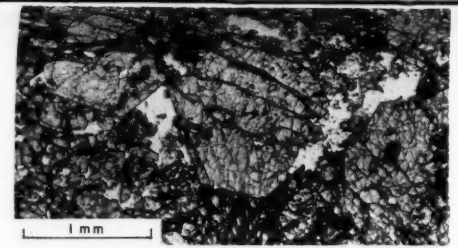

Figure 1

Section showing euhedral crystals of andradite, Cave Canyon deposit. Plain light

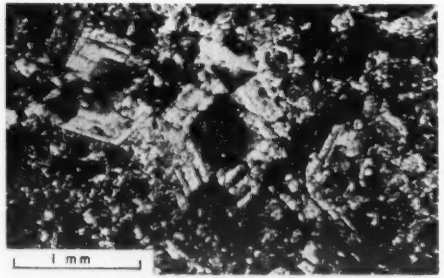

Figure 2

Section showing anisotropic character, twinning, zoning of andradite. Same as Figure 1 but crossed nicols

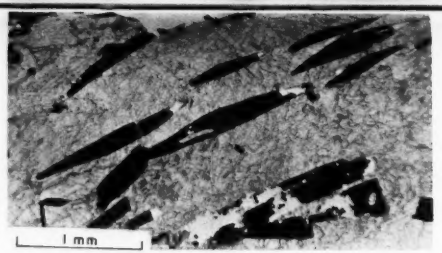

Figure 3

Longitudinal sections of ludwigite in metamorphosed limestone, Cave Canyon deposit. Note tapering of many crystals. Plain light

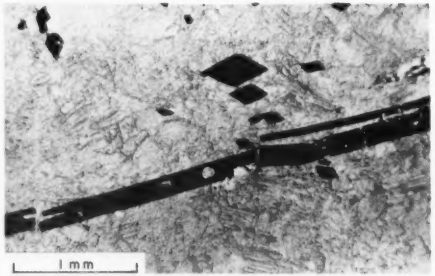

Figure 4

Cross sections and great length of crystals of ludwigite, Cave Canyon deposit. Plain light

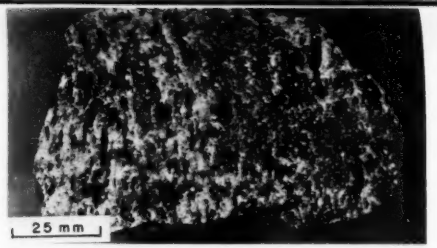

Figure 5

Hand specimen showing elongated crystals of ludwigite in subparallel orientation in metamorphosed limestone, Lava Bed deposit

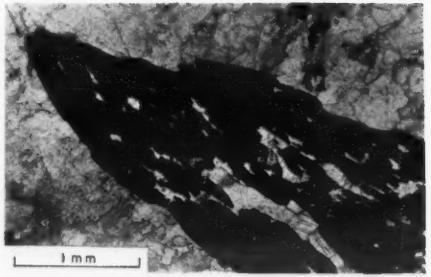

Figure 6

Section from hand specimen shown in Figure 1. Ludwigite occurs in composite crystals showing sieve structure and cleavage or parting perpendicular to length of crystals. Plain light

GARNET AND LUDWIGITE

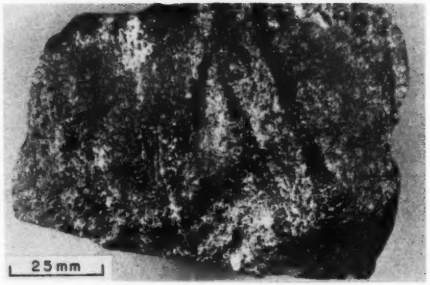

Figure 1

Hand specimen showing interlayered magnetite and humite-group minerals (gray), Lava Bed deposit

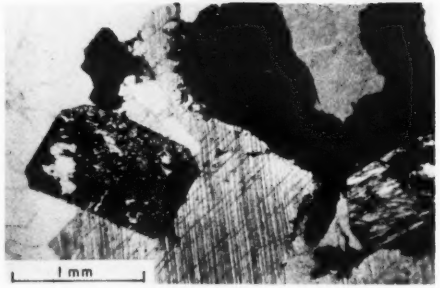

Figure 3

Section from Shasta deposit showing calcite and pyroxene replaced by magnetite (black). Partly replaced euhedral pyroxene at left; magnetite cuts calcite. Plain light

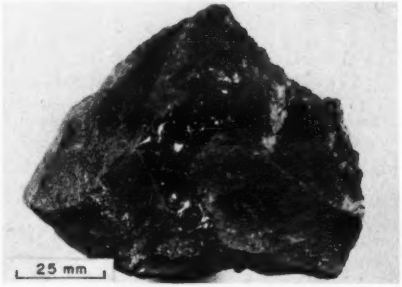

Figure 5

Hand specimen showing vein of specularite (center) in partly epidotized limestone, Iron Hat deposit

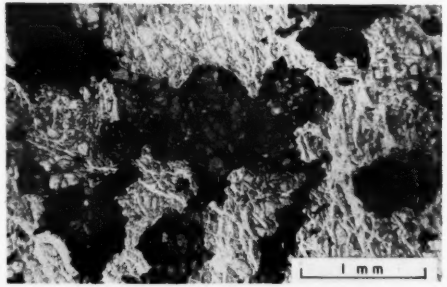

Figure 2

Section from specimen in Figure 1. Magnetite (black), spinel (dark gray), chondrodite partly serpentinized (gray with white streaks of antigorite). Magnetite cuts, embays serpentinized chondrodite and has replaced spinel. Plain light

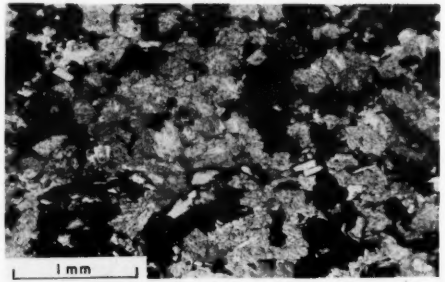

Figure 4

Section from Cave Canyon deposit. Magnetite (black) replaced calcite and corroded and partly replaced phlogopite (whitish, rectangular) along cleavage (lower and right center). Plain light

Figure 6

Section from Iron Hat deposit. Euhedral tabular and partly skeletal specularite cuts and replaces quartz. Bladelike masses show tabular character of specularite. Plain light

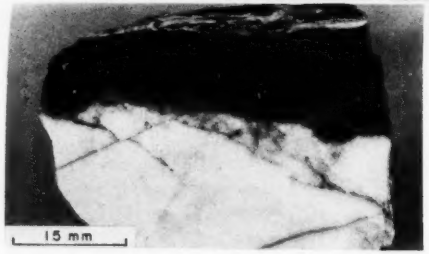

Figure 1

Hand specimen from Iron Hat deposit showing limestone partly replaced by magnetite (black). Note gradational boundary between magnetite and limestone.

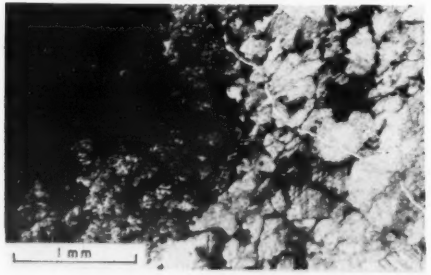

Figure 2

Section from specimen shown in Figure 1. Essentially unreplaced limestone at right; progressive replacement and transition into almost pure magnetite on left. Plain light

Figure 3

Hand specimen from Shasta deposit. Magnetite (black) replaced limestone, chiefly along bedding.

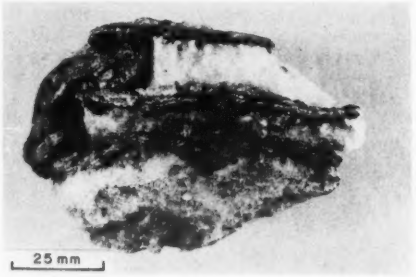

Figure 4

Hand specimen from Shasta deposit. Magnetite (black and some gray) replaced folded limestone along certain beds. Anthophyllite associated with magnetite imparts gray color and fibrous appearance

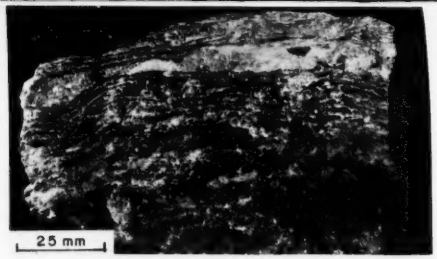

Figure 5

Hand specimen from Silver Lake deposits. Longitudinal section through folded limestone showing selective replacement by magnetite (black). Most layers of magnetite are about 1 mm thick.

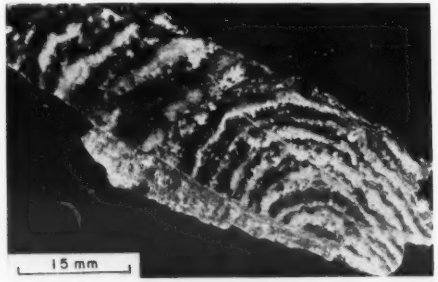

Figure 6

Cross section cut from one end of specimen shown in Figure 5, showing selective replacement of folded limestone by magnetite

REPLACEMENT OF LIMESTONE BY MAGNETITE

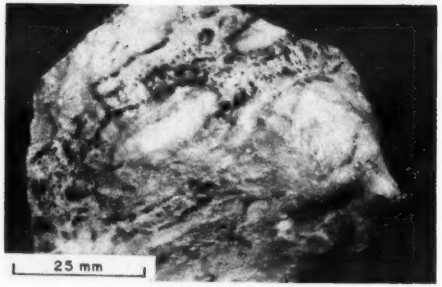

Figure 1

Hand specimen from Vulcan deposit. Black to gray rounded areas and streaks are antigorite. Disseminated replacement is indicated by spherical areas, replacement along bedding by somewhat parallel streaks. *See also* Figure 3.

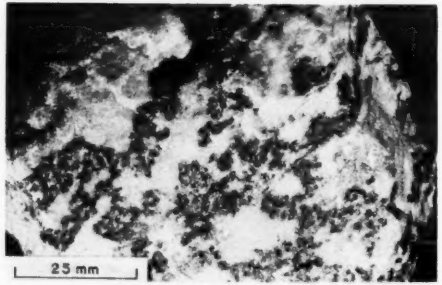

Figure 2

Hand specimen from Vulcan deposit. Apparently antigorite (gray to black) replaced limestone, was later replaced by magnetite (black to gray). Note similarity to replacement pattern shown in Figure 1.

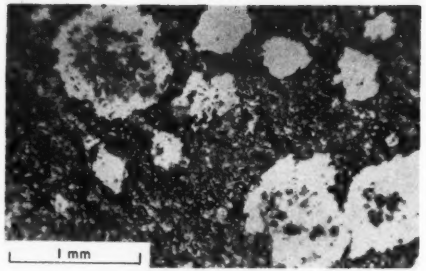

Figure 3

Section of partly serpentinized limestone cut from Vulcan specimen shown in Figure 1. Light-gray, somewhat circular areas are antigorite; some contain remnants of limestone and indicate disseminated replacement. Plain light

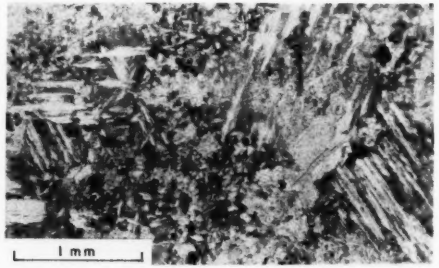

Figure 4

Section of partly serpentinized limestone from Lava Bed deposit. Antigorite (light gray) has replaced calcite along cleavage directions. Plain light.

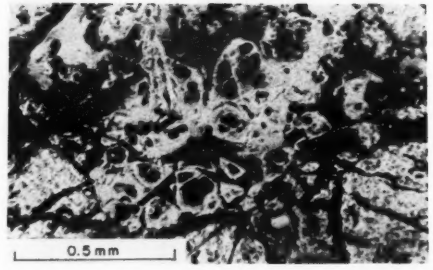

Figure 5

Polished specimen from Vulcan deposit. Magnetite (white to light gray) has replaced antigorite (dark gray to black). Reflected light

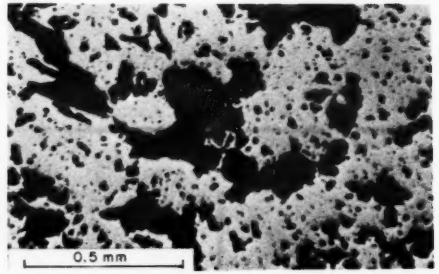

Figure 6

Polished section from Cave Canyon deposit. Magnetite (white to gray) has replaced antigorite (dark gray to black). Reflected light

whereas Schmitt (1939, p. 802, Fig. 4) and Allen and Fahey (1957, p. 894) noted pyroxene formed later than garnet. Schmitt's diagram, however, shows overlapping relationships during part of the formation, and Allen and Fahey state that the formation of manganoan hedenbergite closely followed or overlapped that of garnet. All four investigators state that magnetite generally formed at least slightly later than pyroxene and garnet.

The relationships of minerals of the humite group and of ludwigite to some of the minerals discussed by the writer have been described at various places. Koeberlin (1909, p. 740) has ascertained that the succession at Tilly Foster mine, Brewster County, New York, is (1) spinel, (2) chondrodite, (3) magnetite and serpentine; Geijer (1939, p. 24) described the sequence at Tallgruven, Sweden, as (1) ludwigite, (2) forsterite and humite group, (3) magnetite and spinel, and the sequence at Ostanmossa, Sweden (Geijer, 1927, p. 5) as magnetite probably later than chondrodite at some places and essentially contemporaneous with it at others. Geijer (1925, p. 687) suggests that minerals of the humite group, where occurring with magnetite, have invariably developed earlier than the magnetite. Emmons and Calkins (1913, p. 186) stated that at the Redemption mine in Montana, ludwigite and magnetite apparently were formed together. The observations of Geijer and Koeberlin agree generally with those noted by the writer at the Lava Bed deposit, where both spinel and minerals of the humite group were formed before magnetite. No opportunity was presented for determining the order of formation of ludwigite, since it was not observed with minerals other than calcite.

Replacement

Criteria used. The criteria used to determine the replacement of one mineral by another are essentially the same as those used to determine the sequence of formation of minerals, with the added criteria of an indication of actual substitution by features such as remnants of one mineral that was the host for another (Pl. 2, fig. 3), preservation or partial preservation of crystal form (Pl. 2, fig. 3), structural features of crystals (Pl. 4, fig. 4), evidence of replacement along bedding (Pl. 3, figs. 3–6), and similar features. Where replacement is complete these features are obscured, but even in such cases the texture may resemble that of the unreplaced rock, or progress of replacement from partially replaced to almost completely replaced material may be indicated within a single thin section (Pl. 3, fig. 2) and thus strongly suggest if not establish entire replacement.

Replacements indicated. Replacement of limestone and some metamorphic minerals by iron oxide has been prominent and important in these deposits. The usual replacing mineral is magnetite, but goethite is also found. The most evident features that controlled initial replacement are small fractures, grain boundaries, cleavage cracks, and twinning directions (Pl. 3, fig. 2). Replacement was also controlled by bedding and was highly selective at some places.

Selective replacement is well shown in specimens from the Shasta deposit and from the Silver Lake deposits (Pl. 3, figs. 3–6), where folded beds were replaced; at Silver Lake alternating layers of magnetite and calcite are only about 1 mm thick. The writer suggests that this selectivity may have resulted from a difference in the magnesium content of the original rock layers, the more magnesian ones having been selectively replaced. This is suggested because magnetite replaced antigorite and chondrodite in some deposits; thus a higher magnesium content of some layers may have facilitated replacement of them.

The influence of small fractures as a control for initial deposition and subsequent replacement is indicated at the Iron Hat deposit, where some of the replacement of limestone was in veinlike stringers.

Some replacement was of the disseminated or multiple center type (Bateman, 1950, p. 143), as at Cave Canyon, where magnetite formed tiny spherical masses throughout the limestone.

Metamorphic minerals replaced include chondrodite, spinel, antigorite, pyroxene, and possibly phlogopite. At the Lava Bed deposit magnetite partially or wholly replaced chondrodite, spinel, and antigorite (Pl. 2, fig. 2). At the Shasta deposit magnetite partially replaced pyroxene (Pl. 2, fig. 3), and at the Cave Canyon deposit it may have replaced phlogopite to a small extent (Pl. 2, fig. 4), although the evidence is not decisive. Specimens studied from the Vulcan deposit suggest that limestone was first replaced by antigorite (Pl. 4, figs. 1, 3), and the antigorite was subsequently replaced by magnetite (Pl. 4, figs. 2, 5). Replacement of limestone by antigorite is shown by thin sections from the Lava Bed deposit (Pl.

4, fig. 4), and replacement of antigorite by magnetite is indicated by polished sections from the Cave Canyon deposit (Pl. 4, fig. 6).

Origin and Classification of the Deposits

The writer believes that the deposits originated as a consequence of intrusion of magmatic material into limestone, which caused, from place to place and in varying degrees, recrystallization of the limestone, development of metamorphic minerals, reconstitution and the formation of skarn rocks, and addition of chemical elements and replacement of limestone and some of the metamorphic minerals. These events and the exact sequence in which they occurred probably differed from one deposit to another and from one part of a deposit to another, and probably took place throughout a considerable range of temperature. Iron was added in large amounts and formed abundant magnetite, some specularite and other hematite, and some goethite. Iron probably was added also during the formation of hedenbergite, andradite, ludwigite, ilvaite, and epidote. Fluorine was added during the formation of chondrodite, humite, and clinohumite, and boron during the formation of ludwigite. Magnesium may also have been added during the formation of minerals of the humite group and antigorite. Some recrystallized limestone was replaced by magnetite and by antigorite; some antigorite was replaced by magnetite; some pyroxene, minerals of the humite group, and spinel were replaced by magnetite.

The deposits described are of the type classified as pyrometasomatic (Lindgren, 1922, p. 293), contact metasomatic (Barrell, 1907, p. 117; Bateman, 1950, p. 83–84), or contact metamorphic in much of the older literature. The writer prefers the term contact metasomatic because it clearly indicates that material has been added near the contact of an intrusive mass and avoids a possible confusion regarding temperature of deposition, since *pyrometamorphism* indicates extreme temperature of metamorphism (Turner and Verhoogen, 1960, p. 452). Thus the use of the prefix *pyro* might be misleading. The mineralogy of these California deposits indicates that the temperature probably varied considerably during the entire period of metamorphism and ore deposition and included temperatures generally ascribed to hypothermal and mesothermal deposits.

The complexities and peculiarities of replacement deposits in limestone surrounding intrusive bodies have long been recognized. Lindgren (1905, p. 163, 164), discussing certain deposits in Arizona, stressed the importance of large additions of material and the variations likely to be encountered from one deposit to another. He also noted the formation of the typical metamorphic minerals, tremolite and diposide, along fissure veins in limestone and concluded that the metamorphic and the vein deposits were closely related (Lindgren, 1905, p. 176). Lindgren, Graton, and Gordon (1910, p. 56) noted the transitional nature of contact-metamorphic and vein deposition in some deposits of New Mexico and, in order to emphasize the addition of material associated with contact-metamorphic deposits, Lindgren (1922, p. 293) proposed that they be designated pyrometasomatic. Loughlin and Behre (1933, p. 47, 48) noted the similarities between hypothermal and pyrometasomatic deposits, which they discussed together instead of separately, and suggested (p. 49) that if certain solutions that formed vein deposits in slate, quartzite, and other siliceous rocks had traversed limestone, they would have formed contact-metasomatic deposits. Graton (1933, p. 184) suggested that contact-metamorphic deposits should be considered as a well-individualized division of the hypothermal group, from which they differ chiefly because of the nature of the wall rock, and Knopf (1933, p. 538) noted that the distinguishing feature of pyrometasomatic deposits is their association with contact-metamorphic silicates developed in limestone. The California deposits discussed by the writer illustrate well some of the variations of contact-metasomatic deposits and their probable relationship to hypothermal and even to mesothermal deposits.

REFERENCES CITED

Allen, V. T., and Fahey, J. H., 1957, Some pyroxenes associated with pyrometasomatic zinc deposits in Mexico and New Mexico: Geol. Soc. America Bull., v. 68, p. 881–895

Barrell, Joseph, 1907, Geology of the Marysville mining district, Montana: U. S. Geol. Survey Prof. Paper 57, 178 p.

Bateman, Alan M., 1950, Economic mineral deposits: 2d ed., New York, John Wiley and Sons, 916 p.

Emmons, W. H., and Calkins, F. C., 1913, Geology and ore deposits of the Philipsburg quadrangle, Montana: U. S. Geol. Survey Prof. Paper 78, 271 p.

Geijer, Per, 1925, Processes in contact metasomatism: Econ. Geology, v. 20, p. 687–690

— 1927, Some mineral associations from the Norberg district: Sveriges geol. undersökning, ser. C, no. 343, 32 p.

— 1939, The paragenesis of ludwigite in Swedish iron ores: Geol. Fören. i Stockholm Förh., band 61, no. 416, p. 19–33

Graton, L. C., 1933, The hydrothermal depth-zones, p. 181–197 *in* Ore deposits of the western states (Lindgren volume): Am. Inst. Min. Metall. Engineers, 797 p.

Hadley, J. B., 1948, Iron-ore deposits in the eastern part of the Eagle Mountains, Riverside County, California: Calif. Div. Mines Bull. 129, p. 1–24

Harder, E. C., 1912, Iron-ore deposits of the Eagle Mountains, California: U. S. Geol. Survey Bull. 503, 81 p.

Knopf, A., 1933, Pyrometasomatic deposits, p. 537–557 *in* Ore deposits of the western states (Lindgren volume): Am. Inst. Min. Metall. Engineers, 797 p.

Koeberlin, F. R., 1909, The Brewster iron-bearing district of New York: Econ. Geology, v. 4, p. 713–754

Lamey, C. A., 1948, Iron Mountain iron-ore deposits, Lava Bed district, San Bernardino County, California; Iron Mountain and Iron King iron-ore deposits, Silver Lake district, San Bernardino County, California; Cave Canyon iron-ore deposits, San Bernardino County, California; Vulcan iron-ore deposit, San Bernardino County, California; Iron Hat (Ironclad) iron-ore deposits, San Bernardino County, California; Shasta and California iron-ore deposits, Shasta County, California: Calif. Div. Mines Bull. 129, p. 25–38; 39–58; 68–83; 84–109; 137–164

Lindgren, W., 1905, The copper deposits of the Clifton-Morenci district, Arizona: U. S. Geol. Survey Prof. Paper 43, 364 p.

— 1922, A suggestion for the terminology of certain mineral deposits: Econ. Geology, v. 17, p. 292–294

Lindgren, W., Graton, L. C., and Gordon, C. H., 1910, The ore deposits of New Mexico: U. S. Geol. Survey Prof. Paper 68, 361 p.

Loughlin, G. F., and Behre, C. H., Jr., 1933, Classification of ore deposits, p. 17–55 *in* Ore deposits of the western states (Lindgren volume): Am. Inst. Min. Metall. Engineers, 797 p.

Loughlin, G. F., and Koschmann, A. H., 1942, Geology and ore deposits of the Magdalena mining district, New Mexico: U. S. Geol. Survey Prof. Paper 200, 168 p.

Prescott, B., 1908, The occurrence and genesis of the magnetite ores of Shasta County, California: Econ. Geology, v. 3, p. 465–480

Schmitt, H., 1939, The Pewabic mine: Geol. Soc. America Bull., v. 50, p. 777–818

Skinner, Brian J., 1956, Physical properties of the end-members of the garnet group: Am. Mineralogist, v. 41, p. 428–436

Terrones, A. J., 1958, Structural control of contact metasomatic deposits in the Peruvian Cordillera: Mining Engineer, v. 10, p. 366–372

Turner, Francis J., and Verhoogen, John, 1960, Igneous and metamorphic petrology: 2d ed., New York McGraw-Hill Book Co., 694 p.

Winchell, A. N., and Winchell, H., 1951, Elements of optical mineralogy, Part 2, Descriptions of minerals: 4th ed., New York, John Wiley and Sons, 551 p.

Manuscript Received by the Secretary of the Society, November 10, 1959
Publication Authorized by the Director, U. S. Geological Survey

C. EMILIANI *University of Miami, Coral Gables, Fla.*
T. MAYEDA *University of Chicago, Chicago, Ill.*
R. SELLI *University of Bologna, Bologna, Italy*

Paleotemperature Analysis of the Plio-Pleistocene Section at Le Castella, Calabria, Southern Italy

Abstract: The Plio-Pleistocene boundary has been located at the place where certain northern species of marine invertebrates first appear in the continuous Plio-Pleistocene sections of Italy. The section at Le Castella, near Crotone, southern Italy, consists of clays with diatomaceous layers and a few thin sand layers. The Plio-Pleistocene boundary there is clearly marked by the appearance of *Anomalina baltica* and other northern species of Foraminifera. Calabrian (lower Pleistocene) sediments 210 m thick overlie the boundary, and upper Pliocene sediments 1405 m thick underlie it. The fossil fauna of the Plio-Pleistocene section consists essentially of abundant pelagic and benthonic Foraminifera, and diatoms. The benthonic microfauna indicates a depositional depth of about 500 m. There is no evidence of turbidity currents and submarine slumping.

A section 167.80 m thick, including the paleontologically defined Plio-Pleistocene boundary, was logged and sampled at close stratigraphic intervals. Oxygen isotopic analyses of different species of pelagic and benthonic Foraminifera and of shell fragments of benthonic mollusks at successively higher stratigraphic positions in the section have revealed numerous temperature oscillations. Surface temperatures, probably representing summer averages, as indicated by *Globigerinoides rubra* and *G. sacculifera*, ranged from 21°C. to more than 30°C. in the late Pliocene, from 16°C. to more than 30°C. in the late Pliocene-early Pleistocene, and from 12°C. to 28°C. in the late Pleistocene. Temperatures at some depth and/or at a season other than the summer, as indicated by *Globigerina bulloides* and *G. inflata*, ranged from 20°C. to 28°C. in the late Pliocene, from 11°C. to 22°C. in the late Pliocene-early Pleistocene, and from 9°C. to 18°C. in the late Pleistocene. Temperatures given by benthonic Foraminifera ranged from 14°C. to 20°C. in the late Pliocene and from 11°C. to 22°C. in the late Pliocene-early Pleistocene (no data available for the late Pleistocene). Temperatures above 30°C. may be due, in part, to isotopic effects of the sea water. The above figures clearly indicate a major shift of the temperature ranges toward lower values from the late Pliocene to the late Pleistocene.

No major temperature change seems to have occurred across the paleontologically defined Plio-Pleistocene boundary. Since the secular temperature minima of the late Pliocene are somewhat lower than present average summer temperature, an areal extension of the ice somewhat greater than that at present is suggested. Such extension probably increased at the times corresponding to the even lower temperature minima of the early Pleistocene. Major continental glaciations, however, may not have started until later, because none of the temperature minima in the section at Le Castella appear to have reached values as low as those obtaining during the glacial ages in the eastern Mediterranean.

The temperature changes in the section at Le Castella are paralleled by important changes in the microfauna.

CONTENTS

Introduction 680
Acknowledgments 680
Geology of the Crotone region 681
Section at Le Castella 682
Isotopic analyses 684
References cited 688

Figure

1. Geographic location of the section at Le Castella, Calabria, southern Italy 680
2. Section at Le Castella, Calabria, southern Italy, showing stratigraphy, isotopic temperatures, and variations of the relative abundances of *Globigerinoides rubra rubra* and *G. rubra gomitulus* 683

Table

1. Oxygen isotopic data 685
2. Secular temperature ranges in the Mediterranean 686

Geological Society of America Bulletin, v. 72, p. 679–688, 2 figs., May 1961

INTRODUCTION

Most writers agree that the beginning of the Pleistocene epoch corresponds to the base of the Calabrian stage (Blanc, Tongiorgi, and Trevisan, 1954; di Napoli Alliata, 1954; Gignoux, 1954; Migliorini, 1950; Ruggieri, 1954; Ruggieri and Selli, 1949; 1950; Selli, 1949; 1954), and that the Calabrian age began when

Figure 1. Geographic location of the section at Le Castella, Calabria, southern Italy

certain species of northern marine invertebrates first appeared in the continuous Plio-Pleistocene sections of Italy (International Geological Congress, 1950).

This paper presents and discusses the results of paleotemperature analysis of pelagic and benthonic Foraminifera and benthonic mullusks from the Plio-Pleistocene section at Le Castella, Crotone, southern Italy. From a stratigraphic point of view, it would have been more desirable to study the section at Santa Maria di Catanzaro, 40 km northwest of Le Castella, which is one of the type sections upon which Gignoux (1913) created the Calabrian stage. Unfortunately, the section at Santa Maria di Catanzaro is stratigraphically rather short and tectonically disturbed. Moreover, its sands and sandstones with *Cyprina islandica* (one of the Pleistocene index species for the Mediterranean) were deposited by turbidity currents and contain a mixture of shallow- and deep-water species. The section at Le Castella, on the other hand, is stratigraphically longer, is tectonically undisturbed, and has a rather uniform lithology (marly clay, in places enriched with tripoli and containing very few, thin layers of sand), which suggests essentially quiet, continuous sedimentation. The two sections can be correlated closely by means of the benthonic microfauna.

ACKNOWLEDGMENTS

The National Science Foundation (grants NSF G-1103, G-4536, G-5973, and G-10213) supported financially the paleotemperature work. The Geological Society of America (grants 771-57, 771-57-S58, and 771-57-S59) and the Shell Development Company supported financially the micropaleontological preparations for isotopic analysis. The Consiglio Nazionale delle Ricerche of Italy supported the

field work, and the Department of Geology of the University of Bologna supported taxonomic studies.

GEOLOGY OF THE CROTONE REGION

The section at Le Castella is located on the Ionian shore of Calabria (Fig. 1), on the eastern side of the sedimentary basin of Crotone. This basin is a zeugogeosyncline, bounded on the west by the granitic and metamorphic massif of La Sila, on the north by a large, chaotic mass of "Argille Scagliose" of early Messinian (late Miocene) age and other Miocene formations, and on the south and partly on the east by buried hills of Pliocene age. It has a north-south axis. It subsided extensively from Helvetian (middle Miocene) to middle Pleistocene time.

Sedimentation by turbidity currents and submarine slumpings, facilitated by the steep sides of the basin, was common in the western and northern portion of the basin. Thickenings up to several hundred meters in the area of deposition and elisions of up to 1000 m in the scar areas were produced. A series of buried hills trending north to south interrupted the slope of the basin and kept its central portion free of turbidity-current and slump deposits. Sedimentation in the central portion, where the section of Le Castella is located, was thus relatively quiet and perhaps rather uniform, even though the total thickness of the sediments is very great because of continued subsidence.

The geological history of the central portion of the Crotone basin may be summarized as follows. During the Helvetian a great transgression took place upon a granitic and metamorphic basement of Hercynian age. Continuous marine sedimentation followed from the Helvetian to the early Pleistocene. The area then emerged with numerous interruptions of the uplift movement, as evidenced by marine terraces. The total thickness of the Plio-Pleistocene section, consisting of blue and gray marly clays, is 1615 m. Macrofossils (mollusks, brachiopods, corals) are rare. Microfossils (Foraminifera and diatoms) are very abundant and perfectly preserved.

Detailed field and laboratory work has led to the identification of several geological formations. Material for isotopic analysis was obtained from the two youngest formations, the Tripolaceous and Papanice formations.

TRIPOLACEOUS FORMATION (UPPER PLIOCENE): Blue and gray marly clays with numerous diatomaceous layers 30 cm to a few meters thick. Total thickness of the formation, 255 m. The base of the formation is marked by a thin (2-cm) layer of volcanic ash extending laterally for a few dozens of kilometers. Characteristic Foraminifera: *Anomalina ornata* (Costa), *Globorotalia truncatulinoides* (d'Orb.), and common Lagenidae.

PAPANICE FORMATION (CALABRIAN): Blue and gray marly clays with a few, thin layers enriched with tripoli near the base; scattered, very thin layers of ochreous clay; and a thin layer of sand at the base. Maximum outcropping thickness, 210 m. Characteristic Foraminifera: *Anomalina baltica* (Schröter), *Discorbis mamilla* (Will.), *Discospirina tenuissima* (Carp.), *Eponides frigida* (Cush.), and *Nonionella turgida* (Will.). These species clearly indicate low temperatures. Other species, however, which are present in the same *general* assemblage, indicate warm temperatures. These are: *Articulina tubulosa* (Seg.), *Vaginulinopsis limbata* (Flint), and *V. subaculeata* (Cush.). The presence of both cold and warm species in the same *general* fauna, also evident in other formations of similar age in many parts of Italy and Sicily (*cf.* Emiliani, Gianotti, and Mayeda, 1961), is probably common to many marine Pleistocene deposits throughout the world. The significance of these occurrences will be discussed later.

The sedimentary environment of both the Tripolaceous and the Papanice formations was an open sea. The depth of this sea may be estimated at about 500 m on the basis of the occurrence, throughout both formations, of the following species: *Sigmoilina sigmoidea*, *S. schlumbergeri*, *Nummoloculina irregularis*, *Cornuspira involvens*, *C. foliacea*, *Cristellaria peregrina*, *Lingulina seminuda*, and *Anomalina semipunctata*.

The diatom-rich laminae of the Tripolaceous formation are less than 1 mm to a few millimeters thick and contain abundant pelagic Foraminifera (*Globigerina*, *Globigerinoides*, *Globorotalia*, *Orbulina*) but no benthonic species. Intervening thin veils of volcanic ash, the product of very numerous volcanic explosions in the neighboring areas (La Sila or Ionian Sea), are common. The close association between volcanic ash and diatomaceous layers indicates that the repeated ash falls created conditions favorable to diatom blooms, perhaps by supplying excess SiO_2 (*cf.* Sverdrup,

Johnson, and Fleming, 1942, p. 769) and other suitable elements or compounds. Both ash and tripoli occur only in the southern portion of the Crotone basin, probably because of the local pattern of atmospheric and marine circulation. The great abundance of pelagic Foraminifera in the diatomaceous layers probably resulted from the abundant food supplied by the diatoms. The concurrent absence of benthonic species may have been caused by a temporary excess of decomposing organic material on the bottom. The small gypsum crystals present in some layers are probably epigenetic, formed by the oxidation of iron sulfides, as evidenced by the ochreous bands in the diatomaceous layers.

SECTION AT LE CASTELLA

For the present work, 167.80 m of the section at Le Castella has been accurately logged and sampled (Fig. 2). Isotopic analysis has been limited to a Pliocene section 24.5 m thick and a Plio-Pleistocene section 55.5 m thick. The latter includes the paleontologically defined Plio-Pleistocene boundary. The stratigraphic interval between the two sections is 87.8 m. A total of 22 Pliocene and 25 Pleistocene samples have been analyzed isotopically.

The Pliocene microfauna consists of abundant pelagic and benthonic Foraminifera. Species restricted to the Pliocene are: *Cribrorobulina clericii* (Forn.), *Dentalina tenuis* (Neug.), *Hopkinsina bononiensis* (Forn.), *Cancris auriculus* (Ficht. and Moll.), and *Eponides umbonata stellata* (Silv.). Species more abundant in the Pliocene section than in the Pleistocene section are: *Angulogerina fornasinii* Selli, *Anomalina ornata* (Costa), *Cassidulina bradyi* (Norman), *Globigerinoides rubra gomitulus* (Seg.)[1], and *Globigerinoides sacculifera* (Brady). The total number of species is about 70.

The Pleistocene microfauna consists of very abundant pelagic and abundant benthonic Foraminifera. Species restricted to the Pleistocene section are: *Pyrgo serrata* (Brady), *Lingulina seminuda* (Hantken), *Anomalina baltica* (Schr.), and *A. coronata* (Parker and Jones). Species more abundant in the Pleistocene section than in the Pliocene section are: *Cornuspira carinata* Costa, *Sigmoilina schlumbergeri* Silv., *Cassidulina laevigata* d'Orb., *Angulogerina angulosa* (Will.), and various species of *Bulimina*. Total number of species: about 120. The Pleistocene microfauna is richer than the Pliocene microfauna both in number of species and in number of specimens. The Pleistocene species mentioned above are all extant, preferring cold water or rather deep water in temperate seas. Thus, for instance, *Anomalina baltica* is most abundant in the cold waters of the North Atlantic; *Lingulina seminuda* lives in deep waters with temperatures between 4°C. and 8°C.; *Anomalina coronata* is found almost exclusively in cold seas with temperature between 4°C. and 6°C.; *Sigmoilina schlumbergeri* is abundant in the North Atlantic and, although present also at low latitudes, it prefers waters with temperature between 2°C. and 8°C. In addition to these and other cold-water species, a number of warm-water species are present, as mentioned.

The Plio-Pleistocene boundary is located between samples 50 and 51 (Fig. 2), within a stratigraphic thickness of 1.30 m. Throughout the Ionian Calabria, where one of us (Selli) has studied several thousand samples of Plio-Pleistocene sediments, *Anomalina baltica* and the other cold-water species invariably appear abruptly and all together, so that the Plio-Pleistocene boundary is clearly recognizable. Furthermore, the whole lower Pleistocene is characterized by the frequent occurrence of *Anomalina baltica* and by the scattered occurrence of the other cold-water species mentioned above.

As far as the definition of the Plio-Pleistocene boundary is concerned, the appearance of *Anomalina baltica* has the same value as the appearance of the classic cold-water species of mollusks. Thus, in the section at Santa Maria di Catanzaro, which can be considered the type section for the Plio-Pleistocene boundary, *Anomalina baltica* is invariably absent below the sands with the molluskan index species *Cyprina islandica*, whereas it is invariably present in the overlying clays. A strict association between the two species, however, is exceptional, because of the different habitats. *Cyprina islandica* prefers shallow water and a sandy bottom, whereas *Anomalina baltica* prefers deep water and a muddy bottom.

It is important to observe that, in the section at Le Castella, the microfauna varies remarkably from sample to sample. Thus, for instance, specimens of *Anomalina baltica*,

[1] *Globigerinoides gomitulus* (Seg.) is synonymous with *G. cyclostoma* (Gall. and Wiss.), and we believe it to be a subspecies of *Globigerinoides rubra* (d'Orb.). We prefer the name *gomitulus* because of precedence. Although Seguenza (1880) did not describe his holotype very accurately, Fornasini later (1898; 1899) gave an accurate description.

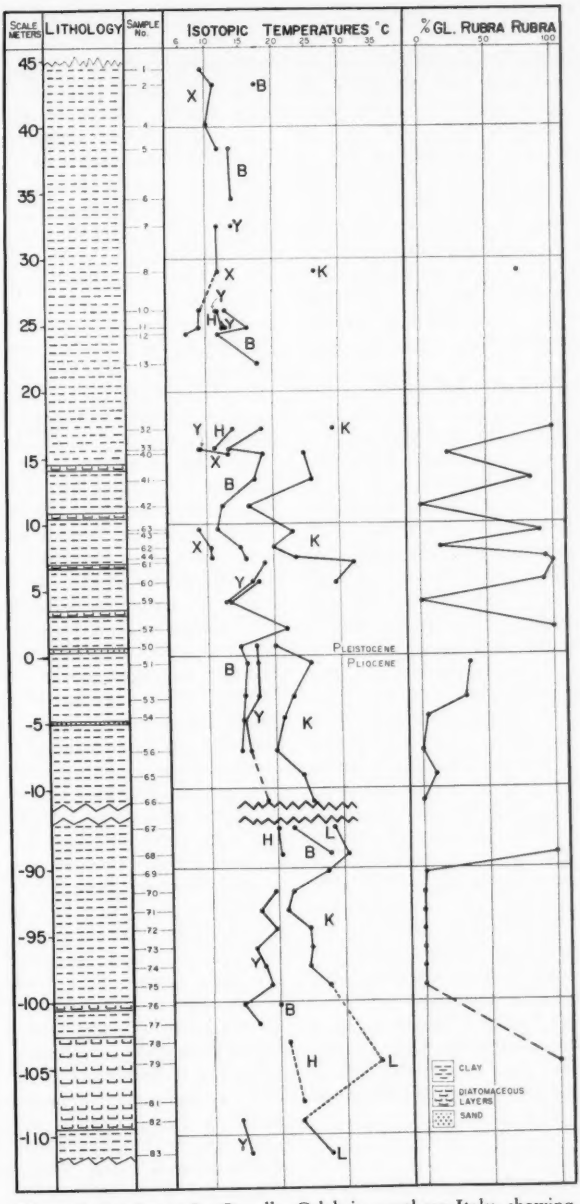

Figure 2. Section at Le Castella, Calabria, southern Italy, showing stratigraphy, isotopic temperatures, and variations of the relative abundances of *Globigerinoides rubra rubra* and *Globigerinoides rubra gomitulus*. B, *Globigerina bulloides;* H, *Globigerina inflata;* K, *Globigerinoides rubra;* L, *Globigerinoides sacculifera;* X, mixed fragments of calcareous benthonic mollusks; Y, mixed species of calcareous benthonic Foraminifera

Angulogerina angulosa, and *Cassidulina laevigata* are very abundant and well developed in sample 42, whereas they are rare and commonly dwarfed in the adjacent samples 41 and 63 (Fig. 2). Stratigraphic intervals of 2.0 m separate sample 42 from sample 41 above and sample 63 below. Marked variations in the relative abundances of *Globigerinoides rubra rubra* and *G. rubra gomitulus* can also be observed. One may conclude, on micropaleontological evidence alone, that environmental conditions (especially temperature, we believe) underwent numerous, important variations.

A 30-cm sand layer with microfossils occurs between samples 50 and 51, *i.e.* at the Plio-Pleistocene boundary. This layer is analogous to the sands with *Cyprina islandica* in the section at Santa Maria di Catanzaro, and occurs, with great variability in thickness, throughout the Ionian Calabria in a similar stratigraphic position (*cf.* Gignoux, 1913). The sand layer in question, which in most places shows evidence of deposition by turbidity current, may have resulted ultimately from a phase of uplift of the crystalline and metamorphic massif of Calabria (La Sila, Serre, Aspromonte) or from a tectonic or even eustatic lowering of sea level.

The section at Le Castella presents several advantages for detailed paleontological and isotopic study of the Plio-Pleistocene boundary. The boundary itself can be identified with great precision. Sedimentation has been continuous and seemingly rather uniform. The lithofacies is almost perfectly uniform. The section was deposited in an open, fairly deep environment. The microfauna is abundant and includes pelagic Foraminifera belonging to the same species used for the isotopic analysis of the Mediterranean deep-sea core 189 (Emiliani, 1955b). The sediments were tectonically undisturbed, except for the final uplift sometime during the middle or late Pleistocene. The main outcrop, a 30-m high falesia, is easily accessible and can be sampled easily and accurately.

ISOTOPIC ANALYSES

All samples collected from the section at Le Castella were washed with cold water (warm or boiling water was not used because of the possibility of isotopic exchange between such water and the calcium carbonate of the shell material). Wherever possible, 500–700 specimens of each of the pelagic foraminiferal species *Globigerinoides rubra* and *Globigerina bulloides*, and in some cases also *Globigerinoides sacculifera* and *Globigerina inflata*, were separated from each sample. Samples of *Globigerinoides rubra* included both subspecies *rubra* and *gomitulus* in varying proportions. It was not considered necessary to treat these subspecies separately because in other analyses they had given either the same temperature or temperatures only 1°–3°C. different, with *G. rubra rubra* giving the higher temperatures[2] (Emiliani, 1955b, Table 2).

The isotopic analyses were carried out according to the procedure previously described (Epstein *et al.*, 1953; Emiliani, 1955a), and a correction of +1.23 per mil for the isotopic composition of the sea water was applied to all isotopic results (*cf.* Emiliani, 1955a, p. 540–544). This correction is the same as that applied to the isotopic results from the Mediterranean deep-sea core 189 (Emiliani, 1955b). Table 1 gives the isotopic data and Figure 2 graphically shows the temperatures.

Globigerina bulloides and *G. inflata* invariably gave temperatures lower than those given by *Globigerinoides rubra* and *G. sacculifera*, a result of deeper habitats and/or growth during some or much of the colder season (*cf.* Emiliani, 1954; 1958). The temperatures given by *Globigerinoides rubra* and *G. sacculifera* should approximate summer means because these two species seem to prefer warmer waters (*cf.* Phleger, Parker, and Peirson, 1953). *Globigerinoides rubra* and *Globigerina bulloides* were not sufficiently abundant for isotopic analysis in some samples: each isotopic analysis requires several hundred specimens. Continuous temperature curves, therefore, could not be determined, but the temperature curves of the two species (Fig. 2) are roughly parallel and complement each other occasionally.

The uncertainty introduced by the unknown isotopic composition of the Ionian Sea water during deposition of the section at Le Castella is probably not greater than that generally obtaining for the open waters of the Atlantic or the Caribbean because of the rapid exchange of the Mediterranean water across the Strait of Gibraltar (Sverdrup, Johnson, and Fleming, 1942, p. 647). At present, the surface salinity of the Mediterranean water increases from 36.25 per mil at the Strait of Gibraltar to

[2] *Globigerinoides rubra rubra* is called "tapering type" and *G. rubra gomitulus* is called "rounded type" by Emiliani (1955b).

more than 39 per mil in the eastern Mediterranean. The O^{18}/O^{16} ratio in the sea water shows a similar trend, increasing from +0.8 per mil at the Strait of Gibraltar and in the western Mediterranean to +1.0 per mil in the Tyrrhenian Sea and to +1.2 per mil in the eastern Mediterranean (unpublished data and data from Epstein and Mayeda, 1953). Similar values may have obtained during much of the Plio-Pleistocene time. However, the amount of continental ice is known to have changed markedly during the Pleistocene, and some changes may have occurred also when the section at Le Castella was being deposited. An increase of continental ice, by preferentially removing isotopically lighter water (*cf.* Epstein and Mayeda, 1953; Emiliani, 1955a), would tend to increase the O^{18} concentration in sea water. A decrease of continental ice, on the other hand, would tend to reduce the

TABLE 1. OXYGEN ISOTOPIC DATA

All figures are expressed as δ per mil with respect to Chicago standard PDB-1.

Sample no.	*Globigerinoides rubra*	*G. sacculifera*	*Globigerina bulloides*	*G. inflata*	*Benthonic Foraminifera*	*Benthonic mollusks*
1	..	..	..	..	..	+3.01
2	..	..	+1.01	..	..	+2.49
4	..	..	..	..	..	+2.79
5	..	..	+1.93	..	..	+2.32
6	..	..	+1.84	..	..	..
7	..	..	..	..	+1.84	+2.40
8	−0.87	..	..	..	..	+2.35
10	..	..	+2.12	+2.40	+2.43	+3.07
11	..	..	+1.31	+2.23	+2.01	+3.13
12	..	..	+2.37	..	..	+3.66
13	..	..	+0.96	+2.09	..	..
32	−1.40	..	+0.86	+1.81	..	..
33	..	..	+2.04	+2.53	+2.82	+3.21
40	−0.53	..	+0.83	..	..	+1.95
41	−0.75	..	+1.13	..	..	..
42	+1.32	..	+2.28	..	..	..
43	−0.19	..	..	..	..	..
44	−0.23	..	+1.44	..	..	+2.63
50	+0.44	..	+1.67	..	+1.09	..
51	−0.69	..	+1.42	..	+1.03	..
53	−0.13	..	+1.55	..	+1.02	..
54	+0.18	..	+1.57	..	+1.54	..
56	+0.43	..	+1.65	..	+1.33	..
57	..	..	..	+0.01	..	..
59	..	..	+1.84	..	+2.09	..
60	−1.47	..	+0.98	..	+1.18	+2.22
61	−2.01	..	..	..	+0.73	..
62	+0.45	..	+1.64	..	..	+2.70
63	..	..	+2.44	..	..	+3.20
65	−0.43	..	..	..	..	..
66	−0.72	−0.88	..	..	+0.78	..
67	..	−1.36	−0.09	+0.39	..	..
68	−1.76	..	−1.24	+0.33	..	..
69	−1.15	..	..	..	..	..
70	−0.02	..	..	..	+0.56	..
71	+0.13	..	..	..	+1.06	..
72	−0.62	..	..	..	+0.50	..
73	−0.64	..	..	..	+1.23	..
74	−0.58	..	..	..	+0.93	..
75	−1.15	..	..	..	+0.70	..
76	..	..	+0.42	..	+1.69	..
77	..	..	..	..	+1.17	..
78	..	..	..	+0.12	..	..
79	..	−2.61	..	..	..	..
81	..	..	..	−0.28	..	..
82	−0.27	..	..	..	+1.79	..
83	..	−1.17	..	..	+1.50	..

latitudinal temperature gradient, decreasing evaporation and, therefore, also the O^{18} concentration in sea water. Areas with greater evaporation rates, such as the Mediterranean, would be especially affected. These isotopic effects, amounting perhaps to 0.5 per mil, would lower by about 2°C. both maxima and minima of the paleotemperature curves (Fig. 2; Emiliani, 1955b, Fig. 1). The analytical error of the isotopic temperatures is ±0.5°C.

The temperature curves of Figure 2 show various oscillations between maxima and minima. Higher maxima and lower minima may have been missed by sampling. Three of the temperature maxima of Figure 2 and one in core 189 (Emiliani, 1955b) exceed 30°C. and give temperatures believed impossible for open-sea waters. These high values may have resulted in part from the evaporation-controlled isotopic effect mentioned above, and the true temperatures may have been a few degrees centigrade lower. The paleotemperature curve of core 189 (Emiliani, 1955b, Fig. 1) shows that the conditions responsible for the excessively high values of the isotopic temperatures were established only exceptionally and persisted for only a short time (perhaps a few thousand years). Epstein and Mayeda (1953) demonstrated the existence of a direct relationship between salinity and O^{18} concentration in open-sea water. From their data it can be seen that a decrease of 0.5 per mil in O^{18} concentration would be accompanied by a salinity decrease of 1–1.5 per mil. Such a salinity decrease in the surface water of the Mediterranean would reduce and even reverse the water exchange across the Strait of Gibraltar and would perhaps cause temporary stagnation of the bottom water. In effect, the highest temperature maximum of core 189 (at 340 cm below the top) corresponds to the layer with the greatest amount of organic carbon and the highest salinity in the interstitial water (Kullenberg, 1952). As Kullenberg (1952) remarks, these conditions suggest stagnation of the bottom water and decreased salinity of the surface water.

The average summer temperature of the surface water off Crotone is 25°C. today, and the winter average about 14°C. The average summer temperature of the surface water, as indicated by *Globigerinoides rubra* and *G. sacculifera*, oscillated from 21°C. to more than 30°C. during the late Pliocene (Fig. 2, section between samples 83 and 67) and from 16°C. to more than 30°C. during the late Pliocene-early Pleistocene (Fig. 2, section between samples 66 and 1). The corresponding temperature ranges of the deeper water and/or colder season, as indicated by *Globigerina bulloides* and *G. inflata*, are 20°C. to 28°C. and 11°C. to 22°C. Isotopic analysis of mixed calcareous benthonic Foraminifera belonging to a variety of species gave temperatures ranging from 14°C. to 20°C. in the lower portion of the section (samples 83 to 67), and from 11°C. to 19°C. in the upper portion (samples 66 to 1). Finally, isotopic analysis of fragments of benthonic mollusks, present only in the upper portion of the section, gave temperatures ranging from 7°C. to 13°C. By comparison, the glacial-interglacial temperature range of the surface water, as indicated by isotopic analyses of *Globigerinoides rubra* from core 189, was generally from 12°C. to 28°C., although values as low as 8°C. (uncorrected) occurred during the Main Würm and values higher than 30°C. occurred for a short time during the last interglacial. The above figures, summarized in Table 2, clearly indicate a major shift of the temperature ranges toward lower values from the late Pliocene to the late Pleistocene.

In a few samples, benthonic Foraminifera gave temperatures up to 4°C. higher than the benthonic mollusks, and in other samples they gave temperatures up to 2°C. higher than the

TABLE 2. SECULAR TEMPERATURE RANGES IN THE MEDITERRANEAN

Numbers are isotopic temperatures in degrees centigrade.

		Globigerinoides rubra and *G. sacculifera*	*Globigerina bulloides* and *G. inflata*	Benthonic Foraminifera	Benthonic mollusks
Core 189		12–28	7–18	..	..
Le Castella	Plio-Pleistocene section	16–>30	11–22	11–19	7–13
	Pliocene section	21–>30	20–28	14–20	..

pelagic foraminifer *Globigerina bulloides* (*See* Fig. 2). These differences could be explained perhaps in terms of different seasonal growth, but the difference between benthonic Foraminifera and mollusks would require a bottom much shallower than the 500 m mentioned previously. It is also possible that the benthonic microfauna consists of a mixture of species of different depth habitats, which were brought to common burial by submarine displacement. In support of this alternative is the fact that separate isotopic analyses of four different species of calcareous benthonic Foraminifera from the lower Pleistocene Ficarazzi Clay of Palermo, Sicily, gave different temperatures, ranging from 14.6°C. to 17.6°C. (Emiliani, Gianotti, and Mayeda, 1960). The temperature given by a mixture of benthonic species of different depth habitats would be higher than the actual temperature at the depth of deposition. Displacement may have occurred by slow and continuous or semicontinuous submarine solifluction rather than by turbidity currents or slumpings, since field evidence for the latter is missing. If so, the temperatures given by the molluscan fragments, the lowest obtained from benthonic material, should approach or coincide with the bottom temperature at the place of deposition.

Of special interest is, of course, the temperature trend in the immediate neighborhood of the Plio-Pleistocene boundary, which is located between samples 51 and 50 (Fig. 2). While surface temperature appears to have decreased by about 5°C. between these two samples, and the temperature given by *Globigerina bulloides* by about 1°C., the first Pleistocene sample (no. 50) shows temperatures similar to those given by samples 56 and 54 which are a few meters below the Plio-Pleistocene boundary. Lower temperatures, however, may have obtained between samples 50 and 51 or 50 and 57 and may have been missed by sampling. The temperature given by *Globigerina bulloides* at sample 57 suggests a high surface temperature, possibly the highest in the Pleistocene section. Sample 57 is only about 1.5 m above the Plio-Pleistocene boundary.

The Pliocene surface temperature minima of the section at Le Castella are only a few degrees centigrade lower than present average summer surface temperature of the Ionian Sea, suggesting absence of major glaciations at that time. The early Pleistocene temperature minima, although several degrees centigrade lower than present temperature, are probably still too high to represent truly glacial conditions, and may reflect only mountain glaciations of various magnitudes preceding the major glaciations.

In the absence of absolute dating, the age of the Plio-Pleistocene boundary, recognized from the temperature decrease in the eastern equatorial Pacific core 58, has been estimated at about 600,000 years (Emiliani, 1955a, p. 562). Some other lower levels in the same core could be also reasonably selected as Plio-Pleistocene boundary, giving an estimated age of 700,000–800,000 years. Correlation of these core levels with the appearance of *Anomalina baltica* in the section at Le Castella is an open question. According to hypothetical correlations by Emiliani (1955a), the age of the first major glaciation (Günz-Nebraskan) would be about 300,000 years. If so, it would seem probable that the Calabrian, Villafranchian, and Sicilian sediments were deposited between 600,000–800,000 and 300,000 years ago (*cf.* Emiliani, Gianotti, and Mayeda, 1961), at a time when recurrent mountain glaciations occurred but large continental ice sheets had not yet developed. In any case, the marine sediments of the lower Pleistocene were certainly not deposited under conditions of uniformly cold temperatures, as many writers have maintained, but rather under oscillating temperatures. The often observed admixture of cold- and warm-water species in the same formation would then not represent a true mixture, but rather an alternation, at close stratigraphic intervals, of colder- and warmer-water faunas. Field sampling, especially of macrofossils, does not seem to have been performed, in general, with sufficient stratigraphic accuracy to permit detection of these alternations.

Changes of the microfauna of the section at Le Castella parallel the changes of the isotopic temperatures. Thus, warm-water species are scarce in the cold levels and are represented, in general, only by dwarfed specimens. In addition, the relative abundances of *Globigerinoides rubra rubra* and *G. rubra gomitulus* vary with temperature as Figure 2 shows.

Since marked temperature changes occur in places even between samples which are only a few decimeters apart (as between samples 61 and 44), a closer sampling of the section at Le Castella would have been advisable. Important temperature maxima and minima may have been missed by the present sampling, and the conclusions presented here are only preliminary.

REFERENCES CITED

Blanc, A. C., Tongiorgi, E., and Trevisan, L., 1954, La limite plio-pléistocène dans la coupe de Monte Mario (environs de Rome): 19th Internat. Geol. Cong., Algiers 1952, Comptes rendus, fasc. 15, p. 218–228

di Napoli Alliata, E., 1954, La limite plio-pléistocène dans la coupe de Castell'Arquato (Plaisance): 19th Internat. Geol. Cong., Algiers 1952, Comptes rendus, fasc. 15, p. 229–234

Emiliani, C., 1954, Depth habitats of some species of pelagic Foraminifera as indicated by oxygen isotope ratios: Am. Jour. Sci., v. 252, p. 149–158

—— 1955a, Pleistocene temperatures: Jour. Geology, v. 63, p. 538–578

—— 1955b, Pleistocene temperature variations in the Mediterranean: Quaternaria, v. 2, p. 87–98

—— 1958, Paleotemperature analysis of core 280 and Pleistocene correlations: Jour. Geology, v. 66, p. 264–275

Emiliani, C., Gianotti, A., and Mayeda, T., 1961, Analisi isotopica dei Foraminiferi siciliani delle Argille di Ficarazzi, Palermo: Quaternaria, v. 5

Epstein, S., and Mayeda, T., 1953, Variation of O^{18} content of waters from natural sources: Geochim. Cosmochim. Acta, v. 4, p. 213–224

Epstein, S., Buchsbaum, R., Lowenstam, H., and Urey, H., 1953, Revised carbonate-water isotopic temperature scale: Geol. Soc. America Bull., v. 64, p. 1315–1325

Fornasini, C., 1898, Decimo contributo alla conoscenza della microfauna terziaria italiana: R. Accad. Sci. Istit. Bologna, Mem. Sci. Nat., ser. 5, v. 7 (1897–1899), p. 205–212

—— 1899, Globigerine adriatiche: R. Accad. Sci. Istit. Bologna, Mem. Sci. Nat., ser. 5, v. 7 (1897–1899), p. 575–586

Gignoux, M., 1913, Les formations marines pliocènes et quaternaires de l'Italie du Sud et de le Sicile: Univ. Lyon, Ann., n.s., I, fasc. 36, 693 p.

—— 1954, Pliocène et quaternaire marins de la Mediterranée occidentale: 19th Internat. Geol. Cong., Algiers 1952, Comptes rendus, fasc. 15, p. 249–258

International Geological Congress, 18th, Great Britain 1948, 1950, Recommendations of commission appointed to advise on the definition of Pliocene-Pleistocene boundary: London, Rept., pt. 9, p. 6

Kullenberg, B., 1952, On the salinity of the water contained in marine sediments: K. Vet. o. Vitterh. Samh. Handl., F. 6, ser. B, v. 6, no. 6, 38 p.

Migliorini, C., 1950, The Pliocene-Pleistocene boundary in Italy: 18th Internat. Geol. Cong., Great Britain 1948, Rept., pt. 9, p. 66–72

Phleger, Fred B, Parker, F. L., and Peirson, J. F., 1953, North Atlantic Foraminifera: Swedish Deep Sea Exped. (1947–1948) Repts., v. 7, fasc. 1, 122 p.

Ruggieri, G., 1954, La limite entre Pliocène et Quaternaire dans la série pliopléistocène du Santerno: 19th Internat. Geol. Cong., Algiers 1952, Comptes rendus, fasc. 15, p. 235–240

Ruggieri, G., and Selli, R., 1949, Il Pliocene e il Postpliocene dell'Emilia: Giornale di Geologia, ser. 3 v. 20, 1948, 14 p.

—— 1950, Il Pliocene e il Postpliocene dell'Emilia: 18th Internat. Geol. Cong., Great Britain 1948, Rept., pt. 9, p. 85–93

Seguenza, G., 1880, Le formazioni terziarie nella provincia di Reggio (Calabria): R. Accad. Lincei, Cl. Sci. Fis. Mat. Nat., Mem., ser. 3, v. 6, p. 3–446, tav. 1–17

Selli, R., 1949, Le conoscenze geologiche sul Quaternario gassifero del Polesine e del Ferrarese settentrionale: IV Convegno Naz. Metano, Padova 1949, Atti, p. 515–535

—— 1954, La limite plio-pléistocène dans les environs d'Ancona (Marche): 19th Internat. Geol. Cong., Algiers 1952, Comptes rendus, fasc. 15, p. 241–247

Sverdrup, H. U., Johnson, M. W., and Fleming, R. H., 1942, The oceans, their physics, chemistry, and general biology: New York, Prentice-Hall, 1087 p.

Manuscript Received by the Secretary of the Society, July 7, 1959
Contribution 303 from the Marine Laboratory, Univ. of Miami, Miami, Fla.

H. BAADSGAARD
R. E. FOLINSBEE
J. LIPSON
Dept. Geology, University of Alberta, Edmonton, Alberta, Canada

Potassium-Argon Dates of Biotites from Cordilleran Granites

Abstract: Biotites from 20 plutons of the Cordillera of North America, principally from British Columbia, have been dated using the potassium-argon method. Samples were selected from well-known intrusive masses in an attempt to compare physically measured dates with relative age established by geological mapping; most dates confirm the geological age interpretations.

The Cordillera underwent granitic intrusion or orogeny at five times separated by long periods of quiescence. The earliest orogeny, of Devonian (Acadian) age, occurred 350–360 million years ago and resulted in intrusion of plutons as widely separated as the Ice River syenite of the Rocky Mountains and the Fitton granite of the northern Yukon.

Early Mesozoic orogeny resulted in the emplacement of the upper Triassic or lower Jurassic Guichon (186 m.y.) and Topley (163 m.y.) batholiths of central British Columbia. The major Cordilleran intrusion occurred 95–100 million years ago, in about the middle of the Cretaceous, with emplacement of the Coast Range batholith and early phases of the Nelson batholith of British Columbia, and the Cassiar and Itsi batholiths of Yukon. In late Cretaceous time, 80 million years ago, the Bayonne pluton, British Columbia, and Boulder batholith and Marysville stock of Montana were emplaced.

During Rocky Mountain orogeny (Eocene), 50–60 million years ago, late phases of the Nelson batholith and a number of plutons such as Coryell were emplaced. Eighteen million years ago, in the Miocene, small granitic bodies intruded the Cascade Range; these are believed to be the youngest exposed batholithic rocks in North America.

CONTENTS

Introduction and acknowledgments 689
Method 690
Cordilleran orogenies 690
Previous investigations 690
Paleozoic orogeny 690
Early Mesozoic orogeny 694
Mid-Cretaceous orogeny 694
Rocky Mountain orogeny 694
Puget orogeny 698
Summary 698
References cited 699

Figure
1. Cordilleran orogenies (after White, 1959) compared with potassium-argon dates of Cordilleran granitic biotites 691
2. Fitton (Yukon) and Ice River (B.C.) Devonian intrusive masses 692
3. Early Mesozoic (186–163 m.y.), mid-Cretaceous (95–101), and early Laramide (77–82) intrusive masses of the Cordillera 693
4. Later Rocky Mountain or Laramide (58–48 m.y.) and Puget or Alpine (36–18 m.y.) intrusive masses in the Cordillera 695

Table
1. K-Ar dates of biotites from Cordilleran granites . 696

INTRODUCTION AND ACKNOWLEDGMENTS

From 1956 to 1959 the writers collected and dated, using the potassium-argon method, biotites from plutons in the western Cordillera, mostly from British Columbia. In general the techniques used are those reported by Evernden, Curtis, and Lipson (1957) in their study of the age of the Sierra Nevada batholith. Large samples (50- to 100-pound blocks) were collected, mostly from recently blasted road cuts. The writers are indebted to Premier Bennett of British Columbia for the accelerated highways program, a service in the interests of geology. The Geological Survey of Canada Map 932-A (1948) of British Columbia was used as a guide to sampling. On geological grounds

Geological Society of America Bulletin, v. 72, p. 689–702, 4 figs., May 1961

the compilers of that map had attempted to assign various batholithic rocks to one of the following age categories: Triassic, Jurassic, post-Lower Cretaceous, Cretaceous, or Tertiary.

J. Rutherford of Northwestern Exploration, Y. Kawase of Pan American Oil, and D. Toms of Dale Mountain Mines contributed samples from remote batholiths such as the Itsi, Fitton, and Cassiar. Prof. W. H. White of the University of British Columbia collected the Guichon batholith sample. The samples of biotite from the jacupirangite phase of the Ice River complex came from the late Dr. J. A. Allan's original Survey collection made in 1910–1912; the writers collected new samples in 1959. Dr. A. Knopf of Stanford University has expressed a continuous interest in the project and provided samples from the Boulder batholith and Marysville stock from his own field collections.

The work at the University of Alberta has been generously supported by grants from the Penrose Bequest of The Geological Society of America, the National Research Council of Canada, the Geological Survey of Canada, and the University of Alberta Research Fund. The grants have made possible the construction of an argon extraction line and mass spectrometer at the University of Alberta. Drs. S. S. Goldich and A. O. Nier of the University of Minnesota assisted greatly when apparatus was being assembled at Alberta, and many of the dates here reported were from runs made on the mass spectrometer at the University of Minnesota. Calibration of the argon-38 spikes, critical in establishing absolute age, has been done in cooperation with the University of Minnesota. Illustrations were drafted by F. Dimitrov. Miss E. Dingman contributed editorial and technical assistance in assembly of the paper. All this is gratefully acknowledged.

METHOD

Ar^{40} in the samples was extracted and purified by a conventional flux-fusion technique. Isotope dilution with mass-spectrometric isotoperatio analysis was used to determine the amount of Ar^{40} in the purified gas (Baadsgaard *et al.*, 1957). J. Lawrence Smith fusion and tetraphenylboron precipitation served to separate quantitatively the potassium in the samples. A. Stelmach, chemist-technician in geochemistry at the University of Alberta, made the potassium determinations. The potassium-40 content of the samples was calculated from the total potassium using the abundance ratio $K^{40}/K = 0.0118_1$ atomic per cent (A.E.C. Nuclear Data Tables, 1959). The constants employed in calculating the ages were: $\lambda e = 0.589 \times 10^{-10}$/yr. and $\lambda\beta = 4.76 \times 10^{-10}$/yr.

CORDILLERAN OROGENIES

Previous Investigations

It is now 5 years since one of the writers first published on the dating of Cordilleran orogenies. With very few data, one date from Canada and a few from the American Cordillera, Beveridge and Folinsbee (1956, p. 24) stated:

". . . it might be said that the geochronological data suggest a main period of Cordilleran batholithic emplacement in mid-Cretaceous time, 100 million years ago, and a late phase of magmatic intrusion in early Laramide time, 70 million years ago. . . ."

Although a lot of argon has flowed through the mass spectrometers since then, the statement stands.

It is now more abundantly clear that field geologists, particularly of the geological surveys of Canada and the United States, have worked out the relative stratigraphic position of the Cordilleran granites remarkably accurately (Armstrong, 1946; Cairnes, 1934, p. 73–74; Dolmage, 1928, p. 85; Knopf, 1950; 1957).

The data are related to the tectonic history of the northern Cordillera set forth by Smith and Stevenson (1955) and especially by White (1959) in his brilliant review paper.

The potassium-argon dates in Table 1 support White's main thesis that the orogenic history of the Cordillera has been longer and more complex than was previously recognized.

White, from field evidence in British Columbia, suggests six major orogenic events in the Cordilleran tectonic history (Fig. 1), commencing with the Proterozoic east Kootenay orogeny. Burwash (1959) and Hunt (1960) are studying the Precambrian orogenic history.

Paleozoic Orogeny

Until 1952, the Paleozoic had not been considered as a period of true orogeny in the Cordillera. The Paleozoic events had been so masked by the major Mesozoic intrusions or confused with Precambrian events as to have almost escaped detection. In 1952, Armstrong suggested that the Wolverine complex represents post-Cambrian, pre-Permian intrusion. The writers have evidence that at least two areas of Paleozoic intrusive rocks exist in the Cordillera.

One is the Ice River complex south of Field, B. C. Allan (1914, p. 191–193) says,

"... the age of the intrusion ... cannot be definitely fixed. It *cuts the lower Ordovician beds*[1] of the Goodsir formation which is the highest member of the sedimentary series represented in the Ottertail Range in which the igneous body occurs. ...

"... For lack of better evidence the Ice River intrusion may be regarded as post-Cretaceous in age and *earlier than the Laramide revolution*[1]. ..."

Gussow and Hunt (1959) have reinterpreted the field relationships and suggested a Precambrian age for the Ice River syenite.

Biotites from a jacupirangite phase and a minette dike cutting Ottertail limestone in this alkalic intrusive mass return potassium-argon dates of 355 and 360 million years, magic numbers turned out on mass spectrometers for biotites from all over the Laurasian or northern continents. Many batholiths and pegmatites of the Maritime provinces of Canada and the New England and southern Appalachian states of the United States, and intrusive masses in the Caledonian Mountains of Europe, the Urals of Russia, and the Variscan or Hercynian ranges of southern England, France, and northern Germany yield 350-million-year-old biotites (Faul and Tilton, 1957; Ovchinnikov, 1958; Faul, 1959; Hurley *et al.*, 1958; 1959; Mayne *et al.*, 1959; Damon and Kulp, 1957; Tilton *et al.*, 1958). The writers place less reliance on a date of 304 m.y. obtained for a very coarse, possibly slightly altered biotite from a pegmatitic phase of the Ice River intrusive mass.

The second Cordilleran Paleozoic granite dated is the Fitton batholith of the Yukon, one of several plutons in Paleozoic rocks of the Barn Mountains. Biotite from this granite returns 353 m.y. The granite lies more than 1500 miles from the Ice River intrusive mass but in a similar geologic environment (Fig. 2).

At present a controversy, almost a cold war, is raging over the position that these 325–375-

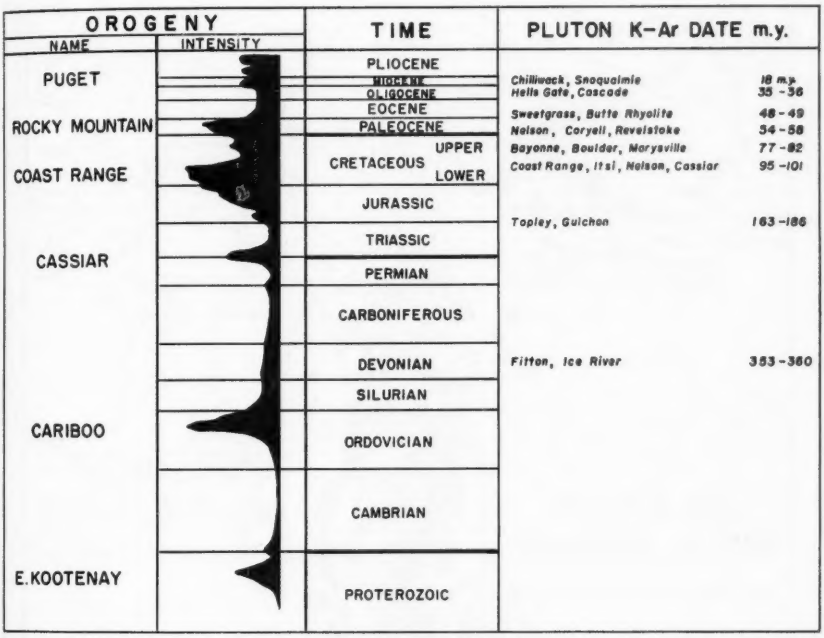

Figure 1. Cordilleran orogenies (after White, 1959) compared with potassium-argon dates of Cordilleran granitic biotites

[1] Italics the writers'

million-year-old batholiths occupy in the time scale—this is the Paleozoic age problem (Davidson, 1959). These dates are probably post-Early Devonian (Acadian), since the 350-million-year-old Fitton granite intrudes a complete and conformable section of rocks including all the Ordovician and Silurian and perhaps some Devonian rocks (Martin, 1959).

The discovery of datable Paleozoic plutons in the Cordillera and Arctic means that the oil possibilities of the Peel Plateau area of the Yukon, and presumably of the Arctic islands

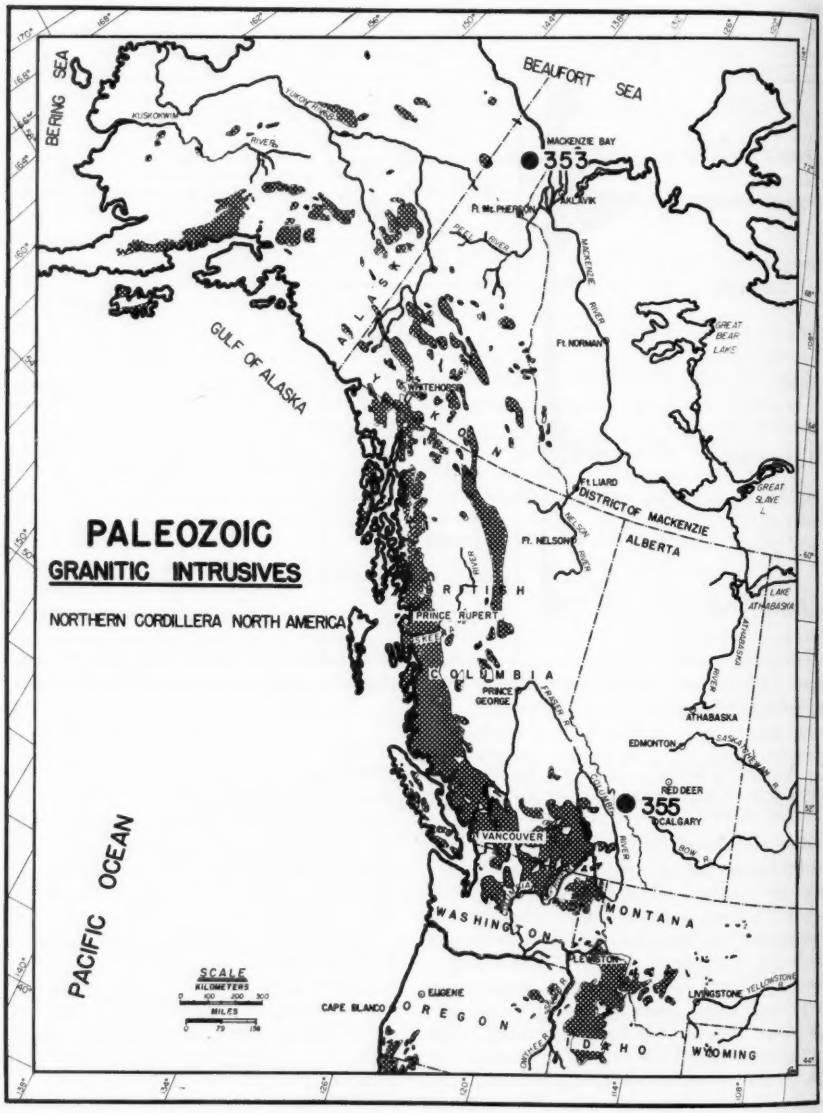

Figure 2. Fitton (Yukon) and Ice River (B.C.) Devonian intrusive masses

extension of this Arctic geosyncline, will have to be reappraised. Ore deposits may exist around these early intrusive masses; oil deposits may occur in stratigraphic pinchouts over these buried granite hills; either oil or ore may be masked by Mesozoic cover.

Finally the dates suggest that a very intimate relationship existed during the Paleozoic between North America and Europe; this is reflected in the simultaneity of the early Paleozoic orogeny throughout the Laurasian continents.

Figure 3. Early Mesozoic (186–163 m.y.), mid-Cretaceous (95–101), and early Laramide (77–82) intrusive masses of the Cordillera

Early Mesozoic Orogeny

The Guichon Creek batholith date, 186 m.y. (Fig. 3), is for an intrusive mass of which Duffell and McTaggart (1952, p. 79) say:

". . . because of the batholith's relations with rocks of the Nicola group and the Ashcroft Jurassic rocks it is possible to date its period of intrusion closely. The Nicola rocks intruded by the batholith belong to the Karnic stage of Upper Triassic time, whereas the Jurassic rocks overlying it are of early Middle and Upper Jurassic age. Therefore, the batholith was emplaced between early Upper Triassic and early Middle Jurassic time, most probably during the Lower Jurassic. . . ."

Warren and Stelck (1959) suggest the late Triassic as a possible period of orogeny because of worldwide continental Rhaetic red beds.

Hanson and Phemister (1928) were the first to recognize the Topley intrusive masses as early Mesozoic; the masses appear on Geological Survey of Canada maps as possibly Triassic. The Topley granite cuts Permian strata and is overlain by fossiliferous sedimentary rocks containing flora characteristic of Jurassic time, but which may be Cretaceous. In Tipper's opinion (1959), based on convincing field evidence, the Topley intrusions are post-Late Triassic, pre-Middle Jurassic. The potassium-argon date, 163 m.y., is much older than that of any other dated major batholith of the Cordillera, except the Guichon and Ice River masses.

Mid-Cretaceous Orogeny

After the intrusion of the Topley granite, there was a long period of comparative quiet, and the northern Cordillera was unaffected by what has classically been regarded as the late Jurassic, Nevadan, revolution. The mid-Cretaceous appears to have been the time of major intrusion in British Columbia (Dolmage, 1928, p. 85), with the emplacement of the Coast Range intrusive mass, the Cassiar-Omineca batholith, early elements of the Nelson batholith, and outlying plutons such as the Itsi batholith of the Yukon.

A large number of lead-alpha age determinations on zircon by the U.S. Geological Survey (Larsen *et al.*, 1958; Matzko, Jaffe, and Waring, 1958) indicate an "early Late Cretaceous" date for the southern California, the Sierra Nevada, the Idaho, and the Coast Range (Washington, British Columbia, and Alaska) batholiths. Potassium-argon age determinations confirm this. The writers have as yet no evidence of a late Jurassic orogeny (Nevadan) in the northern Cordillera such as that reported for California and Oregon by Evernden, Curtis, and Lipson (1958).

The Nelson batholith illustrates the difficulties that plague interpreters of potassium-argon dates. Zircon extracted from granite at Whatshan Lake returns a lead-alpha date of 105 m.y. (Beveridge and Folinsbee, 1956), or 108 m.y. (Larsen *et al.*, 1958). Biotite from this granite gives a potassium-argon date of only 54 m.y. However, only 10 miles to the west, biotite, apparently from another part of the same pluton, returns a 96 m.y. potassium-argon date. The Nelson batholith in this area is autochthonous; zircons show overgrowth phenomena similar to those figured by Poldervaart and Eckelmann (1955) and Beveridge and Folinsbee (1956, p. 25). Possibly the situation is analogous to that reported by Wetherill *et al.* (1959) for the Baltimore gneiss. As both biotites are equally chloritized (Table 1), the mechanism for differential argon leakage cannot be invoked. Potassium content appears to group significantly with dates in most instances (Table 1); the Nelson granite is the one conspicuous exception in this study.

The discrepancy in dates could indicate that a Paleozoic or older sedimentary series was intruded and metamorphosed during the Tertiary and that the zircons retained some radiogenic lead during recrystallization (*See* Geol. Soc. America Map of North America, 1946, legend for Nelson batholith.) However, strontium-rubidium dates and isotopic-lead dates for the zircon are required to check this hypothesis.

Rocky Mountain Orogeny

Orogeny continued on into Late Cretaceous times with the emplacement of small plutons such as Bayonne (British Columbia), Boulder (Montana), and Marysville (Montana) (Knopf, 1950; 1956; 1957), believed to be Late Cretaceous and assignable to the Laramide orogeny. The Maestrichtian stage of the Cretaceous period and Mesozoic era ended about 63 million years ago, on the basis of potassium-argon and lead-alpha dates for minerals from late Cretaceous ash falls on the plains of Alberta (Folinsbee, Baadsgaard, and Lipson, 1958; 1961).

After a 20-million-year period of quiescence covering latest Cretaceous and Paleocene time, orogeny, accompanied by alkalic intrusions, occurred again. This was the Rocky Mountain

or Laramide revolution proper, apparently occurring 48–58 million years ago toward the end of Paleocene time or during the Eocene.

Russell (1951, p. 47) has this to say:

"... One of the most widely accepted generalizations of historical geology is the doctrine that the eras terminated in world-wide or at least continental disturbances, the so-called revolutions. Of these, the Laramide revolution, during which the eastern ranges of the Rocky Mountains were formed by overthrusting and folding, is assigned

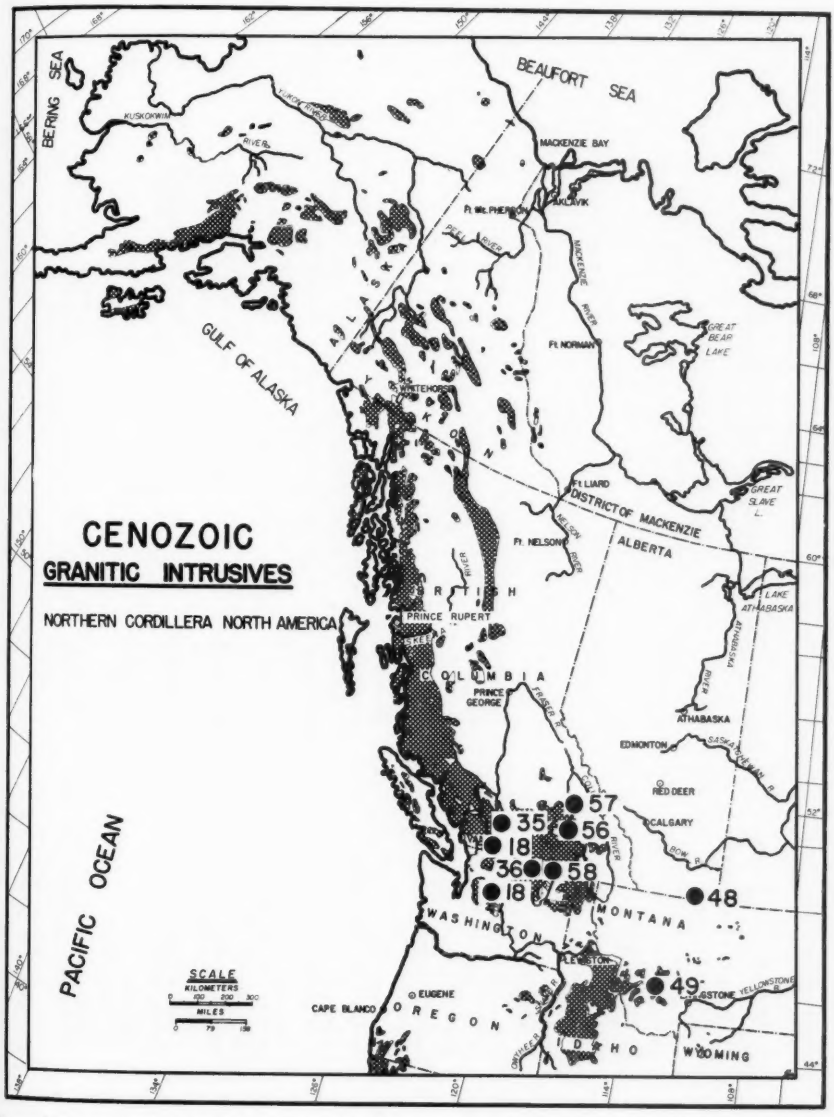

Figure 4. Later Rocky Mountain or Laramide (58–48 m.y.) and Puget or Alpine (36–18 m.y.) intrusive masses in the Cordillera

TABLE 1. K-AR AGE OF BIOTITES FROM CORDILLERAN GRANITES

Constants: $\lambda e = 0.589 \times 10^{-10}$/yr., $\lambda\beta = 4.76 \times 10^{-10}$/yr., $K^{40}/K = 0.0118_1$ atomic per cent. Assumed deviation in dates is ±5 per cent.

No.	Pluton and locality	Rock type	Latitude, longitude	Geologic age (authority)	%K	Ar^{40}/K^{40}	Date (m.y.)
	PALEOZOIC PLUTONS (Cariboo orogeny)						
AK 51	*Fitton* North Yukon	quartz monzonite	68° 30′ N., 138° 01′ W.	Late Devonian? (Martin, 1959, p. 2442)	6.47	0.0229	353
Ak 46	*Ice River* Field, B.C.	jacupirangite	51° 10′ N., 116° 23′ W.	post-Ordovician (Allan, 1914) or Precambrian (Gussow and Hunt, 1959)	5.19	0.0230	355
Ak 83		minette	51° 08′ N., 116° 24′ W.		6.89	0.0234	360
AK 84		pegmatite	51° 11′ N., 116° 27′ W.		6.63	0.0194	304
	EARLY MESOZOIC PLUTONS (Cassiar orogeny)						
AK 44	*Guichon* Highland Valley, B.C.	quartz diorite	50° 29′ N., 120° 58′ W.	Early Jurassic (Duffell and McTaggart, 1952)	3.31	0.0115	186
AK 23	*Topley* Fort Fraser, B.C.	granite	54° 04′ N., 124° 41′ W.	post-Late Triassic, pre-mid-Jurassic (Tipper, 1959)	3.60	0.0100	163
	MID-CRETACEOUS PLUTONS (Coast Range orogeny)						
AK 50	*Cassiar-Omineca* Southern Yukon	quartz monzonite	60° 04′ N., 130° 29′ W.	Late Jurassic or Early Cretaceous (Armstrong, 1946)	6.16	0.00611	101
KA 126	*Coast Range* Vancouver, B.C.	granodiorite	49° 22′ N., 123° 16′ W.	Cretaceous or Jurassic (Armstrong, 1953)	6.39	0.00596 0.00572	99 95
KA 125	*Itsi* Eastern Yukon	granodiorite	62° 55′ N., 130° 10′ W.	Cretaceous or later (Kindle, 1945)	6.64	0.00578	96
AK 47	*Nelson* Monashee Pass, B.C.	porphyritic granite	49° 58′ N., 118° 18′ W.	Late Cretaceous (Cairnes, 1934, p. 73–75)	2.97	0.00581	96
	LATE CRETACEOUS PLUTONS						

	Late Cretaceous Plutons (Early Laramide orogeny)						
AK 48	Kain quarry, *Boulder* batholith Helena, Montana	granodiorite	46° 28′ N., 112° 01′ W.	Late Cretaceous? (Knopf, 1957, p. 89–90)	4.86	0.00494	82
AK 63	*Marysville* Montana	granodiorite	46° 45′ N., 112° 18′ W.	Late Cretaceous? (Knopf, 1950)	5.43	0.00470	78
KA 118	*Bayonne* Kootenay Lake, B.C.	granite or alkaline granodiorite	49° 15′ N., 116° 39′ W.	Probably Cretaceous, possibly Late Cretaceous (Rice, 1941, p. 37)	6.46	0.00465	77
	Early Tertiary Plutons (Later Laramide orogeny)						
AK 26	*Coryell* Rossland, B.C.	syenite	49° 04′ N., 117° 58′ W.	post-Eocene (Daly, 1912, p. 372–375)	4.13	0.00346	58
AK 29	*Revelstoke* 10 miles north of Revelstoke, B.C.	gneissic granodiorite	51° 08′ N., 118° 11′ W.	unmapped	5.44	0.00342	57
AK 28	*Coryell* Santa Rosa, B.C.	syenite	49° 03′ N., 118° 03′ W.	post-Eocene (Daly, 1912)	3.82	0.00324	54
AK 27	*Nelson* Whatshan Lake, B.C.	granite	50° 00′ N., 118° 06′ W.	Late Cretaceous (Cairnes, 1934)	3.30	0.00327 0.00333	55 56
KA 156	Dike, *Big Butte* Butte, Montana	rhyolite	46° 01′ N., 112° 35′ W.	Late Miocene (Weed, 1912, p. 45)	7.21	0.00294	49
AK 53	Pinhorn Butte, *Sweetgrass* Southern Alberta	minette	49° 01′ N., 111° 10′ W.	Early Tertiary (Alden, 1924)	7.02	0.00289	48
	Later Tertiary Plutons (Puget orogeny)						
AK 25	*Cascade* Christina Lake, B.C.	gneissic granite	49° 01′ N., 118° 18′ W.	Jurassic? (Daly, 1912, p. 387–388)	6.32	0.00215	36
AK 24	*Hell's Gate* Fraser Canyon, B.C.	granodiorite	49° 47′ N., 121° 26′ W.	Jurassic (Geol. Survey Canada Map 737A, 1942)	5.71	0.00207	35
AK 31	*Chilliwack* Wahleach, B.C.	quartz diorite	49° 15′ N., 121° 41′ W.	Miocene (Daly, 1912, p. 546)	6.56	0.00104	18
AK 45	*Chilliwack* Cheam View, B.C.	quartz diorite	49° 15′ N., 121° 41′ W.	Middle Cenozoic (Crickmay, 1930)	6.63	0.00107	18
AK 91	*Snoqualmie*	granodiorite	47° 23′ N., 121° 27′ W.	Miocene (Grant, 1941)	5.67	0.00104	18

to the close of the Mesozoic era. Studies on the Tertiary rocks of Western Canada, and on their vertebrate and molluscan fossils, have convinced me that the major Rocky Mountain orogeny occurred much later, that is, in the Eocene epoch. . . ."

Geochronological data support this and other observations by Russell (1959). The major period of intrusion is dated as occurring 48–58 million years ago (Fig. 4), 10 million years after the close of the Cretaceous, and perhaps during Eocene time. Matzko, Jaffe, and Waring (1958) obtained a similar group of dates for intrusive masses of central Alaska using the lead-alpha method. Evernden, Kistler, and Curtis (1959) proposed a Cenozoic time scale with the base of the Paleocene 55–60 million years ago and base of the Eocene 48–50 million years ago. The orogeny that the present writers have dated involved intrusion of syenites into and around the Nelson batholith and the intrusion of the Sweet Grass laccoliths of northern Montana, with their dike equivalents in southern Alberta (Alden, 1924).

The writers hope that these data will help to correct what Russell deplores, the textbook insistence that the Laramide revolution marked the close of the Cretaceous period.

Puget Orogeny

White (1959) postulates a late Tertiary Cordilleran orogeny which he calls the Puget orogeny and places in the Miocene. Evernden, Kistler, and Curtis (1959) place the base of the Miocene 25–27 million years ago and the base of the Pliocene 12–13 million years ago. The present writers found only one intrusive mass in British Columbia which gives a Miocene date. It was long ago recognized by Daly (1912, p. 535) and by Crickmay (1930) as a mid-Cenozoic intrusive mass. Crickmay assigned a mid-Cenozoic age to the fresh and unaltered bodies of quartz diorite that lie across the Harrison River valley below the efflux of the lake and extend across Fraser River to the southeast, continuing into the mountains beyond Wahleach Lake, there joining Daly's (1912) Chilliwack batholith. The quartz diorite cuts across the great thrust fault and all the associated high-angled structures that separate the Coast and Cascade ranges.

Biotite dates show this quartz diorite to be 18 million years old, far younger than the 100-million-year-old Coast Range batholith at Vancouver a few miles to the west. It is a miarolitic rock whose cavities yield quartz crystals (D. C. MacArthur, personal communication) correlative petrographically and by K-Ar dating (Lipson, Folinsbee, and Baadsgaard, 1961) with the epizonal Snoqualmie batholith of Washington (Buddington, 1959), which is late Oligocene or early Miocene (Grant, 1941). It is thus one of the youngest exposed batholiths in the world (Knopf, 1955). Jäger and Faul (1959) found Alpine micas of identical date. Lowdon (1960) reports correlative young (11–16 m.y.) granites in the Valhalla complex of the Nelson batholith.

These Miocene dates support Crickmay's contention that the Cascade Range is a re-elevated Laramide range, indicating Alpine orogeny, as distinct from the Coast Range which Crickmay believed to be a re-elevated Jurassic system. The Coast Range of British Columbia is now believed from potassium-argon dates to represent mainly mid-Cretaceous orogeny.

SUMMARY

This reconnaissance study of the geochronology of the batholithic rocks of British Columbia, Yukon, Alberta, and the northwestern United States vindicates the opinions set forth mainly by geologists working for the geological surveys of Canada and the United States over the past half century or more.

The paper emphasizes the geological importance of an early Paleozoic orogeny, possibly correlated with the Caledonian of Europe or the Acadian orogeny of eastern North America, and confirms suggestions by Dolmage (1928) and by Larsen and his coworkers of the U.S. Geological Survey assigning the Coast Range orogeny of British Columbia to the mid-Cretaceous. The dates emphasize that many of the intrusions accompanying the Laramide or Rocky Mountain orogeny were post-Mesozoic. Dates obtained suggest a renewal of orogeny, *i.e.* White's "Puget" orogeny 36 million years ago, and the continuance of granite intrusion into the Cordillera at least to mid-Miocene time, only 18 million years ago. The data may be of some use in regional petrologic studies (Moore, 1959), in interpreting metallogenic epochs in the Cordillera, and in reappraisal of the oil possibilities of certain areas such as the Peel Plateau of the Yukon, the geosyncline of the Canadian Arctic islands, and the Groundhog River area of British Columbia west of Prince George.

The writers believe that these biotites give dates which are as reliable as those any single method of absolute age determination can give. The dates can be taken at present to indicate

only the last major heating of the rock from which the biotite came (Curtis and Reynolds, 1958) and therefore require careful geologic evaluation. The potassium-argon ratios of biotites can be measured to within ±5 per cent; the dates calculated assume no postcrystallization effects. Considerable evidence indicates that later intrusion may update earlier granitic rocks: for example, the Nelson granite at Whatshan Lake is believed to have first crystallized as a mid-Cretaceous granite (95 million years ago); subsequently it was updated by reason of its proximity to early Tertiary (Coryell) syenite intrusive masses (50–60 million years).

Carr and Kulp (1957) have discussed some problems relating to the potassium-argon method of geochronometry. In the present paper, with a comparatively small body of data from potassium-argon dates of biotites alone, and no certain confirmation by other dating methods, the writers suggest only that there is good agreement between the data presented and Cordilleran geologic history as determined by field methods.

Buddington (1959) has recently reviewed, in masterly fashion, granite emplacement with special reference to North America. His work suggests a host of plutons to which potassium-argon dating might be applied. Batholiths such as those he discusses, with a wealth of accumulated geologic knowledge, offer excellent promise for geological study using absolute dating methods.

Knopf (1950), perhaps with tongue in cheek, concluded his paper on the Marysville stock as follows:

"Nearly fifty years have been required to formulate a reasonable answer to the problem of the relationship between Boulder bathylith, Marysville stock and the geographically associated gold-silver veins; perhaps, when, as physicists promise us, five grams of a rock will suffice for a determination of its absolute age, the answer will come more rapidly and more positively."

The Marysville stock was dated with destruction of a total of 3.46 gms of biotite extracted from a hand specimen submitted by Dr. Knopf. Perhaps the millenium (plus or minus a few million years) has been reached.

REFERENCES CITED

Alden, W. C., 1924, Physiographic development of the northern Great Plains: Geol. Soc. America Bull., v. 35, p. 385–424

Allan, J. A., 1914, Geology of field map-area, B.C. and Alberta: Geol. Survey Canada Mem. 55, 312 p.

Armstrong, J. E., 1946, Geology and mineral deposits of northern British Columbia west of the Rocky Mountains: Geol. Survey Canada Bull. #5, 46 p.

—— 1952, Fort St. James map-area, Cassiar and Coast district, British Columbia: Geol. Survey Canada Mem. 252, 210 p.

—— 1953, Preliminary map, Vancouver North, British Columbia: Geol. Survey Canada Paper 53–27, 7 p.

Baadsgaard, H., Goldich, S. S., Nier, A. O., and Hoffman, J. H., 1957, The reproducibility of A^{40}/K^{40} age determinations: Am. Geophys. Union Trans., v. 38, p. 539–542

Beveridge, A. J., and Folinsbee, R. E., 1956, Dating Cordilleran orogenies: Royal Soc. Canada Trans., v. 50, ser. 3, p. 19–43

Buddington, A. F., 1959, Granite emplacement with special reference to North America: Geol. Soc. America Bull., v. 70, p. 671–747

Burwash, R. A., 1959, Pre-Beltian basement in southern Alberta and adjacent British Columbia (Abstract): Geol. Soc. America Bull., v. 70, p. 1576

Cairnes, C. E., 1934, Slocan mining camp: Geol. Survey Canada Mem. 173, 137 p.

Carr, D. R., and Kulp, J. L., 1957, Potassium-argon method of geochronometry: Geol. Soc. America Bull., v. 68, p. 763–784

Crickmay, C. H., 1930, The structural connection between the Coast Range of British Columbia and the Cascade Range of Washington: Geol. Mag., v. 67, p. 482–491

Curtis, G. H., and Reynolds, J. L., 1958, Notes on the potassium-argon dating of sedimentary rocks: Geol. Soc. America Bull., v. 69, p. 151–160

Daly, R. A., 1912, Geology of the North American Cordillera at the 49th Parallel: Geol. Survey Canada Mem. 38, 546 p.

Damon, P. E., and Kulp, J. L., 1957, Argon in mica and the age of the Beryl Mt., N.H., pegmatite: Am Jour. Sci., v. 255, p. 697–704

Davidson, C. F., 1959, How old is the Cambrian system?: Nature, v. 183, p. 768–770

Dolmage, V., 1928, Gun Creek map-area, British Columbia: Geol. Survey Canada Summary Rept., Part A, p. 78–93

Duffell, S., and McTaggart, K. C., 1952, Ashcroft map-area, British Columbia: Geol. Survey Canada Mem. 262, 122 p.

Evernden, J. F., Curtis, G. H., and Lipson, J., 1957, Potassium-argon dating of igneous rocks: Am. Assoc. Petroleum Geologists Bull., v. 41, p. 2120–2127

—— 1958, Potassium-argon dates for the intrusives of northern and central California (Abstract): Geol. Soc. America Bull., v. 69, p. 1684

Evernden, J. F., Kistler, R., and Curtis, G. H., 1959, Cenozoic time scale of the West Coast (Abstract): Geol. Soc. America Bull., v. 70, p. 1718

Faul, H., 1959, Doubts of the Paleozoic time scale (Abstract): Jour. Geophys. Research, v. 64, p. 1102

Faul, H., and Tilton, G. R., 1957, Age of some Hercynian granites in Europe: Assoc. Internat. de Volcanologie, Union Géodésique et Géophysique Internationale, XI Assemblée Générale, Toronto, p. 18–19

Folinsbee, R. E., Baadsgaard, H., and Lipson, J., 1958, Potassium-argon age dating of sediments (Abstract): Am. Assoc. Petroleum Geologists, Program 43rd Ann. Mtg., p. 17

—— 1961, Potassium-argon dates of Upper Cretaceous ash falls, Alberta, Canada, p. 362–363 *in* Kulp, J. L., *Editor*, Geochronology of rock systems: New York Acad. Sciences Annals, v. 91, p. 159–590

Grant, R. V., 1941, A John Day vertebrate fossil discovered in the Keechelus series of Washington: Am. Jour. Sci., v. 239, p. 590–593

Gussow, W. C., and Hunt, C. W., 1959, Age of Ice River complex, Yoho National Park, British Columbia: Alberta Soc. Petroleum Geologists Jour., v. 7, p. 62

Hanson, G., and Phemister, T. C., 1928, Topley map-area, British Columbia: Geol. Survey Canada Summary Rept., Part A, p. 56–59

Hunt, G. H., 1960, Time of intrusion of the Purcell sills, southeastern British Columbia (Abstract): Geol. Soc. America Bull., v. 71, p. 1893

Hurley, P. M., Boucot, A. J., Albee, A. L., Faul, H., Pinson, W. H., and Fairbairn, H. W., 1959, Minimum age of the Lower Devonian slate near Jackman, Maine: Geol. Soc. America Bull., v. 70, p. 947–950

Hurley, P. M., *et al.*, 1958, The Paleozoic time scale problem; variations in isotopic abundances of strontium, calcium and argon and related topics: Mass. Inst. Technology Dept. Geology and Geophysics, 6th Ann. Progress Rept. for U.S. Atomic Energy Comm., p. 107–109

Jäger, E., and Faul, H., 1959, Age measurement on some granites and gneisses from the Alps: Geol. Soc. America Bull., v. 70, p. 1553–1557

Kindle, E. D., 1945, Geological reconnaissance along the Canol road, from Teslin River to Macmillan Pass, Yukon: Geol. Survey Canada Paper 45–21, 26 p.

Knopf, A., 1950, The Marysville granodiorite stock, Montana: Am. Mineralogist, v. 35, p. 834–844

—— 1955, Bathyliths in time, p. 685–702 *in* Poldervaart, Arie, *Editor*, Crust of the earth: Geol. Soc. America Special Paper 62, 762 p.

—— 1956, Argon-potassium determinations of the age of the Boulder bathylith, Montana: Am. Jour. Sci., v. 254, p. 744–745

—— 1957, The Boulder bathylith of Montana: Am. Jour. Sci., v. 255, p. 81–103

Kulp, J. L., 1959, Absolute age determination of sedimentary rocks: 5th World Petrolcum Cong., Proc. Sec. 1, p. 689–704

—— 1959, The geological time-scale: Nature, v. 184, p. 62–63

Larsen, E. S., Gottfried, D., Jaffe, H. W., and Waring, C. L., 1958, Lead-alpha ages of the Mesozoic batholiths of western North America: U.S. Geol. Survey Bull. 1070–B, 27 p.

Lipson, J., Folinsbee, R. E., and Baadsgaard, H., 1961, Periods of orogeny in the western Cordillera, p. 459–463 *in* Kulp, J. L., *Editor*, Geochronology of rock systems: New York Acad. Sciences Annals, v. 91, p. 159–590

Lowdon, J. A., 1960, Age determinations by the Geological Survey of Canada: Geol. Survey Canada Paper 60–17, 51 p.

Lyons, J. B., Jaffe, H. W., Gottfried, D., and Waring, C. L., 1957, Lead-alpha ages of some New Hampshire granites: Am. Jour. Sci., v. 255, p. 527–546

Martin, L. J., 1959, Stratigraphy and depositional tectonics of North Yukon-Lower Mackenzie area, Canada: Am. Assoc. Petroleum Geologists Bull., v. 43, p. 2399–2455

Matzko, J. J., Jaffe, H. W., and Waring, C. L., 1958, Lead-alpha age determinations of granitic rocks from Alaska: Am. Jour. Sci., v. 256, p. 529–539

Mayne, K. I., Lambert, R. St.J., and York, D., 1959, The geological time scale: Nature, v. 183, p. 212–214

Moore, J. G., 1959, The quartz diorite boundary line in the western United States: Jour. Geology, v. 67, p. 198–210

Ovchinnikov, L. N., 1958, Determinations of the absolute age of the ore deposits of the Urals: Geochemistry, No. 6, p. 689–698

Poldervaart, A., and Eckelmann, F. D., 1955, Growth phenomena in zircons of autochthonous granites: Geol. Soc. America Bull., v. 66, p. 947–948

Rice, H. M. A., 1941, Nelson map-area, east half, British Columbia: Geol. Survey Canada Mem. 228, 86 p.

Russell, L. S., and Landes, R. W., 1940, Geology of the southern Alberta plains: Geol. Survey Canada Mem. 221, 223 p.

— 1951, Age of the Front Range deformation in the North American Cordillera: Royal Soc. Canada Trans., v. 45, ser. 3, p. 47–69

— 1959, Fossil mammals and intercontinental connections (Abstract): Royal Soc. Canada Proc., v. 53, ser. 3, Appendix C, p. 18

Smith, A. R., and Stevenson, J. S., 1955, Deformation and igneous intrusion in southern British Columbia, Canada: Geol. Soc. America Bull., v. 66, p. 811–818

Tilton, G. R., Wetherill, G. W., Davis, G. L., and Hopson, C. A., 1958, Ages of minerals from the Baltimore gneiss near Baltimore, Maryland: Geol. Soc. America Bull., v. 69, p. 1469–1474

Tipper, H. W., 1959, Revision of the Hazelton and Takla groups of central British Columbia: Geol. Survey Canada Bull. 47, p. 31–32

Warren, P. S., and Stelck, C. R., 1959, Continental margins of western Canada: Alberta Soc. Petroleum Geologists Jour., v. 6, p. 29–42

Weed, W. H., 1912, Geology and ore deposits of the Butte district, Montana: U.S. Geol. Survey Prof. Paper 74, 262 p.

Wetherill, G. W., Tilton, G. R., Davis, G. L., and Hopson, C. A., 1959, Mineral ages in the Baltimore-Washington area (Abstract): Jour. Geophys. Research, v. 64, p. 1129–1130

White, W. H., 1959, Cordilleran tectonics in British Columbia: Am. Assoc. Petroleum Geologists Bull., v. 43, p. 60–100

Manuscript Received by the Secretary of the Society, November 16, 1959

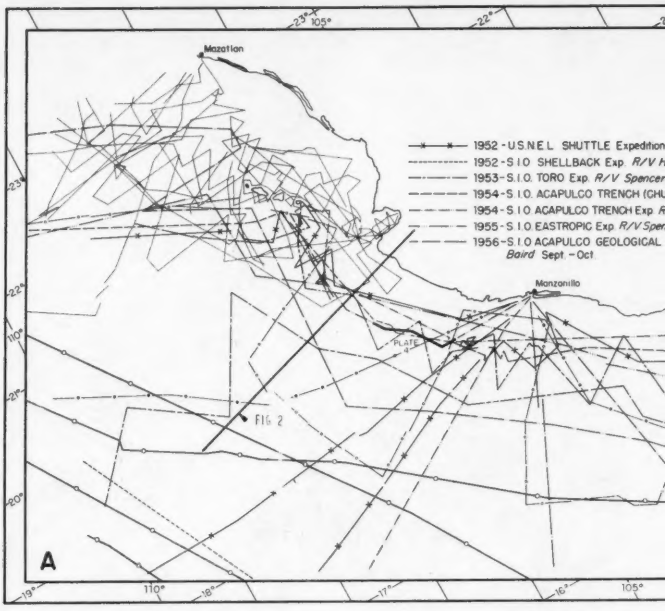
Mazatlan
1952 - U.S.N.E.L. SHUTTLE Expedition
1952 - S.I.O. SHELLBACK Exp. R/V
1953 - S.I.O. TORO Exp. R/V Spencer
1954 - S.I.O. ACAPULCO TRENCH (CHU
1954 - S.I.O. ACAPULCO TRENCH Exp. R
1955 - S.I.O. EASTROPIC Exp. R/V Spen
1956 - S.I.O. ACAPULCO GEOLOGICAL
Baird Sept. - Oct.
Manzanillo
PLATE 4
FIG. 2
A

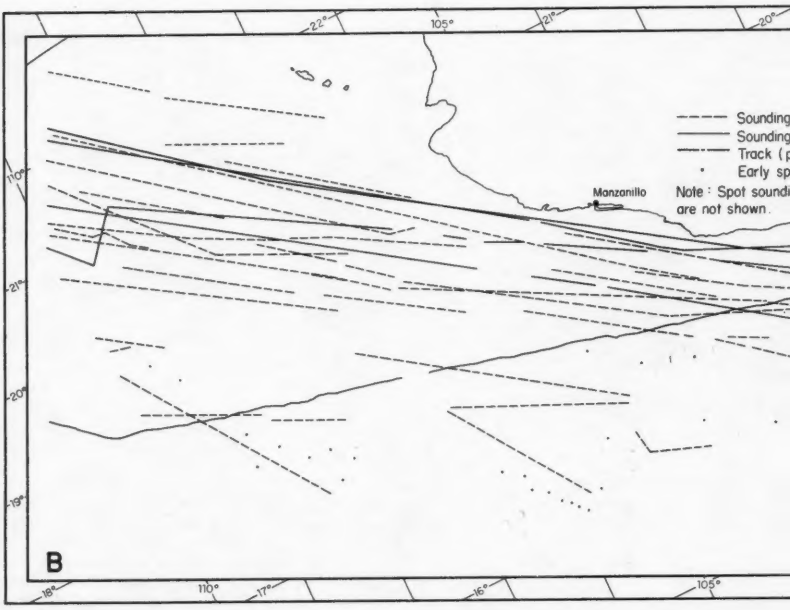

FISHER, PLATE 1
Geological Society of America, volume 72

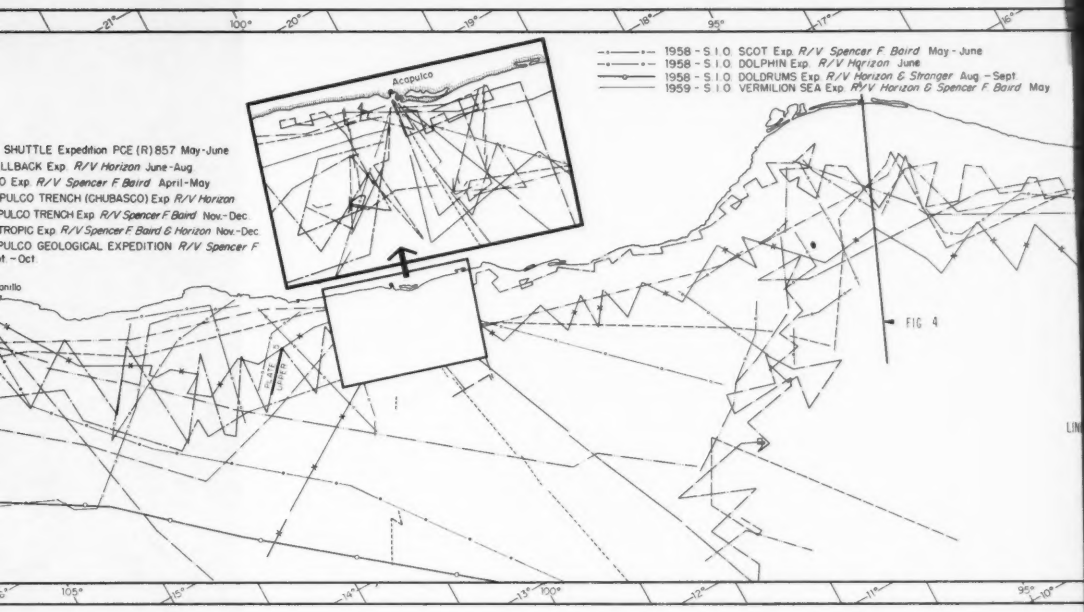
1958 - S.I.O. SCOT Exp. R/V Spencer F. Baird May - June
1958 - S.I.O. DOLPHIN Exp. R/V Horizon June
1958 - S.I.O. DOLDRUMS Exp. R/V Horizon & Stranger Aug. - Sept.
1959 - S.I.O. VERMILION SEA Exp. R/V Horizon & Spencer F. Baird May
SHUTTLE Expedition PCE (R) 857 May-June
LLBACK Exp. R/V Horizon June-Aug.
O Exp. R/V Spencer F. Baird April-May
PULCO TRENCH (CHUBASCO) Exp. R/V Horizon
PULCO TRENCH Exp. R/V Spencer F. Baird Nov.-Dec.
TROPIC Exp. R/V Spencer F. Baird & Horizon Nov.-Dec.
PULCO GEOLOGICAL EXPEDITION R/V Spencer F
t - Oct.
anillo
Acapulco
FIG. 4
105°
15°
14°
13°
100°
12°
11°
95°
10°

A. Index map: S.I.O. and N.E. L. exploration of the Middle America Trench

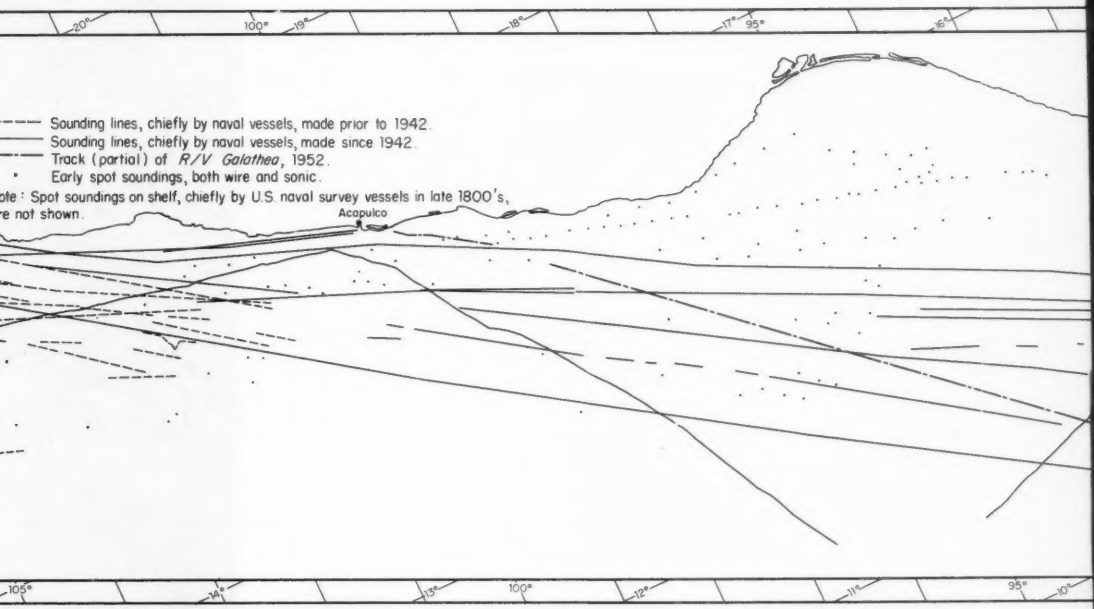

B. Index map: Sounding lines furnished by the U.S. Hydrographic Office

ECHO-SOUNDING LINES USED IN THE PREPARATION OF PLATES 2, 3, A

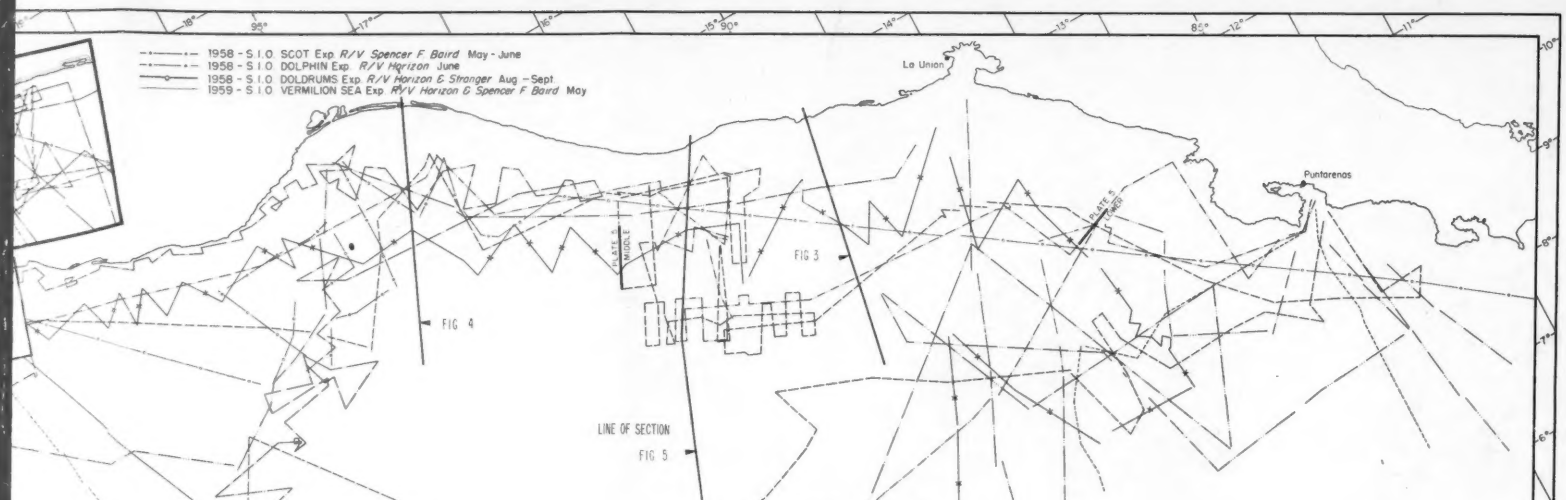
1958 - S.I.O. SCOT Exp. R/V Spencer F. Baird May - June
1958 - S.I.O. DOLPHIN Exp. R/V Horizon June
1958 - S.I.O. DOLDRUMS Exp. R/V Horizon E. Stronger Aug - Sept.
1959 - S.I.O. VERMILION SEA Exp. R/V Horizon E. Spencer F. Baird May
La Union
Puntarenas
FIG 3
FIG 4
LINE OF SECTION
FIG 5
W

dex map: S.I.O. and N.E. L. exploration of the Middle America Trench

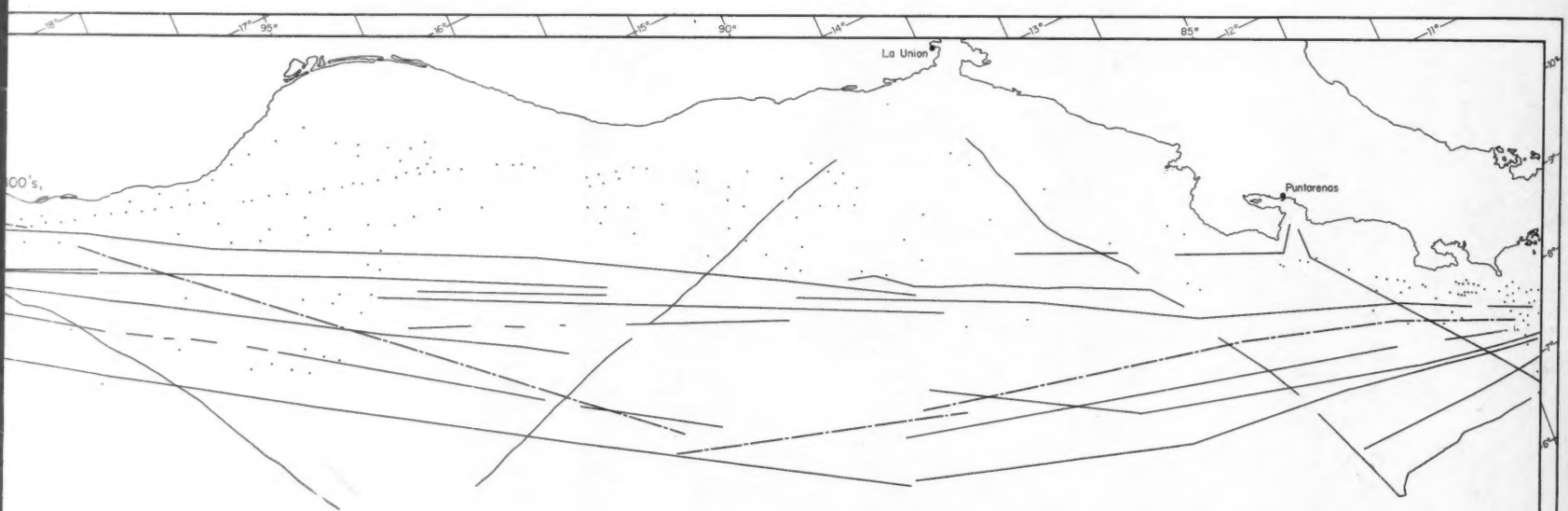

ndex map: Sounding lines furnished by the U.S. Hydrographic Office

DING LINES USED IN THE PREPARATION OF PLATES 2, 3, AND 6

ROBERT L. FISHER *Scripps Institution of Oceanography, University of California, La Jolla, Calif.*

Middle America Trench: Topography and Structure

Abstract: From 1952 to 1959, during nine expeditions of the Scripps Institution of Oceanography and one of the U. S. Navy Electronics Laboratory, research vessels recorded 31,950 miles of echo-sounding traverses in and adjacent to the Middle America Trench, which extends from the Islas Tres Marías off western Mexico to the Cocos Ridge southwest of Costa Rica.

The Middle America Trench is continuous at depths greater than 2400 fathoms (4400 m) for 1260 miles, except off Manzanillo and Zihuatanejo, Mexico, where submarine mountains lie in the trench. It is deeper than 3000 fathoms (5500 m) for 380 miles as the Guatemala Deep. Northwest of Acapulco it is generally U-shaped in cross section, with a steeper shoreward flank and a flat bottom suggesting sedimentary fill. From Acapulco southeast to the west side of the Gulf of Tehuantepec, the trench shoals, in a series of basins, to 2700 fathoms (5000 m). To the southeast it widens and deepens abruptly to a maximum 3500 fathoms (6400 m) off western Guatemala, then shoals gradually to merge into the sea floor off Costa Rica. The southeast segment is also asymmetrical in cross section but is V-shaped with irregular bottom. A northeast-trending band of ridge-and-trough topography, 60 miles wide, separates the 1800- to 1900-fathom sea floor outside the trench off southern Mexico from the 2100- to 2200-fathom Guatemala Basin. This zone has been traced from several hundred miles offshore to an intersection with the trench near the west side of the Gulf of Tehuantepec.

Seismic-refraction studies reported in an accompanying paper (Shor and Fisher, 1961) were employed in determining the trench structure. Three refraction stations were taken along the axis of the trench west of Acapulco and two along its axis off Guatemala and El Salvador. Another station was shot on the shelf and one 60 miles seaward of the trench off Guatemala. Thick sediments were found in the Tres Marías Basin off Manzanillo and at the shelf station off Guatemala. Arrivals from rock with compressional wave velocity of 4–6 km/sec were observed at the Tres Marías Basin and Guatemala shelf stations. Off Guatemala, on a section normal to the trench, the depth below sea level to the M discontinuity is interpreted from these seismic data as about 9 km (Pacific Basin), 10 km (outer ridge), 16 km (trench), and 17 km (shelf). Below the sea floor the crust thickens from 5–7 to 10–17 km along this section. The M discontinuity is deeper and the crust below the sediments thicker under the two southern stations than under the two central trench stations. The mantle is deeper under the Tres Marías Basin, where thick (1½ km) sediments are found, than under the central stations.

The Gulf of Tehuantepec marks a major change in trench configuration and possibly in age. Northwest of Tehuantepec the flat trench bottom developed in most places suggests a greater age. Southeast of the gulf the deep V-shaped trench, with thicker crustal layers but very little fill, borders a volcanically active coast. The zone of ridge-and-trough topography trending southwest from Tehuantepec may be another evidence of this boundary.

CONTENTS

Introduction 704
Regional relations 704
Scope of the present study 704
Acknowledgments 706
Previous work 706
Bathymetry 706
Gravity measurements 706
Topography 707
Preparation of the charts 707
Topography within and shoreward of the Middle America Trench 708
Topography seaward of the Middle America Trench 711
Topography of the Gulf of Tehuantepec . . . 712
Bathymetric evidence for sedimentary fill in the Middle America Trench 713
Discussion 714
References cited 717

Figure
1. Index map: seismic setting of the Middle America Trench 705
2. View to northwest from Banderas Bay 708
3. View to southeast from La Libertad, El Salvador 710
4. View to northwest from Gulf of Tehuantepec . 712
5. Schematic structure section off western Guatemala 715

Geological Society of America Bulletin, v. 72, p. 703–720, 5 figs., 6 pls., May 1961

Plate Facing
1. Echo-sounding lines used in the preparation of Plates 2, 3, and 6 703
2. Submarine topography, from Islas Tres Marías to Acapulco, Mexico 706
3. Submarine topography, from Acapulco, Mexico, to San José, Guatemala 710
4. Echogram of traverse along trench, near Manzanillo, Mexico 714
5. Echograms of three crossings of the Middle America Trench 715
6. Submarine topography, from San José, Guatemala, to Punta Burica, Panama 720

Table
1. Maximum depth of fill in the Middle America Trench, as deduced from bathymetric records 714
2. Velocities of refracting layers 717

INTRODUCTION

Regional Relations

A narrow depression, 20–100 miles offshore, extends 1550 miles along the west coasts of Mexico and Central America, from the Islas Tres Marías to the Golfo de Dulce (Fig. 1). This deep area includes the Acapulco Trench or Deep and the Guatemala Trench of various authors (*e.g.*, Agassiz, 1906; Whitcroft, 1944; Fisher and Revelle, 1955). Following Heacock and Worzel (1955), the writer now favors the name Middle America Trench for the entire structure.

Miocene to Recent volcanic rocks, folded and faulted Paleozoic, Mesozoic, and Cenozoic sedimentary and metamorphic rocks, and granitic rocks largely of late Cretaceous age, are exposed along the mountainous coasts of Jalisco, Colima, Michoacan, Guerrero, and Oaxaca (Schuchert, 1935, p. 129–131). Coastal mountains trend nearly parallel to the shore line. The east-west line of recently active Mexican volcanoes intersects the trench near 19° N. (Fig. 1). The Pacific coastal plain of Tehuantepec has a thin cover of undeformed Pleistocene marine sedimentary rocks lying on the pre-Carboniferous basement. The isthmus was downfaulted, probably in Late Miocene time, then raised slightly during late Pliocene and Pleistocene to its present low elevation (Webber and Ojeda R., 1956, p. 78). From southeastern Chiapas to Lake Nicaragua, the coastal plain is bordered on the east by late Cenozoic to Recent andesitic volcanoes. Rocks extruded by these young volcanoes have buried the western ends of east-trending mountain ranges of folded and faulted upper Paleozoic rocks (Schuchert, 1935, p. 314–320). The Pacific coasts of southern Nicaragua and Costa Rica are mountainous and composed chiefly of Tertiary and Quaternary volcanic rocks and igneous detritus. The recently active "Volcanic Range" of Costa Rica trends southeast, and passes inland from the Nicaragua-Costa Rica border (Schuchert, 1935, p. 592–600).

Along the trench axis and to the east of it, a very active zone of shallow earthquakes follows the Mexican coast from Jalisco to Oaxaca, crosses the Gulf of Tehuantepec, and continues, with reduced activity, to western Panama (Fig. 1). Outside the trench shallow activity is most frequent west of Colima, but several shocks have occurred off Oaxaca. Intermediate shocks follow the volcanic belts on land. No deep shocks are known from this area (Gutenberg and Richter, 1954, p. 36). The earthquake distribution has been studied by Benioff; he concluded that from the Islas Tres Marías to Panama a "marginal reverse fault complex," with an "intermediate component" extending to a depth of about 220 km, dips eastward beneath the continent (Benioff, 1954, p. 390).

Gunn (1947) attempted a quantitative treatment of the Middle America Trench–Coastal Mountain–Volcanic Chain relations. He assumes a strong elastic lithosphere supported on a weak magma and examines the mechanics of a "compressed shear thrust fault" formed in such a crust. From his calculations, Gunn states that shear faults resulting from horizontal compression would be localized at continental margins and that with continuing compression the higher continental mass would overthrust the ocean basin and simultaneously form a linear deep at the toe of the overriding block and a line of volcanoes, parallel to the deep, 50–90 km inland from the continental margin.

Scope of the Present Study

This work represents one of the results of research carried out under contracts with the Office of Naval Research and the Bureau of Ships, U. S. Navy.

The bathymetric studies were made during the 1952 U. S. Navy Electronics Laboratory Shuttle Expedition (bathymetry, bottom-sampling, hydrography) and the Scripps Institution of Oceanography expeditions: Shellback (1952; hydrography, bathymetry), Toro (1953; bathymetry, seismic-reflection studies, bottom-sampling), Acapulco Trench (1954; bathymetry, seismic-refraction studies, heat-flow and

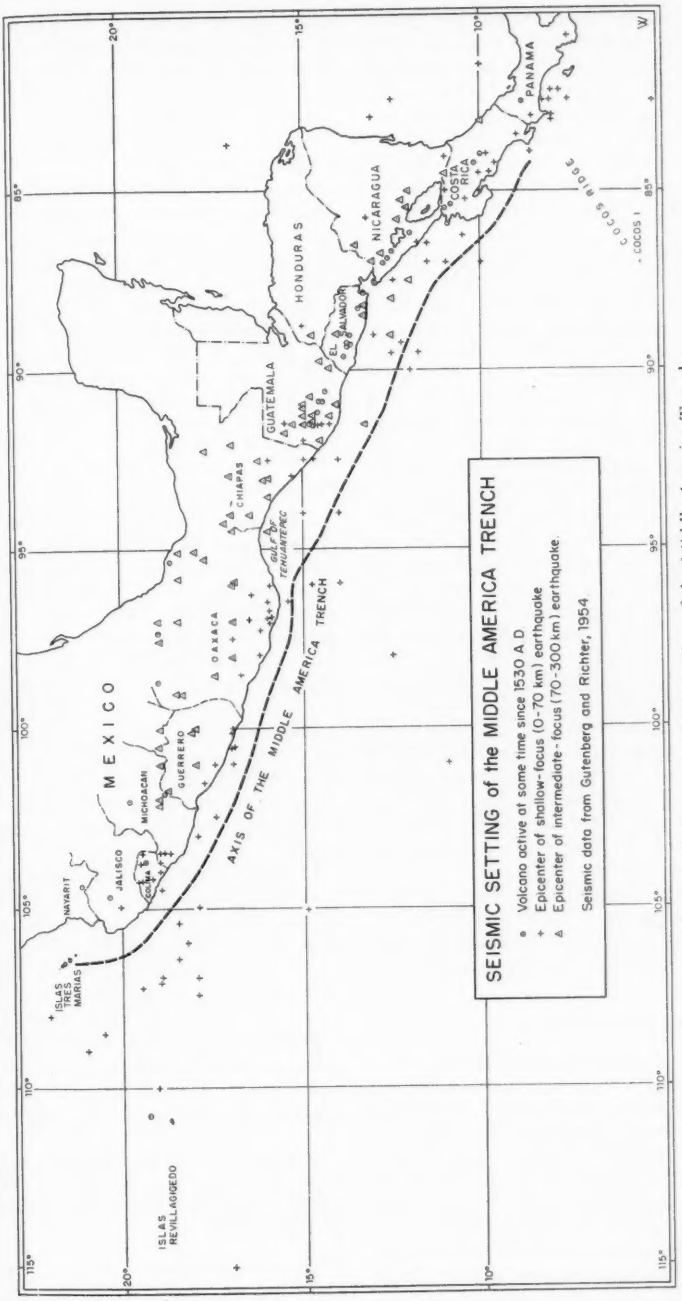

Figure 1. Index map: seismic setting of the Middle America Trench

magnetic measurements), Eastropic (1955; hydrography, bathymetry), Acapulco Geological (1956; bathymetry, bottom sampling), Dolphin (1958; magnetic measurements, hydrography), Scot (1958; biology, hydrography), Doldrums (1958; hydrography, biology), and Vermilion Sea (1959; bathymetry, seismic-refraction, and heat-flow studies, biology, bottom sampling). About 190 ship days were spent in the area.

Seismic-refraction data reported in an accompanying paper (Shor and Fisher, 1961) were collected on the 1954 Acapulco Trench Expedition. A short paper on the topography and structure of the Middle America Trench contains some discussion of the techniques and evaluation of the seismic-refraction data (Fisher and Shor, in press). On the 1954 cruise, other refraction data were taken in the homeward run, well seaward of the trench; one station of this later series lies on the seaward extension of the Champerico profile discussed below. An interpretation of the data from this station (Raitt, personal communication) has been included in the structural cross section (Fig. 5). Interpretation of the reflection records taken on the Toro Expedition in 1953 has not been completed, although preliminary results have been taken into account in following discussions of probable sediment thickness.

Similarly, bottom samples, taken both by gravity and piston corers, have not been studied microscopically but logged macroscopically in the field and stored for laboratory examinations. Statements regarding sedimentation in and bordering the trench are made on the basis of these field data.

Heat-flow and magnetic measurements were made by Arthur E. Maxwell and Ronald G. Mason, respectively. Their results, also bearing on inferred structure, will be reported elsewhere.

ACKNOWLEDGMENTS

The task of collecting sounding or seismic data on the nine Scripps expeditions was shared with 58 members of the scientific parties. On the N.E.L. Shuttle Expedition the author was assisted by Edwin L. Hamilton and Maxwell Silverman. The officers and men of the U. S. Navy Electronics Laboratory research vessel PCE(R) 857 and of the Scripps Institution of Oceanography research vessels Spencer F. Baird and Horizon and Stranger executed difficult ship operations and shared in the scientific program. Their help is gratefully acknowledged. Special thanks are due Maxwell Silverman, Alan C. Jones, M. Allan Beal, and Gene A. Rusnak. Warren Wooster, Townsend Cromwell, John Knauss, and Robert Holmes made available the echo-sounding data from the Shellback, Eastropic, Dolphin, Scot, and Doldrums expeditions.

Ing. Carlos Acosta del Campo of the Instituto Nacional de Recursos Minerales kindly provided copies of unpublished geological and structural maps of the Isthmus of Tehuantepec and of southern Chiapas, Mexico.

Robert C. Winsett, Howard Taylor, and James Moriarty prepared the illustrations. Russell Raitt, H. W. Menard, Roger Revelle, J. B. Hersey, and J. Lamar Worzel read and made suggestions in the manuscript.

PREVIOUS WORK

Bathymetry

The earliest systematic bathymetric observations, from Baja California to the Gulf of Panama, were the coastal surveys of the U.S.S. Narragansett (1873–1875), U.S.S. Tuscarora (1878–1879, 1880), and the U.S.S. Ranger (1882, 1884–1885). Deep soundings were taken by the U. S. Fish Commission Steamer Albatross in 1888, and especially during two expeditions (1891, 1904–1905) led by Alexander Agassiz, who noted (1906, p. 5) the very steep continental slope (Jalisco to Guerrero), the near-shore Tres Marías, Manzanilla (sic), and Acapulco Basins, and the Guatemala Basin lying 150–200 miles off San José, Guatemala.

In 1923 the Coast and Geodetic Survey Steamer Guide discovered the 3500-fathom Guatemala Deep at the base of the continental slope. Other survey vessels traversing the area include the Emden, the U.S.S. Chopper (1949), and the Galathea (1952). Thousands of soundings of varying quality have been reported by military and commercial vessels en route between Panama and the United States west coast or Hawaii; however, their courses generally lie well outside the trench area, except between long. 97° and 106° W.

Bathymetric charts and discussions of the topography have been published by Whitcroft (1944), Tamayo (1949), and Heacock and Worzel (1955).

Gravity Measurements

In 1926, aboard a Dutch submarine, F. A. Vening Meinesz made gravity observations

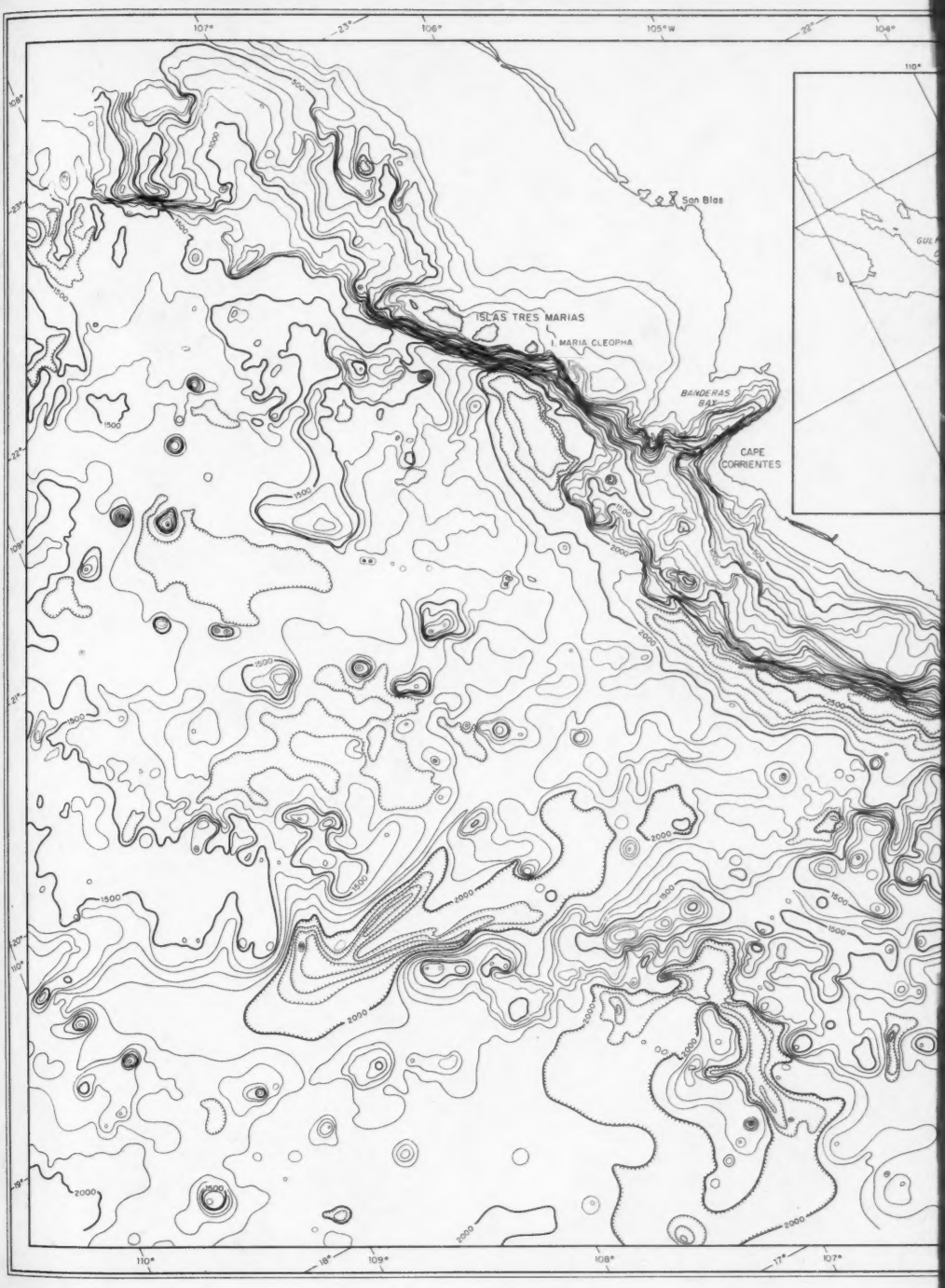

SUBMARINE TOPOGRAPHY

FISHER, PLATE 2
Geological Society of America, volume 72

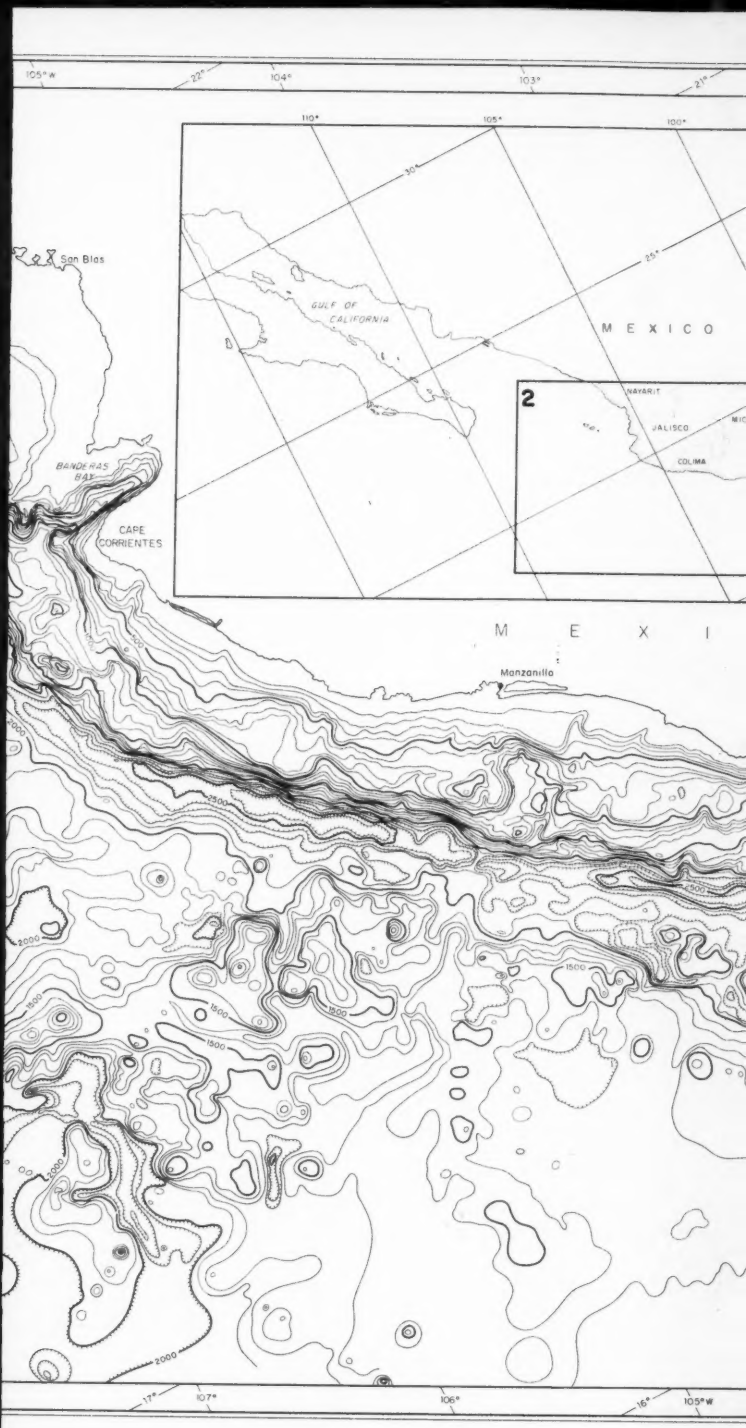

SUBMARINE TOPOGRAPHY, FROM ISLAS TRES MARÍAS TO ACAPUL

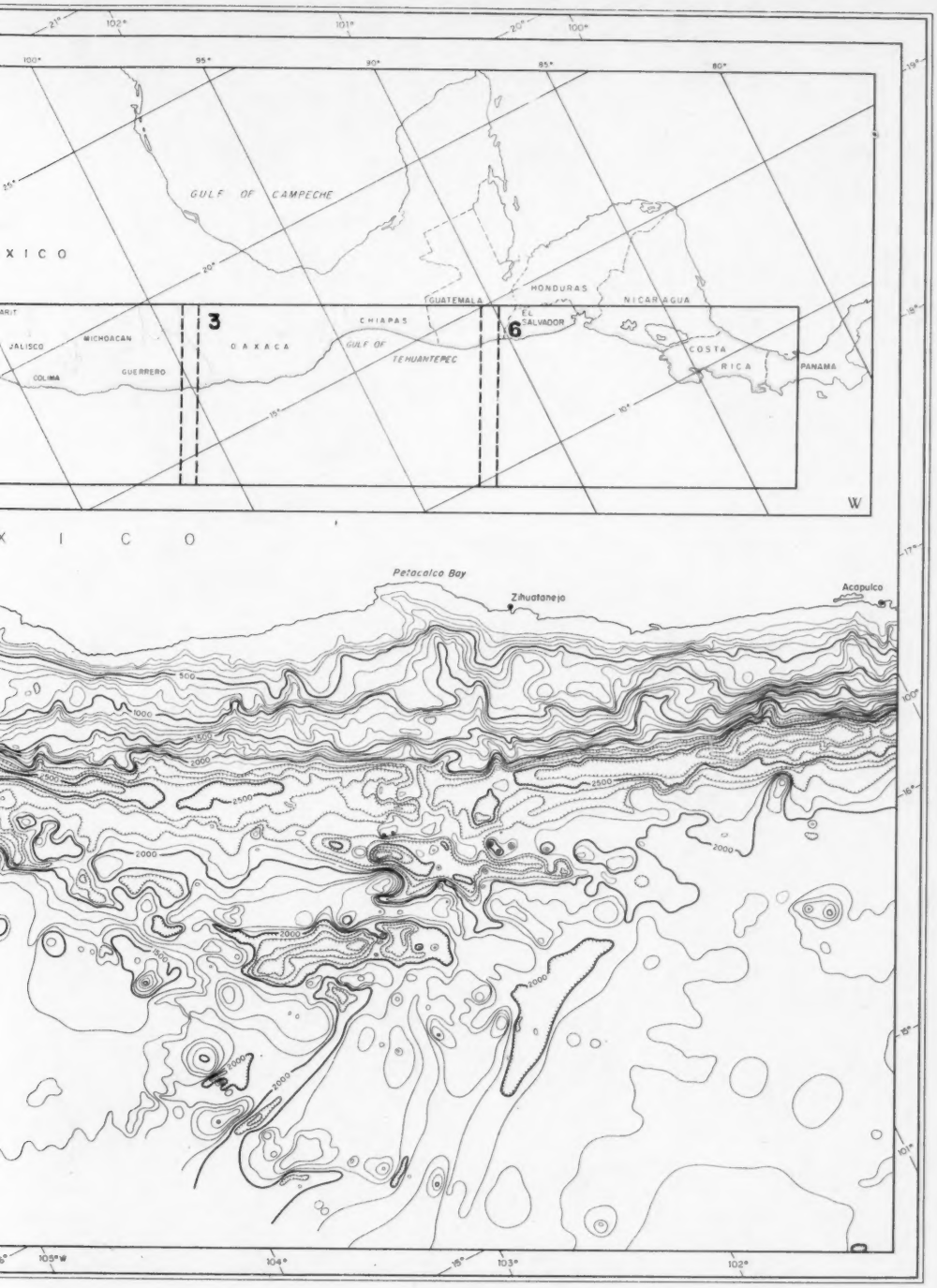

TO ACAPULCO, MEXICO

west of Mexico and Central America. Two north-south profiles, totaling seven stations, cross the trench at 98°20′ W. and 103°25′ W. According to Vening Meinesz (1948, p. 116), adjusted values suggest that off this coast a landward crustal block is riding over a seaward block, depressing it to form the trench.

In 1949, John G. Heacock, Jr., made 41 stations aboard the U.S.S. CHOPPER, along 1750 miles of track, in this area (Worzel and Ewing, 1952, p. 455). Heacock's gravity observations and interpretations are not yet published.

TOPOGRAPHY

Preparation of the Charts

During Scripps and N.E.L. expeditions of 1952–1958, research vessels recorded 27,900 miles of echo-sounding traverses in and adjacent to the Middle America Trench (Pl. 1A). On the 1959 Vermilion Sea Expedition 4050 miles of track was run in the region bounded by Banderas Bay, Mazatlan (23°10′ N., 106°28′ W.), and the southern tip of Baja California (22°52′ N., 110° W.). Each ship was equipped with Edo echo sounder modified to permit shoal scale recording speed on all ranges and calibrated to correct for instrument errors. On six of the cruises, input to each sounder was held at 60 cycles per second by a constant-frequency unit. Soundings from these instruments are precise to ±5 fathoms. During the Shellback and Eastropic expeditions, line frequency was noted, and the sounding as recorded was corrected to its equivalent at the standard 60 cycles. On the 1956–1959 expeditions the ships were equipped with "Precision Depth Recorder" similar to that described by Luskin *et al.* (1953). This unit, a modified commercial facsimile printer, records the output of the Edo echo sounder on a greatly expanded scale, so that soundings can be read with a precision of ±1 fathom under all conditions when a recordable bottom echo is detected. However, the relatively precise values recorded are subject to the usual difficulties of interpretation of echo sounding: side-echo effects, slope corrections, and sweeping by the sound cone as the ship rolls. Soundings were recorded in fathoms, assuming a nominal sounding velocity of 4800 feet/second. With the temperature-pressure-salinity conditions prevailing at depths of more than 500 fathoms in the region of the Middle America Trench, the true sounding velocity ranges from 4880 to 4960 feet/second. Soundings recorded on the Edo echo sounder, from which Plates 2, 3, and 6 were constructed, are 1½–3½ per cent too shoal. In deep water the increase in sounding velocity with depth is about 1 per cent per 1500 fathoms, so that conclusions as to bottom slopes within a basin, for example, are relatively accurate. Ships' positions were established by visual bearings on land, or by star sights that have a probable error of about 2 miles.

Plates 2, 3, and 6, plots of sea-floor topography contoured at 100-fathom intervals, were prepared from Scripps data, published and unpublished U. S. Hydrographic Office sheets, and 1150 miles of sounding lines recorded by the R/V GALATHEA. Sounding lines that agreed within 10 fathoms at crossings were accepted without adjustment. Preference was given to Scripps and N.E.L. soundings, then to GALATHEA and recent Navy soundings, then to old H. O. lines which crossed well with recent traverses (Pl. 1B). Many additional older or stray soundings were rejected. Slope corrections have not been applied. At great depths and steep slopes, the usually accepted first arrival echo distance may be significantly less than the depth beneath the ship (*e.g.*, Fisher, 1954). Occasionally in this study when an especially clear echogram was obtained, and particularly when clear echoes from a narrow but flattish trench bottom returned later than echoes from the walls, the wave trains were analyzed and the nominal true depth—the probable distance to the trench bottom vertically beneath the ship— was noted.

Dredged bedrock from Pacific seamounts investigated to date has been volcanic, and bathymetric surveys of seamounts usually show the peak to be conical, or nearly conical (see Menard, 1955, for example). Therefore, for this study stray or isolated shoal soundings have been contoured as conical peaks unless data on nearby lines strongly indicate the presence of a ridge. This practice may cause an unreal abundance of contoured peaks, since some shoals must be slightly mislocated duplicated soundings. The ridges, presumably of volcanic rocks, are contoured as nearly conical peaks rising from a low swell, not as small peaks between fairly shallow saddles, such as might be expected along fault-bounded ridges.

In the descriptions that follow, topographic characteristics such as shelf-break depth, trench bottom, trench terminations, and the nature of the landward and seaward flanks, each is discussed proceeding along the trench from northwest to southeast. The sea-floor relief outside

the seaward flank of the trench is discussed below under Topography Seaward of the Middle America Trench. Because the Gulf of Tehuantepec marks a boundary in the submarine topography, just as the Isthmus of Tehuantepec forms a boundary between two major structural provinces on land, the Tehuantepec region, both Isthmus and Gulf, is discussed in a separate section.

Topography Within and Shoreward of the Middle America Trench

Conclusions that may be drawn from Plates 2, 3, and 6 and study of Edo echograms are:

(1) The trench, sigmoid in plan, in general follows the Mexican-Central American shore line. The sharpest change in direction occurs just west of Tehuantepec, where it leaves the coast and trends nearly east-southeast for 400 miles. The change in trend is most marked at depth shallower than 1000 fathoms but persists to the bottom of the trench at 2600–2800 fathoms.

(2) At 2400 fathoms the trench is only 5–25 miles wide, but it is continuous at this depth for 1260 miles, except off Manzanillo and Zihuatenejo, where submarine mountain ranges intersect the axis. At 2700 fathoms it extends for 660 miles and at 3000 fathoms it continues for 380 miles as the Guatemala Deep.

(3) From configuration of the trench bottom, the Middle America Trench can be divided into two sections, with the boundary near 15° N., 95° 30′ W., off Tehuantepec.

From Islas Tres Marías to Tehuantepec, the bottom of the trench consists of flat-floored, elongate basins separated by ridges or seamounts (Pl. 2, 3). The bottom deepens, in a series of nearly horizontal steps, to a maximum depth of 2965 fathoms southwest of Acapulco. Such steps, especially well developed west and northwest of Manzanillo, suggest that sediment is being ponded behind hills or spurs of the trench flank (Pl. 4). Ponding in the Puerto Rico Trench has been reported by Ewing and Heezen (1955, p. 256). Similar basins, with much smaller flat floors at depths of 2780–2900 fathoms, continue to about 15° 15′ N., 96° W.

Southeast of 15° N., 95° W., the trench bottom drops steeply to a maximum of 3510 fathoms near 14° N., 93° 40′ W., continues deep in a series of very narrow elongated basins to 87° 30′ W., then shoals and widens gradually, with several basins, to end at about 84° W. (Pls. 3, 6).

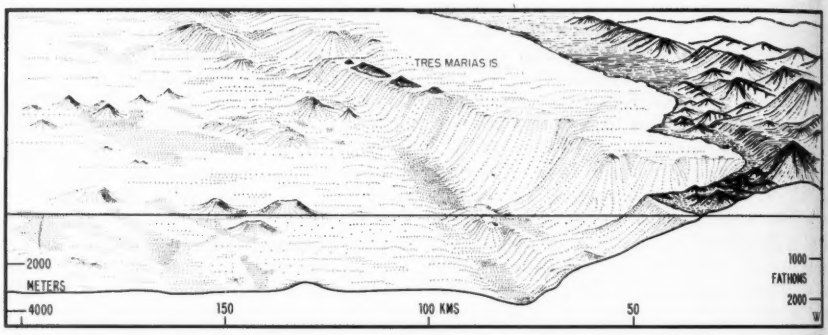

Figure 2. View to northwest from Banderas Bay. Vertical exaggeration 10 X. *See* Plate 1A for location of section.

(4) At 20° N. the trench axis bends northward and sharply intersects the Islas Tres Marías (Pl. 2). The north flank of the Tres Marías Basin, where the trench apparently ends, is a steep (>21°) slope. Several seamounts and a region shoaler than 1600 fathoms bound the basin on the northwest (Fig. 2). If projected, the axis of the rather straight Gulf of California would pass near 22° N., 108° W., about 60–75 miles west of the Islas Tres Marías. The present topographic study indicates that the Gulf probably is not a direct extension of the Middle America Trench.

To the southeast, the trench ends gradually against the northeast-trending Cocos Ridge (Pl. 6). Near 85° W., it is sharply constricted by a bulge in the continental slope and a group of seamounts on the trench south flank.

(5) Submarine canyons, like those off Cali-

fornia (Shepard and Emery, 1941), indent the shelf and upper continental slope, particularly along the narrow shelf northwest of Acapulco (Pl. 2). None of these canyons has been traced to the trench bottom; many, however, extend to depths of 600–800 fathoms. More detailed sounding may show that some of these canyons, V-shaped in cross section, continue to the bottom of the trench. Several canyons appear related in position to present-day river mouths.

Larger re-entrants, some branching and traversing the entire continental slope, occur off Banderas Bay (Fig. 2; Pl. 2), Manzanillo and Petacalco Bay (Pl. 2). Salina Cruz (Pl. 3), and San José and Puntarenas (Pl. 6). Banderas Bay is a structural trough, separating outcrop areas of middle Cenozoic intrusive rocks and early Cenozoic extrusive rocks on the north from Paleozoic metamorphic rocks on the south (Sanchez Mejorada, 1956). A very narrow, deep chasm extends along the south shore to the head of the bay. A shelf 5–7 miles wide borders the north shore of Banderas Bay and is developed west and south of Cape Corrientes. No shelf exists along the south shore of the bay; depths greater than 100 fathoms lie less than 1000 feet from shore. The trough near Manzanillo has slope reversals along the axis and several peaks bordering the broad valleys. Others are asymmetrical in cross section. Most have wide heads and steplike longitudinal profiles. Similar large sea valleys on the north flank of the Aleutian Trench have been described by Gates and Gibson (1956, p. 139–143). Those authors suggest a fault origin for the valleys and show that some of them lie along or near projected trends of faults mapped on the islands. Udintsev (1955, Fig. 4) reports such features bordering the Kuril-Kamchatka Trench. Unlike their possible counterparts in the Aleutian region, most of the Middle America Trench sea valleys are aligned nearly normal to the continental slope. However, the reversals in slope and the U-shaped cross sections commonly developed suggest a tectonic origin, at least in part, for these interlobate valleys; they are probably related to the unusually irregular topography, both within and just outside the trench, adjacent to most of them.

During the 1952–1959 cruises, 121 echo-sounding profiles were made across the Middle America Trench. Echograms of parts of three such profiles are reproduced in Plate 5. Additional conclusions from a study of all the echograms include:

(6) From Islas Tres Marías to Manzanillo, the shelf break is at 55–60 fathoms, where a nearly horizontal shelf is terminated rather sharply.[1] Possible evidence of local warping exists in two tilted benches, which deepen landward, cut on a submerged pinnacle southeast of María Cleopha Island.

Off Acapulco, the depth of the shelf break ranges from 55 to 140 fathoms within a distance of 20 miles, as determined from crossings nearly normal to the coast. The steeply dipping shelf shoreward of the deeper breaks suggests that here the shelf has been locally warped or faulted downward.

From 30 miles southeast of Acapulco to just west of Port Angeles, except for the somewhat anomalous shelf topography of Tartar Shoal, the shelf is very narrow to nonexistent. The shelf break ranges in depth from 65 to 100 fathoms; most normal crossings indicate depths of 70–90 fathoms. Here faulting is suggested; the depths do not increase or decrease progressively along the coast.

The depth of the shelf breaks south of the Isthmus of Tehuantepec was the subject of special study on the 1956 Acapulco Geological Expedition and is discussed below.

From Champerico to the Golfo de Nicoya the shelf break, at 59–90 fathoms, sharply terminates the wide shelf.

(7) Continental slope morphology differs east and west of the Gulf of Tehuantepec, although in both areas steepness generally increases with depth, and one or more deep breaks in slope occur in many places.

To the northwest, average slope of the landward wall of the trench is 10°–14°; some slopes are as low as 5° and, off María Cleopha Island (Fig. 2) and Acapulco, as great as 24°. The surface is irregular, and peaks rise 50–300 fathoms; there are many submarine canyons on the upper part of the slope.

Southeast of Tehuantepec the slope is more gentle, ranging from 4° to 8°, and smoother; its few pinnacles are only 20–50 fathoms high. Some large valleys traverse the slope (Fig. 3).

(8) Most profiles northwest of Acapulco show a broad, nearly flat trench bottom (Pl. 5, upper profile), except where mountain ranges intersect the axis, as near Manzanillo and Zihuatanejo. On these basin floors, the bottom

[1] In this discussion of the depth of the shelf break the writer assumes that along this coast the shelf break is due primarily to wave abrasion related to some past lowered sea level, as discussed by Dietz and Menard (1951).

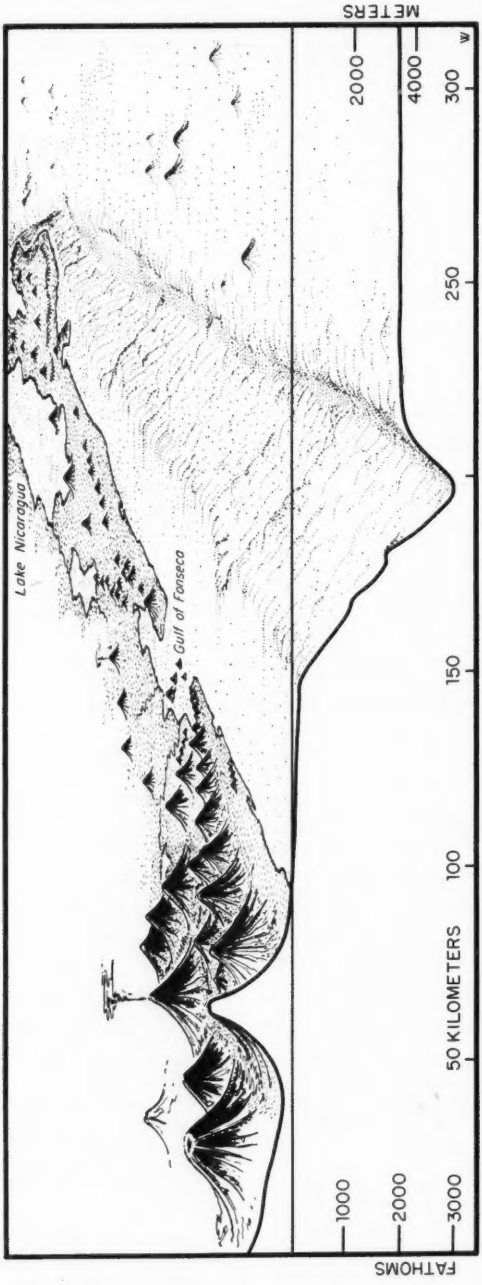

Figure 3. View to southeast from La Libertad, El Salvador. Vertical exaggeration 10 X. *See* Plate 1A for location of section.

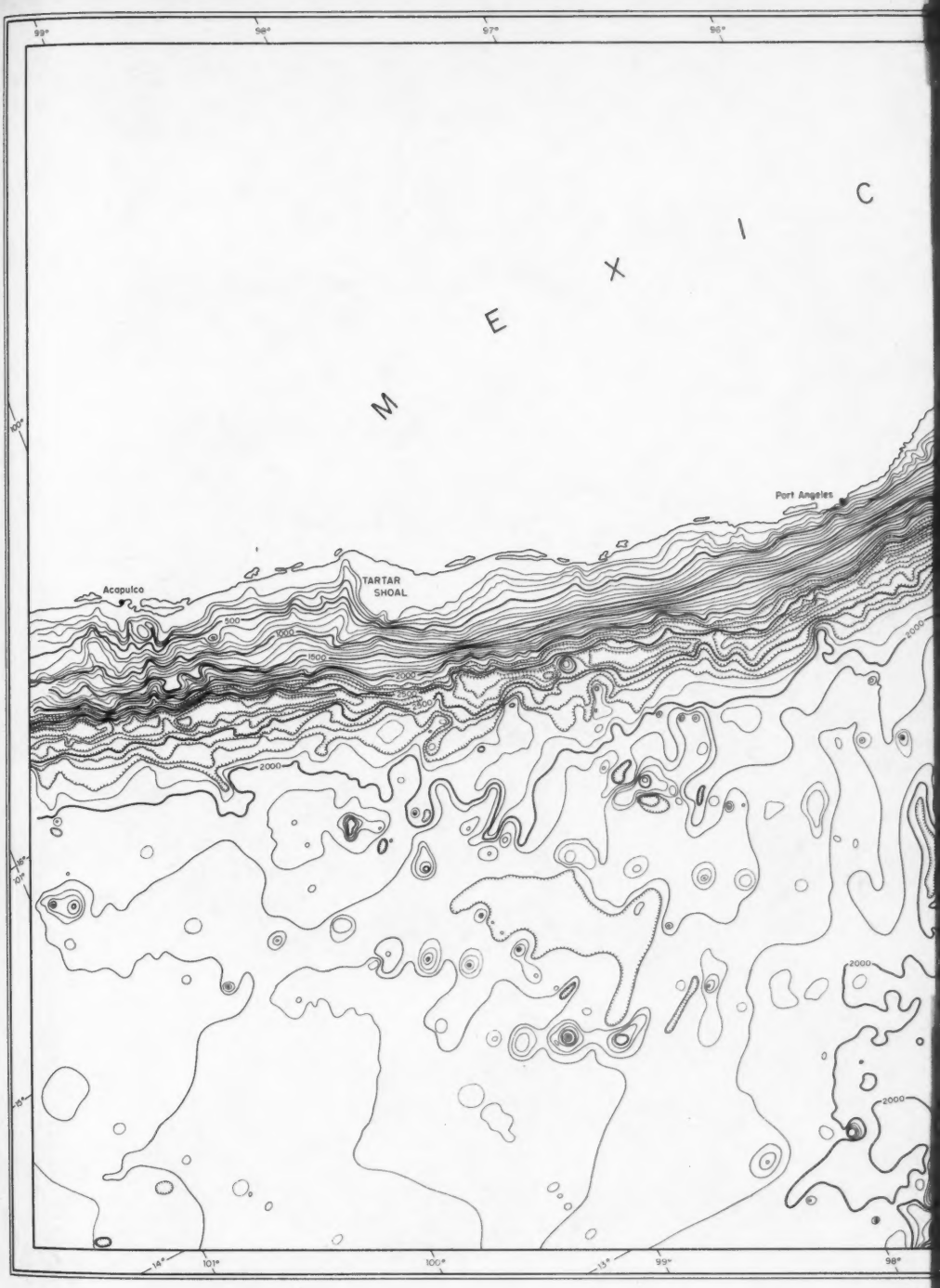

SUBMARINE TOPOGRAPHY,

FISHER, PLATE 3
Geological Society of America, volume 72

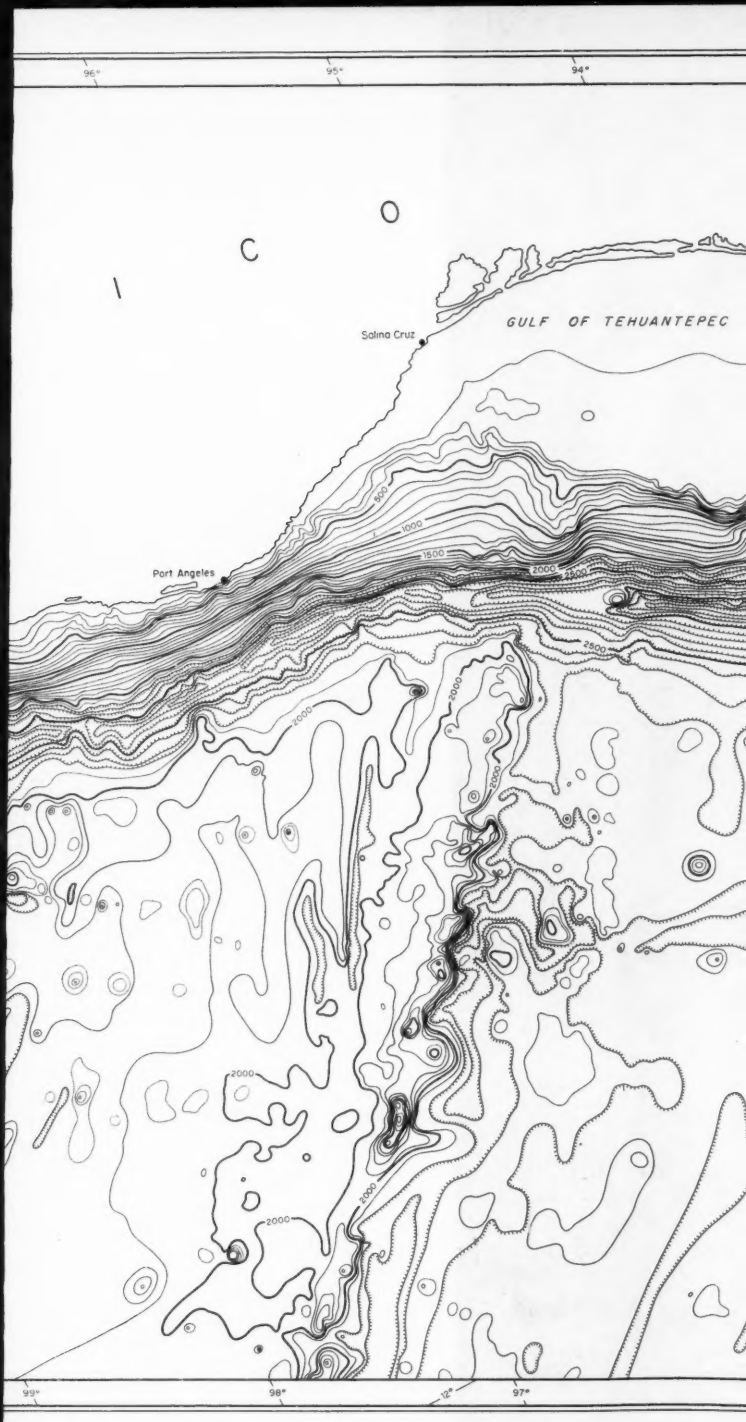

SUBMARINE TOPOGRAPHY, FROM ACAPULCO, MEXICO, TO SAN JOS

SAN JOSÉ, GUATEMALA

commonly rises 5–10 fathoms toward the land and seaward flanks, although sharp breaks in slope occur at the edges of the basin. Some echograms show knolls projecting 50–100 fathoms above the trench floor.

In the deepest portion of the trench, extending from the east side of the Gulf of Tehuantepec to the Gulf of Fonseca, the trench is V-shaped in profile, with little bathymetric evidence of sedimentary fill (Fig. 3; Pl. 5, middle profile). As the trench shoals toward the Cocos Ridge, its bottom widens, but the deepest portions are not quite flat (Pl. 5, lower profile).

(9) Off Jalisco, the seaward flank of the trench is smooth and rises gently (at ½°–2°); off Colima, Michoacan, and northwestern Guerrero it is steeper (3°–10°) and irregular, and peaks 150–300 fathoms high project from the slope. Off southeastern Guerrero and Oaxaca the outer slope rises smoothly, at 1°–3°, to depths of 1800–1900 fathoms.

Southeast of Tehuantepec, the seaward flank slopes upward at 2°–6° to a low swell or to nearly flat bottom, except southwest of Nicoya where isolated groups of seamounts locally constrict the trench, steepening the outer flank.

Topography Seaward of the Middle America Trench

Sea-floor topography west and south of the trench differs in character in four regions where rough bottom is best developed.

(1) West of 105° W., between 15° N. and 23° N. (Pl. 2), the sea floor is shallow (1500–1800 fathoms) with many seamounts, probably volcanoes, capping broad swells. The trends of some of the swells are real as shown; other trends merely follow ships' tracks. In this volcanic field a random distribution of peaks seems likely. Nearly all the earthquakes seaward of the trench occur in this region; all are shallow shocks, with computed epicenters plotting north of 17° N. and west of 105° W. (Gutenberg and Richter, 1954, p. 168–169; Coast and Geodetic Survey, 1948–1958). The only extensive deep areas within this region lie 100–250 miles east of the volcanic island of San Benedicto; they may be part of the east-trending Revillagigedo structure.

(2) Southwest of Zihuatanejo, two elongate deeps, separated from the trench axis and from each other by pinnacle-topped ridges, lie subparallel to the trench (Pl. 2). Steep-walled and flat-floored, at 2450 and 2800 fathoms, they are 150–450 fathoms deeper than the trench proper adjacent to them, where an irregular ridge intersects the axis. The writer suggests that such bordering deeps are fault troughs, and that formation of the deeps and ridges occurred as adjustments after the trench was formed. Generally off Mexico the trench cross section is regular, though asymmetrical; the sea floor drops steeply to a flat or nearly flat trench bottom, then rises more gently offshore. Near Zihuatanejo, however, the trench bottom is both shallow and irregular and has peaks several hundred fathoms high. Locally the offshore flank is the steeper, with one or more peaks apparently superposed on the more normal gentle offshore slope. The flat bottoms in the troughs mentioned above probably resulted from the sediment moving downslope from the neighboring peaks, though no aprons were detected.

(3) A band of irregular topography, 60–120 miles wide, separates the gently rolling, 1850- to 1950-fathom sea floor off southern Guerrero and Oaxaca from the even flatter 2100- to 2200-fathom Guatemala Basin off Chiapas and Guatemala. This zone, termed the Tehuantepec Ridge by Menard and Fisher (1958), extends at least 420 miles southwest from the seaward flank of the trench off southern Oaxaca. The best explored segment, between 12° N. 98° W. and the trench, is shown in Plate 3. Here 24 echo-sounding lines give very similar profiles. Along a northwest to southeast traverse, the zone begins in most places with a broad depression, 100–150 fathoms deeper than the regional depth to the west. The sea floor then rises gently to a swell or ridge with a depth along its axis that has been contoured on Plate 3 as less than 1700–1800 fathoms in most places. Because of the spacing of the soundings, possibly the 1600-fathom contour should be drawn more extensively, to indicate a shoaler ridge than has been shown in Plate 3. However, of the 11 accepted sounding lines that might be considered random in that the ships reporting them were just passing through the area, only five show soundings shoaler than 1750 fathoms. Several seamounts, one with a minimum depth of 990 fathoms, have been found along the ridge. The east flank descends sharply into one of a series of narrow, nearly flat-bottomed elongated depressions. The sea floor then rises 150–250 fathoms to the regional depth of 2100–2200 fathoms in the Guatemala Basin off Chiapas and Guatemala. A marginal depression 150–200 fathoms deep, lying 50–90 miles east

of the ridge and trending nearly east-west, has been contoured from an older, generally reliable line.

(4) The Guatemala Basin shoals to the southeast. West of Costa Rica, isolated seamounts rise from a smooth, 1700- to 1800-fathom bottom (Pl. 6). One notable group lies just outside the southeast end of the trench and another at 9° 30′ N. Guardian Bank, largest and shoalest of the shallow areas reported off Costa Rica, was not found by ships on the 1952, 1954, and 1955 cruises, despite special searches at and near its various reported positions.

Topography of the Gulf of Tehuantepec

A linear structure such as that described in the preceding section, an asymmetrical ridge with narrow flanking deeps, separating large areas with several hundred fathoms difference in regional depth, is characteristic of the "fracture zones" of the northeastern Pacific, as described by Menard (1955). The best-explored zones discussed by Menard have been traced several hundred miles seaward from the North American coast and projected landward across the continental margin. If the linear structure off Oaxaca is part of such a major zone, it might be expected to continue seaward for hundreds of miles and, in the landward direction, to cross the trench and shelf and affect the structure of the Isthmus of Tehuantepec (Pl. 3).

Three weeks of the scientific program of the 1956 Acapulco Geological Expedition consisted of making echo-sounding runs across the upper continental slope and the shelf in the Gulf of Tehuantepec, and in exploring the westward extension of the zone of ridge-and-trough topography. Plate 1A shows the track of the expedition. A detailed discussion of this "fracture zone" (?) has been published (Menard and Fisher, 1958): the northeast trend has been traced definitely from the south flank of the trench to 10° N., 100°–101° W., where it joins the nearly east-trending "Clipperton fracture zone" indicated by Menard. Apparently the northeast-southwest "fracture zone" (?) intersects the trench between 95° W. and 96° W., as suggested by (1) the shoal axial depth at that point, (2) constriction of the trench by peaks on the south flank and a bulge, to 1000 fathoms or greater, on the north side, (3) the peak lying along the trench axis just south of 15° N., 95° W., and, possibly, (4) by the irregularities in the 100-, 200-, and 300-

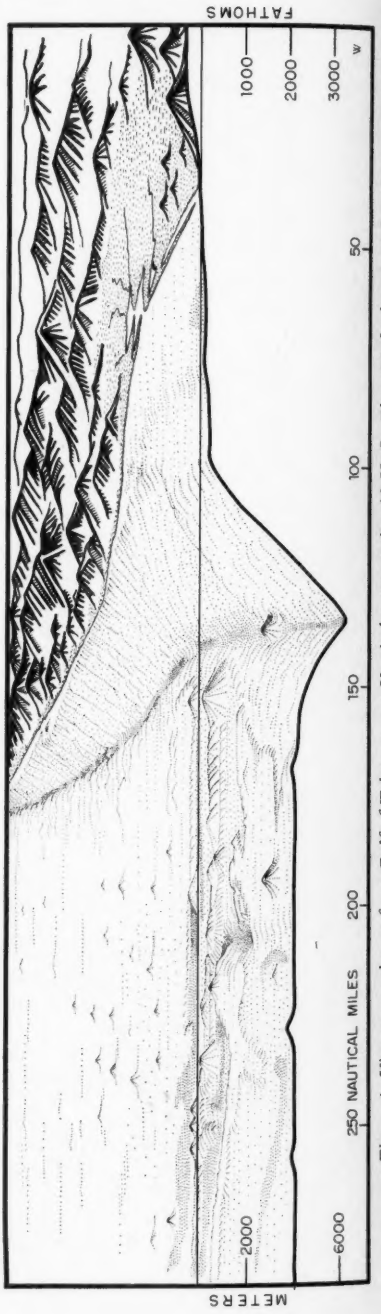

Figure 4. View to northwest from Gulf of Tehuantepec. Vertical exaggeration 10 X. *See* Plate 1A for location of section.

fathom contours south of Salina Cruz (Fig. 4).

On the 1956 cruise, 23 echo-sounding profiles nearly normal to the shelf break and upper slope were made between 97° W., near Port Angeles, and the Guatemala border. Eighteen of these lines show a deep shelf or terrace, with a drop-off at 155–200 fathoms, lying downslope from the more usual 70- to 90-fathom shelf break. The occurrence of this deep shelf detected farthest west is just east of Port Angeles, and it continues with a recognizable break in slope at about 200 fathoms to near 95° 15′ W., south of Salina Cruz. Between Salina Cruz and the large canyon near 93° 30′ W. the deep break lies at 165–175 fathoms, and the shallow shelf break is not well developed. It may represent warping rather than a stillstand at sea level. Southeast of Champerico only one shelf break, at 65–90 fathoms, was found. West of Salina Cruz both the shallow and deep shelves are narrow and thus steep in slope. East of Salina Cruz the shallow and deep parts of the shelf are wide; a steep-sided depression, 5–10 fathoms deeper than the adjacent shelf, was found shoreward of the possible shallow shelf break on four sounding lines. Apparently the canyon south of Salina Cruz forms a boundary for both shelves. The deeper part of the shelf begins to slope upward at about 95° W. Southeast of the canyon at 93° 30′ W. the deeper shelf slopes upward more sharply and narrows until it merges with the upper shelf.

The above description indicates that along the trench as explored to date a series of deep breaks in slope, suggesting a downwarped or downfaulted shelf below the more normal shallow shelf, is developed only in the Gulf of Tehuantepec. The variation laterally in vertical separation of the two breaks in slope and the depression shoreward of the shallower shelf break indicate that faulting across the shelf may have been important south of the Isthmus of Tehuantepec.

The most detailed recent survey of the geologic structure of the Pacific side of the Isthmus is summarized by Webber and Ojeda R. (1956). These authors conclude that Tertiary deformation in this region consisted of faulting, chiefly vertical, along two fault systems. The chief event was the dropping and slight tilting to southward of a triangular block with its base in the present gulf. This block, bounded on the west by northeast trending faults passing near 16° 30′ N., 96° W., and on the east by a north-trending fault system near 94° 20′ W., dropped 1500 feet in relation to the Chiapanecan block to the east. The motion had an unspecified lateral component. This faulting was Miocene, probably Late Miocene, as established by offset of dated volcanic flows.

Although this information from the nearby land establishes neither the date nor magnitude of possible faulting on the shelf, it shows that vertical movements of considerable extent have occurred very near the shelf. This faulting has taken place along fairly extensive fault systems, some members of which have been traced to the present shore line, and may represent a shoreward expression of the extensive linear structure seaward of the trench off the Tehuantepec region.

Bathymetric Evidence for Sedimentary Fill in the Middle America Trench

Most of the echograms recorded during the 1952–1959 explorations of the Middle America Trench are of sufficiently high quality to permit analysis in an attempt to learn the nature and the thickness of the material that constitutes the nearly flat floor of the trench over much of its length.

Several echograms have been studied to determine bottom slopes within three of the basins or ponds on the trench floor. The echogram shown in Plate 4 includes traverses along three steps in the trench bottom, finishing on the southeast with a crossing at about 50° to the trend of the trench. Since frequency input to the Edo echo sounder was held at 60 cycles per second and the records are clear, the soundings can be read to ±5 fathoms. In these basins the depths recorded vary in a consistent manner. Hence, the slight slopes indicated are believed real. Bottom slopes within one or another of the three ponds or basins range from nearly horizontal to as much as 0.01⁻, the steepest slopes occur near the trench walls, and most slopes are 0.001–0.003.

In a discussion of deep-sea cores from the North Atlantic, Ericson, Ewing, and Heezen (1952) state that large quantities of sediment of shallow-water origin have been deposited in the deep basins by turbidity currents flowing down steep submarine slopes and out over the very gently sloping deep-sea floor. Their principal criteria for shallow-water origin of these sediments are graded sand and silt layers and tests of shallow-water benthonic organisms, chiefly Foraminifera. In the Atlantic, cores containing an abundance of such material have been taken in areas where bottom slopes are only 0.001–0.002. Foraminifera from the

Figure 4. View to northwest from Gulf of Tehuantepec. Vertical exaggeration 10 X. *See* Plate 1A for location of section.

Middle America Trench cores have not been examined in detail, but studies already made indicate the presence of displaced fauna. Piston cores from the trench bottom off Acapulco contain graded sand and silt layers and fragments of organic debris, possibly wood, at depths of 8–10 feet in the core. The writer suggests that the flat trench bottom results from deposition of sediments carried down the trench walls by turbidity currents on the nearshore flank and by slumps down the offshore flank. Such mass movements might be expected in a region of frequent earthquake activity, such as coastal Mexico. As these sediment-laden currents moved out from the trench walls they slowed and deposited their loads as the very gently sloping aprons now observed. Similar occurrences have been discussed by other authors (*e.g.*, Hersey and Rutstein, 1958).

Table 1. Maximum Depth of Fill in the Middle America Trench, as Deduced from Bathymetric Records

Region	Possible range of thickness (in km)	Probable thickness (in km)
Tres Mar'as Basin, near seismic station 1	0.2 –0.65	0.6+
Tres Marías Basin, near seismic station 1	0.5	0.5
Tres Marías Basin, near seismic station 1′	0.4+	0.4
Tres Marías Basin, near seismic station 1′	0.45	0.4
West of Manzanillo	0.45–1.0	1.0
Southwest of Manzanillo	0.2 –0.4	0.4
South of Manzanillo	0.08–0.2	0.2
Southwest of Petacalco Bay	0.45–0.9	0.7
Southwest of Acapulco	0.04–0.05	0.05
South of Acapulco	0.3 –0.4	0.35
Southwest of Champerico	0.01–0.02	0.02
South of Champerico	Not detected	
South of San José	0.02–0.04	0.035
South of Gulf of Fonseca	0.02–0.04	0.03
Southwest of San Juan del Sur	0.07	0.07
West of Gulf of Nicoya	0.03	0.03
South of Gulf of Nicoya	0.05	0.05

Echograms of most of the 121 trench crossings, such as those shown in Plate 5, have been examined to obtain data on the probable thickness of the material partially filling the trench and resulting in a nearly flat trench bottom off most of Mexico, Nicaragua, and Costa Rica (Pl. 5, upper and lower profiles). On each crossing, the apparent width of the flat bottom giving a strong echo was noted. The slopes of the trench walls were computed and, where necessary, slope corrections made. Several crossings were normal to the trench axis; others have been projected to normal crossings, in which apparent width of the flat bottom is at a minimum and slope of the trench walls is at a maximum. These corrections tend to balance one another, as far as computed fill is concerned. For each profile, the observed side slopes were projected to intersection, and the maximum value for possible fill noted. This operation was then repeated using the extreme values of side slope for each region in order to cover the probable range in thicknesses and to allow for changes in the wall slopes with depth.

Computations from these bathymetric data suggest that moderately thick fill is present only in the Tres Marías Basin and near Manzanillo and that there is almost no fill off Guatemala. They also indicate rapid changes in the amount of fill in short distances along the trench, as for example near Manzanillo. Representative values computed from bathymetric data are presented in Table 1.

A similar calculation was made to learn the thickness of fill in one of the suggested fault troughs offshore of the trench off Zihuatanejo; very tentatively, a value of 0.3–0.4 km seems likely.

DISCUSSION

The Middle America Trench, though bordering a continent and shallower than the western Pacific trenches, exhibits most of the phenomena associated with trench—island-arc systems (Gutenberg and Richter, 1954, p. 36). It has negative gravity anomalies and many shallow-focus earthquakes along its length and active vulcanism and intermediate-focus shocks landward of the Central American section. The abundance of seamounts and the shallow seismicity seaward of the trench west of Colima and Jalisco, and the irregular topography interrupting the trench off Michoacan, are considered indicative of tectonic activity that may postdate the early stages of the formation of the trench.

Echo sounding and seismic interpretations (Shor and Fisher, 1961) differ as to amount of sediment in the trench bottom, except that

ECHOGRAM OF TRAVERSE ALONG TRENCH NORTHWEST OF MANZANILLO, MEXICO

Vertical exaggeration 15 X. *See* Plate 1A for track. The dark zone recorded at 2400–2450 fathoms is the outgoing signal. The slightly lighter zone at 2500–2600+ fathoms on the tape is the corresponding return from the "deep scattering layer," which in this case actually lies at 100–200+ fathoms.

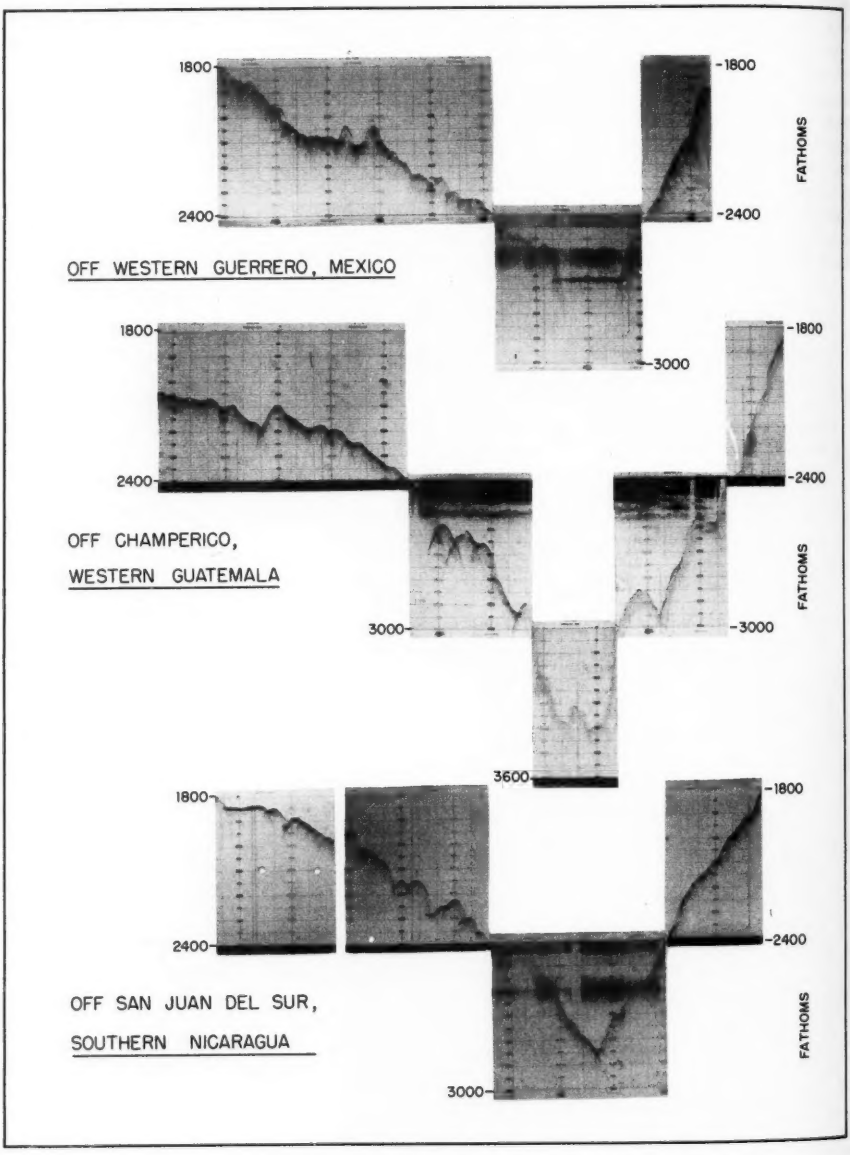

ECHOGRAMS OF TRAVERSES ACROSS THE MIDDLE AMERICA TRENCH

Vertical exaggeration about 15 X. *See* Plate 1A for tracks. Note the strong echo from the flat trench floor off Guerrero and from the narrow flat floor off Nicaragua.

sediments are considerably thicker in the Tres Marías Basin and near Manzanillo than elsewhere along the trench axis. Little significance is attached to apparent differences in sediment thickness found on other seismic lines. Inserting a totally masked layer of about 4 km/sec velocity below the 2.15 km/sec sedimentary layer reduces the computed thickness of sedimentary fill to agree more nearly with values obtained from interpretation of the echograms. Bathymetric profiles strongly suggest more fill off Central Mexico than off Chiapas, Guatemala, El Salvador, and Nicaragua, despite possible important contributions of ash from the Central American volcanoes to the southern part of the trench. The apparently thicker fill off Mexico may be due to a greater age of this portion of the trench, to a more ample source of sediment, or to the narrowness of the indented shelf northwest of Acapulco, which could allow land-derived material to move more readily across the shelf to the steep trench flank and thence downward by slumping to the bottom. Southeast of Tehuantepec, such material would more probably settle on the broad shelf; there trench-bottom deposits would be largely ash. The average thickness of sediments in the Middle America Trench appears intermediate between the very thin (<200 m) volcanic (?) detritus of the Tonga Trench (Raitt, Fisher and Mason, p. 249, 1955) and the reportedly 2- to 3-km-thick turbidity-current deposits of the Puerto Rico Trench (Ewing and Heezen, p. 265, 1955; Talwani *et al.*, 1959, p. 1550).

The crustal structure deduced for the Middle America Trench may be compared with that of the Tonga Trench reported by Raitt *et al.* (1955). The presence of a basement layer with velocity of 5.2±0.1 km/sec was observed beneath and landward of the Tonga Trench. The presence of layers with similar intermediate velocity several kilometers thick was detected beneath the continental shelf off Guatemala, and a layer perhaps 1 km to 2 km thick probably exists beneath the sediments in the Middle America Trench. Thickness of the lower crustal layer (velocity 6.5–7.0 km/sec) increases from 4.5, 5.0, and 5.2 km on the Tres Marías Basin, Manzanillo, and Acapulco trench-axis lines, respectively, to 7.6 and 7.7 km on the corresponding lines off Central America. The latter values are comparable to the thickness (more than 8 km) found for the corresponding layer beneath the Tonga Trench, which is 3.5–4 km deeper (Raitt *et al.*, 1955, p. 248).

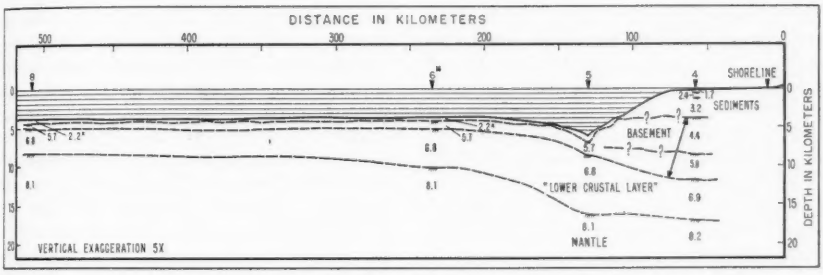

Figure 5. Schematic structure section off western Guatemala. *See* Plate 1A for location.

The mantle, with velocities of 7.7–8.5 km/sec, lies at about 10.8 km below sea level in the Tres Marías Basin, 11.7 and 12.2 km off Manzanillo and Acapulco, then deepens to 16.2 and 14.9 km off Guatemala and Nicaragua, respectively. By any method of interpretation tried, present travel-time data indicate that, along the trench axis, the crust is thicker off Guatemala and Nicaragua than off Central Mexico, notwithstanding the greater thickness of sediments in the Tres Marías Basin and near Manzanillo.

Figure 5 is a schematic structural cross section, normal to the trench off western Guatemala, based on interpreted travel-time data of seismic lines on the shelf, in the trench, and offshore. The section crosses near the midpoint of profile 4–4′ and of profile 5–5′ (Shor and Fisher, 1961, Fig. 1), and that of 8 well outside the trench; station 6 has been shifted westward to fall on the section. At the positions where seismic lines cross the section, depths of the various layers, computed using regional

velocities, are indicated by hachured interfaces. The dashed lines are possible interpolations, if the upper three layers of the shelf lines are considered as sediments in different stages of compaction, and the fourth and fifth layers are combined as basement complex (volcanic rocks?, plutonic rocks?). Any sediment-basement and basement-lower crustal layer contacts are probably more irregular than shown here. Although the subsurface information is sparsely distributed, several conclusions can be made regarding trench structure off western Guatemala:

(1) Below the trench axis, the M discontinuity is 6 km deeper than in the Pacific Basin to the west, and less than 1 km shallower than beneath the outer shelf 70 km to the northeast. There is no indication of a tectogene-like bulge of crustal material into the mantle beneath the trench. At station 6 the estimated depth to the mantle, about 10 km, is shallower than its depth at the average Pacific Basin station (Shor and Fisher, 1961, Table 2). Thus the depth to the mantle beneath the trench is about 5 km greater than in the average of the Pacific stations.

(2) A thick section of material with velocity of 3.5–6 km/sec (volcanic rocks?, metamorphosed sedimentary rocks?, sialic intrusive rocks?) is present beneath the outer portion of the shelf. This section thins rapidly seaward, although it may persist as a thin basement layer beneath and outside the trench.

(3) Whether or not basement rocks are present beneath and outside the trench, the lower crust is about half again as thick beneath the trench as beneath the outer station or the average Pacific Basin station. Though of smaller dimensions, this Middle America Trench section more nearly resembles the Tonga Trench structure deduced by Raitt *et al.* (1955, p. 253) and the Peru-Chile Trench structure reported by Raitt (1958, p. 37) than the Mindanao or Puerto Rico trench sections as interpreted by Worzel and Shurbet (1955, p. 93–96) or the Tonga Trench reinterpretation offered by Talwani, Worzel, and Ewing (1959).

However, differences in crustal sections proposed may be more a matter of the kind of data available than of actual structure. For the Tonga, Peru-Chile, and Middle America trenches work, seismic-refraction data were used, with records from waves traveling in the layers down to and including the upper mantle beneath the trenches. Worzel and Shurbet constructed "standard" oceanic and continental crustal sections from gravity and averaged seismic data. Working from the standard sections, they based their schematic crustal structure of the Mindanao Trench on gravity computations and that of the Puerto Rico Trench on gravity computations supported by seismic data from the sediment layer in the trench proper and from some of the deeper layers outside the trench. Both computed sections contain a locally thinned (lower) crustal layer overlain by more or less sediment along the trench axis. According to Ewing and Heezen (1955, p. 266), "The fact that a local thinning of the crust can better explain the gravity results leads one to the conclusion that tension rather than compression may be the dominant force involved in the formation of the trenches." Without going more deeply into the question of forces forming trenches, the present writer wishes to point out that the interpreted results for the Middle America Trench off western Guatemala as here reported, and those from the Tonga and Peru-Chile trenches, apparently do not support this conclusion. Additional gravity and seismic observations in the Puerto Rico Trench, reported by Shurbet and Worzel (1957, p. 263–266), have been interpreted by those writers as indicating that sediments in that trench are not so thick as they previously supposed and that "Some thickening of the crustal rock section under the trench is shown by the seismic data and confirmed by the gravity calculations" (p. 266).

Talwani, Sutton, and Worzel (1959) give a detailed seismic and gravity section across the Puerto Rico Trench. They show (Fig. 3, p. 1550) a considerably greater depth to the M discontinuity under the trench axis from seismic- refraction observations than by gravity computations. They note that the difference could be due to structural variations transverse to the section. The refraction measurements reported in greater detail by Officer *et al.* (1957) indicate a crustal thickness there of about 10 km and a lower crustal-layer thickness of 7–8 km, very similar to those reported for the Middle America and Tonga trenches.

Heacock's gravity observations should prove of special significance in this connection. According to a published station chart (Worzel and Ewing, 1952, p. 455), five of Heacock's stations, numbers 960–964, lie within 60 miles of the Champerico section figured here; the two profiles cross at about 60° near station 6.

Since the depth below sea level to basement along the axis of the Middle America Trench,

from the Islas Tres Marías to the Gulf of Fonseca, probably is of the order of only 5–7 km, and since the trench borders a continental structure rather than an island arc, perhaps it is more appropriate to compare its deduced structure to that found at, for example, the continental slope off southern California rather than the postulated structure of the classic deeps of the western Pacific or the Puerto Rico Trench.

A recent paper by Shor and Raitt (1958) describes their seismic-refraction studies in the southern California continental borderland. They include a schematic structure section (Fig. 2, p. 249) drawn from the deep sea across the slope and borderland to the mainland. The section is a composite, based on work during several years. The western 60 km of the section, with five stations included, passes from the deep Pacific across the continental rise and slope up to the 1-km-deep shoal known as Patton Ridge, the ridge directly shoreward of the Patton Escarpment (Shepard and Emery, 1941, Pl. 1), and may be compared with the structure section drawn off Guatemala (Fig. 5).

From the structure sections as drawn, the following comparisons seem valid:

(1) Velocities obtained and layer identifications are similar (Table 2).

(2) At the base of the continental slope, the depth from sea level to basement is 5–6 km, about 1 km shallower than in the trench off Guatemala.

(3) Off the borderland, the mantle lies at so-called "oceanic depth," 9–11 km, as close to the base of the continental slope as it can be measured. Beneath the trench, at the base of the slope, the depth below sea level to the mantle is 15–17 km.

(4) Beneath the 1-km-deep Patton Ridge, 30–35 km northeast of the base of the continental slope, the computed depth to the M discontinuity is 17 km, very similar to the 15–18 km depth to the mantle beneath the outer, 0.1-km-deep shelf 70 km northeast of the trench off Guatemala.

(5) A thick shallow mass, with velocity of about 5 km/sec, lies beneath Patton Ridge but thins rapidly at the continental slope. A possibly similar mass, with velocity of 4–6 km/sec, underlies the outer shelf off Guatemala but thins rapidly toward the trench.

Table 2. Velocities of Refracting Layers

Layer	California velocities (km/sec)	Guatemala velocities (km/sec)
Sediments	1.8–2.8	1.7–3.2
Basement complex, possibly volcanic rocks or consolidated sediments	4.6–5.1 5.9–6.2	4.4 5.7–5.9
"Lower crustal layer"	6.7–7.0	6.8–6.9
Mantle	8.1–8.2	8.1–8.2

(6) The "lower crustal layer" (velocity 6.7–7.0 km/sec) thickens in the landward direction from 4.5 to 8 km in a distance of 45 km in the schematic section off California. Off Guatemala (observations were more widely spaced here), it increases from 5 km at 6 to 7.6 km at 5, then thins to 5 km beneath the outer shelf, in a horizontal distance of 175 km.

The most striking difference in the two sections is that off the borderland the rapid transition to a deep mantle occurs landward of the base of the continental slope, and off Guatemala the deepening of the mantle occurs seaward of the trench. In this respect, the structure of the moderately deep trench off the continental margin of Central America more nearly resembles that of the very deep trench off the Tonga island arc than of the seaward margin of the southern California continental borderland.

REFERENCES CITED

Agassiz, A., 1906, Reports on the scientific results of the expedition to the eastern tropical Pacific . . . 1904–5 . . ., v. 5, General report of the expedition: Cambridge, Mass., Harvard Coll., Mus. Comp. Zool. Mem., v. 33, 75 p.

Benioff, Hugo, 1954, Orogenesis and deep crustal structure—additional evidence from seismology: Geol. Soc. America Bull., v. 65, p. 385–400

Coast and Geodetic Survey, 1948–1958, Preliminary determination of epicenters: Washington, D. C., U. S. Dept. Commerce

Dietz, R. S., and Menard, H. W., Jr., 1951, Origin of abrupt change in slope at continental shelf margin: Am. Assoc. Petroleum Geologists Bull., v. 35, p. 1994–2016

Ericson, D. B., Ewing, M., and Heezen, B. C., 1952, Turbidity currents and sediments in North Atlantic: Am. Assoc. Petroleum Geologists Bull., v. 36, p. 489–511

Ewing, M., and Heezen, B. C., 1955, Puerto Rico trench topographic and geophysical data, p. 255–267 *in* Poldervaart, A., *Editor*, Crust of the earth: Geol. Soc. America Special Paper 62, 762 p.

Fisher, R. L., 1954, On the sounding of trenches: Deep-Sea Research, v. 2, p. 48–58

Fisher, R. L., and Revelle, R., 1955, The trenches of the Pacific: Sci. Am., v. 193, no. 5, p. 36–41

Fisher, R. L., and Shor, G. G., Jr., in press, Topography and structure of the Middle America Trench: Mexico, 20th Intern. Geol. Cong. Proc.

Gates, O., and Gibson, W., 1956, Interpretation of the configuration of the Aleutian Ridge: Geol. Soc. America Bull., v. 67, p. 127–146

Gunn, Ross, 1947, Quantitative aspects of juxtaposed ocean deeps, mountain chains and volcanic ranges: Geophysics, v. 12, p. 238–255

Gutenberg, B., and Richter, C. F., 1954, Seismicity of the earth: Princeton, N. J., Princeton Univ. Press, 310 p.

Heacock, J. G., Jr., and Worzel, J. L., 1955, Submarine topography west of Mexico and Central America: Geol. Soc. America Bull., v. 66, p. 773–776

Hersey, J. B., and Rutstein, M. S., 1958, Reconnaissance survey of Oriente Deep (Caribbean Sea) with a precision echo sounder: Geol. Soc. America Bull., v. 69, p. 1297–1304

Luskin, B., Heezen, B. C., Ewing, M., and Landisman, M., 1953, Precision measurement of ocean depths: Deep-Sea Research, v. 1, p. 131–140

Menard, H. W., Jr., 1955, Deformation of the northeastern Pacific basin and the west coast of North America: Geol. Soc. America Bull., v. 66, p. 1149–1198

Menard, H. W., Jr., and Fisher, R. L., 1958, Clipperton fracture zone in the northeastern equatorial Pacific: Jour. Geology, v. 66, p. 239–253

Officer, C. B., Ewing, J., Edwards, R. S., and Johnson, H. R., 1957, Geophysical investigations in the Eastern Caribbean; Venezuelan Basin, Antilles Island Arc, and Puerto Rico Trench: Geol. Soc. America Bull., v. 68, p. 359–378

Raitt, R. W., 1958, Seismic surveys, p. 36–38 *in* Fisher, R. L., *Editor*, Preliminary report on Expedition Downwind: Washington, D. C., IGY World Data Center A, IGY Gen. Rept., Ser. 2, 58 p.

Raitt, R. W., Fisher, R. L., and Mason, R. G., 1955, Tonga Trench, p. 237–254 *in* Poldervaart, A., *Editor*, Crust of the earth: Geol. Soc. America Special Paper 62, 762 p.

Sanchez Mejorada, S. H., 1956, Carta geologica de la Republica Mexicana (1:2,000,000): Mexico, 20th Intern. Geol. Cong.

Schuchert, Charles, 1935, Historical geology of the Antillean-Caribbean region: New York, John Wiley & Sons, 811 p.

Shepard, F. P., and Emery, K. O., 1941, Submarine topography of the California coast; canyons and tectonic interpretation: Geol. Soc. America Special Paper 31, 171 p.

Shor, G. G., Jr., and Fisher, R. L., 1961, Middle America Trench: seismic-refraction studies: Geol. Soc. America Bull., v. 72, p. 721–730

Shor, G. G., Jr., and Raitt, R. W., 1958, Seismic studies in the southern California continental borderland: Mexico, 20th Intern. Geol. Cong. Proc. Section 9, Geofisica Aplicada, v. 2, p. 243–259

Shurbet, G. L., and Worzel, J. L., 1957, Gravity anomalies and structure of the West Indies, part III: Geol. Soc. America Bull., v. 68, p. 263–266

Talwani, M., Sutton, G. H., and Worzel, J. L., 1959, A crustal section across the Puerto Rico Trench: Jour. Geophys. Research, v. 64, p. 1545–1555

Talwani, M., Worzel, J. L., and Ewing, M., 1959, Gravity anomalies and crustal section across the Tonga Trench (Abstract): Jour. Geophys. Research, v. 64, p. 1126

Tamayo, J. L., 1949, Geografia general de Mexico, tome 2 (Geografia fisica): Mexico, Talleres Graficos de la Nacion, 583 p.

Udintsev, G. B., 1955, Topography of the Kuril-Kamchatka Trench: Trud. Inst. Okeanology, v. 12, p. 16–61

Vening Meinesz, F. A., 1948, Gravity expeditions at sea, 1923–1938, v. 4: Delft, Netherlands Geod. Comm. Pub., 233 p.

Webber, B. N., and Ojeda R., J., 1956, Estructuras geologicas del sureste de Oaxaca y sur de Chiapas, Mexico: Mexico, 20th Intern. Geol. Cong. Guidebook to Excursion G-15, p. 75–82

Whitcroft, H. T., 1944, The bathymetry of the Central America region, west coast of Mexico and northern Central America: Am. Geophys. Union Trans., Pt. 4, p. 606–608

Worzel, J. L., and Ewing, M., 1952, Gravity measurements at sea, 1948 and 1949: Am. Geophys. Union Trans., v. 33, p. 453–460

Worzel, J. L., and Shurbet, G. L., 1955, Gravity interpretations from standard oceanic and continental crustal section, p. 87–100 *in* Poldervaart, A., *Editor*, Crust of the earth: Geol. Soc. America Special Paper 62, 762 p.

Manuscript Received by the Secretary of the Society, February 25, 1959
Contribution from the Scripps Institution of Oceanography, New Series

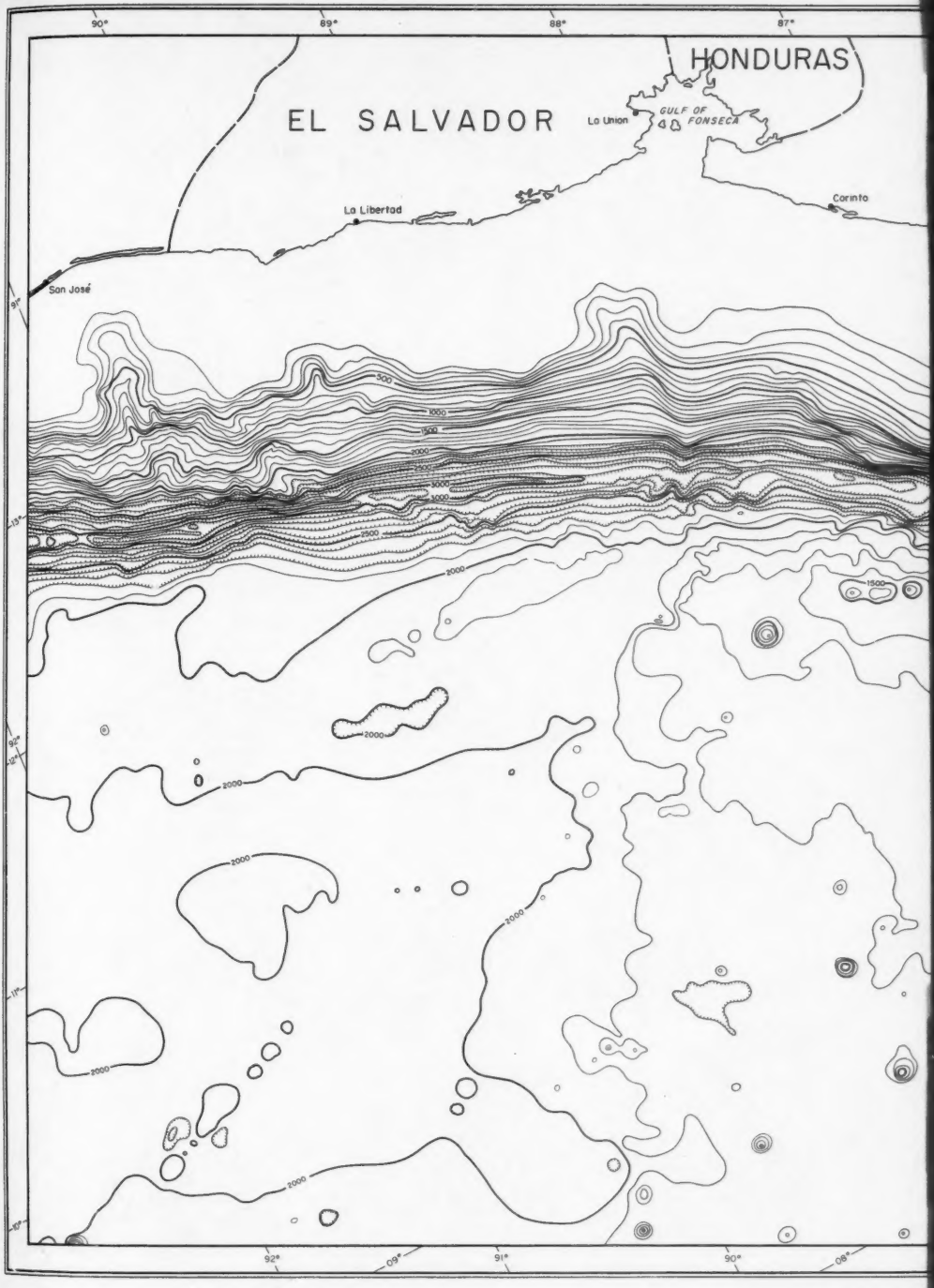

SUBMARINE TOPOGRAPHY, I

FISHER, PLATE 6
Geological Society of America, volume 72

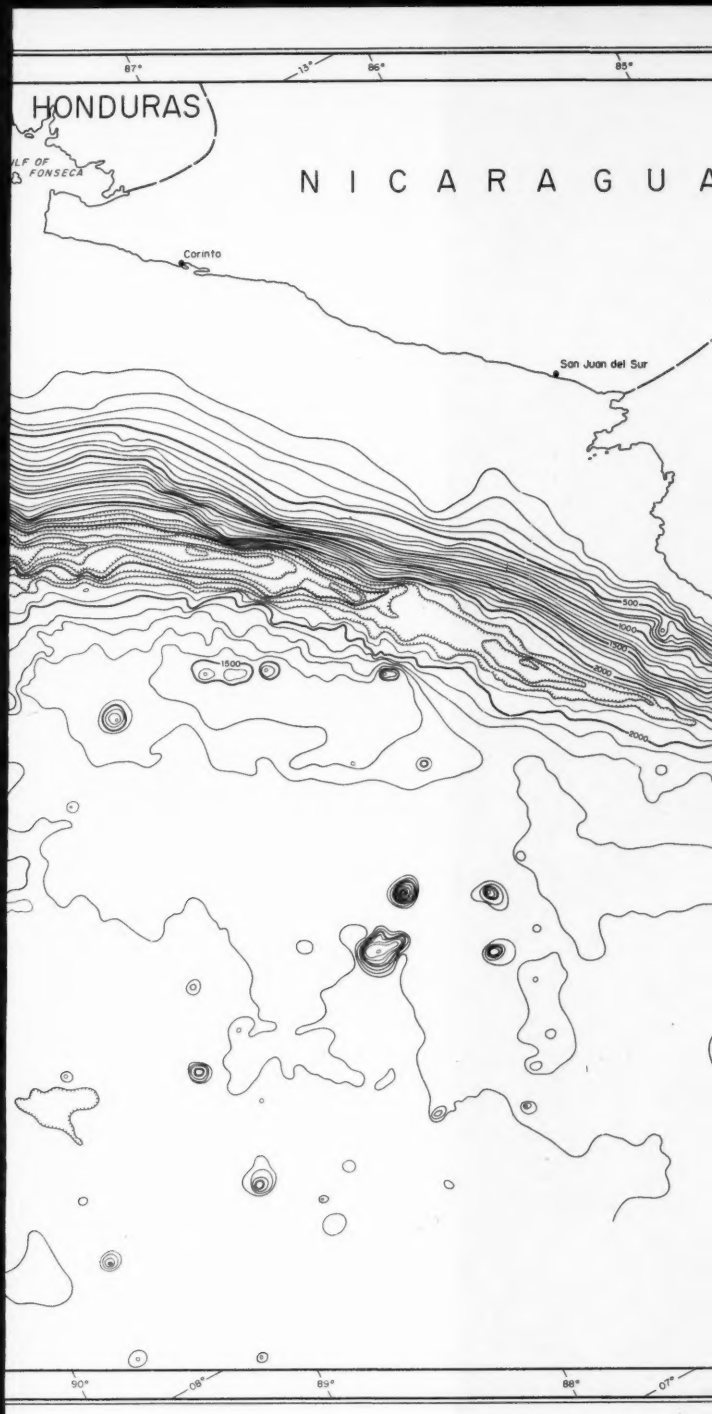

UBMARINE TOPOGRAPHY, FROM SAN JOSÉ, GUATEMALA, TO PUNT

TO PUNTA BURICA, PANAMA

GEORGE G. SHOR, JR.
ROBERT L. FISHER
University of California, The Scripps Institution of Oceanography, La Jolla, Calif.

Middle America Trench: Seismic-Refraction Studies

Abstract: Seismic-refraction profiles in the Middle America Trench show that the main crustal layer ranges from normal oceanic thickness (about 5 km) to half again as thick. Sediments are thicker than in the Pacific Basin. Because of the increased depth of water and sediment at all stations and thickening of the main crustal layer at some stations, the M discontinuity bows down beneath the trench. At the outer edge of the continental shelf near Guatemala, the water is replaced by sediments and rocks which may be either consolidated sediments or volcanic rocks; the M discontinuity is at little greater depth than beneath the trench.

CONTENTS

Introduction 721
Acknowledgments 721
Field methods 722
Computation 723
Interpretation of results 726
Sedimentary and basement layers 726
Main crustal layer 728
Mantle 729
Structure 729
References cited 729

Figure
1. Locations of stations 722
2. Travel-time plots for stations 1 and 1′ (Tres Marias Basin) 722
3. Travel-time plots for stations 2 (near Manzanillo) and 3 (near Acapulco) 724
4. Travel-time plots for stations 4 and 4′ (on continental shelf near Champerico) 724
5. Travel-time plots for stations 5 and 5′ (on axis of trench near Champerico) 726
6. Travel-time plots for stations 6 (on outer ridge, near Champerico) and 7 (on axis of trench near La Union) 727
7. Structural sections based on individual station solutions 727
8. Structural sections based on the assumption of regionally uniform velocities 728

Table
1. Equations of arrival times 723
2. Seismic velocities and layer thicknesses 725
3. Layer thicknesses computed by assuming regional uniformity of velocities 726

INTRODUCTION

On the 1954 Acapulco Trench Expedition seismic-refraction work was done by the Scripps Institution of Oceanography ships SPENCER F. BAIRD and HORIZON at seven locations (Fig. 1) in and near the Middle America Trench. Five of the stations were along the trench axis, near Puerto Vallarta, Manzanillo, and Acapulco, Mexico; Champerico, Guatemala, and La Union, El Salvador. The other two were on the outer edge of the continental shelf and on the ridge seaward of the trench, both near Champerico. The choice of station positions was based on previous bathymetric studies by Fisher which, with bathymetry and structural interpretations from this and later trips, are reported separately (Fisher, 1961). The purpose of the seismic work was to measure the depth of the M discontinuity beneath the trench.

ACKNOWLEDGMENTS

In the work at sea the authors were aided greatly by Alan C. Jones and Maxwell Silverman; computational work ashore was assisted by Gloria Slack and Frieda James. The seismic-refraction program has been under the general direction of Prof. Russell W. Raitt. Illustrations have been prepared by Christine Baldwin. The authors are indebted to Russell Raitt and J. B. Hersey for critical reading of the manuscript, and to the officers, crews, and scientific parties of the vessels SPENCER F. BAIRD and HORIZON for their help.

This work represents results of research sponsored by the U. S. Navy, Bureau of Ships,

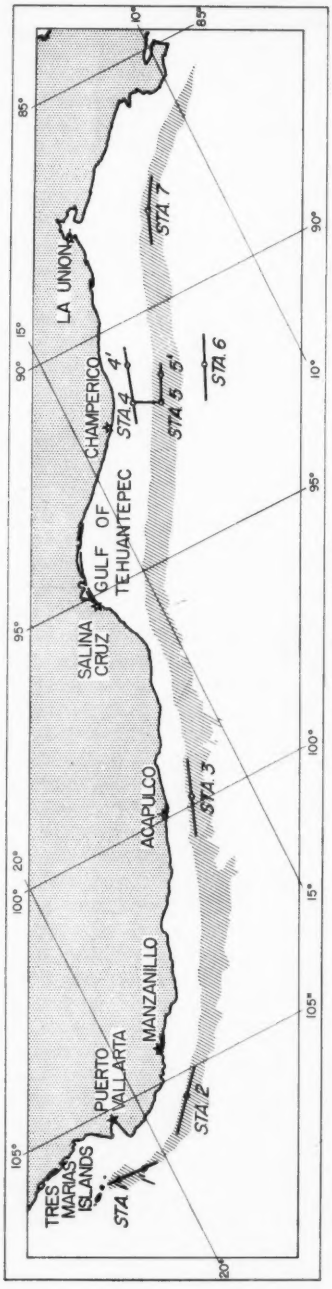

Figure 1. Locations of stations

under contract Nobsr 72512 and the Office of Naval Research under contract Nonr 2216(05).

FIELD METHODS

Recording was done aboard the SPENCER F. BAIRD, while the HORIZON, dropping charges,

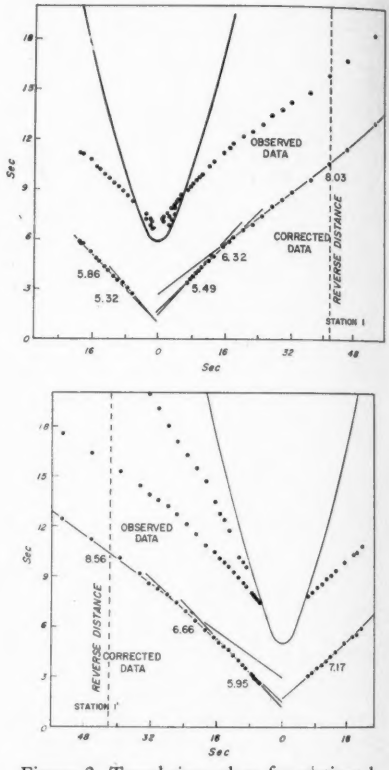

Figure 2. Travel-time plots for stations 1 and 1′ (Tres Marias Basin). Upper points are observed data; lower points are corrected to sea floor.

steamed toward the BAIRD, passed it close abeam, and continued onward. Stations 2, 3, 6, and 7 were split profiles. At stations 1, 4, and 5 two receiving positions were occupied; the outbound shooting track from the first position was followed on the inbound track to the second, so that each station consisted of a reversed profile with unreversed short profiles on the ends.

Both shipboard operations and data analysis

are more difficult to execute for a narrow trench than for either a broad trench (such as the Puerto Rico Trench) or ocean-basin areas, because of the rapid changes in water depth and sediment thickness transverse to the trench, which require that both ships stay closely on the trench axis. On stations in the narrow portion of the trench (2, 3, 5, and 7) an attempt was made to have the shooting ship follow the trench axis as defined by prior exploration instead of following a straight track. The receiving ship moved back to the trench axis whenever it drifted appreciably toward the trench walls. Effects of structural variations along and across the trench are still probably large and have given difficulty in interpretation.

Receiving and shooting procedures otherwise were as described by Raitt (1952; 1956); signals from four hydrophones were recorded in three frequency bands at two levels. Shots were half a pound to 300 pounds of high explosives.

COMPUTATION

Travel times were corrected first for firing-mark delay and then for water delay to sea

TABLE 1. EQUATIONS OF ARRIVAL TIMES

Station	Northwest line	Southeast line
1	$\left\{\begin{matrix}0.94\pm.04+X/5.86\pm.07\\0.91\pm.02+X/5.32\pm.22\end{matrix}\right.$	$1.41\pm.05+X/5.49\pm.12$
		$1.73\pm.08+X/6.32\pm.13$
		$2.65\pm.07+X/8.03\pm.09$
1′	$1.19\pm.01+X/5.95\pm.02$	
	$1.51\pm.08+X/6.66\pm.13$	$1.70\pm.03+X/7.17\pm.10$
	$2.86\pm.12+X/8.56\pm.15$	
2	$0.94\pm.08+X/5.45\pm.24$	
	$1.08\pm.06+X/6.18\pm.13$	$1.32\pm.10+X/7.32\pm.24$
	$1.58\pm.07+X/7.50\pm.07$	$1.67\pm.13+X/7.77\pm.15$
3	$0.51\pm.03+X/5.86\pm.09$	$0.15\pm.09+X/4.75\pm.19$
	$1.19\pm.13+X/7.00\pm.28$	$0.62\pm.09+X/6.66\pm.21$
	$1.58\pm.17+X/7.98\pm.19$	$1.77\pm.21+X/8.52\pm.28$
4	$0.00^{*}\quad+X/1.78\pm.16$	$0.00^{*}\quad+X/1.78\pm.16^{\dagger}$
	$0.44\pm.07+X/2.60\pm.10$	$0.42\pm.04+X/2.55\pm.05$
	$0.84\pm.04+X/3.16\pm.05$	$0.91\pm.05+X/3.16\pm.06$
	$1.84\quad+X/4.64$ **	$1.82\pm.02+X/4.41\pm.03$
	—	$3.20\pm.02+X/5.76\pm.02$
		$4.21\pm.10+X/6.78\pm.10$
		$5.66\pm.14+X/8.27\pm.10$
4′	$0.00^{*}\quad+X/1.64\pm.07$	$0.00^{*}\quad+X/1.64\pm.07^{\dagger}$
	$0.48\pm.03+X/2.29\pm.02$	$0.47\pm.09+X/2.22\pm.07$
	$1.55\pm.04+X/3.33\pm.05$	$1.44\pm.11+X/3.21\pm.12$
	$2.32\pm.03+X/4.39\pm.03$	$2.38\pm.04+X/4.74\pm.05$
	$3.99\quad+X/5.90$ **	$3.55\pm.15+X/6.09\pm.20$
	$4.79\pm.07+X/6.97\pm.09$	
	$5.85\pm.19+X/8.09\pm.14$	
5		$0.61\pm.30+X/5.65\pm.82$
		$0.88\pm.08+X/6.32\pm.11$
		$2.53\pm.25+X/8.34\pm.27$
5′	$1.06\pm.04+X/7.11\pm.07$	$0.99\pm.15+X/6.69\pm.39$
	$1.97\pm.76+X/7.76\pm.65$	
6	$0.74\pm.02+X/6.91\pm.04$	$0.67\pm.03+X/6.62\pm.06$
	$1.19\pm.04+X/7.68\pm.04$	$1.31\pm.02+X/7.85\pm.03$
7	$1.13\pm.12+X/6.39\pm.33$	
	$0.97\pm.06+X/6.77\pm.07$	$1.01\pm.04+X/6.53\pm.06$
	$3.04\pm.27+X/8.72\pm.27$	$2.69\pm.10+X/8.47\pm.12$

* Intercept assumed to be 0.00
† Solution for points on both sides of receiving position together
** Line fitted to 2 points; no least-squares solution

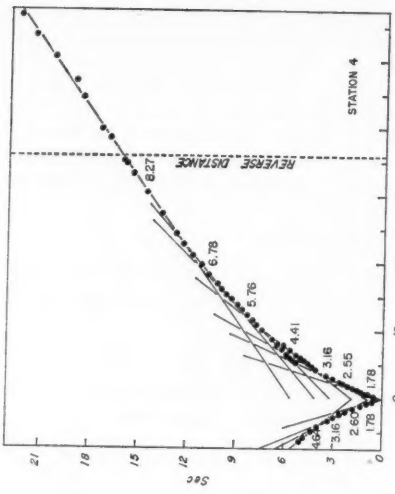

Figure 4. Travel-time plots for stations 4 and 4' (on continental shelf near Champerico)

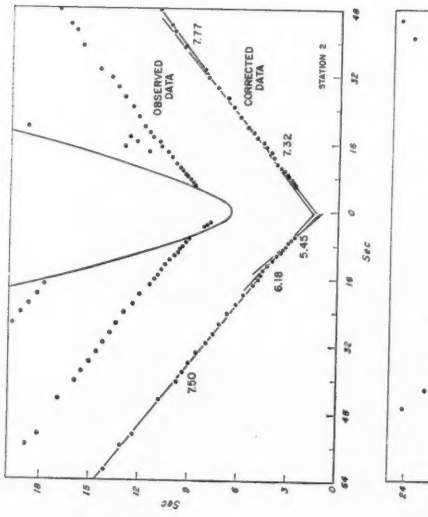

Figure 3. Travel-time plots for stations 2 (near Manzanillo) and 3 (near Acapulco). Both are along axis of trench.

floor, by using correction cosines determined from the observed slopes of the uncorrected travel-time plots. Distances were determined from the travel time of the direct water wave and velocities of sound in water computed from hydrographic casts at each station by using Kuwahara's (1939) tables. If the direct water wave was not observed, its travel time was computed from that of the bottom-reflected waves by a method similar to that of Katz and Ewing (1956, p. 507).

single section computed. For the reversed profiles only the data for the reversed pair were used; the velocities were again the harmonic mean, but the intercepts were used separately to obtain sections for each end of the reversed profile.

Difficulties arise in the computation and in comparison of the results because of the possible presence of a "basement layer" with velocity between 4 and 6 km/sec, intermediate between those of the sediments and the main

TABLE 2. SEISMIC VELOCITIES AND LAYER THICKNESSES
Data for each station were computed independently.

	Water		Sediment		Basement		Crust		Mantle	
Station	h_0	c_0	h_1	c_1	h_2	c_2	h_3	c_3	c_4	Σh
1	4.40	1.54	1.64	2.15	1.77	5.71	3.84	6.49	8.29	11.65
1′	3.76	1.54	1.38	2.15	1.79	5.71	6.05	6.49	8.29	12.98
2	4.91	1.54	1.36	2.15			2.86	6.70	7.64	9.13
3	5.14	1.54	0.39	2.15	2.31	5.25	3.93	6.82	8.24	11.77
4	0.12	1.50	0.50 0.74 1.83	1.71 2.41 3.25	3.84 4.03	4.40 5.83	6.53	6.88	8.18	17.59
4′	0.12	1.50	0.58 1.75 1.14	1.71 2.41 3.25	4.81 2.61	4.40 5.83	4.33	6.88	8.18	15.34
5	6.18	1.54	1.00	2.15			9.84	6.69	8.04	17.02
5′	6.02	1.54	1.20	2.15			5.36	6.69	8.04	12.58
6	3.62	1.53	0.80	2.15			3.69	6.76	7.76	8.11
7	5.13	1.53	1.13	2.15			9.71	6.65	8.60	15.97
Pacific average	4.34		0.30	2.15	1.18	5.23	4.78	6.81	8.20	10.60

Travel-time plots are shown in Figures 2–6. The upper points in each plot are the observed data; the lower points are refracted arrivals corrected for water delay. On station 4, the observed and corrected data coincided to the scale of the figure in most cases, so that only the corrected points are shown. Straight lines were fitted to the arrivals by least squares; equations of the lines are given in Table 1. The deviations listed are the standard deviations of the velocity and intercept time.

Structural computations by a number of methods are possible. The simplest method, in which a "horizontal layer" computation is made for each station independently, is presented in Table 2. In this method the harmonic mean of the velocities and the direct mean of the intercept times were taken from the least-squares solutions for the split profiles and a

crustal layer. This layer was recorded reliably on three of the four profiles of station 1 and on both profiles of station 3. Its presence is indicated, with very poor determination of velocity, on one of two profiles of station 2 and two of four profiles of station 5. On station 4, in shallow water, there are two well-observed layers with velocity in the 4–6 km/sec range. On stations 6 and 7 the layer was not indicated. The line with velocity 6.4 km/sec on station 7 has too high an intercept time to be a separate layer and is probably caused by variation in sediment thickness.

For solutions based only on the observed data from each station separately, the "basement" can be included only on stations 1, 3, and 4. The results of these computations are plotted in Figure 7. To make it easier to compare stations and to take account of the possi-

Figure 3. Travel-time plots for stations 2 (near Manzanillo) and 3 (near Acapulco). Both are along axis of trench.

Figure 4. Travel-time plots for stations 4 and 4′ (on continental shelf near Champerico)

bility that variations in velocity from station to station (and the resulting variations in structure computed) are due to changes in dip along the individual profiles, the stations have been reworked using regional velocities and a uniform number of layers (in all but the continental shelf station, number 4). In this computation the harmonic mean of all observed velocities for each layer was taken, and for each station the mean delay times were computed. Where no basement layer was observed it was assumed to be at the time of the first refracted arrival. The remainder of the solution was as before; the results appear in Table 3 and Figure 8.

INTERPRETATION OF RESULTS

Sedimentary and Basement Layers

Computations for all except station 4 were made using an assumed velocity of 2.15 km/sec for the sediments. No first arrivals were received from this layer, and second arrivals were indistinct. The velocity of 2.15 km/sec was obtained by Raitt (1956) from reflection studies on deep-water lines in the central Pacific. Reflection data for similar analysis on the trench stations were examined but had too large a scatter to determine a velocity; presumably this was caused by variations in sediment thickness. Wobbles in the refraction travel-time plots also indicate considerable variation in sediment thickness, as does a perceptible shift in the crust arrival line on the first profile of

TABLE 3. LAYER THICKNESSES COMPUTED BY ASSUMING REGIONAL UNIFORMITY OF VELOCITIES

Station	Water depth	Layer 1 2.15 km/s	Layer 2 5.74 km/s	Layer 3 6.75 km/s	Depth below sea level to 8.11 km/sec (M discontinuity)
1	4.1	1.3	2.9	4.5	12.8
2	4.9	1.2	0.6	5.0	11.7
3	5.1	0.6	1.3	5.2	12.2
5	6.2	0.8	1.6	7.6	16.2
6	3.6	0.6	1.0	5.0	10.2
7	5.2	1.0	1.0	7.7	14.9

station 7. This latter occurred at the time of a relatively small shift of the receiving position during the course of the run. Bathymetric results (Fisher, 1961) indicate ponding of sediments in the low parts of the trench; this would mask rough topography and create a scatter of the refraction arrivals.

Sediment-thickness values in Table 2 for lines 2, 5, 6, and 7 are maxima because no basement layer has been introduced. If this layer is

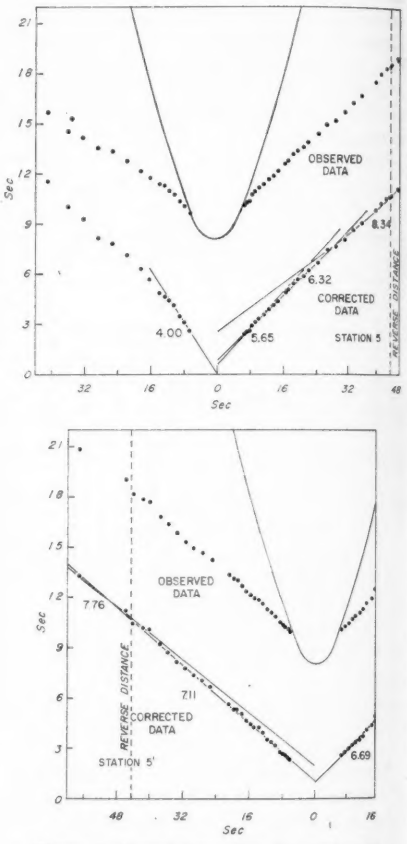

Figure 5. Travel-time plots for stations 5 and 5′ (on axis of trench near Champerico)

present but masked, the sediment thickness is decreased by some hundreds of meters, as shown in Table 3.

All observed early arrivals interpreted as being from the basement layer could be explained by deviations in the crustal arrival times caused by variations in sediment thickness of the order of 100 m. Some evidence for interpretation as an extra layer is found in subbottom reflections on stations 1, 2, and 6 and in the presence of arrivals with apparent veloc-

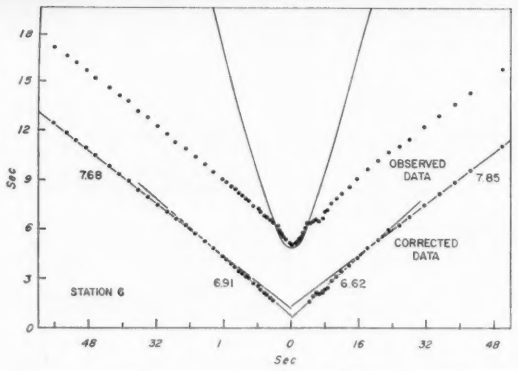

Figure 6. Travel-time plots for stations 6 (on outer ridge, near Champerico) and 7 (on axis of trench near La Union)

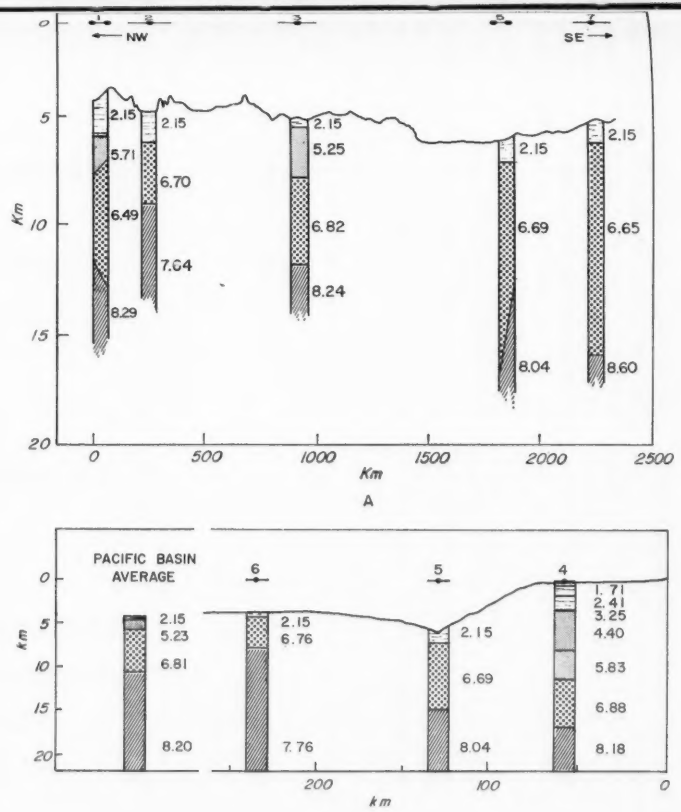

Figure 7. Structural sections based on individual station solutions. A—along trench; B—transverse to trench

ity 4.0 km/sec and zero intercept on a line up the trench wall from station 5.

Station 4, on the shelf near Champerico, is a special case. Layers with velocities of 1.7, 2.4, 3.2, 4.4, and 5.8 km/sec were found above the main crustal layer. The first three layers could be interpreted equally as a single layer with a continuous increase of velocity with depth. The 4.4 km/sec layer is a definite entity as shown by a sharp break in travel-time slope and a long straight plot of arrivals. The 5.8 km/sec layer is strongly shown on one of the reversed lines and one of the unreversed lines but is masked on the other reversed line. The first three layers probably represent sediments of varying stages of compaction. The fourth and fifth layers could, lithologically, be sedimentary rocks or igneous intrusive or extrusive rocks, as could the corresponding basement layer in the deep-sea stations. Vulcanism in the neighboring area of Guatemala and southern Mexico suggests that they may be volcanic rocks.

Main Crustal Layer

Arrivals with velocity between 6 and 7 km/sec were found at every station; the "true velocity" ranged from 6.5 to 6.9 km/sec; the mean of all observations was 6.75 km/sec. This is almost the same as the mean for the main crustal layer in the central Pacific as found by

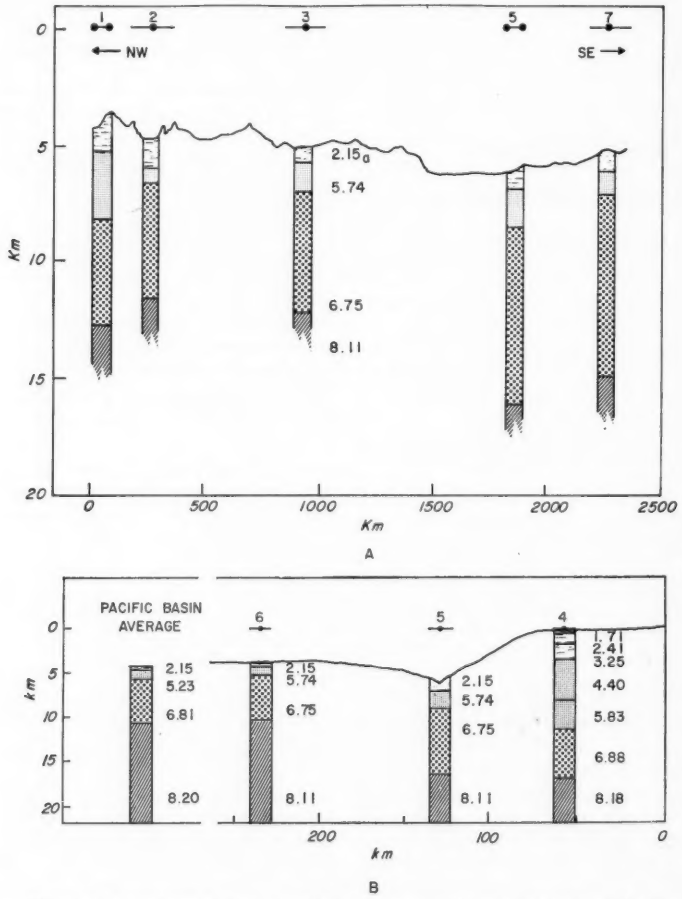

Figure 8. Structural sections based on the assumption of regionally uniform velocities. A—along trench; B—transverse to trench

Raitt (1956, p. 1634) and does not differ significantly from values obtained by Ewing and others in the Atlantic. The evidence indicates that this layer is continuous from the deep sea under the trench to at least the outer edge of the continental shelf.

Mantle

Arrivals with mantle velocity were obtained on all stations; computed "true velocity" scatters widely from 7.6 to 8.6 km/sec; the mean of all observations was 8.11 km/sec. This mean is not significantly different from values obtained on either oceanic or continental lines in the past. The scatter in velocities, although it may be real, could be explained by variations in structure along the length of each profile, as could the scatter in velocities in the crust.

Structure

The M discontinuity is depressed beneath the trench. In the central sector (stations 2 and 3) the main crustal layer is not significantly thickened; the depression corresponds only to the deepening of the water and the thickening of the sediments. At the southern trench stations (5 and 7) the crust is thickened. The thickening is not great, however, and does not approach that implied in the tectogene hypothesis. This thickening at the southern stations is independent of the form of layer solution, although regional velocity solutions smooth out the extremes. The section transverse to the trench shows the M discontinuity dipping beneath the trench and then descending only a little more beneath the edge of the shelf. The M discontinuity must be deeper landward.

The crustal thickness beneath the Middle America Trench is not less than that beneath the Pacific basin, and in places it is greater. This is essentially the same conclusion as that derived for the Tonga Trench by Raitt, Fisher, and Mason (1955) and for the Puerto Rico Trench by Officer *et al.* (1957) from seismic data; it does not agree with the interpretation from gravity data for the latter two trenches and others by Worzel and Shurbet (1955) and Talwani, Worzel, and Ewing (1959).

REFERENCES CITED

Fisher, Robert L., 1961, Middle America Trench: Topography and structure: Geol. Soc. America Bull., v. 72 p. 703–720

Katz, S., and Ewing, M., 1956, Seismic-refraction measurements in the Atlantic Ocean. Pt. VII, Atlantic Ocean basin west of Bermuda: Geol. Soc. America Bull., v. 67, p. 475–510

Kuwahara, Susumu, 1939, Velocity of sound in sea water and calculation of the velocity for use in sonic sounding: Hydrog. Rev., v. 16, no. 2, p. 123–140

Officer, C. B., Ewing, J., Edwards, R. S., and Johnson, H. R., 1957, Geophysical investigations in the Eastern Caribbean; Venezuelan Basin, Antilles Island Arc, and Puerto Rico Trench: Geol. Soc. America Bull., v. 68, p. 359–378

Raitt, R. W., 1952, Geophysical measurements in oceanographic instrumentation: Natl. Res. Council of Natl. Acad. Sci. Pub. 309, p. 233

— 1956, Seismic-refraction studies of the Pacific Ocean Basin. Pt. I, Crustal thickness of the central equatorial Pacific: Geol. Soc. America Bull., v. 67, p. 1623–1640

Raitt, R. W., Fisher, R. L., and Mason, R. G., 1955, Tonga Trench, p. 237–254 *in* Poldervaart, A., *Editor*, Crust of the earth: Geol. Soc. America, Special Paper 62, 762 p.

Talwani, M., Worzel, J. L., and Ewing, M., 1959, Gravity anomalies and crustal section across the Tonga Trench (Abstract): Jour. Geophys. Research, v. 64, p. 1126

Worzel, J. L., and Shurbet, G. L., 1955, Gravity interpretations from standard oceanic and continental crustal sections, p. 87–100 *in* Poldervaart, A., *Editor*, Crust of the earth: Geol. Soc. America Special Paper 62, 762 p.

Manuscript Received by the Secretary of the Society, February 25, 1959
Contribution from the Scripps Institution of Oceanography, New Series

HIROSHI NIINO *Tokyo University of Fisheries, Tokyo, Japan*
K. O. EMERY *Dept. Geology, University of Southern California, Los Angeles, Calif.*

Sediments of Shallow Portions of East China Sea and South China Sea

Abstract: Nearly 1000 bottom samples from the shallow portions of the East China and South China seas were studied and compared with source areas and oceanographic conditions. Sediments of the Gulf of Pohai and central Yellow Sea are fine-grained, low in calcium carbonate, and contain many unstable minerals and a moderately high percentage of organic matter. Most are contributed by the Hwangho (which carries much eroded loess), Yangtze, and many smaller rivers. The thickness of these sediments is so great as to constitute a modern zeugogeosyncline.

Sediments on the inner half of the continental shelf between Shanghai and Hainan and in the Gulf of Tonkin are similar to those of the central Yellow Sea; they comprise modern detrital materials contributed to the continental shelf by many rivers, but in amounts as yet insufficient to cover the shelf everywhere. Seaward of these sediments, on the outer half of the continental shelf between Korea and Hainan, is a broad belt of coarse sandy sediment from which finer sediments are winnowed away or prevented from being deposited by the strong Kuroshio Current. The sediment contains glauconite and much calcium carbonate in the form of foraminiferal tests and broken mollusk shells but very little organic matter. Because the inorganic portion is much coarser than that nearer shore, it is believed to constitute a littoral deposit left from a Pleistocene time of glacially lowered sea level. Locally on the shelf small areas of residual sediment near rock outcrops commonly contain reworked fossils. Pieces of pumice and many small shards of volcanic glass are present in the sediments but nowhere are they abundant enough to form a dominantly volcanic sediment. The shelf sediments are similar in most respects to those on the continental shelf of California, and they clearly indicate deposition below present base levels of equilibrium.

Seaward of the continental shelf, in deep water of the continental slope, the sediments are finer-grained and contain more calcium carbonate. These sediments consist of the finer-grained terrigenous material that bypasses the shelf and is deposited so slowly in the quiet deep water that Foraminifera make up a large percentage of the total sediment.

CONTENTS

Introduction 732
Topography and regional geology 732
Land 732
Sea floor 736
Climate 736
Oceanography 740
General 740
Temperature 740
Salinity 741
Currents 741
Bottom data 742
Notations on charts 742
Samples 743
Rocks 745
Total sediment 745
General texture 745
Color 749
Terrigenous fraction 749
Median diameter 749
Sorting 752
Mineralogy 753
Volcanic fraction 753
Authigenic fraction 753
Organic fraction 753
Calcium carbonate 753
Silica 757
Organic carbon 757
Summary and conclusion 758
Origin of sediments 758
Comparison with ancient sediments and sedimentary environments 760
References cited 761

Figure
1. Index map, East China and South China seas . 733
2. General topography of region. 734
3. Detailed topography of East China Sea and adjoining Yellow Sea and Gulf of Pohai. . 735
4. Detailed topography of Taiwan Strait and adjacent areas. 737
5. Detailed topography of shelf off coast of south China. 738
6. Detailed topography of northern South China Sea and Gulf of Tonkin. 739

Geological Society of America Bulletin, v. 72, p. 731–762, 21 figs., May 1961

Figure
7. Wind direction and velocity, summer and winter. 740
8. Surface-water temperature, summer and winter. 741
9. Surface-water salinity, summer and winter. . 742
10. Surface currents, summer and winter. 743
11. General sediment chart of area north of Taiwan, East China Sea 744
12. General sediment chart of area southwest of Taiwan, South China Sea 746
13. Color and general description of total sediment, and median diameter and sorting coefficient of noncalcareous part of sediments from East China Sea 747
14. Color and general description of total sediment, and median diameter and sorting coefficient of noncalcareous part of sediments from Taiwan Strait and shelf off coast of south China 748
15. Color and general description of total sediment, and median diameter and sorting coefficient of noncalcareous part of sediments from Gulf of Tonkin 750
16. Distribution of samples containing pumice and glauconite 752
17. Organic constituents of sediments from East China Sea 754
18. Organic constituents from Taiwan Strait and shelf off coast of south China 755
19. Organic constituents of sediments from Gulf of Tonkin 756
20. Areas of maximum catch of bottom fishes, 1928–1939 758
21. General structure and bottom sediment according to origin 760

Table
1. Summary of composition of sediment samples, Yellow Sea, continental shelf, and Gulf of Tonkin 751
2. Summary of sediment characteristics, Yellow Sea and Gulf of Pohai, continental shelf, and Gulf of Tonkin 757

INTRODUCTION

Many of the sedimentary strata laid down during the geological past accumulated in partly enclosed, wide, flat, shallow, marine embayments. Some of the embayments were sites of accumulation of geosynclinal sediments, and others were sites of accumulation of epicontinental platform sediments. Because some of these ancient sediments are economically important, it is highly desirable that their conditions of deposition be understood. Attempts have been made to interpret conditions of deposition from the geological record, but the evidence provided by sedimentary rocks and fossils is incomplete and leads to uncertain interpretations. Thus, studies must be made of modern shallow seas where temperature, salinity, oxygen content, currents, winds, and other parameters can be measured and their seasonal and other kinds of variations be recognized. This paper relates the sediments of a modern wide shallow marine area to their depositional conditions and provides information that may be useful in interpreting the sediments of somewhat similar ancient areas.

The region described is the East China and South China seas (Figs. 1, 2). No previously published study of the sediments is known except for compilations based on bottom-sediment notations on navigational charts by Shepard, Emery, and Gould (1949) and by Klenova (1958) and a generalized chart of part of the East China Sea based on fishery samples by T. Kumada (*in* Kasawara, 1948). Kumada's samples were destroyed before being properly studied; however, many additional samples were obtained by other Japanese fishing boats between 1920 and 1940, when the boats were able to visit all parts of the region. All are small snapper samples, except a few rocks that were caught up in nets, and all had been dried after collection. Niino brought the samples to University of Southern California and made sample descriptions, using a binocular microscope, determined organic carbon, and compiled background oceanographic data. An assistant, George Keller, made analyses for calcium carbonate and grain-size distribution. Emery was responsible for general organization, writing, and drafting. These studies were made possible by funds provided by the Office of Naval Research (Contract Nonr 228-12), by facilities of Allan Hancock Foundation, and by research time given by Tokyo University of Fisheries and University of Southern California.

About 300 of the samples were made available for foraminiferal studies as master's theses at University of Southern California; the results were published by Polski (1959) for the northern half of the area and by Waller (1960) for the southern half.

TOPOGRAPHY AND REGIONAL GEOLOGY

Land

This study covers a range of latitude from 15° N. to 41° N. The land consists of hills bordered by a narrow coastal plain and large deltas (Fig. 2). Most conspicuous is a delta that

covers an area of about 750,000 sq km, a composite feature built on both sides of the hilly peninsula of Shan-Tung by the Hwangho and Yangtze rivers. Draining from mountainous areas far to the west, both rivers carry large volumes of sediment, much of which is yellow eroded fine-grained loess, which earned the name Yellow River, or Hwangho. Both Hwangho and Yangtze rivers are subject to devastating floods. Natural and artificial levees confine the Hwangho, but the power of the river is so great that many times it has cut through the dikes and changed its mouth from one to the other side of Shan-Tung.

As though attempting to encircle the huge delta and adjacent Gulf of Pohai and Yellow Sea, the peninsula of Korea extends southward, and the hills of south China extend northeastward but do not meet. Neither arm is mountainous; only a few peaks are higher than 1500 m. The structural trends of each arm are northeast-southwest.

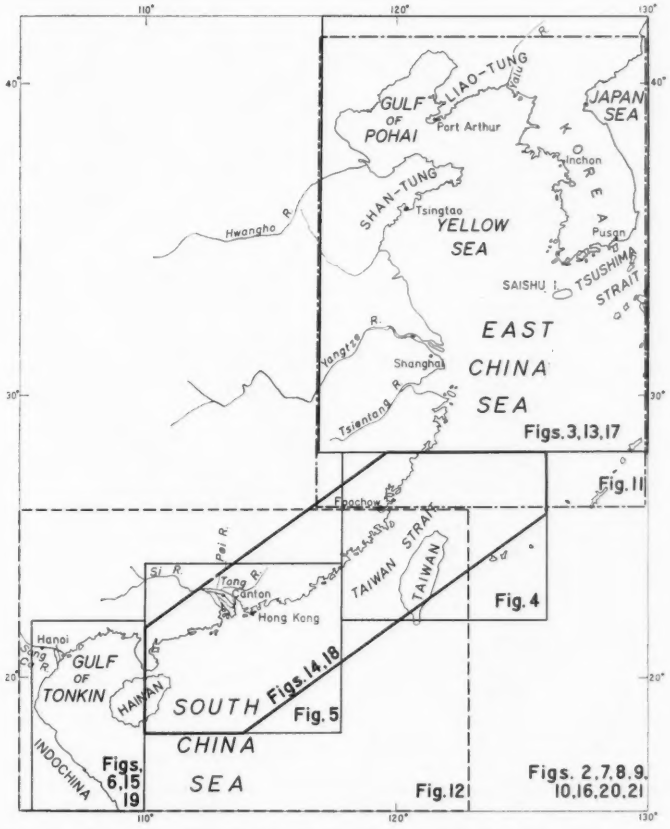

Figure 1. Index map, East China and South China seas. Enclosed areas refer to text figures, as numbered in lower right-hand corner of each area.

The west side of Korea is low and consists of coastal plains, small hills, and many rocky islands. Along the coast of south China is a narrow but densely populated coastal plain; the two large cities, Canton and Hong Kong, are located at its widest point where the Si River from the west and the Tong River from the east join and form a delta. Similar topogra-

phy of narrow coastal plain backed by hills extends westward and around the Gulf of Tonkin to Indochina.

Islands present varying degrees of relationship to the mainland. Those to the north and east, belonging to the Ryukyu Chain, consist of small volcanic islands and larger ones of tectonic origin, such as Okinawa. Since they are separated from the continental shelf by a trench, they contribute little sediment to the shelf and are not further considered here. Far north in Tsushima Strait is Saishu Island; even though it is small, its peak is higher than any in Korea. Along the coasts of South Korea and south China are many small islets, all representing drowned portions of the hilly mainland coast. The larger islands of Taiwan and Hainan are also closely related to the mainland. Taiwan is a fault block tilted up on its east side so that its peak, nearly 4000 m, is the highest point of the entire region shown in Figure 2. Hainan is an oval island with a

Figure 2. General topography of region. Same contour interval is used for sea floor and land. Contours of sea floor are based on soundings given on charts of Japan Hydrographic Office supplemented by data from sample sites; drawn only to maximum depth of 1800 m, part way down the slope of Ryukyu Trench. Contours on land have been taken from U. S. Coast and Geodetic Survey's World Aeronautical Charts; no reliable information exists for blank areas along western margin.

high point in the middle surrounded by coastal plain.

Rocks of the region include igneous, metamorphic, and sedimentary types. The oldest are Precambrian gneiss and schist at Liao-Tung, Korea, and south China. The similarity in structural trend of these rocks shows them to be part of a single structure, the Fukien-Reinan massif (Kobayashi, 1952), which probably connects Korea and south China beneath

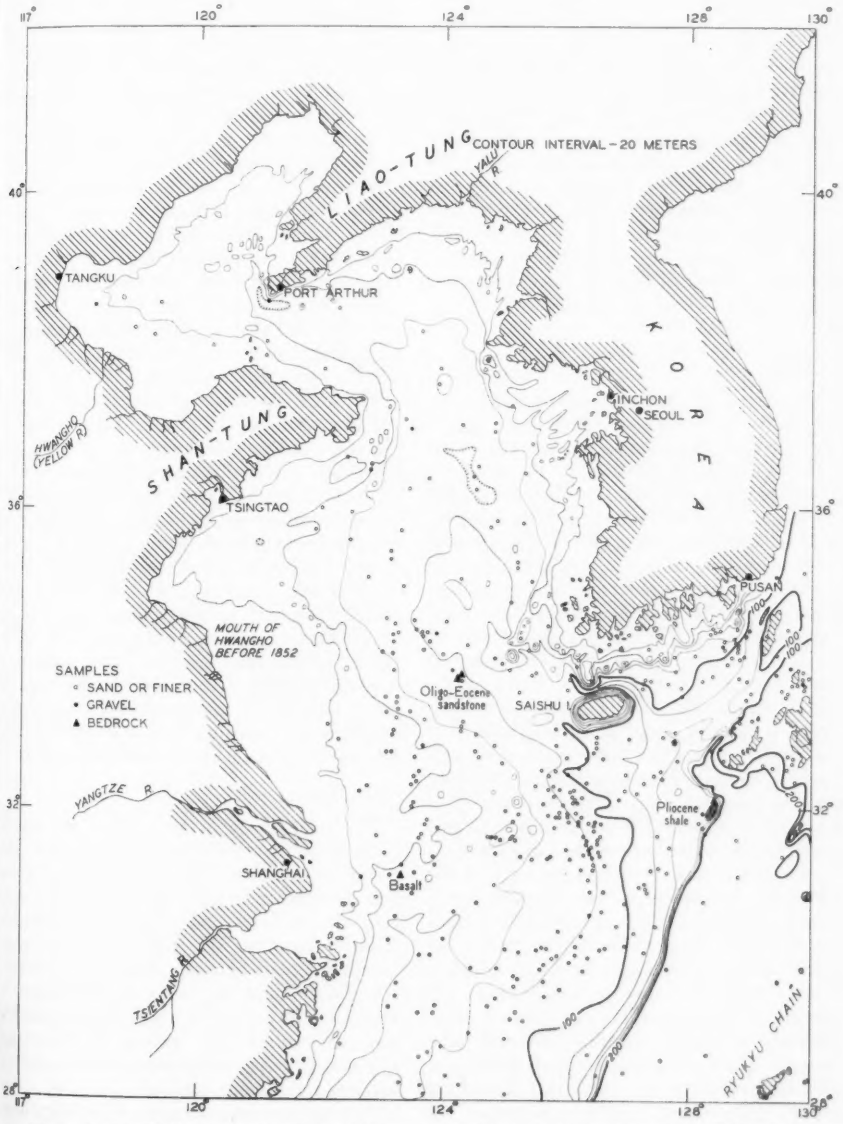

Figure 3. Detailed topography of East China Sea and adjoining Yellow Sea and Gulf of Pohai

the East China Sea. Paleozoic sedimentary and intrusive (granite and syenite) rocks occur in North Korea, north of Gulf of Pohai, western Shan-Tung, near Nanking, and in the Ryukyu Chain. Mesozoic granite and diorite crops out in eastern Shan-Tung, South Korea, and Kyushu, Hainan, and Indochina. Tertiary marine sedimentary rocks occur in South Korea, Saishu, Kyushu, the Ryukyu Chain, and Taiwan, whereas Tertiary non-marine strata are widespread in China and Korea. The most widespread Pleistocene strata is loess in north China, including the large deltas, but there are marine terrace deposits along the coasts, laterite in south China, and coral reefs on the Ryukyu Chain, Taiwan, and along the southern Indochina shores. Additional details of stratigraphy in the region are given by Lee (1939) and on various geological maps (Central Research Institute of Electric Power Industry, 1959; Tokyo Geographical Society, 1929; 1952).

Sea Floor

The part of the sea floor that is of interest in this study is the shallow region that extends from the shore to the shelf-break—outer edge of shelf (Dietz and Menard, 1951)—at about 120 m depth. Beyond the shelf-break are trenches and abyssal sea floor described in part by Hess (1948) and Dietz (1954). The greatest width of shallow bottom occurs along the axis of the embayment that includes the Gulf of Pohai, Yellow Sea, and East China Sea, about 850 km (Fig. 3). The northern two-thirds of this area, consisting of about 500,000 sq km, is partly enclosed by the arcuate trend of the hills of Korea and south China, and it may represent the remainder of an originally oval and island-studded sea now more than half filled by sediments of the combined deltas of the Hwangho and Yangtze rivers. This area is flat, shallower than 100 m, and has its axis nearer the Korea side than the China side, as though in response to eastward growth of the deltas. The average slope from the shore to the 40-m contour of the deltas is 0°00′15″, comparable to the slope of the delta at the head of the similarly shallow Persian Gulf (Emery, 1956). Among the minor irregularities is a depression in the Strait of Pohai off Port Arthur, evidently caused by scouring action of tidal currents. There also are many small submerged hills, some of which are rocky extensions of the granitic Shan-Tung. Others northeast of Shanghai probably represent incompletely eroded and unburied remnants of the enclosing arc of hills.

Southeast of a line connecting Shanghai and the tip of Korea (Fig. 3) is a 300,000-sq-km area of outer shelf that is probably less closely related to the Yellow Sea than to the continental shelf off the south coast of China between Shanghai and Hainan (Figs. 4, 5). Both parts of the continental shelf total about 600,000 sq km and range in width between 230 and 460 km; the maximum is about seven times the world average width of continental shelves. Existing soundings indicate that the shelf slopes seaward more or less continuously to the shelf-break, except in the southern part of Taiwan Strait where rocky outcrops produce the Pescadores Islands and the submerged reefs and banks just southwest of them. Between the Pescadores Islands and the southwest side of Taiwan is a deep submarine canyon described by Yabe and Tayama (1929). At least one other submarine canyon, undescribed, occurs about 400 km northeast of Taiwan.

The crescentic Gulf of Tonkin is the southernmost area of the study. Lying west of Hainan, it is a shallow embayment of the South China Sea. The entire submarine area landward of the shelf-break (Fig. 6) totals about 170,000 sq km. Soundings are sparse, but they appear to reveal a broad smooth flat-floored area having its axis slightly nearer Hainan than Indochina, the probable source of most of its detrital sediments. The only notable minor irregularities occur between Hainan and the mainland to the north, where tidal currents have scoured a depression about 5 m below the sea floor at either end. Debris eroded from the depression or sediment prevented from settling there has formed a tidal delta at each end of the strait.

CLIMATE

The wide range of latitude of the region gives rise to some variety in the climate. At the north in the Gulf of Pohai and northern Yellow Sea the climate is Koppen's *Dwa* type: very cold dry winters and wet warm summers (Goode, 1943, p. 21). The rest of the area, except the coast between Shanghai and northern Taiwan and the coast of Indochina, is Koppen's *Cw* type, which is similar but has less rigorous winters. The exceptions above are *Cfa* and *Af*, respectively; both are warm to hot and wet throughout the year.

Average summer and winter air temperatures

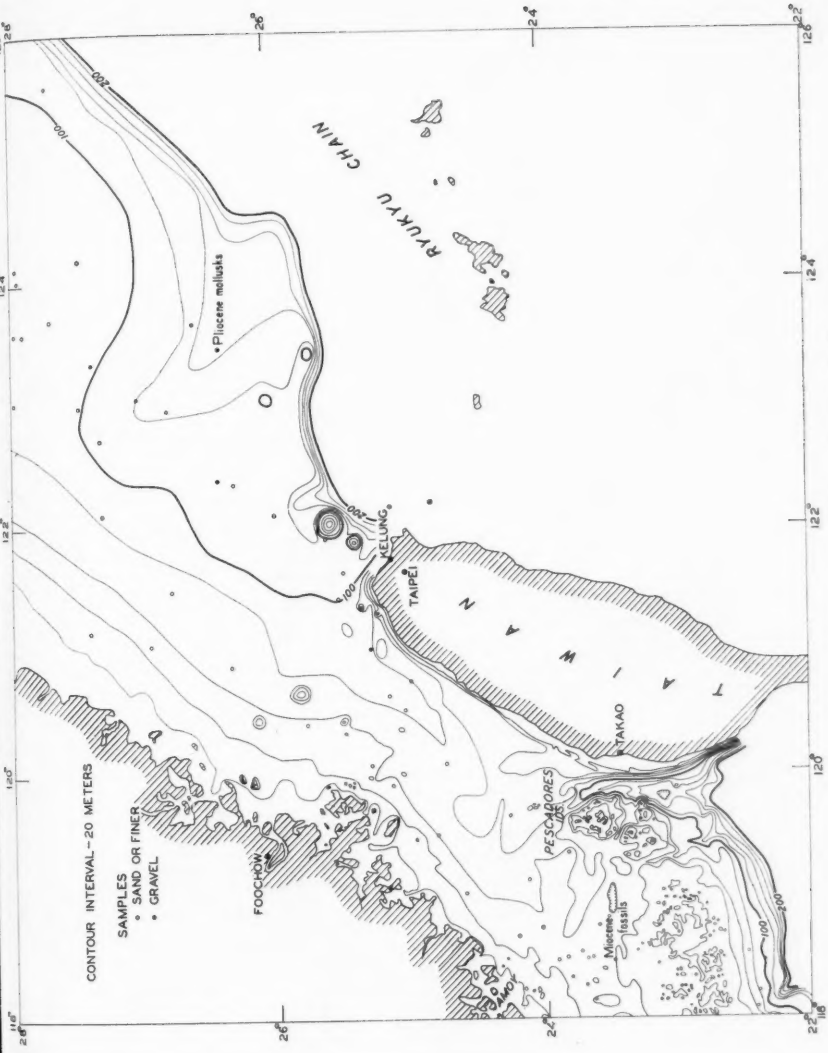

Figure 4. Detailed topography of Taiwan Strait and adjacent areas

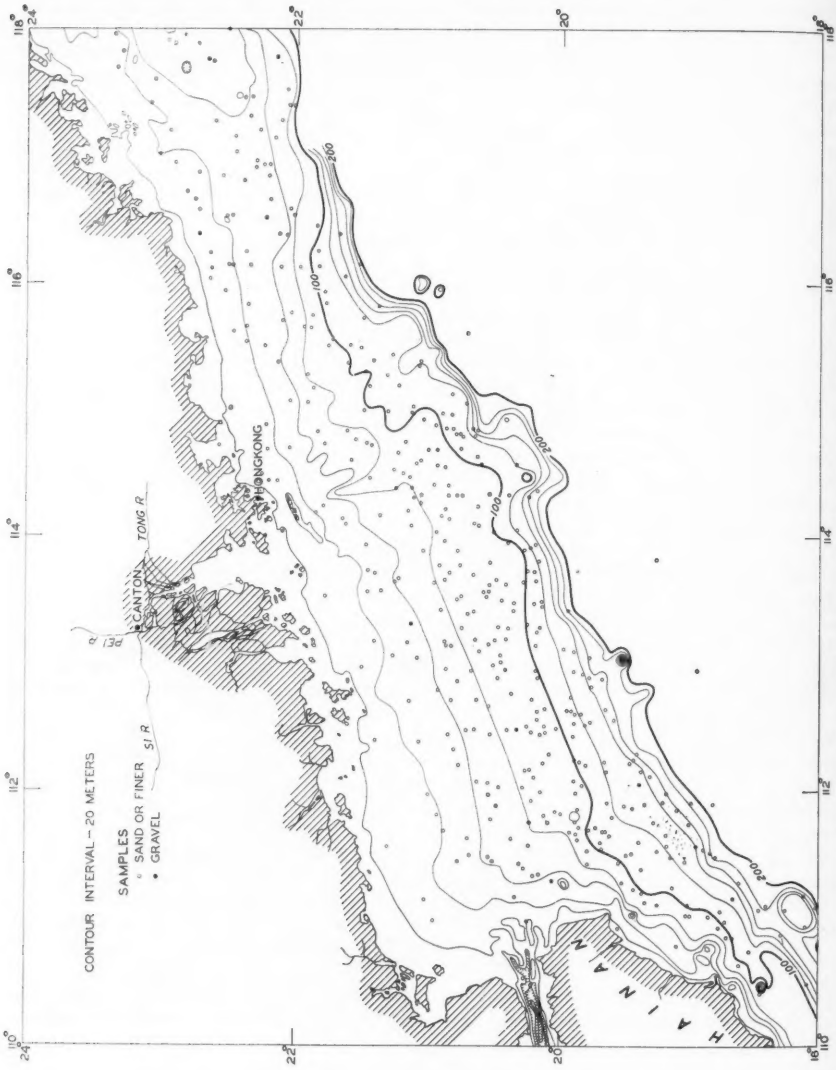

Figure 5. Detailed topography of shelf off coast of south China

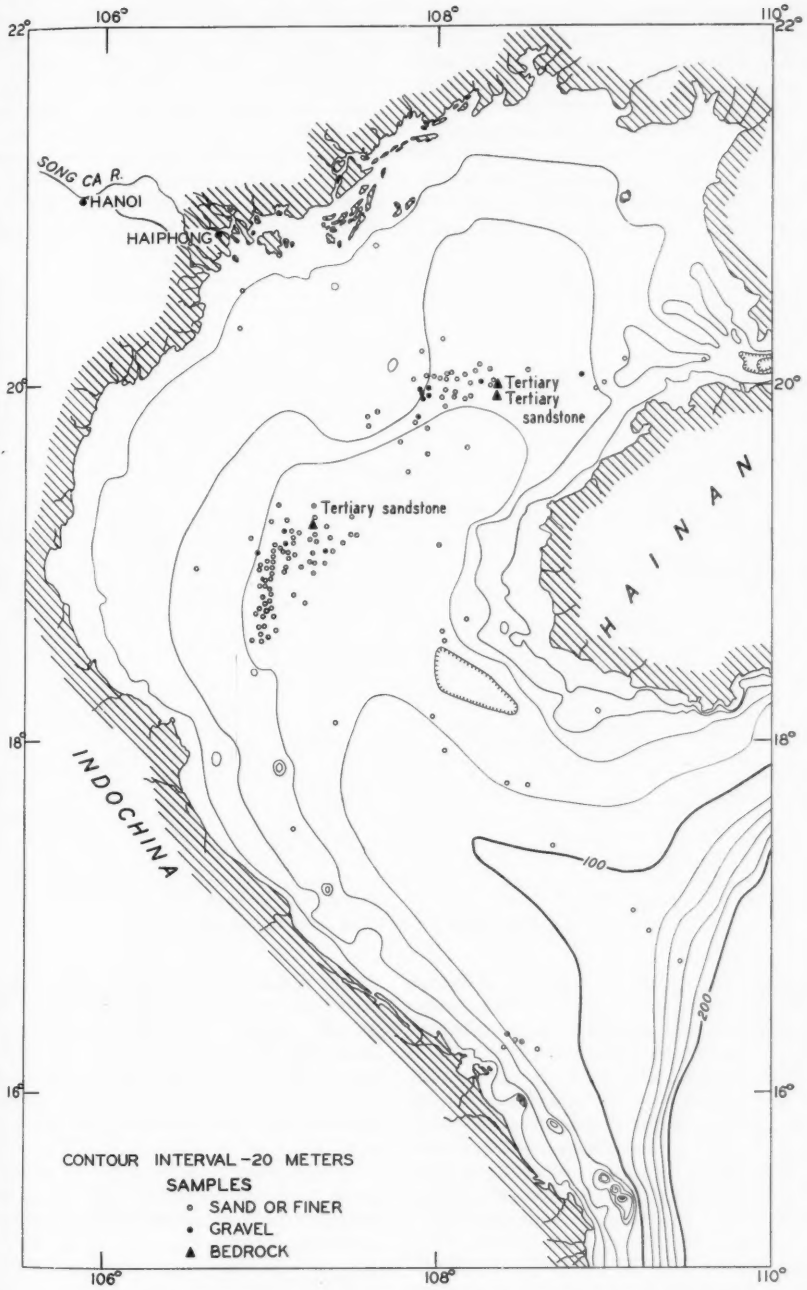

Figure 6. Detailed topography of northern South China Sea and Gulf of Tonkin

Figure 5. Detailed topography of shelf off coast of south China

over the ocean (Royal Netherlands Meteorological Institute, 1935) range between 25° and −6°C in the Gulf of Pohai, 28° and 14° near Taiwan, and 29° and 18° in the Gulf of Tonkin. Thus the range in degrees between the averages for summer and winter is nearly three times as great in the northern as in the southern part of the region. The annual rainfall ranges from less than 50 cm in the north to more than 200 cm in the south; since most of it falls during summer, this is the usual season of river floods.

Winds, studied from the same source compilation, are very different in summer and winter (Fig. 7). During the summer they blow onshore with low velocities, in response to a seasonal low-pressure area over China developed by solar heating. During winter the winds blow southerly offshore and southwestward parallel to the coast and have high velocities, especially where confined in straits between islands and the mainland. Typhoons are most common in the summer months; in early summer they move landward in the direction of the prevailing wind and in late summer northward parallel to the coast. During the winter they are rare and occur only in the south.

OCEANOGRAPHY

General

Comparison of results obtained by different cruises to various parts of the region show considerable changes from year to year in temperature, salinity, and currents. For this reason the writers considered it preferable to present results obtained during particular cruises, rather than results obtained by averaging the data of many. In addition, averages reported by hydrographic offices (Japan Hydrographic Office, 1910; Royal Netherlands Meteorological Institute, 1935; U.S. Dept. Commerce, 1938) are based on ship's log books that contain much inexpertly taken data, especially for sea-surface temperatures. Unfortunately, no general oceanographic cruises have been made throughout the whole region, so that the results presented here are the composite products of several cruises of different dates and places.

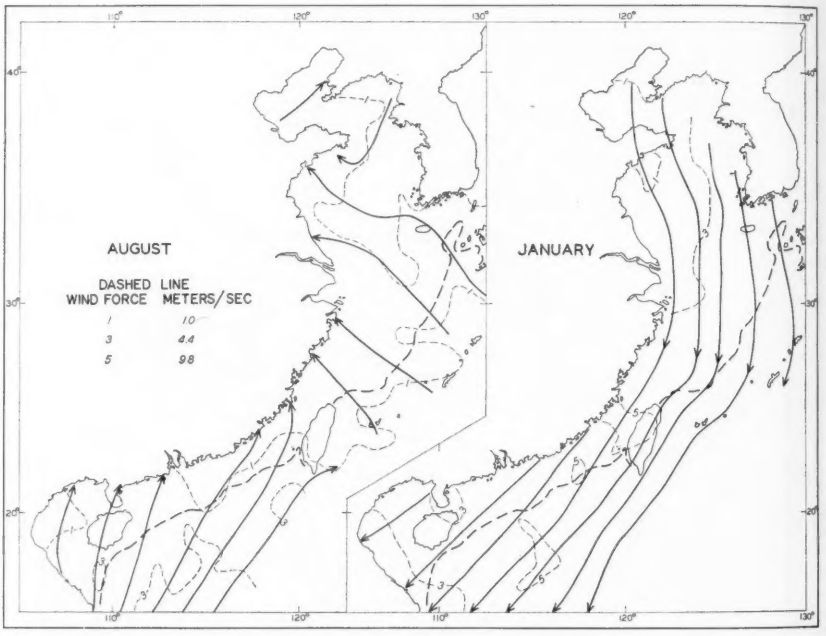

Figure 7. Wind direction and velocity, summer and winter

Temperature

Surface temperature for the summer (Fig. 8) is based on a cruise during August 1931 in

the Gulf of Pohai (Okamoto, 1950), fishing cruises of several summers in the Yellow Sea (Anonymous, 1931–1936; 1956), a cruise during June and July 1929 off the south China coast (Uda, 1949), and a cruise from July to September 1929 to the Gulf of Tonkin (Yasuhara, 1932). Winter temperatures are based on data from many cruises in the Yellow Sea and off the south China coast (Anonymous, 1931–1936; 1956) and a cruise from December 1929 to February 1930 in the Gulf of Tonkin (Yasuhara, 1932). Although many data have been obtained in the Yellow Sea, owing to the intense fishing effort there, little information is available for the Gulf of Tonkin, and winter data for all areas is sparse.

The results (Fig. 8) show a summer to winter range of 26° in the north and only 7° in the south, more or less paralleling the ranges in air temperature. During winter in the Gulf of Pohai temperatures are so low that much sea ice forms (U.S. Navy, 1946). Average nearshore temperatures are always lower and more changeable with the seasons than those offshore; thus, the seaward gradient of temperature is greater in winter than in summer. Local upwelling occurs east of Hainan, north of Taiwan, and possibly also south of Shan-Tung during summer. The smoother isotherms of winter are doubtless only the result of contouring sparser data.

Salinity

Data on the salinity of the surface water were obtained from the same composite sources as temperature but are less detailed. Salinity increases with distance from shore, reaching values of about 34 ‰ in the open sea near the shelf-break and 35 ‰ in the Kuroshio beyond (Fig. 9). The lowest salinity in the Yellow Sea (30 ‰) unaccountably appears to occur during winter, rather than during summer when the Hwangho and Yangtze rivers are in flood. South of Hong Kong the river discharge during summer produces a marked local decrease of salinity to less than 27 ‰, but salinity data for winter are lacking.

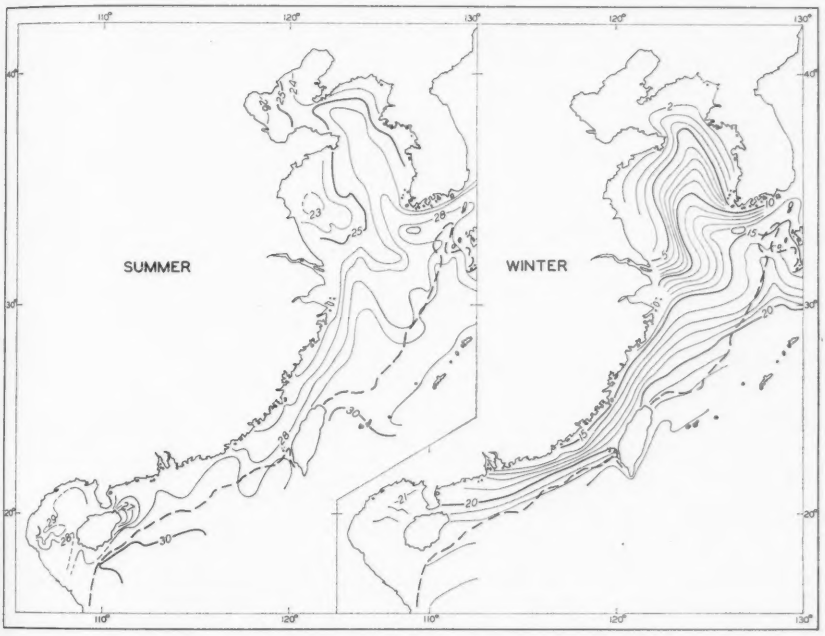

Figure 8. Surface-water temperature, summer and winter (°C)

Currents

Currents of the region are dominated by the warm high-salinity Kuroshio (Fig. 10) which is widest and fastest during the summer (Koe-

numa, 1939). Like the Gulf Stream (Stommel, 1958), the Kuroshio maintains a meandering pattern (Uda, 1951), shifting laterally several hundred kilometers. Most of the Kuroshio water moves eastward out of the region just south of Japan, but one branch passes around the west side of Taiwan and rejoins the main stream, especially during summer. Another branch, the Tsushima Current, enters the Japan Sea through Tsushima Strait between Japan and Korea, also mostly during the summer. Other smaller branches enter the east sides of the Gulf of Tonkin and the Yellow Sea during summer.

Near shore a southward-flowing countercurrent is best developed during winter when the Kuroshio is weakest. This current consists of cold low-salinity water partly derived from the large rivers. Extending south of Shan-Tung, the current moves along the shore, reversing the summer flow in the Strait of Taiwan and reaching as far as Hainan.

Comparison with the average wind pattern (Figs. 7, 10) suggests that the wind is largely responsible for the near-shore countercurrent, though the Kuroshio is produced by piling up of tropical water against the west side of the ocean by the trade winds. The northward shift of the belt of trade winds during the summer strengthens the Kuroshio in that season.

BOTTOM DATA

Notations on Charts

Before this study the chief source of information about bottom materials of the shallow portions of the East China Sea and the South China Sea was that of bottom notations on charts. These notations were derived from brief shipboard examination of bits of sediment adhering to the tallowed lead used in early hydrographic surveys. Owing to Japan's interest in fishing and navigation, about 53,000 notations of bottom materials appear on charts of the region published by the Japanese Hydrographic Office before 1941. These data were compiled into bottom-sediment charts by Shepard, Emery, and Gould (1949), who published some of them. Patterns from five of the original charts were redrawn to bring together

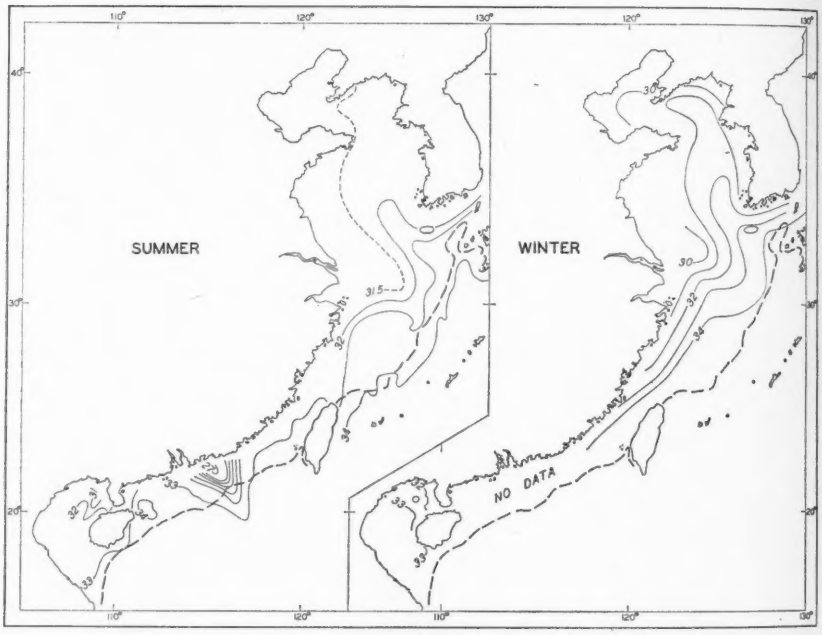

Figure 9. Surface-water salinity, summer and winter (o/oo)

into two sheets all the information for the East China Sea and the South China Sea (Figs. 11, 12).

At first glance the sediment charts appear to present only a random patchiness of bottom materials, but analysis shows some system to the pattern. Rock bottom occurs in straits, atop submarine hills, off rocky points and islands, and near the shelf-break; at these places strong wave and/or current action prevents deposition of fine-grained sediment. Gravel is commonly associated with the rock bottom. A few areas of rock are reported in the flat central basins of the Gulf of Pohai and the Gulf of Tonkin, but not of the Yellow Sea. Rock also is more common on the broad missle areas of the continental shelf bordering the Yellow Sea and the south China coast. Mud, at the other extreme, is the common bottom material in the middle areas of the Gulf of Pohai, Yellow Sea, and Gulf of Tonkin, where partly encircling coasts offer some protection from waves and currents. Mud bottom close to shore between Shanghai and Hainan evidently owes its presence to a more rapid supply by rivers than removal by currents. Sand bottom occupies positions intermediate in exposure between those of rock and of mud. It is dominant near the outer edge of the shelf from Korea to Hainan, probably largely in response to the winnowing of finer grains by the Kuroshio (Fig. 10). Frequent notations of shell sand indicate that much of the sand is produced locally by organic growth.

Samples

The total of 982 samples represents an average of only 1 per 1500 sq km, in contrast to the average for bottom notations of 1 per 26 sq km. Although the number of samples is less than 2 per cent of the number of bottom notations on navigational charts, laboratory examination of them provides information far exceeding their relative proportion. The combination of thousands of notations and a few hundred samples is perhaps ideal for learning about the distribution and origin of the sediments.

The total number of samples from the Gulf of Pohai and Yellow Sea northwest of a line between the tip of Korea and Shanghai is 96

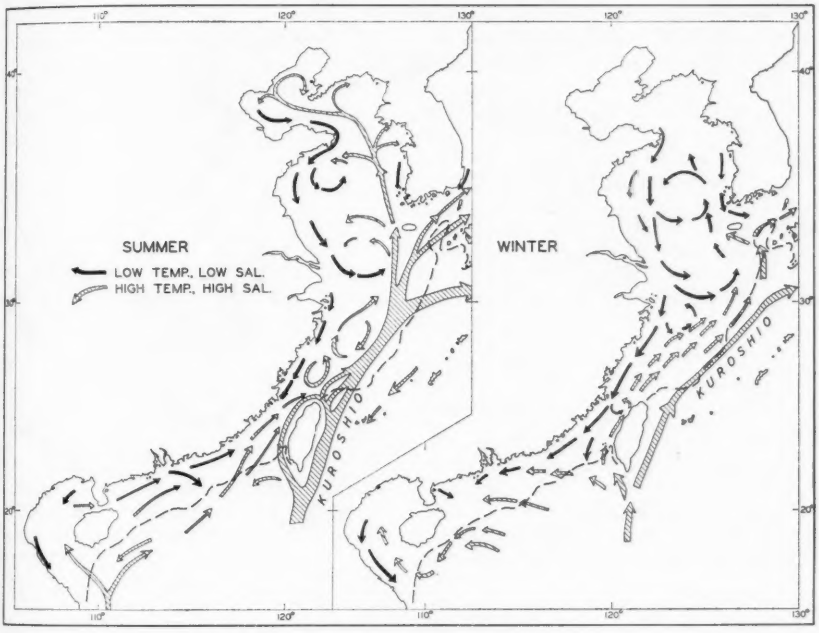

Figure 10. Surface currents, summer and winter

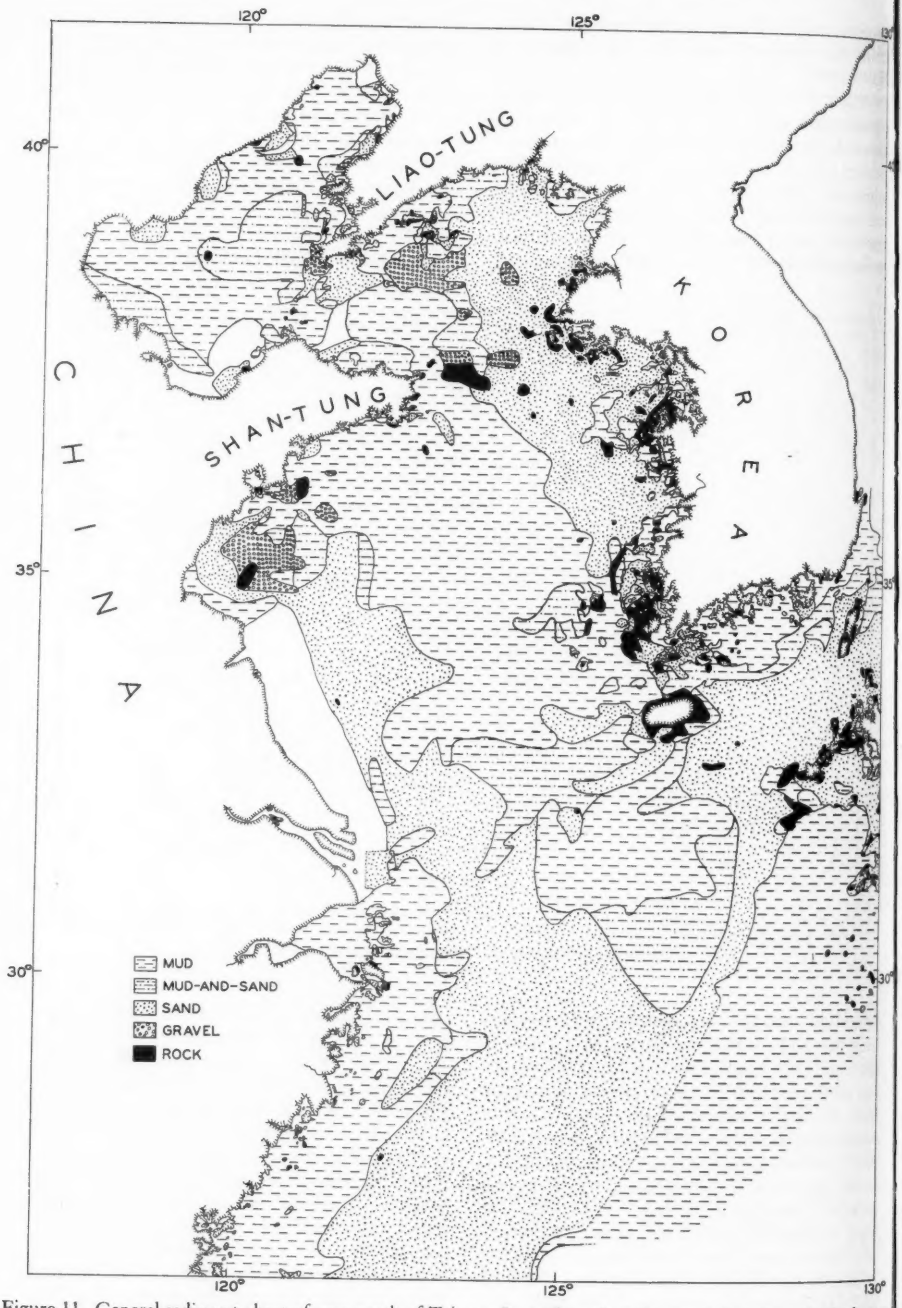

Figure 11. General sediment chart of area north of Taiwan, East China Sea. Pattern is based on 45,000 bottom notations of navigational charts. Partly from Shepard, Emery, and Gould (1949)

(Fig. 3). They are fairly evenly distributed except for sparseness in the Gulf of Pohai where fishing is poor, northwest of Shanghai where the water is very shallow, and near Korea where Japanese may not fish. Seaward of this arbitrary line, in the shallow area of the East China Sea (Fig. 3) are 277 well-distributed samples. Near Taiwan Strait (Fig. 4) are 55 samples, and on the continental shelf off the south China coast (Fig. 5) are 414. The 8 samples from the outer part of the Gulf of Tonkin (Fig. 6) bring to a total of 754 the samples from open continental shelves. Within the Gulf of Tonkin are 132 samples, about 50 per cent more than the number in the Yellow Sea, but these are very poorly distributed owing to political restriction of near-shore waters to the fishing industry.

The depth distribution of the samples is as follows:

Meters	*Per Cent*
0– 20	1
20– 40	8
40– 60	16
60– 80	27
80–100	25
100–120	13
120–140	5
140–160	2
160–180	1
180–200	1
200+	1
	100

Thus, 90 per cent of the samples are from depths shallower than the average shelf-break at 120 m. Because of danger to navigation and the lack of fish only 9 per cent are from depths shallower than 40 m.

Rocks

Among the bottom samples are many that contain rounded gravel and a few with pieces of rock believed to be bedrock because of fresh fractures or fragileness. On the outer shelf of the Yellow Sea (Fig. 3) olivine basalt was found in place off Shanghai, and sandstone containing Eocene or Oligocene mollusks was found at two adjacent stations west of Saishu Island (Niino, 1934). Southeast of Saishu Island one sample contains angular pieces of shale so soft that a nearby outcrop is indicated and another sample probably in place consists of similar shale with Pliocene mollusks and crabs (Niino, 1952). Exposures of bedrock in these areas support the suggestion of a former arcuate mountain connection between Korea and the mountains of south China, the middle part of which has eroded to form the flat and shallow sill or entrance to the Yellow Sea.

Only gravel was found among the samples from the area near Taiwan (Fig. 4), but two of the gravel samples contain fossils: Pliocene mollusks northeast of Taiwan and Miocene west of the Pescadores Islands. Samples from the shelf off the south China coast (Fig. 5) include no bedrock, though rounded gravel was found in several of them.

Many samples from the deep middle area of the Gulf of Tonkin (Fig. 6) contain gravel, and three have sandstone bedrock lithologically similar to sedimentary strata on Hainan.

Bedrock and gravel identified on the basis of chart notations and samples show that large areas of the Gulf of Pohai, the outer Yellow Sea, the shelf off the south China coast, and the Gulf of Tonkin contain only a thin cover of sediment atop bedrock. One of the areas of bedrock is about 200 km directly off the mouths of the large Yangtze and Tsientang rivers, which shows that the deltas of these rivers are not of great thickness there. Only in the central Yellow Sea southwest of Shan-Tung and west of South Korea is there a possibility of thick modern sediments.

TOTAL SEDIMENT

General Textures

A general description of the total dried sediment was prepared before separating its six main components: detrital, organic, authigenic, residual, relict, and volcanic. For some purposes in this report detrital, residual, and relict sediments are grouped under the term terrigenous.

Each sample was examined by a binocular microscope and assigned to one of four types: sand, muddy sand, sandy mud, or mud. Designation as sand required that at least an estimated 90 per cent of the bulk of the sample consist of grains of sand size (coarser than 0.062 mm). Mud required that 90 per cent of the bulk must consist of grains of silt or clay size (finer than 0.062 mm). Muddy sand and sandy mud are intermediate; 50–90 per cent is composed of sand grains in the former, and 50–90 per cent of silt and clay grains in the latter. Distribution maps (Figs. 13, 14, 15) were drawn on the basis of these estimated textures.

In the Gulf of Pohai and the Yellow Sea mud occurs mostly along the west side, extending as far southwest as Taiwan. A small area of mud is present at the south end of

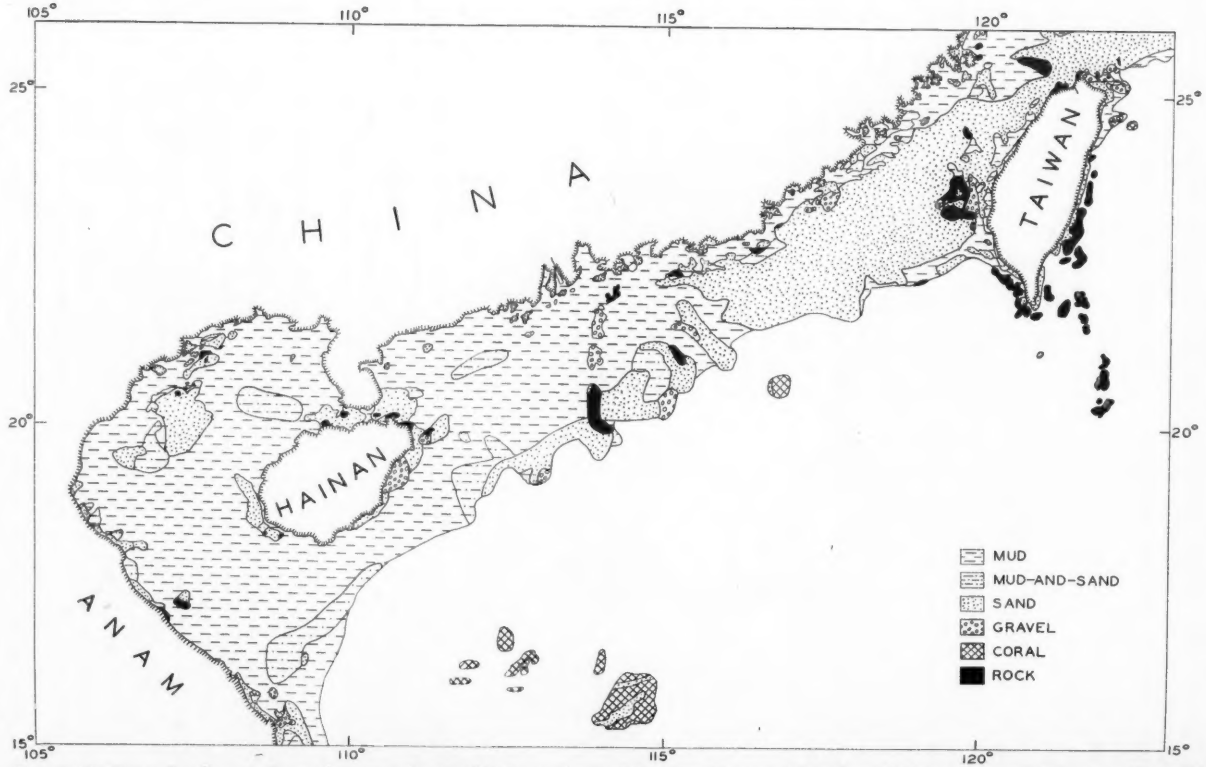

Figure 12. General sediment chart of area southwest of Taiwan, South China Sea. Pattern is based on 8000 bottom notations of navigational charts. Partly from Shepard, Emery, and Gould (1949)

Korea, and another is shown by the limited samples from the Gulf of Tonkin off the mouth of the Song Ca River (at Hanoi). Sand occupies the east side of the Yellow Sea and the outer half of the continental shelf from Korea to Hong Kong. A small patch is also present in the strait between Hainan and the mainland. Most of this sand, particularly that on the shelf, has a high content of shell fragments. The muddy sand and sandy mud occupy an intermediate position between sand and mud in the Yellow Sea. Little of either is present on the continental shelf between Shanghai and Hong Kong, but southwest of Hong Kong and in the

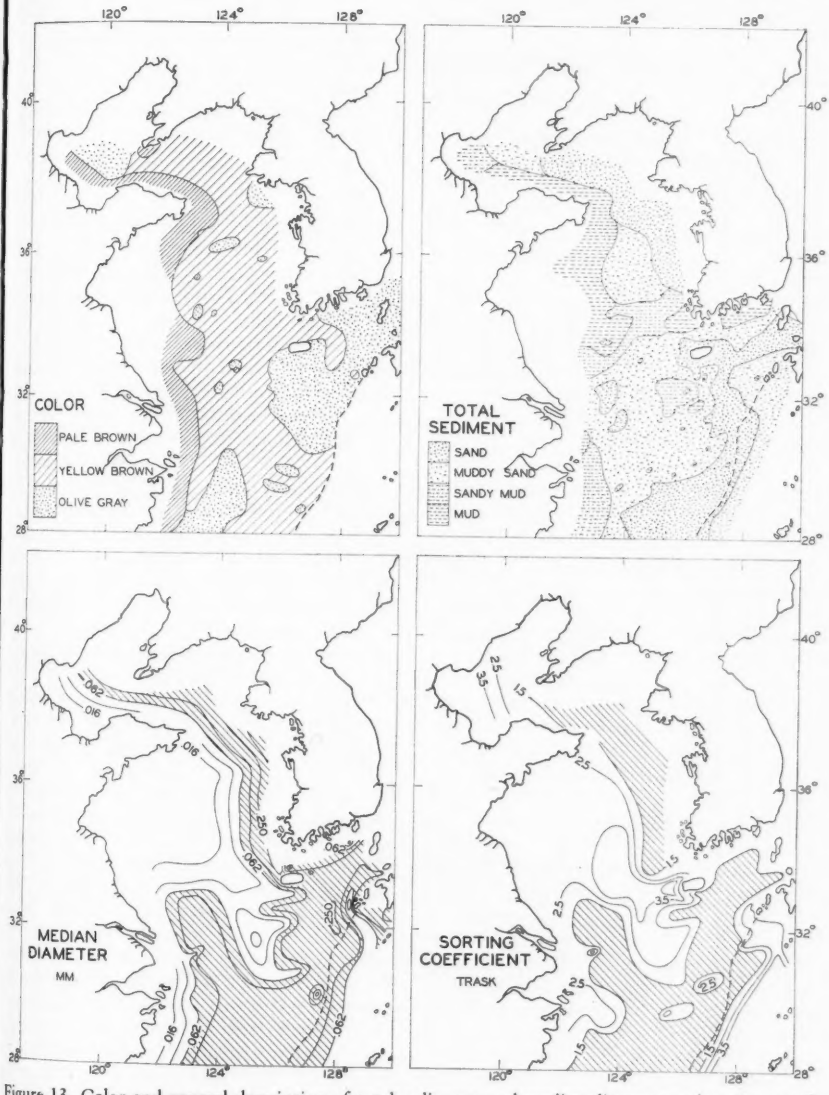

Figure 13. Color and general description of total sediment, and median diameter and sorting coefficient of noncalcareous part of sediments from East China Sea

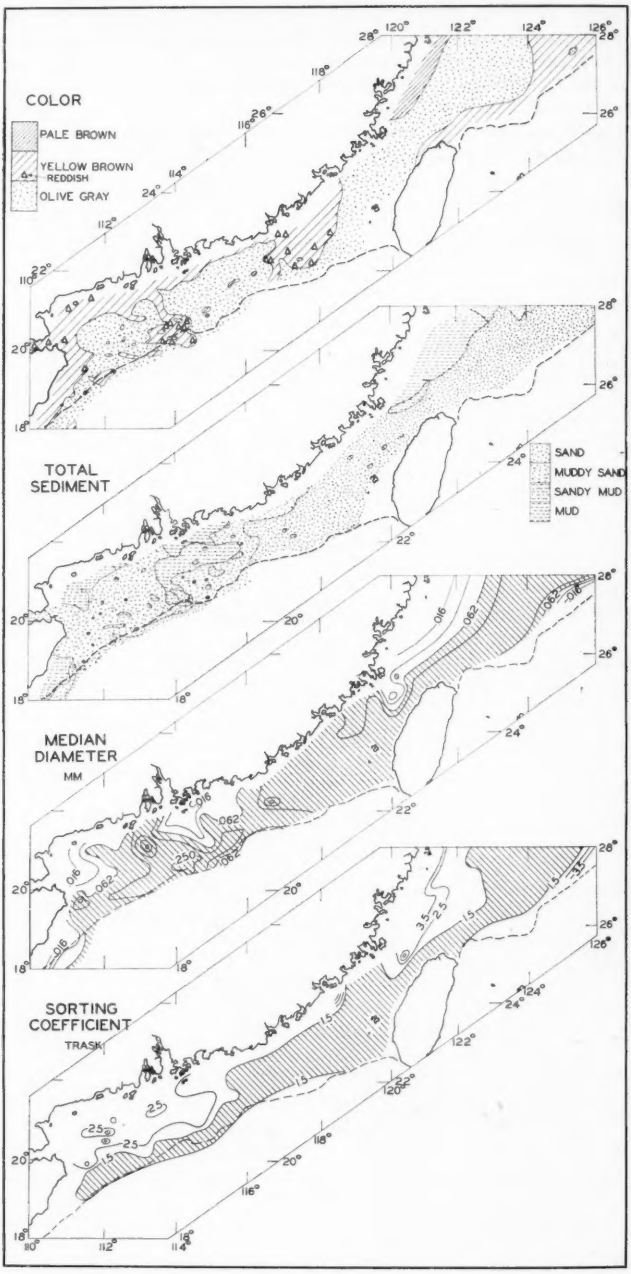

Figure 14. Color and general description of total sediment, and median diameter and sorting coefficient of noncalcareous part of sediments from Taiwan Strait and shelf off coast of south China

Gulf of Tonkin muddy sand is dominant and accompanied by small patches of sandy mud.

As one might expect, the bottom-sediment charts showing general textures of whole sediment (Figs. 13, 14, 15) correspond closely to the charts based on published navigational chart notations of bottom materials (Figs. 11, 12). The chief differences are the result of subdividing the mud and sand of the latter into two textures. Minor differences occur because of the denser sampling grid permitted by the more numerous chart notations and because of the more nearly precise and uniform identifications of the samples made by a single observer in the laboratory.

Color

Color of the dry samples was estimated using the Rock-Color Charts devised by Goddard *et al.* (1948). Nearly all samples could be approximated by three main colors: 5 YR 5/2—pale brown, 10 YR 5/4—yellow brown, and 5Y 5/2—olive gray. Maps of color distribution (Figs. 13, 14, 15) show that each of the differently colored sediments occupies a particular kind of environment, and a comparison with other parameters shows that each has a different composition.

The pale-brown sediment occupies the smallest area, near the China shore from the Gulf of Pohai to Taiwan, plus a small area near the Indochina shore of the Gulf of Tonkin. The sediment is fine-grained, well sorted, and slightly calcareous or noncalcareous. These characteristics, together with its presence near the mouths of the large rivers that drain the interior, indicate that it consists of loess reworked by streams and brought to the ocean where the near-shore marine currents carried it southward (Fig. 10) for redeposition in the marine environment.

Olive-gray sediment covers the widest area. It is medium- to coarse-grained and ranges from highly calcareous shell sand on the continental shelf to slightly calcareous muddy sand in the Gulf of Pohai and Gulf of Tonkin. For the coarse sediment the color was taken as an average of the white or cream-colored shell fragments and the darker detrital grains. For the more homogeneous fine sediments the color approaches but does not quite reach the green typical of fine-grained detrital marine sediments found at moderate depths at many other places of the world (about 5 Y 3.5/2 to 3 GY 4/3).

Yellow-brown sediment commonly occupies an intermediate position between sediments of the other two colors. Most is of intermediate grain size, sandy mud to muddy sand. These characteristics suggest that its color may be due to mixing of sediments of the two other colors. Some samples within the area of yellow-brown sediment off south China have a reddish tinge (Fig. 14) suggesting possible reworking of lateritic soils of south China (Lee, 1939, p. 8).

TERRIGENOUS FRACTION

Median Diameter

After the acid-soluble part of the sediment samples had been removed by treatment with dilute hydrochloric acid, the insoluble residue was washed and wet-sieved through a wire screen having openings 0.062 mm in diameter. The fraction remaining on the screen was dried and weighed. If large compared to the fine fraction, its size distribution was measured in a settling tube. The fraction passing through the screen was dried and weighed if it was small compared with the coarse fraction. If the fine fraction was large, it was dispersed with sodium hexametaphosphate, filtered several times to remove traces of the acid, and its size distribution measured by the pipette method.

The analyses of insoluble residue are essentially of the detrital fraction alone, because only negligible amounts of insoluble grains of organic, volcanic, authigenic origin are present. The resulting areal distribution of median diameters (50 per cent of weight coarser and 50 per cent finer than the median diameter) differs markedly from the distribution of textures of whole sediment (Figs. 13, 14, 15), owing to removal of shell fragments and foraminiferal tests, most of which are coarse compared with the accompanying detrital grains.

In the Gulf of Pohai and the Yellow Sea (Fig. 13) median diameters exhibit a smooth increase from the west to the east coasts. This is probably an effect of the large Hwangho, Yangtze, and Tsientang rivers on the west that dump sediments which are much finer-grained than those that are contributed by the shorter steeper Korean streams on the east side. At the outer part of the Yellow Sea, where bedrock closely underlies the bottom, the detrital sediments are of about the same coarseness as those along the east side of the Yellow Sea. Detrital sediments seaward of the shelf-break again become fine, so that the shelf south of Shanghai is fine-grained near shore, coarse offshore, and fine beyond the shelf. A tongue of coarse-

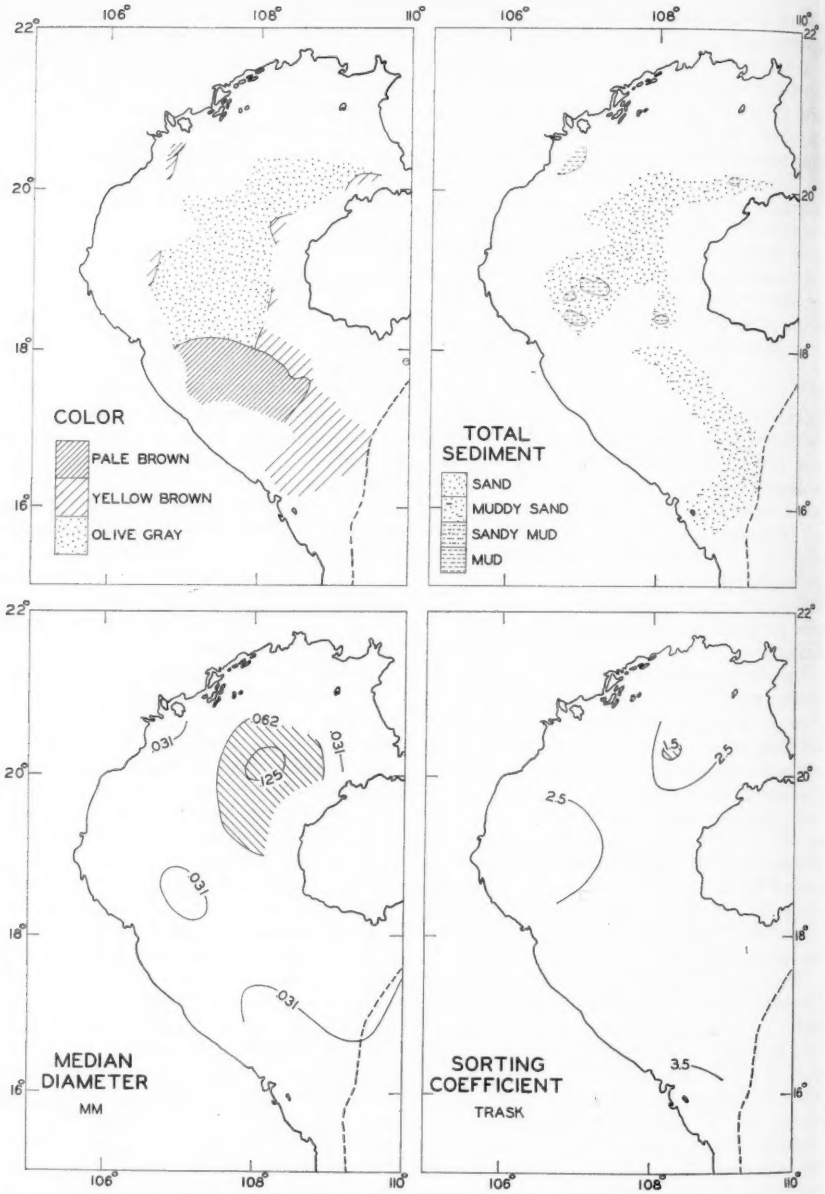

Figure 15. Color and general description of total sediment, and median diameter and sorting coefficient of noncalcareous part of sediments from Gulf of Tonkin

grained detrital sediment that extends northward to a point east of Shanghai probably results in part from the presence of outcrops of bedrock that provide residual sediment. Farther south between Taiwan and Hainan the shelf again has three general zones. Fine sediment occurs near shore, especially off the Si and Tung rivers at Hong Kong and in the sheltered area east of Hainan. Coarse sands are present on the outer half of the shelf, and these grade into finer sediment in deeper water beyond the shelf-break. The coarsening on the outer half of the continental shelf has its counterpart elsewhere in the world where it probably marks a zone of coarse shore and littoral sediment deposited during Pleistocene glacial epochs of

TABLE 1. SUMMARY OF COMPOSITION OF SEDIMENT SAMPLES, YELLOW SEA, CONTINENTAL SHELF, AND GULF OF TONKIN

(In weight per cent)

	Yellow Sea		Continental shelf		Gulf of Tonkin
	West side (3)*	East side (3)	Outer half (6)	Inner half (6)	(4)
Organic					
Carbonate					
Shells	27	34	51	20	18
Foraminifera	44	59	47	52	29
Miscellaneous	29	7	2	28	53
	100 = 10.9	100 = 9.0	100 = 34.3	100 = 13.7	100 = 17.8
Silica	3.0	2.3	tr	tr	tr
Organic matter	1.2	.3	.3	1.0	1.2
Authigenic					
Glauconite	.5	.3	2.5	.0	.8
Terrigenous					
Silt and clay	57.8	.8	6.4	64.7	39.0
Sand					
Light minerals					
Quartz	50	67	73	49	64
Plagioclase	16	16	13	20	17
Orthoclase	9	11	7	10	4
Rock fragments	25	6	7	21	15
	100 = 26.0	100 = 86.1	100 = 55.7	100 = 20.3	100 = 40.9
Heavy minerals					
Hornblende	23	31	33	25	25
Alterite	24	14	17	27	14
Olivine	14	11	10	7	15
Magnetite	7	7	6	11	11
Leucoxene	8	7	4	6	5
Ilmenite	5	5	7	6	5
Garnet	6	14	tr.	3	tr.
Augite	2	4	3	3	3
Zircon	5	tr.	6	tr.	3
Hematite	tr.	tr.	tr.	2	7
Epidote	tr.	tr.	2	2	tr.
Biotite	tr.	tr.	tr.	tr.	3
Sphene	tr.	tr.	2	2	tr.
Hypersthene	0	0	5	0	0
Serpentine	tr.	0	tr.	tr.	tr.
Enstatite	tr.	tr.	0	tr.	tr.
Rutile	0	tr.	0	0	0
Muscovite	0	0	0	0	tr.
Kyanite	0	0	0	tr.	0
	100 = 0.6	100 = 1.2	100 = 0.8	100 = 0.3	100 = 0.3
	100.0	100.0	100.0	100.0	100.0

*Numbers in parentheses show number of samples on which the averages are based.

lowered sea level and left behind as a relict sediment when sea level rose after that glacial time. These sediments also are believed to be relict, as suggested also by the inclusion in them of some pre-Recent foraminiferans, worn and replaced by phosphorite and glauconite (Polski, 1959; Waller, 1960). At present tidal and other currents prevent burial of the relict sediment under fine-grained modern detrital sediments.

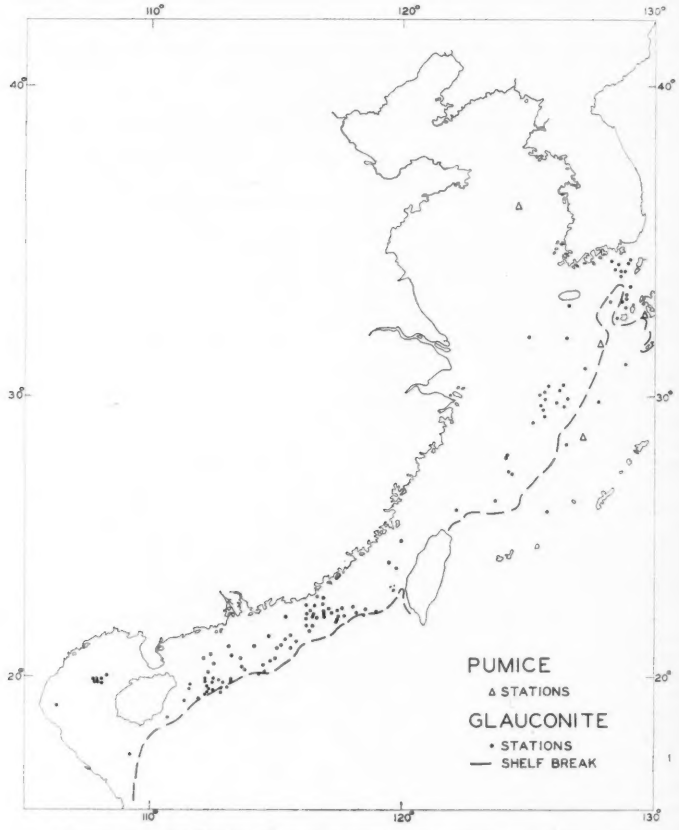

Figure 16. Distribution of samples containing pumice and glauconite

Sorting

The Trask sorting coefficient ($So = \sqrt{Q_c/Q_f}$) is based on the coarse and the fine quartiles of the weight distribution of the grains. According to Trask (1932, p. 71–72), a coefficient smaller than 1.5 indicates good sorting, whereas one larger than 4.5 indicates poor sorting. As discussed by Emery (1954), it seems desirable to drop the use, in an absolute sense, of the terms well-, moderately well, and poorly sorted and instead use the sorting coefficient only for describing the relative degrees of sorting within a given environment.

In the Gulf of Pohai and the Yellow Sea (Fig. 13) the sorting coefficients indicate poorer sorting along the west side and better along the east side. On the outer half of the Yellow Sea and along the continental shelf (Fig. 14) the sorting is poorest near the shore, best on the

outer part of the shelf, and poor again beyond the shelf-break. The Gulf of Tonkin, with its fine-grained sediment, is characterized by poorer sorting than is the area of coarse sediments of the shelf.

The areal distribution of sorting coefficients (Figs. 13, 14, 15) shows a markedly close relationship with that of median diameter; the coarsest sediments are the best sorted. This relationship is probably a confirmation of Inman's (1949) finding that where a single depositional agent is involved, the best sorting occurs in sediments of fine sand size (0.125–0.250 mm), and the sediments are relatively poorly sorted as they are finer or coarser than this optimum size.

Mineralogy

A separation of the sand-size insoluble residue into light and heavy minerals was made by floating or sinking with the heavy-liquid, acetylene tetrabromide. The light minerals were identified by standard staining techniques and the heavy minerals by their optical characteristics (Table 1).

Light minerals are dominated by quartz, but the feldspar/quartz ratio averages 1:3, and the sands must be classified as arkosic. Many of the samples, however, contain rock fragments, largely of metamorphic origin, and 50 per cent or more of silt and clay, which indicates that graywacke is a better general term for most of the sediments, especially the fine-grained ones.

More than a quarter of the total heavy minerals consists of hornblende. Olivine, magnetite, leucoxene, ilmenite, and garnet are intermediate in abundance. Nearly a fifth of the heavy-mineral group comprises one or more minerals that are so highly altered that identification proved to be very uncertain. These are termed alterite. In general, there is little difference in the compositions of heavy-mineral suites in the different areas; this suggests a reasonably uniform source and degree of weathering. Both the light and heavy fractions are characterized by unstable mineral species.

Radioactivity of the acid-insoluble coarse fraction was measured by placing the tube of a Geiger counter 1 cm above a tray containing sediment spread in a layer 5 cm long, 2 cm wide, and 0.2 cm deep. Counts per minute were determined and corrected for background. Results showed counts of between 1 and 17 above background. Highest counts (more than 10) were found along the Korean side of the Yellow Sea and immediately off the mouths of the Yangtze and Tsientang rivers.

VOLCANIC FRACTION

The volcanic fraction found in the insoluble residue consists of pieces of pumice as large as 1 mm and shards of volcanic glass that are much smaller. The pumice is white to pinkish brown and is probably andesite. Only the pumice was mapped (Fig. 16); it was most abundant on the continental shelf between Saishu Island and Taiwan. It probably was floated by currents from volcanoes on Saishu Island, northern Taiwan, Pescadores Islands, and many islands of the Ryukyu Chain to the east.

AUTHIGENIC FRACTION

The two most common authigenic minerals in continental-shelf sediments of the world are glauconite and phosphorite; manganese oxide occurs locally as films on exposed rocks. In this region, no manganese oxide was noted, and phosphorite, though sought by optical and chemical methods, was not found in the samples, except rarely as phosphatized foraminiferal tests. Glauconite was found in 127 samples (Fig. 16), about one-eighth of the 982 bottom samples. Most is from the outer half of the shelf. In some samples only a few grains were found. Glauconite constitutes more than about 5 per cent of the total sediment in only a few samples. Most of it is in the form of pellets, but some occupies the cavities of foraminiferal tests or gastropod shells. Most grains are dark green, but some, especially toward the north, are light green. Some pellets have a network of cracks that contain white or yellow filling.

ORGANIC FRACTION

Calcium Carbonate

The fraction of the whole sediment that is soluble in dilute hydrochloric acid is termed for convenience calcium carbonate, though it contains some magnesium carbonate. Figures 17, 18, and 19 show that calcium carbonate is most abundant in sediments of the outer half of the continental shelf between Korea and Hainan; values of more than 20 per cent are typical, and values of more than 60 per cent are present locally. The lowest percentages of calcium carbonate characterize the embayments of the Gulf of Pohai, Yellow Sea, and Gulf of Tonkin, in each of which 10 per cent is typical, but the range is about 1–20 per cent. Intermediate

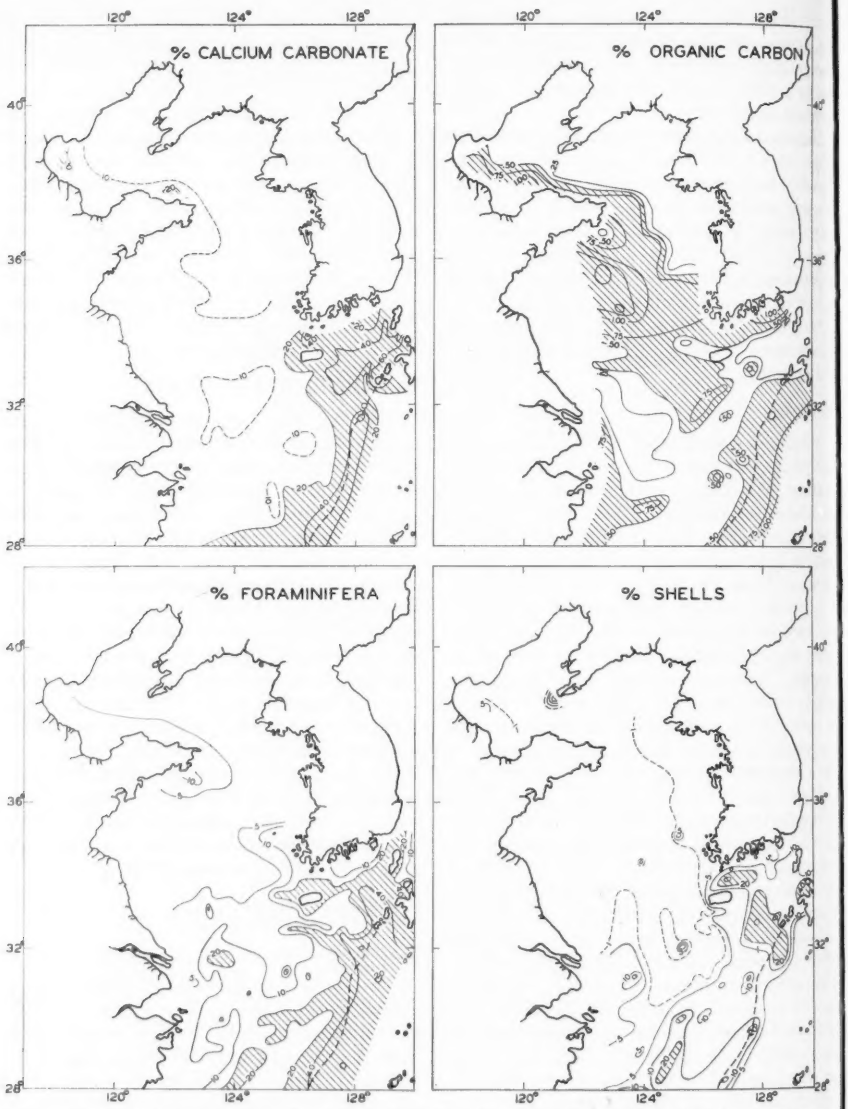

Figure 17. Organic constituents of sediments from East China Sea. Percentage of calcium carbonate, organic carbon, Foraminifera, and shell fragments. Lined pattern indicates areas of high percentages.

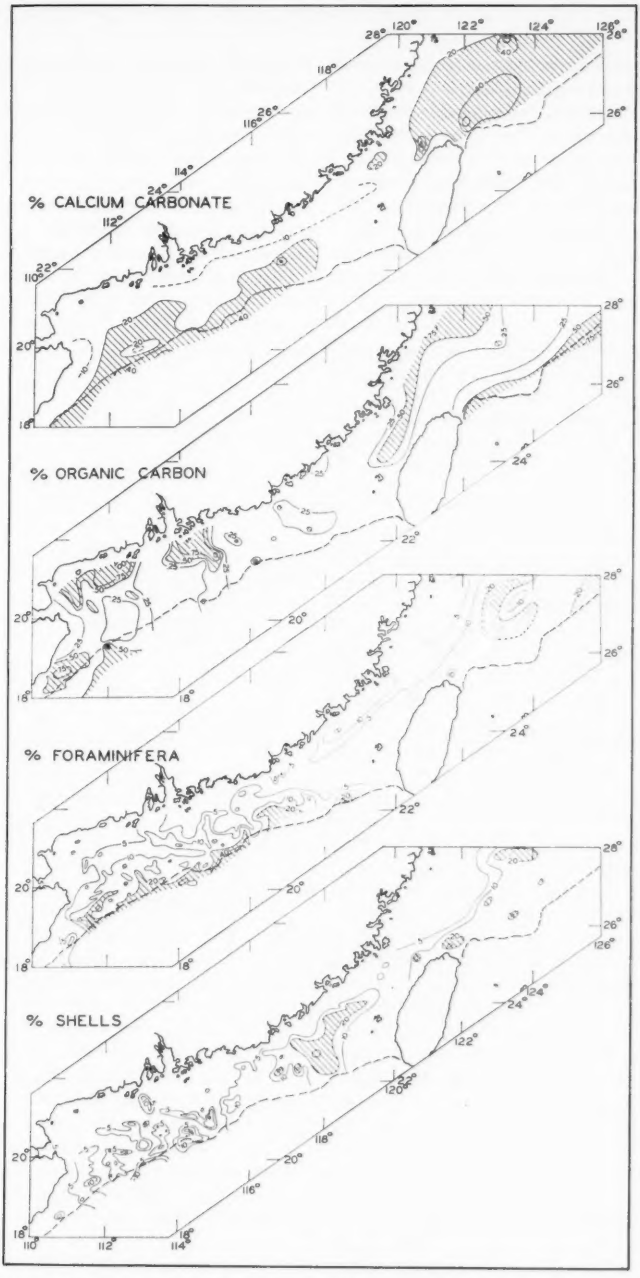

Figure 18. Organic constituents from Taiwan Strait and shelf off coast of south China. Percentage calcium carbonate, organic carbon, Foraminifera, and shell fragments. Lined pattern indicates areas of high percentages.

percentages of 10–20 per cent occur along the inner half of the continental shelf.

Three sources of the calcium carbonate are possible: organic debris, reworked limestone, and chemical precipitation. No acicular crystals, such as might be expected of chemical precipitates, were noted, but they may be present in minor amounts as fine silt and clay-sized grains. Small pieces of reworked limestone are probably present locally, but only in neglibible quantities. Most of the calcium carbonate is of direct organic origin, chiefly in the form of foraminiferal tests, followed in order by broken shells of mollusks (mostly pelecypods, gastropods, and pteropods), echinoid spines, and bryozoans. Only foraminiferal tests and shell fragments proved abundant enough to assign estimates of percentage abundance by binocular examination. In the fine-grained sediments the sum of the per-

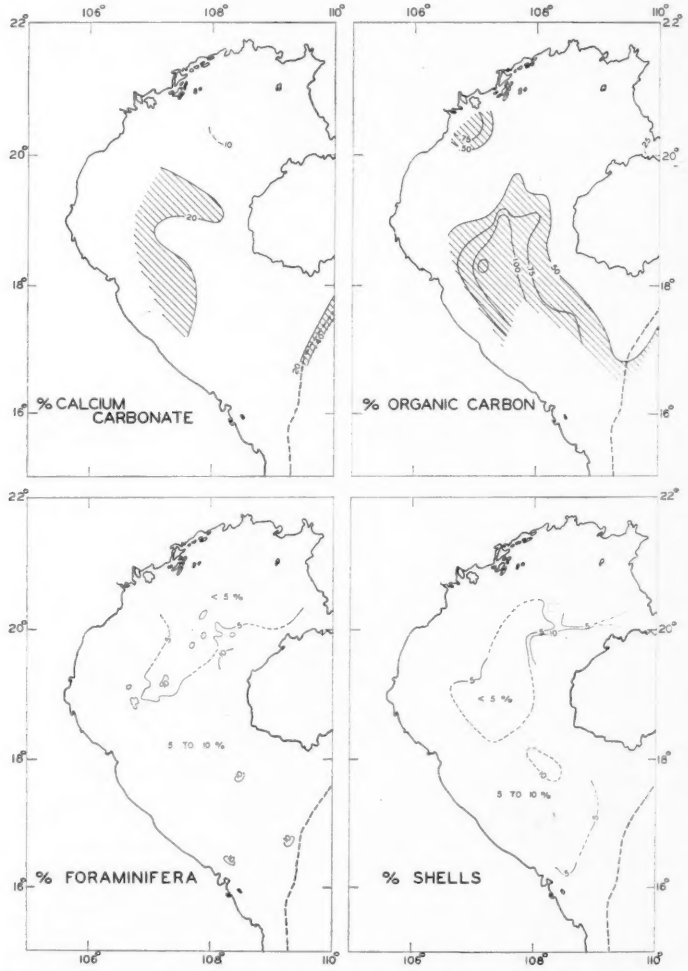

Figure 19. Organic constituents of sediments from Gulf of Tonkin. Percentage calcium carbonate, organic carbon, Foraminifera, and shell fragments. Lined pattern indicates areas of high percentages.

centages of Foraminifera and shells is commonly less than the percentage of total acid-soluble material; this deficiency is ascribed to organic debris so finely comminuted that it is not apparent in binocular examination of the samples.

The areal distribution of both foraminiferal tests and shell fragments (Figs. 17, 18, 19) closely follows that of total calcium carbonate: each is most abundant on the outer half of the continental shelf between Korea and Hainan, least abundant in the enclosed seas, and of intermediate abundance on the inner half of the shelf. The ratio of tests to shells is highly variable throughout the region, but some generalizations are possible. Shells are the more abundant in straits near Taiwan, Saishu, and Hainan, and in the upper part of the Gulf of Tonkin, whereas foraminiferal tests are the more abundant in the Gulf of Pohai, the Yellow Sea, the continental shelf fronting the Yellow Sea, and the shelf between Hong Kong and Hainan. In a general way, shell fragments dominate in sandy sediments and foraminiferal tests in finer sediments, as is perhaps reasonable considering the greater wall thickness and, thus, greater resistance to comminution exhibited by shells than by foraminiferal tests. The relative initial abundence of shells and tests is unknown.

Table 2. Summary of Sediment Characteristics, Yellow Sea and Gulf of Pohai, Continental Shelf, and Gulf of Tonkin

(Figures are averages.)

	Yellow Sea and Gulf of Pohai	Continental shelf	Gulf of Tonkin
Area (sq km)	500,000	600,000	170,000
Depth (m)	50	60	50
Annual temperature range (°C)	5–26	17–28	23–28
Annual salinity range (o/oo)	31–32	33–34	32–33
Median diameter (mm)	0.06	0.12	0.04
Sorting coefficient	2.5	1.5	3.0
Calcium carbonate (%)	10	30	15
Foraminiferal tests (%)	6	14	7
Shell fragments (%)	2	14	5
Organic carbon (%)	0.8	0.3	0.6

Silica

The chief siliceous organic remains in the samples are spicules of many kinds of sponges. These are most abundant in the central Yellow Sea and Gulf of Pohai, where they constitute as much as 10 per cent of the total organic fraction, but only 1 or 2 per cent of the whole sample. They are less common in the Gulf of Tonkin but are rare on the continental shelf. Planktonic diatoms are less abundant but were observed in samples from the same general areas having sponge spicules. *Coscinodiscus* is most common, followed by *Chaetoceras* and *Navicula*. A fresh-water kind of *Pennatae* was noted in some samples off the mouths of the Hwangho and Yangtze rivers. A few broken Radiolaria occur in samples from the continental shelf but are very rare in the enclosed seas and thus have a distribution opposite that of diatoms.

Organic Carbon

Organic carbon present in organic matter was determined by the potassium dichromate—ferrous ammonium sulfate titration method of Allison (1935). This method oxidizes the carbon that is not already completely oxidized, as is carbonate. Because it is based on the assumption that the organic matter in all sediments is at the same state of oxidation, it yields only approximate, though reproducible, results; since the samples had previously been dried, a more precise determination was not justified. Multiplication of the percentage organic carbon by the factor 1.7 corrects for proportional amounts of oxygen, nitrogen, and hydrogen that must be present, yielding an approximate percentage for total organic matter.

The highest percentages of organic carbon (1.60 to 1.80) were found in the west-central Yellow Sea, and the next highest (1.20 to 1.30) in the west-central Gulf of Tonkin. Large areas in both partly enclosed bodies of water have sediments containing more than 0.50 per cent organic carbon. The outer half of the continental shelf has areas of low concentrations of organic carbon, mostly less than 0.50 per cent, and some large areas have less than 0.25 per cent. An increase to 0.75 or 1.00 per cent occurs on the inner half of the shelf and on the slope seaward of the shelf-break.

Comparisons of Figures 13 and 17, 14 and 18, 15 and 19 show close inverse correlation of organic carbon with median diameter. Similar relationships are common elsewhere in the world where the relatively low content of organic matter in coarse sediment has been attributed to winnowing of the light organic

matter and to concentration of it in the same quiet areas where fine-grained sediments accumulate.

The intensive fishing industry provides data for an interesting comparison with bottom sediments. Records of the Nippon Suisan Company compiled by Kasawara (1948) show the areal distribution of trawlings for bottom-living fishes made between 1928 and 1947 in the Gulf of Pohai, Yellow Sea, and the continental shelf of the East China Sea. In order to avoid bias due to fuel restriction during the war and political restriction of near-shore waters in postwar years, only the data for 1928 to 1939 were plotted (Fig. 20), but during those years more than half a million trawlings were made by boats of this large company. Comparison of the map of fishing intensity (Fig. 20) with maps of median diameter (Figs. 13, 14, 15) and organic carbon (Figs. 17, 18, 19) shows the preference of bottom fishes for areas floored by fine-grained organic-rich sediments, probably a result of the greater abundance of worms and other small mud-digesting organisms in those areas.

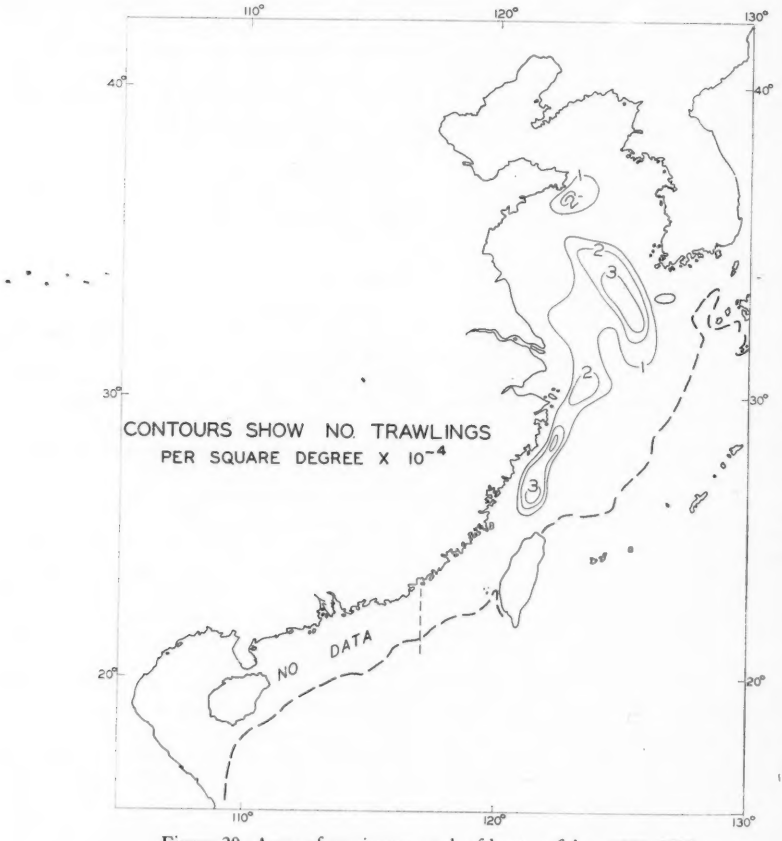

Figure 20. Areas of maximum catch of bottom fishes, 1928–1939

SUMMARY AND CONCLUSION

Origin of Sediments

Examination of all the maps and a compilation of some of their data into Table 2 indicate that the partly enclosed Gulf of Pohai, Yellow

Sea, and Gulf of Tonkin have sediments markedly different from those of the exposed continental shelf. The partly enclosed areas have sediments that are finer, less well sorted, have less calcium carbonate, fewer foraminiferal tests, fewer shell fragments, and more organic matter. Six different origins of the sediment appear to be worthy of consideration for this region: organic, authigenic, volcanic, residual, relict, and modern detrital. A similar classification was worked out for the continental shelf of southern California (Emery, 1952).

The organic portion of the sediments consists of soft organic matter and of shells and tests composed of calcium carbonate and some magnesium carbonate and of silica. Calcareous remains form the great bulk of the total organic contribution. The organic debris, both hard and soft parts, that accumulates in the top layers of sediment amounts to about 12 per cent of total sediment in the Yellow Sea and Gulf of Pohai, 16 per cent in the Gulf of Tonkin, but 30 per cent on the continental shelf. Siliceous organisms, mostly sponge spicules and diatoms, make up somewhat less than 1 per cent of the total sediment in the enclosed seas and a negligible amount on the shelf. In contrast, authigenic and volcanic sediments constitute about 1 per cent of total sediment on the shelf and a negligible amount in the enclosed seas.

There remains about 69 per cent of the total sediment on the shelf, 84 per cent in the Gulf of Tonkin, and 88 per cent in the Gulf of Pohai and Yellow Sea that must be divided between residual, relict, and modern detrital origin. Perhaps the chief means of distinguishing these three kinds of sediment is grain-size distribution, although composition, shape, and degree of weathering provide supplementary information. Residual sediments, derived from subaerial or submarine weathering of underlying bedrock, may be expected to be coarse, poorly sorted, and to occupy areas not reached and covered by modern detrital sediments. A few small areas of residual sand were identified on the outer part of the continental shelf where samples of especially coarse sand are associated with hilltops and bedrock.

Relict sediments, those left from conditions of deposition different from those existing now, are exemplified by beach sands deposited during a time of lower sea level during the Pleistocene glacial epochs. Such relict sands should occur in belts parallel to shore and should be most easily recognized as coarse-grained, well-sorted sands seaward of a belt of finer-grained modern detrital sands. In this region they are represented by the belt of relatively coarse sand at the sill of the Yellow Sea and on the outer half of the continental shelf southwest of Taiwan. Relict sediments cover about a quarter of the sea floor of this region.

Modern detrital sediments exhibit a reasonably uniform decrease in grain size seaward from their source at the shore. Examination of the charts and Table 1 indicates that these sediments dominate especially in the enclosed seas. Most are contributed by the large rivers. Though data on loads are scanty, the Hwangho is reported (White and Renner, 1948, p. 339) to discharge about 2,500,000,000 tons of sediment annually. Grabau (1932) put the figure at 472,500,000 cu m, or about 1,000,000,000 tons annually, and for the Yangtze River at 182,000,000 cu m, or about 400,000,000 tons. The Mississippi River discharges about 500,000,000 tons annually (Fisk, McFarlan, Kolb, and Wilbert, 1954). Because of the finer grain size of the sediments of the large Hwangho River, as compared with those of the smaller Korean streams, the sediments of the Gulf of Pohai and the Yellow Sea exhibit a decrease of grain size toward their main source. Sediments discharged by the Hwangho, Yangtze, Tsientang, Si and Tong, Song Ca, and other smaller rivers are recognizable on the various maps by their fine grain size and related parameters. Some of the rivers have formed large deltas that have prograded the shore. The seas into which some of the rivers empty are so shallow that the deltas appear to have no fore-set beds, but the top-set beds of very low slope extend far seaward and finally merge into the floors of the basins. In this respect the deltas are similar to that of the Tigris and Euphrates rivers (Emery, 1956) which also has been built into a shallow sea.

Limited data on the thickness of the delta are provided from a well drilled from an elevation of 5 m above sea level to a depth of 740 m (Grabau, 1940, p. 35); sands and muds containing shells of fresh-water and terrestrial mollusks made up the bulk of material found. The Japanese Army also drilled many water wells north of Shan-Tung during 1938. These penetrated unconsolidated sediments to more than 400 m below sea level; fresh water was found near the surface and salt water at depth.

These relationships strongly suggest that deltaic deposits extend from the surface to considerable depth.

Comparison with Ancient Sediments and Sedimentary Environments

Most ancient sediments which are studied by geologists were deposited in geosynclines or on the mouth of the Yellow Sea, forming a rock platform which is thinly mantled by sediments (Figs. 3, 11), judging from the presence of outcrops. Other rock outcrops occur on the shelf off south China and within the Gulf of Tonkin (Figs. 4, 6, 12). Where modern sediments are present, they consist largely of calcareous debris and authigenic material (both indicative of

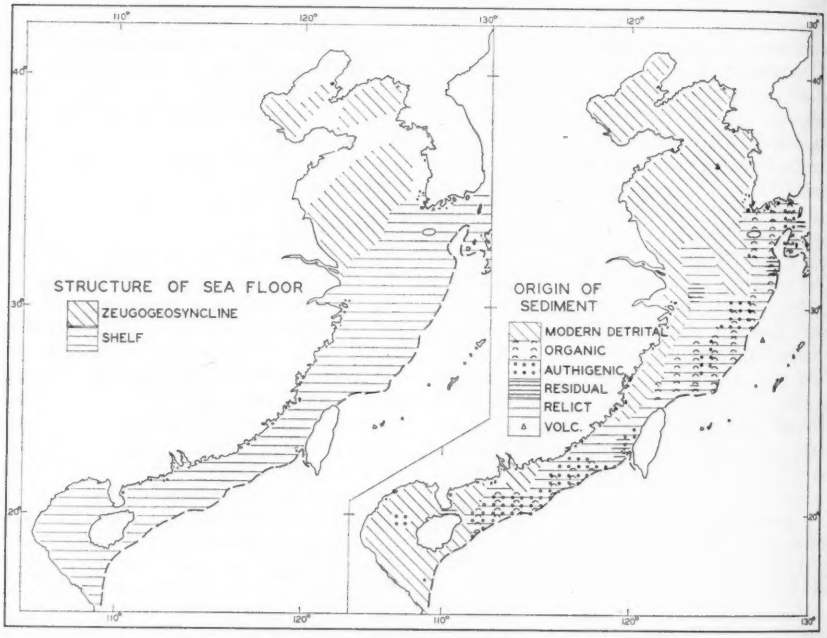

Figure 21. General structure and bottom sediment according to origin

stable platforms. Those in geosynclines generally form thick, narrow, long bodies, whereas those on platforms (shelves or cratons) are thin and tabular. Examined within the framework of geosynclines and platforms (Fig. 21), the East China and South China seas may provide modern examples in which the conditions of deposition are fairly well known.

The present surface of continental shelves wherever it has been studied is a feature formed by marine erosion during the Pleistocene followed by marine deposition in Pleistocene and subsequent times. As far as can be inferred from existing information, the shelf off the East Asiatic coast is no exception. Rocks of Korea and south China appear to extend across slow deposition) on the seaward part of the shelf and coarse to fine modern detrital sediment on the landward part. In time, the detrital sediment should prograde and cover the entire shelf unless its deposition on the outer part is prevented by the high velocity of the Kuroshio Current. The facts that the shelf is long and narrow, that detrital sediments come from only one side, and that winnowing of finer-grained detrital sediments occurs on the seaward side of the shelf result in a sharp lateral change of grain size. This change is far sharper than should occur atop a stable platform covered by a broad partly enclosed epicontinental sea of the type that covered central United States during the Paleozoic era. The

writers are not aware of any ancient platform deposits that are similar to those of the present East Asiatic shelf.

The large elliptical area of the combined deltas of the Hwangho and Yangtze rivers has been considered a geosyncline in which sediments have partly buried a central erosional remnant of granitic rocks, Shan-Tung (Figs. 1, 2) (Grabau, 1940, p. 50; Gilluly, Waters, and Woodford, 1951, p. 508). The sediments range from more than 740 m thick (probably much more) on the mainland to essentially zero at the mouth of the Yellow Sea. Sediments in the central Yellow Sea are of unknown thickness but at least are thick enough that no rocks crop out in an area of about 200 by 500 km. The rocky platform at the mouth of the Yellow Sea may be taken as an associated foreland, though it is narrower than most forelands. According to Kay's (1951) classification, the central Yellow Sea and possibly the Gulf of Pohai (Fig. 21) may be the northeastern margin of a modern zeugogeosyncline (subsiding area atop the craton adjacent to local uplifts which contribute significant amounts of detrital sediment). As pointed out by Gilluly, Waters, and Woodford, the sediments of this area resemble those of the Devonian delta in the Appalachian geosyncline. Deltaic sediments are also well-known in geosynclines along the Gulf of Mexico and in the Persian Gulf.

REFERENCES CITED

Allison, L. E., 1935, Organic carbon by reduction of chromic acid: Soil Sci., v. 40, p. 311–320

Central Research Institute of Electric Power Industry, 1959, Geological map of South-East Asia, scale 1:4,000,000, 2 sheets: Tokyo

Dietz, R. S., 1954, Marine geology of northwest Pacific: Description of Japanese Bathymetric Chart 6901: Geol. Soc. America Bull., v. 65, p. 1199–1224

Dietz, R. S., and Menard, H. W., 1951, Origin of abrupt change in slope at continental shelf margin: Am. Assoc. Petroleum Geologists, v. 35, p. 1994–2016

Emery, K. O., 1952, Continental shelf sediments of southern California: Geol. Soc. America Bull., v. 63, p. 1105–1108

— 1954, Some characteristics of southern California sediments: Jour. Sed. Petrology, v. 24, p. 50–59

— 1956, Sediments and water of Persian Gulf: Am. Assoc. Petroleum Geologists Bull., v. 40, p. 2354–2383

Fisk, H. N., McFarlan, E., Jr., Kolb, C. R., and Wilbert, L. J., Jr., 1954, Sedimentary framework of the modern Mississippi delta: Jour. Sed. Petrology, v. 24, p. 76–99

Gilluly, J., Waters, A. C., Woodford, A. O., 1951, Principles of geology: San Francisco, W. H. Freeman & Co., 631 p.

Goddard, E. N., Trask, P. D., DeFord, R. K., Rove, O. N., Singewald, J. T., Jr., and Overbeck, R. M., 1948, Rock-color chart: Washington, D. C., National Research Council, Committee on Rock-Color Chart, 6. p. (distributed by Geological Society of America)

Goode, J. P., 1943, School atlas: New York, Rand McNally & Co., 286 p.

Grabau, A. W., 1932, Principles of stratigraphy: New York, A. G. Seiler Co., 1185 p.

— 1940, The rhythm of the ages: Peking, China, Henri Vetch, 561 p.

Hess, H. H., 1948, Major structural features of the western north Pacific, an interpretation of H. O. 5485, bathymetric chart, Korea to New Guinea: Geol. Soc. America Bull., v. 59, p. 417–446

Inman, D. L., 1949, Sorting of sediments in the light of fluid mechanics: Jour. Sed. Petrology, v. 19, p. 51–70

Japan Hydrographic Office, 1910, Japanese oceanic current charts near Japan: Navy special chart no. 555, Pls. 1–22 (folio)

Kasawara, A., 1948, Fisheries resources of the trawl fishing grounds of East China Sea and Yellow Sea: Research Inst. Nippon Fisheries Co., Ltd., Jour., v. 3, 194 p.

Kay, M., 1951, North American geosynclines: Geol. Soc. America Mem. 48, 143 p.

Klenova, M. V., 1958, Ocean bottom character chart: Oceanologia et Limnologia Sinica, v. 1., no. 3, p. 243–254

Kobayashi, T., 1952, On the southwestern wing of the Akiyoshi orogenic zone in Indochina and South China and its tectonic relationship with the other wind in Japan: Japanese Jour. Geology and Geography, v. 22, p. 27–37

Koenuma, K., 1939, On the hydrography of the south-western part of the North Pacific and the Kurosio. Part III. Oceanographic investigations of the Kurosio area and its outer region; development of ocean currents in the North Pacific: Imp. Marine Observatory Mem., v. 7, p. 41–114

Lee, J. S., 1939, The geology of China: London, Thos. Murby & Co., 528 p.

Niino, H., 1934, On the fossil locality at the sea bottom of Korean Strait: Jour. Geog. Soc. Tokyo, v. 9, no. 12, p. 33–39

—— 1952, The bottom character of the banks and submarine valleys on and around the continental shelf of the Japanese islands: Tokyo Univ. Fisheries Jour., v. 38, no. 3, p. 191–403

Okamoto, Y., 1950, Oceanographical research of East China Sea and Yellow Sea: Nagasaki, West Dist. Fisheries Expt. Sta. Jour., v. 3, p. 53–78

Polski, W., 1959, Foraminiferal biogacies off the north Asiatic coast: Jour. Paleontology, v. 33, p. 569–587

Royal Netherlands Meteorological Institute, 1935, Oceanographic and meteorological observations in the China Seas and in the western part of the North Pacific Ocean: The Hague, Netherlands, Govt. Printing Office folio 115, 80 p.

Shepard, F. P., Emery, K. O., and Gould, H. R., 1949, Distribution of sediments on East Asiatic continental shelf: Allan Hancock Found. Occasional Paper 9, 64 p.

Stommel, H., 1958, The Gulf Stream: Berkeley, Calif., Univ. Calif. Press, 202 p.

Tokyo Geographical Society, 1929, Geological atlas of Eastern Asia, scale 1:2,000,000, 17 sheets

—— 1952, Geology and mineral resources of Far East: North China, Central China, South China and Taiwan: Symposium, 595 p.

Trask, P. D., 1932, Origin and environment of source sediments of petroleum: Houston, Gulf Pub. Co., 323 p.

Uda, M., 1949, The results of hydrographical surveys in China Sea in summer: Tokyo, Imp. Fisheries Expt. Sta. Jour., v. 11, p. 39–75

—— 1951, On the fluctuations of the main stream axis and its boundary line of Kuroshio: Oceanographic Soc. Japan Jour., v. 6, p. 181–189

U.S. Department of Commerce, 1938, Atlas of climatic charts of the oceans: Washington, D. C., Weather Bur. Pub. 1247, 129 charts (folio)

U.S. Navy, 1946, Ice atlas of the Northern Hemisphere: Washington, D. C., Hydrographic Office, 106 p. (folio)

Waller, H. O., 1960, Foraminiferal biofacies off the south China coast: Jour. Paleontology, v. 34, p. 1164–1182

White, C. L., and Renner, G. T., 1948, Human geography: New York, Appleton-Century-Crofts, Inc., 692 p.

Yabe, H., and Tayama, R., 1929, On some remarkable examples of drowned valleys found around the Japanese Islands: Oceanographic Works in Japan Rec., v. 2, p. 11–15

Yasuhara, Y., 1932, Expedition to fisheries ground near Hainan Island: Taiwan, Fisheries Expt. Sta. Jour., v. 25, 107 p.

Anonymous, 1931–1936, Semi-annual report of oceanographic investigations: Tokyo, Imp. Fisheries Expt. Sta. Jour., v. 48–57 (tables)

—— 1956, Fishery ground chart of East China Sea and Yellow Sea: Nagasaki, West Dist. Fisheries Expt. Sta. Jour., v. 11, 93 p.

MANUSCRIPT RECEIVED BY THE SECRETARY OF THE SOCIETY, OCTOBER 20, 1959

Short Notes

EMANUEL AZMON

MARINE TO NONMARINE TRANSITION OF SEDIMENTS ACROSS LITTLE SYCAMORE BEACH, CALIFORNIA

Abstract: Grain-size distribution and mineral frequencies in Recent sediments reflect the longshore drift of sand which supplies Little Sycamore Beach with much more sand than does the canyon above it. The study also shows, as expected, marked differences between marine and nonmarine sediments.

One of the most critical transition zones in sedimentary geology is a beach. It occupies a relatively small area between the terrestrial and submarine environments and is exposed alternately to both marine and nonmarine erosion. the immediate submarine area. A study of this type of transition in Recent sediments may render useful information for deciphering ancient environments.

Little Sycamore Beach (Fig. 1) was selected

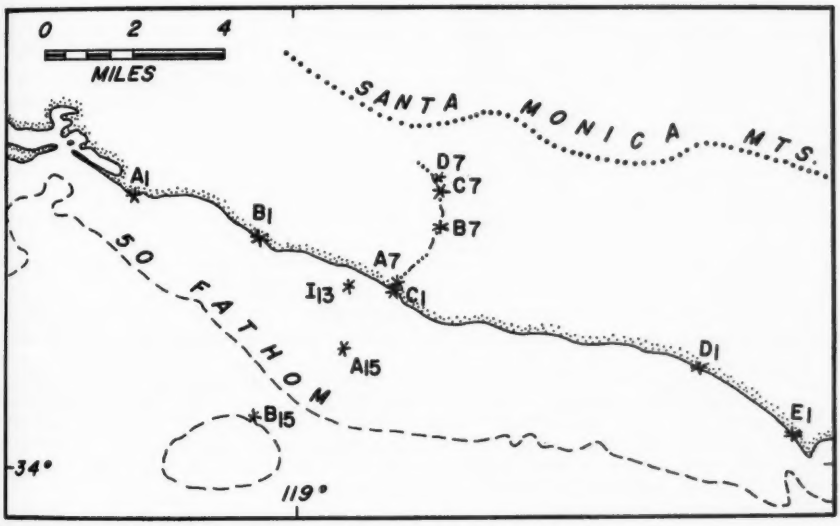

Figure 1. Index map showing sampling stations. A1—Point Mugu Beach; B1—Sycamore Beach; C1—Little Sycamore Beach; D1—Trancas Beach; E1—Westward Beach; A7, B7, C7—Little Sycamore Canyon; D7—outcrop; I13, A15, B15—offshore samples

In many cases it is difficult to identify and accurately locate a beach zone in a geological formation, especially when only the marine side of this zone is sampled, because of apparent lithological similarities between the beach and at random for a trial study of such a transition. One set of samples was collected from Little Sycamore Canyon, Little Sycamore Beach, and the offshore area below the beach. A second set of samples was collected east and west of

Geological Society of America Bulletin, v. 72, p. 763–766, 2 figs., May 1961

Little Sycamore Beach from Point Mugu Beach, Sycamore Beach, Trancas Beach, and Westward Beach.

Different sampling techniques and handling procedures had to be adapted for each of the environments. In the canyon, about 500 gms of sediment was wet-sieved, and the 62–1000-mu fraction was split for analysis. At the beaches, about 20 gms of sand was scraped into a vial from the surface layer and the entire sample split for analysis. The marine samples were collected aboard the R/V Velero IV, of the Marine Laboratory of the Hancock Foundation for Scientific Research, University of Southern California. Only the fraction finer than 62 mu was eliminated by wet-sieving, and a split of the coarse fraction was used for analysis.

All the samples were weighed and treated with dilute HCl (about 2 normal) to remove the carbonates and the iron oxide coating. The dry weight of the residue was recorded for later computation of the hydraulic ratio (Rittenhouse, 1943) and carbonate content.

The heavy minerals were then concentrated by sedimentation in acetylene tetrabromide (specific gravity 2.96) and mounted in Aroclor (index of refraction 1.66 to 1.67) on glass slides for a petrographic analysis.

A preliminary count of at least 100 mineral grains per sample showed the general distribution of the minerals in the two sets of samples. On the basis of analyses, zircon and opaque minerals (magnetite, ilmenite, leucoxene, hematite) were selected and repeat counts of several hundred grains made so that at least 15–20 grains of each of the trace minerals were

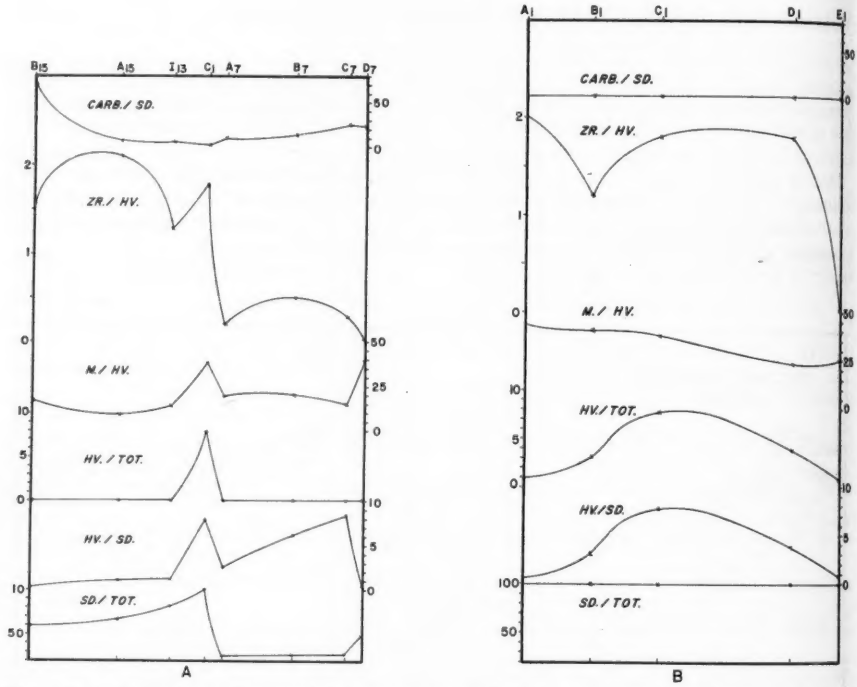

Figure 2. A. Six analyses of canyon-beach-marine transition. B. Six analyses of beach samples. *See* subcaption of Figure 1 for explanation of locality symbols. SD/TOT—sand ratio to total sample, in weight per cent; HV/SD—heavy-mineral ratio to sand, in weight per cent; HV/TOT—heavy-mineral ratio to total sample, in weight per cent; M/HV—opaque minerals (mainly magnetic) ratio to heavy minerals, in number of grains per cent; ZR/HV—zircon ratio to heavy minerals, in number of grains per cent; CARB/SD—carbonate ratio to sand, in weight per cent

included in each count. All the minerals other than the tracers were recorded as "other minerals."

A comparison of six related analyses of the canyon-beach-marine samples (Fig. 2A) with the same type of analyses of the beach samples (Fig. 2B) shows, very strikingly, the outstanding features of the beach sediments.

The first analysis shows ratio of sand to the total sample in weight per cent. As expected, the canyon deposits show considerably less sand than the beach material, and the marine sediments contain progressively less sand with increased distance from shore (Fig. 2A). All the beaches (Fig. 2B), are composed of approximately 100 per cent sand.

The second analysis shows the ratio of heavy minerals to sand in weight per cent. The great increase in the heavy-mineral content from the outcrop to the sediment is probably due to the greater weathering and elimination of feldspars in the light-mineral fraction. From the foot of the outcrop to the ocean the heavy-mineral content gradually decreases. At the beach, however, this content is twice as high as it is immediately above or below it, with no apparent relationship to either the canyon or the ocean (Fig. 2A). Little Sycamore Beach shows the highest percentage of heavy minerals, but the change in mineral content from one beach to another (Fig. 2B) is gradual and continuous.

The third analysis shows heavy-mineral concentration, represented as the ratio of the heavy minerals to the total sample and expressed in weight per cent. The inflation of the denominator in this ratio makes the relative amounts of heavy minerals look nil, except on the beaches, where the total sediment is sand.

The fourth analysis shows the ratio of opaque minerals (magnetite, ilmenite, leucoxene, and hematite) to the total heavy minerals, expressed in per cent number of grains. Here too, the opaque content gradually changes from the foot of the outcrop to the ocean, except at Little Sycamore Beach where this content is considerably higher than it is immediately above or below it (Fig. 2A). The change in mineral content from one beach to another (Fig. 2B) is gradual and continuous.

The fifth analysis shows the ratio of zircon to the total heavy minerals, expressed in per cent number of grains. It shows a general increase in zircon content from the outcrop, through the canyon and Little Sycamore Beach, to the ocean. Along the beaches no trend can be recognized.

Sixth, and last, is a carbonate to sand ratio expressed in weight per cent. The carbonate content is practically nil at the beaches, slightly higher near the outcrop, and considerably higher farther offshore.

It would be statistically unjust to arrive at detailed and comprehensive conclusions on the basis of only two profiles and approximately 12 samples. Yet, one major trend predominates in practically all the analyses. There is a definite relationship between Little Sycamore Beach and the beaches east and west of it and a distinct nonrelationship of this beach to the canyon above it or the ocean below it. This probably reflects the longshore drift of sand which supplies Little Sycamore Beach with a greater quantity of opaque minerals and total heavy minerals than does the canyon above it. At least four of the six analyses show a marked difference between the marine and nonmarine sediments, as should be expected.

References Cited

Layne, M. M., 1950, The gasoline method for the disintegration of argillaceous shales: The Micropaleontologist, v. 4, no. 1, p. 21

Rittenhouse, G., 1943, The transportation and deposition of heavy minerals: Geol. Soc. America Bull., v. 54, p. 1725–1780

4129 Buckingham Rd., Los Angeles 8, California

Manuscript Received by the Secretary of the Society, December 28, 1960

J. A. WHELAN

UNUSUAL SOLUTION(?) CAVITIES IN THE MANNING CANYON SHALE NEAR FAIRFIELD, UTAH

Abstract: One bed of the Manning Canyon shale in Manning Canyon, Utah, contains numerous elongate cavities, rectangular in cross section, all oriented down dip. The cavities contain a small amount of residue consisting of fine-grained iron-stained quartz. The solution of carbonate veins is postulated as the origin of the cavities.

During the fall of 1958, the writer was assisting some students in a study of clay minerals in the Southern Oquirrh Mountains about 35 miles southwest of Salt Lake City, Utah. In an abandoned clay pit in the W.½ SW.¼ Sec.23, T.6 S., R.3 W., about 3½ miles northwest of Fairfield, one bed of the Manning Canyon shale (Mississippian-Pennsylvanian) was found which contained numerous elongated cavities, almost rectangular in cross section, and oriented parallel to the dip of the bed. The bed strikes N. 25° W. and dips 75° E. For the geology of Manning Canyon, which contains the pit, the reader is referred to Gilluly (1932) and to Bissel, Rigby, Procter, and Moyle (1959). The Oquirrh Mountains contain numerous small structures, but in general the Manning Canyon shale in this locality strikes N. 30° W. and dips 60° E.

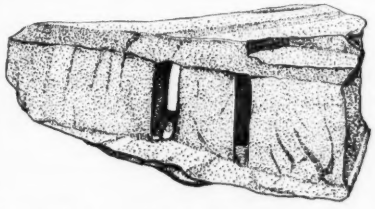

Figure 1. Drawing of hand specimen containing two of the cavities described. The bed is about 2 cm thick. The difference in lithology between the bedding surfaces and the center of the bed is very apparent.

A typical specimen containing two cavities is shown in Figure 1. The bed in which the cavities occur is about 2 cm thick. The cavities have a vertical dimension of about 1.7 cm and range from 1.0 to 6.0 mm in width. The cavities contained varying amounts of a rust-colored residue. At first the cavities were thought to be molds of anhydrite crystals, but this was not so because: (1) only the width of the cavities varied; the vertical dimension is constant, just slightly less than the thickness of the bed; (2) one of the samples showed that the bed was lenticular and pinched out; the cavity it contains is terminated by a decreasing vertical dimension only. No crystal faces are present on the termination.

This bed shows a macroscopic variation of lithology between its top and bottom surfaces and its center. For about 1.5 mm from both top and bottom, the bed is greenish black with a talcose luster. The center of the bed, which contains the cavities, is brownish black and is not talcose. When powdered for X-ray diffraction, the top and bottom of the bed is dark gray, the center portion light gray. X-ray-diffraction patterns show that the outer surfaces of the beds are composed chiefly of pyrophyllite and quartz, while the dominant mineral in the center of the bed is a septachlorite. Pyrophyllite was first noted in the Manning Canyon shale by Ehlmann (1958, Ph.D. Thesis, Univ. Utah). The fact that the top and bottom of the bed contain considerably more pyrophyllite than the center may support Ehlmann's hypothesis that the pyrophyllite was formed by the action of hydrothermal solutions.

The brown residue in the cavities gave an X-ray-diffraction pattern of quartz. A spectrochemical analysis of this material is given in Table 1.

The samples collected contained cavities up to 9 cm long.

A satisfactory explanation of the origin of the cavities must explain (1) their regular cross sections, (2) their orientation down dip,

Geological Society of America Bulletin, v. 72, p. 767–768, 2 figs., May 1961

TABLE 1. SPECTROCHEMICAL ANALYSIS OF RESIDUE IN CAVITIES IN THE MANNING CANYON SHALE NEAR FAIRFIELD, UTAH

Analyst, B. J. Anderson

Al	X	Cu	Tr	Mo	Tr	V	Tr
B	Tr (?)	Fe	M	Ni	Tr		
Ca	O.X–X.	Mg	P	Si	M		
Co	Tr	Mn	X	Ti	O.OX		

Looked for and not found: Sb, As, Ba, Be, Bi, Cd, Cr, Ga, Ge, Pb, Ag, Na, Sn, Zn, and Zr

M, major (probably more than 10%); X, 1–9%; P, present; Tr, trace

and (3) the fact that they were confined to one thin bed of the Manning Canyon shale, but were common, at least for a short distance along the strike, in that bed.

It seems probable that the cavities represent the solution of veins, probably carbonate veins which contained some quartz, during weathering of the outcrop. Perhaps the veins were in an en echelon pattern; this would account for the orientation of the cavities. The iron and manganese residue in the cavities could have formed from the oxidation of ferrous and manganous carbonate originally present as a solid solution in the carbonate of the vein.

This study was made incidental to a study of clay minerals supported by the University of Utah Research Fund.

References Cited

Bissel, H. J., Rigby, J. K., Proctor, P. D., and Moyle, R. W., 1959, Geology of the Southern Oquirrh Mountains and Fivemile Pass–Northern Boulder Mountain Area, Tooele and Utah Counties, Utah: Utah Geol. Soc. Guidebook 14, 269 p.

Gilluly, J., 1932, Geology and ore deposits of Stockton and Fairfield quadrangles, Utah: U. S. Geol. Survey Prof. Paper 173, 171 p.

DEPT. MINERALOGY, UNIVERSITY OF UTAH, SALT LAKE CITY, UTAH

MANUSCRIPT RECEIVED BY THE SECRETARY OF THE SOCIETY, JULY 12, 1960

ROBERT BOWEN

PALEOTEMPERATURE ANALYSES OF MESOZOIC BELEMNOIDEA FROM AUSTRALIA AND NEW GUINEA

Abstract: Paleotemperature analyses were carried out on more than 60 Belemnoidea obtained from Mesozoic strata in West and South Australia and New Guinea. One set of data records mean rostral temperatures, and another derived by analyzing successive increments of powdered carbonate from the rostra shows the variations of temperature during ontogenies. The latter probably represent and in this event would confirm seasonal changes during the Mesozoic. The former demonstrate a cooling from the Jurassic into the Cretaceous and are consistent with the extension of the Albian and Coniacian-Santonian climatic maxima, previously demonstrated in Europe, into the Australian area. The Cretaceous readings dispose of the idea of an ice age in South Australia at that time. It appears that the Belemnoidea were eurythermal through most of their evolutionary history. The paleotemperature results are in accord with a possibly large migration of Australia during the Mesozoic.

Since the preliminary work of Urey (1947; 1948) showed that the abundance of the O^{18} isotope in calcium carbonate is related to the temperature of deposition of this compound, measurement by means of sensitive mass spectrometers has been used to reconstruct past climates. This paper is concerned with data derived from such analyses of a number of Mesozoic Belemnoidea from Australia and New Guinea. The original standard gas used by Urey *et al.* (1951) was CO_2 obtained from a *Belemnitella americana* from the Peedee formation (Upper Cretaceous : Maestrichtian) of North Carolina, and this is known as PDB-1. It has no delta value—*i.e.*, its delta can be regarded as zero. A new standard derived from Jurassic belemnoids from the island of Skye off the coast of Scotland was used in the present work, and the machine results obtained by comparison of CO_2 samples with it were corrected so as to relate them to PDB-1.

I : Data Obtained from Analyses of Whole Specimens

These give mean rostral temperatures and were obtained by cutting a complete cross section representing accumulative growth, cleaning it of contaminants, and grinding it to a powder; the necessary aliquot for investigation was taken from this.

1 : Jurassic

Thirty six specimens from the Newmarracarra Limestone (Middle Jurassic : Bajocian) of Bringo Cutting 19 miles east of Geraldton, Western Australia, were analyzed. The minimum delta value obtained was $-0.45‰$; assuming the mean ocean delta in the Jurassic to be $0.00‰$, this corresponds to a temperature of 18.5°C. The maximum delta value was $-2.72‰$ (29.2°C). The average delta value for the entire assemblage was $-1.73‰$ (24.4°C), and about two-thirds of the belemnoids were within 3°C of this figure. A single specimen was obtained from the Kuabgen group (Upper Jurassic) of the Upper Fly River, New Guinea. It probably belongs to the species *Belemnopsis gerardi* and gave a delta value of $+0.13‰$ (15.9°C).

2 : Cretaceous

In Western Australia specimens were derived from strata of the Alinga formation (Albian to Turonian age). Thirteen came from the Murchison River area; 8 of these were from cliffs west of Murchison House station; these gave delta values ranging from $-0.28‰$ (17.7°C) to $-2.1‰$ (26.1°C), the average temperature being 20.6°C. Four specimens collected from another locality (cliffs north of an emergency aerodrome on the telegraph line at Murchison House station) gave an average temperature close to this figure, namely 18.8°C with a delta range from $-0.26‰$ to $-0.74‰$. A specimen from a third locality in this area gave a delta value of $-0.24‰$ (17.5°C). Evidence from Europe (Bowen, 1961) indicates a climatic minimum there in the Cenomanian following an earlier maximum during Albian time. Possibly these were world-wide variations; if so, the reading of 17.5°C may derive from the Cenomanian part of the

Geological Society of America Bulletin, v. 72, p. 769–774, 2 figs., May 1961

Alinga formation. Four additional specimens obtained from Junnawa Hill in the lower Murchison River area may also be from the Alinga formation, but they may come from the overlying Toolonga Calcilutite (Coniacian-Santonian to Maestrichtian). They gave an average temperature of 19.8°C (delta values ranging from −0.54‰ to −0.85‰); comparison with Europe would suggest they are either Cenomanian (if Alinga) or Campanian (if Toolonga); both were times of climatic minima. Two specimens were collected from the Gearle Siltstone on Cardabia Creek in the Giralia area. This formation is Albian to Turonian in age, and the specimens gave very different results, namely 20.3°C and 30.1°C.

All the preceding Cretaceous specimens came from various parts of Western Australia. Six were obtained from South Australia—from Fossil Creek 35 miles from Oodnadatta—and are Albian in age. They gave delta values ranging from −0.85‰ to −2.45‰, and the average temperature obtained from them is 21.9°C. These results are particularly interesting because they show that Lowenstam and Epstein (1954) were in error in assuming that in Albian time the lowest average temperatures were in Australia. They obtained readings of 15.2°C and 16.6°C from Australian Upper Albian specimens, but these came from a locality almost 1000 miles from the present one. Dorman and Gill (1959) gave readings ranging from 12.2°C to 16.5°C for specimens derived from the Aptian of Lake Eyrie area—close to Oodnadatta. However, they also record seasonal analyses of some of these specimens, and from these it can be seen that Aptian temperatures reached a maximum of 21°C. Bowen (1961) has shown that in Europe Aptian temperatures were substantially lower than those of Albian time. The author concludes that there was considerable temperature fluctuation in South Australia (*i.e.*, in the Cretaceous Tambo Sea area) from Aptian time through the Albian. Two points must be borne in mind: (1) the Tambo Sea became a lake later in the Cretaceous, hence large ecological and climatic changes are to be expected during this period; (2) differences undoubtedly arise from the probable different living habits of the various species of Belemnoidea. In other words, differences in isotopic composition could result from ecological differences. This interpretation is in general agreement with the opinion of Gill who stated (personal communication) that "the present evidence favours your ideas of considerable variations in climatic conditions . . . there were differences due to actual climatic fluctuation and others due to the considerable variation which one would anticipate in a comparatively shallow transcontinental sea."

TABLE 1. ANALYSES OF JURASSIC SPECIMENS

Specimen number	Layer number	Corrected delta (‰)	Temperature (°C)
1	1 (Outer)	−1.6	23.7
	2	−1.3	22.3
	3	−1.2	21.9
	4	−1.8	24.7
	5	−1.6	23.7
	6	−1.3	22.3
	7	−1.5	23.3
	8 (Center)	−1.3	22.3
2	1 (Outer)	−1.1	21.4
	2	−1.2	21.9
	3	−1.2	21.9
	4	−1.3	22.3
	5	−2.1	26.1
	6	−1.6	23.7
	7	−1.6	23.7
	8 (Center)	−1.3	22.3
3	1 (Outer)	−1.9	25.2
	2	−2.0	25.7
	3	−2.1	26.1
	4	−2.5	28.1
	5	−2.5	28.1
	6	−2.8	29.6
	7	−2.4	27.6
	8 (Center)	−2.8	29.6
4	1 (Outer)	−1.1	21.4
	2	−0.9	20.5
	3	−0.8	20.0
	4	−1.0	20.9
	5	−1.5	23.3
	6	−2.4	27.6
	7	−2.0	25.7
	8 (Center)	−3.1	31.2

II : Data Obtained from Successive Increments of Powdered Carbonate from the Rostra

Several explanations of these are available. The most likely is that they represent seasonal changes in temperature in which case the highs may be interpreted as summer maxima and the lows as winter minima. This would give an indication of the life span of the animal or at least that part of it during which the rostrum was formed. This hypothesis is accepted by the author as being most in accord with the facts. Another possibility however is that the temperature fluctuations represent the results of migrations. Lowenstam and Epstein (1954) noted that in some cases the belemnoid tem-

perature trends parallel those of associated benthonic forms—here, the relevant belemnoids (although nektonic in habits) must have passed much of their lives in the seasonal climatic ranges of their areas of burial (at least the parts of the ontogenies during which the rostra grew). Thus, while no evidence of migration can be advanced, some evidence against it can; hence it is inadvisable to accept this interpretation. A third possibility is that the delta fluctuations represent not alternations between warmer and cooler conditions, but salinity changes. However, again there is no evidence to support this idea.

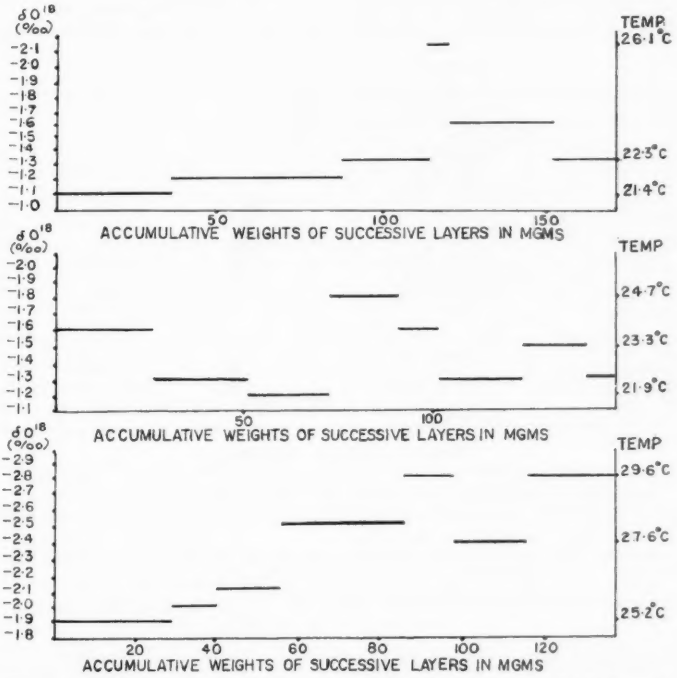

Figure 1. Variation analyses. Three of the four analyses made on Middle Jurassic (Bajocian) specimens from the Geraldton area of Western Australia to show changes in temperature during rostral growth (interpreted as seasonal in character by the author). Details are recorded in Table 1, and the graphs represent specimens 2 (top), 1, and 3.

Four specimens of Jurassic age from the Newmarracarra Limestone of Bringo Cutting near Geraldton, Western Australia were analyzed (Table 1; Fig. 1).

Some of these results, *e.g.*, those for specimen 1, show very well a probable seasonal rise and fall. In specimen 1 at least two maxima (probably summers) and two minima (probably winters) can be observed, and thus the animal probably lived through 2 or more years. Similar variation analyses were made on some of the Cretaceous specimens. As with the Jurassic ones, the range of temperature variation during ontogeny was small—of the order of 2°–5°C.

Clearly, the climates of many parts of the world have altered considerably since the Mesozoic. Widespread evidence indicates that the Jurassic and Cretaceous equator ran through the southern United States and Europe. No longer is this the case, and the reason may be polar wandering, continental drift, etc. Paleomagnetic investigations summarized by Cox and Doell (1960) yield a number of Jurassic and Cretaceous virtual geomagnetic poles which (if, as most workers believe, the average geocentric dipole is always directed along the axis

of rotation) closely approximate or coincide with the geographic poles. In the Jurassic, some are located in Asia, and some in North America, while in the Cretaceous some are in the Pacific and Alaska, and others are located elsewhere. Obviously, the utility of this work in reconstructing climatic belts of the Mesozoic is limited. As Cox and Doell (1960) remark: "the geomagnetic pole positions from the Mesozoic . . . are quite scattered (and) no conclusive statements concerning drift or wandering can be made."

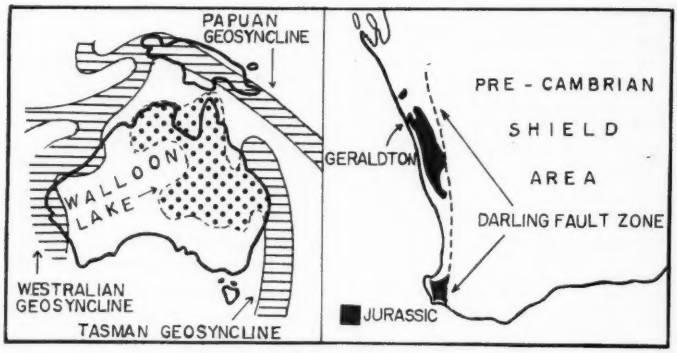

Figure 2. Geology of Australia

Left: Paleogeography of Australia during the late Cretaceous. The interconnection of the Westralian geosyncline with the Papuan is evident, and through this link contact was made with the Tethys. The Walloon Lake succeeded the Tambo Sea (referred to in the text).

Right: Map of southwest Australia showing Jurassic outcrops and their relation to the town of Geraldton. The Darling fault zone separates the Jurassic from the great Precambrian shield to the east.

At present, the variation of temperature with latitude attains a maximum of about 60°C, and there still exist polar ice caps. In the Jurassic certainly and probably in the Cretaceous also, there were no appreciable bodies of ice anywhere. Seasons existed (Fig. 1). A cooling from the Jurassic to the Cretaceous is apparent in the Australian area. The temperatures recorded in this note are closely comparable with those of Western Europe (Bowen, unpublished analyses): *e.g.*, *cf.* the Albian of England—20°C, 21.1°C, 23.3°C; of France—22.7°C, 24.7°C, 25.1°C. This means that the Albian and Coniacian-Santonian climatic maxima spread over most of the planet (except for Japan where the Albian gave a reading of only 16.8°C). Neocomian and Cenomanian minima recorded in Europe and elsewhere are consistent with the Australian results. The world Jurassic shows even greater consistency. Unpublished data show this very clearly; *e.g.*, in Argentina temperatures of 23.7°C and 25.6°C average 24.6°C (very close to the average from Western Australia); in Europe, temperatures of from 20°C to 25°C are common, and this is true also in North America. Low temperatures were recorded from Alaska and India, however, and also, as was seen earlier, in New Guinea.

Some inferences may be drawn from the paleotemperature results.

(1) They show that the belemnoids (known to have been nektonic in their habits) were eurythermal during most of their evolutionary history. They were successful in colonizing cool and hot bodies of water—the Australasian data record a minimum of 15.9°C and a maximum of 31.2°C (a range of more than 15°C). The South Australian Cretaceous readings dispose of the idea of an ice age at that time in this area.

(2) The Australian data are consistent with the world climatic picture derived from analyses made on specimens from many other countries. Comparison with these specimens shows that the Westralian geosyncline (Fig. 2), although warm, was cooler than the Tethys in Jurassic time. The Cretaceous emerges as a more diversified climatic period, and the

climatic maxima and minima, although not certainly identified in Western Australia (because of poor stratigraphical control of the relevant specimens), very probably took place at the same time there as elsewhere. Climatic maxima and minima do of course occur between the Albian and Turonian, and until there is any evidence to the contrary it is logical to locate them in accordance with more exact data obtained from Europe, etc.

(3) The positions of the poles must be considered. Work to be published later shows that the north pole probably lay in the general area of the Bering Sea, and the south pole in the general area of South Africa. Irving (1958) suggested that "from Carboniferous to Eocene times Australia was situated in what is nowadays the position of southern South America and has subsequently moved to its present position." Irving and Green (1958) gave the Mesozoic (probably Jurassic) pole position as: Lat. 50 S. and Long. 157 E. The latitude is possible, but the author believes the true position is much west of this. The paleotemperature data show high temperatures in the Upper Jurassic of Argentina and suggest that this region has rotated southward away from the equator since the Jurassic. During early Jurassic time, therefore, Australia could have occupied this position and later migrated. During later Jurassic time and in part of the Cretaceous, it may have been near South Africa, and New Guinea may have been a separate unit with locally cool-water conditions. India, also, is believed to have migrated over a considerable distance at about the same time.

Acknowledgments

The author is grateful to Dr. Harold C. Urey for his advice and encouragement, to Dr. Peter X. Eberhardt for his assistance, and to Dr. Cesare Emiliani for his suggestions. M. F. Glaessner, B. F. Glenister, and N. H. Fisher supplied specimens. The author is indebted to Dr. G. W. Bain, Mr. B. E. Balme, Dr. E. D. Gill, Dr. B. F. Glenister, and Dr. E. Irving for their comments. The author also wishes to thank the Atomic Energy Commission for support of the project, through grant number AT(11-1)-34, and the National Science Foundation for support of the project through grant number G-10220.

References Cited

Bowen, Robert, 1961, Paleotemperature analyses of Mesozoic Belemnoidea from Germany and Poland: Jour. Geology, v. 69, p. 75–83

Cox, Allan, and Doell, Richard R., 1960, Review of paleomagnetism: Geol. Soc. America Bull., v. 71, p. 645–768

Dorman, F. H., and Gill, E. D., 1959, Oxygen isotope paleotemperature measurements on Australian fossils: Roy. Soc. Victoria Proc., n. ser., v. 71, pt. 1, p. 73–98

Irving, E., 1958, Paleogeographic reconstruction from paleomagnetism: Geophys. Jour. Royal Astron. Soc., v. 1, p. 224–237

Irving, E., and Green, R., 1958, Polar movement relative to Australia: Geophys. Jour. Royal Astron. Soc., v. 1, p. 64–72

Lowenstam, H. A., and Epstein, S., 1954, Paleotemperatures of the post-Aptian Cretaceous as determined by the oxygen isotope method: Jour. Geology, v. 62, p. 207–248

Urey, H. C., 1947, The thermodynamic properties of isotopic substances: Jour. Chem. Soc., p. 562–581

— 1948, Oxygen isotopes in nature and in the laboratory: Science, v. 108, no. 2810, p. 489–496

Urey, H. C., Lowenstam, H. A., Epstein, S., and McKinney, C. R., 1951, Measurement of paleotemperatures of the Upper Cretaceous of England, Denmark, and the south-eastern United States: Geol. Soc. America Bull., v. 62, p. 399–416

School of Science and Engineering, University of California, La Jolla, Calif.
Manuscript Received by the Secretary of the Society, December 17, 1959

PRIESTLEY TOULMIN, 3D

GEOLOGICAL SIGNIFICANCE OF LEAD-ALPHA AND ISOTOPIC AGE DETERMINATIONS OF "ALKALIC" ROCKS OF NEW ENGLAND

Abstract: Recent age determinations indicate that at least two groups of "alkalic" igneous rocks exist in New England, with ages of about 185 and 270 million years. Because of their lithologic and geologic similarities, all these rocks had previously been grouped with the White Mountains plutonic-volcanic series of New Hampshire. Until reliable petrographic or geologic criteria become available for distinguishing these age groups, caution should be exercised in assigning any undated body of "alkalic" rock to one or the other group.

In recent years, a number of age determinations have been made on "alkalic" plutonic rocks of New England (Webber, Hurley, and Fairbairn, 1956; Tilton *et al.*, 1957; Lyons *et al.*, 1957; Quinn *et al.*, 1957; Aldrich *et al.*, 1958; Jaffe *et al.*, 1959; Hurley *et al.*, 1960). Tables 1 and 2 summarize these age determinations, and Figure 1 shows the sample localities.

Table 1. Isotopic Age Determinations on "Alkalic" Rocks of New England

Specimen and location	Mineral	Method	Age (10^6 yrs.)	Reference
Conway granite, quarry, Redstone, N. H.				
Green granite	Zircon	U^{238}-Pb^{206}	187 ± 5	Tilton *et al.* (1957, p. 364)
Green granite	Zircon	U^{235}-Pb^{207}	184 ± 5	
Green granite	Zircon	Pb^{207}-Pb^{206}	140 ± 60	
Green granite	Zircon	Th^{232}-Pb^{208}	190 ± 5	
Green granite	Biotite	Rb^{87}-Sr^{87}	190	Aldrich *et al.* (1958, p. 1129)
Green granite	Biotite	K^{40}-Ar^{40}	168	
Red granite	Biotite	Rb^{87}-Sr^{87}	183	
Red granite	Biotite	K^{40}-Ar^{40}	137	
Conway granite, Redstone, N. H.	Biotite	K^{40}-Ar^{40}	178 ± 8	Hurley *et al.* (1960, p. 254)
Conway granite, Redstone, N. H.	Biotite	Rb^{87}-Sr^{87}	170 ± 9	
Quincy granite, Swingle quarry, Quincy, Mass.	Whole rock	K^{40}-Ar^{40}	280 ± 15	

Most of the known bodies of "alkalic" rocks in New England are in New Hampshire, where they are known collectively as the White Mountains plutonic-volcanic series (Billings, 1956, p. 69–88). The rocks of the White Mountains series postdate the principal orogenies in northern New England and form ring dikes, stocks, and one batholith in the White Mountains. Stocks and a small batholith of similar rocks, also posttectonic, occur in Vermont[1] (Eggleston, 1918; Daly, 1903; Chapman, 1954), Maine (Jenks, 1934; Wandke, 1922), Massachusetts (Clapp, 1921; Warren, 1913; Warren and McKinstry, 1924; Toulmin, 1958, Ph. D. thesis, Harvard Univ.; 1960), and Rhode Island (Warren and Powers, 1914; Quinn, Ray, and Seymour, 1949).

Emerson (1917, p. 188) mentioned two additional small masses of "Quincy granite" near Sharon and Fall River, Massachusetts; Chute (1950) mentioned a stock of undetermined extent near North Easton, Massachusetts, consisting of porphyritic albite-riebeckite granite. The writer (1957) has described a granite

[1] The alkalic rocks at Cuttingsville, Vermont, described by Eggleston, are surrounded by Precambrian rocks and so cannot be demonstrated on local evidence to be younger than the Paleozoic orogenies.

Geological Society of America Bulletin, v. 72, p. 775–780, 1 fig., May 1961

similar to those of Peabody and Cape Ann, Massachusetts, from Cashes Ledge, in the Gulf of Maine. All these rocks have usually been considered to be roughly correlative on the basis of general petrographic similarity and posttectonic emplacement. One of these intrusive masses, the Quincy granite of Massachusetts, is demonstrably pre-Pennsylvanian, and on the basis of its supposed equivalence to the White Mountain series, Billings (1956, p. 105) and Williams and Billings (1938, p. 1025) tentatively assigned a Mississippian(?) age to the White Mountains series.

Tables 1 and 2 and Figure 1 show that the

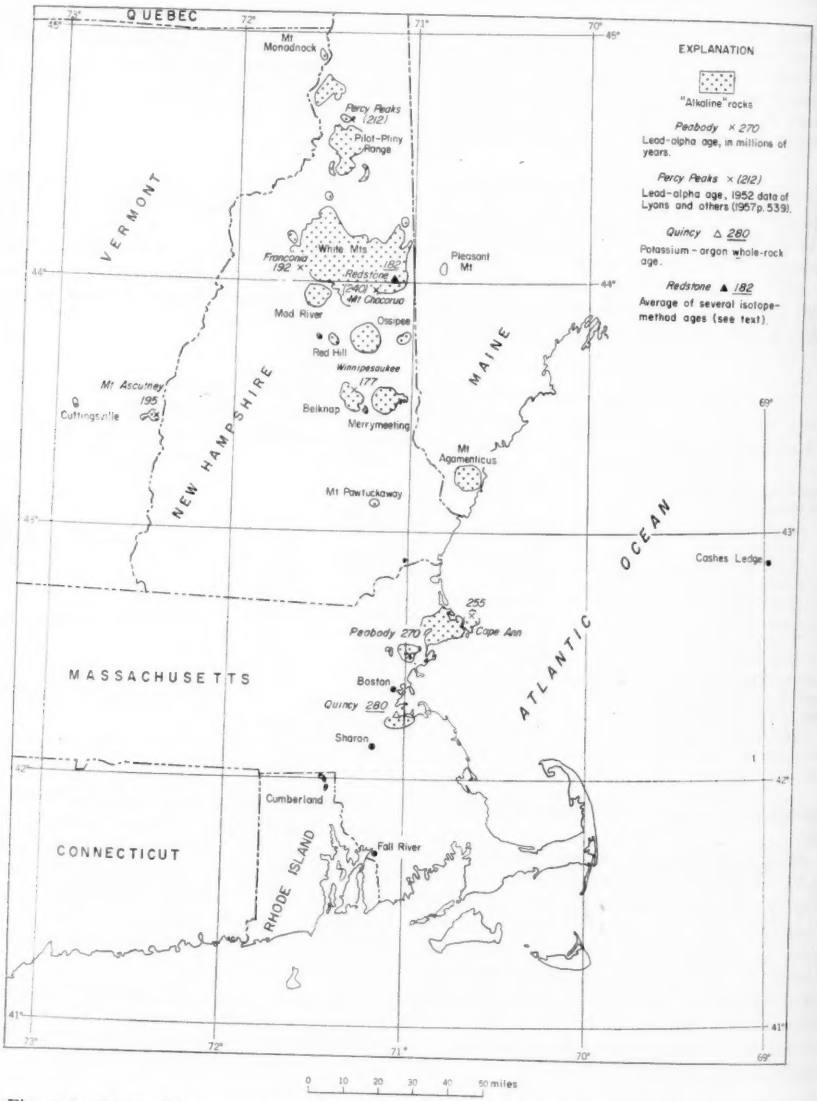

Figure 1. Geographic distribution of age determinations of "alkalic" rocks in New England

age data do not support the correlation of all the "alkalic" intrusive rocks of New England. The rocks studied from the Boston area appear to be significantly older (260–270 m.y.) than the similar rocks studied from New Hampshire (185 m.y.). This age difference obviously implies at least two periods of emplacement of "alkalic" rocks in New England and thus poses problems of assignment of many bodies of such rocks to one or the other group.

Recent improvements in spectrographic analytical methods for lead in zircon (Rose and Stern, 1960) necessitate careful re-evaluation of pre-existing lead-alpha age determinations. The error in previous lead determinations is not entirely systematic, but most of the lead-alpha age determinations discussed in this note were made on specimens with lead contents in the range where preliminary results with the new method suggest that the errors are least (T. W. Stern, oral communication). Furthermore, the fact that the ages determined fall into two groups, each of which contains one rock dated by isotopic methods in good agreement with the lead-alpha ages, at least supports the conclusion that the rocks discussed are of different ages, regardless of the size of the absolute error in the ages.

The age of the Conway granite at Redstone, New Hampshire, must be regarded as well established, inasmuch as concordant lead-isotope age data for zircon agree very well with Rb-Sr and K-Ar ages on mica from the same rock and the mica ages have been run independently by two laboratories (Carnegie Institution of Washington and Massachusetts Institute of Technology). The further agreement with lead-alpha ages on the same granite from the same locality lends additional support to the lead-alpha ages for the other rocks in New Hampshire, all of which had been assigned to the White Mountains series on geologic and petrographic grounds.[2]

As noted by Hurley *et al.* (1960, p. 253), the K-Ar whole-rock age on Quincy granite from Quincy, Massachusetts, is probably a minimum age. The fact that the same workers determined a K-Ar age for mica of the Conway granite from Redstone, New Hampshire, in very good agreement with the age well established for that rock (*See* Table 1) justifies comparison of their results on the Quincy granite with the results of Tilton *et al.* on the Conway granite at Redstone, New Hampshire.

The ages of the granites and syenites of the Peabody and Cape Ann intrusive masses, northeast of Boston, have not been determined by isotopic methods, but the agreement of the lead-alpha zircon ages with the age determination just discussed for the Quincy granite at Quincy, Massachusetts, makes it reasonable to assume that these rocks are correlative with the Quincy granite and therefore are older than those rocks of the White Mountains series of New Hampshire given in Table 1. Aside from the lead-alpha ages at Mt. Ascutney, no age

TABLE 2. AVERAGE LEAD-ALPHA AGE DETERMINATIONS ON "ALKALIC" ROCKS OF NEW ENGLAND

Locality on Figure 1	Rock types	Age (10^6 Yrs.)	Reference
Redstone	Conway granite	182	Lyons *et al.* (1957); Jaffe *et al.* (1959)
Mt. Ascutney	Conway granite, syenite	195	Lyons *et al.* (1957)
Franconia	Mt. Osceola granite	192	Lyons *et al.* (1957)
Winnipesaukee	Monzodiorite	177	Lyons *et al.* (1957)
Percy Peaks	Syenite	(212)*	Lyons *et al.* (1957)
Mt. Chocorua	Mt. Osceola granite	(240)*	Lyons *et al.* (1957)
Cape Ann	Cape Ann granite of Clapp (1910) and Warren and McKinstry (1924)	255 ± 12	Webber *et al.* (1956)
Peabody	Peabody granite of Clapp (1910)	270 ± 15	Webber *et al.* (1956)

*These determinations, made in 1952, are regarded by Lyons *et al.* (1957, p. 538–540) as less reliable than the other results here quoted from this paper.

[2] Three of the samples reported on by Lyons *et al.* (1957, p. 539) gave lead-alpha ages intermediate between the 185 m.y. of the other New Hampshire rocks and the 260–270 m.y. of the Massachusetts rocks. These determinations were made in 1952 and were regarded as less reliable than the other lead-alpha ages on New Hampshire rocks even before the isotopic data of Tilton *et al.* (1957) became available (Lyons *et al.*, 1957, p. 538–540). The 1952 determinations are reported here only for completeness.

determinations exist for the similar rocks from Vermont, Maine, Rhode Island, or Cashes Ledge.

The geologic and petrographic resemblance of the "alkalic" rocks in Massachusetts to those of New Hampshire is very striking, and the writer knows of no certain field or petrographic criteria to distinguish them. It is true that ring-dike structures are not well developed in Massachusetts but are characteristic of the White Mountains plutonic-volcanic series in New Hampshire. Moreover, plutonic mafic varieties, which are common in New Hampshire, are not found in the "alkalic" rocks of Massachusetts, unless the gabbro at Nahant, Massachusetts (LaForge, 1932, p. 24; Clapp, 1921, p. 31–33, 100–101), belongs to the "alkalic" group. On the other hand, some stocks assigned to the White Mountains series in New Hampshire lack ring dikes and gabbros or diorites. Furthermore, most of the ring dikes are porphyritic quartz syenite and granite porphyry; the equicrystalline granites in New Hampshire characteristically form stocks, some of which are irregular in outline. It is also true that biotite granite similar to most of the Conway granite of New Hampshire is lacking in eastern Massachusetts, but again not every intrusive center of the White Mountains series of New Hampshire contains Conway granite.

Figure 1 shows that the ages so far determined strongly suggest a geographic grouping of younger rocks to the north and older to the south. However, there is no clearcut geographic break in the distribution of the "alkalic" rocks, and the age-group assignment of the "alkalic" rocks of southern New Hampshire and Maine is particularly uncertain.

Future geologic and petrologic studies may establish reliable criteria for distinguishing the two age groups, or more detailed age studies may conceivably show a complete gradation in age among all the "alkalic" rocks of New England. For the present, however, temporal and genetic correlations among these rocks should be made with great caution.

Multiple periods of emplacement of post-tectonic (or "late tectonic") alkalic rocks are also known in other mountain systems, as for example the Caledonides of northern Europe: alkalic intrusive masses of Loch Loyal and the Assynt district of Scotland apparently predate major movement on the Moine thrust (Phemister, 1948, p. 48–49, 54) and are therefore presumably pre-Old Red Sandstone, whereas the similar alkalic rocks of the Oslo district of Norway are Permian (Holtedahl and Dons, 1957, p. 24–32).

References Cited

Aldrich, L. T., Wetherill, G. W., Davis, G. L., and Tilton, G. R., 1958, Radioactive ages of micas from granitic rocks by Rb-Sr and K-A methods: Am. Geophys. Union Trans., v. 39, p. 1124–1134

Billings, M. P., 1956, The geology of New Hampshire. Part 2, Bedrock geology: Concord, New Hampshire State Planning Devel. Comm., 203 p.

Chapman, R. W., 1954, Criteria for the mode of emplacement of the alkaline stock at Mount Monadnock, Vermont: Geol. Soc. America Bull., v. 65, p. 97–114

Chute, N. E., 1950, Bedrock geology of the Brockton quadrangle, Massachusetts: U.S. Geol. Survey Geol. Quad. Map GQ-5

Clapp, C. H., 1910, The igneous rocks of Essex County, Massachusetts (Abstract of thesis): Mass. Inst. Technology, 12 p.

—— 1921, Geology of the igneous rocks of Essex County, Massachusetts: U.S. Geol. Survey Bull. 704, 132 p.

Daly, R. A., 1903, Geology of Ascutney Mountain, Vermont: U.S. Geol. Survey Bull. 209, 122 p.

Eggleston, J. W., 1918, Eruptive rocks at Cuttingsville, Vermont: Am. Jour. Sci., ser. 4, v. 45, p. 377–410

Emerson, B. K., 1917, Geology of Massachusetts and Rhode Island: U.S. Geol. Survey Bull. 597, 289 p.

Holtedahl, Olaf, and Dons, J. A., 1957, Geological guide to Oslo and district: Norske Vidensk. Akad. i Oslo, Skr., I. Mat.-Nat. Kl., 1957, no. 3, 86 p.

Hurley, P. M., Fairbairn, H. W., Pinson, W. H., and Faure, G., 1960, K-A and Rb-Sr minimum ages for the Pennsylvanian section in the Narragansett Basin: Geochim. Cosmochim. Acta, v. 18, p. 247–258

Jaffe, H. W., Gottfried, David, Waring, C. L., and Worthing, H. W., 1959, Lead-alpha age determinations of accessory minerals of igneous rocks (1953–1957): U.S. Geol. Survey Bull. 1097-B, p. 65–148

Jenks, W. F., 1934, Petrology of the alkaline stock at Pleasant Mountain, Maine: Am. Jour. Sci., ser. 5, v. 28, p. 321–340

LaForge, Laurence, 1932, Geology of the Boston area, Massachusetts: U.S. Geol. Survey Bull. 839, 105 p.

Lyons, J. B., Jaffe, H. W., Gottfried, David, and Waring, C. L., 1957, Lead-alpha ages of some New Hampshire granites: Am. Jour. Sci., v. 255, p. 527–546

Phemister, James, 1948, British regional geology; Scotland, the Northern Highlands: 2d ed., Great Britain Geol. Survey and Museum, 93 p.

Quinn, A. W., Jaffe, H. W., Smith, W. L., and Waring, C. L., 1957, Lead-alpha ages of Rhode Island granitic rocks compared to their geologic ages: Am. Jour. Sci., v. 255, p. 547–560

Quinn, A. W., Ray, R. G., and Seymour, W. L., 1949, Bedrock geology of the Pawtucket quadrangle, Rhode Island-Massachusetts: U.S. Geol. Survey Geologic Quad. Map GQ-1

Rose, Harry, Jr., and Stern, Thomas W., 1960, The spectrochemical determination of lead in zircon for lead-alpha age measurements: Am. Mineralogist, v. 45, p. 1243–1256

Tilton, G. R., Davis, G. L., Wetherill, G. W., and Aldrich, L. T., 1957, Isotopic ages of zircon from granites and pegmatites: Am. Geophys. Union Trans., v. 38, p. 369–371

Toulmin, Priestley, 3d, 1957, Notes on a peralkaline granite from Cashes Ledge, Gulf of Maine: Am. Mineralogist, v. 42, p. 912–915

—— 1960, Compositions of feldspar and crystallization history of the granite-syenite complex near Salem, Essex County, Massachusetts, U.S.A.:XXI Internat. Geol. Cong., Rept. pt. XIII, p. 275–286

Wandke, Alfred, 1922, Intrusive rocks of the Portsmouth Basin, Maine and New Hampshire: Am. Jour. Sci., ser. 5, v. 4, p. 139–158

Warren, C. H., 1913, Petrology of the alkali granites and porphyries of Quincy and the Blue Hills, Mass., U.S.A.: Am. Acad. Arts Sci. Proc., v. 49, no. 5, p. 203–331

Warren, C. H., and McKinstry, H. E., 1924, The granites and pegmatites of Cape Ann, Massachusetts: Am. Acad. Arts Sci. Proc., v. 59, no. 14, p. 313–368

Warren, C. H., and Powers, Sidney, 1914, Geology of the Diamond Hill-Cumberland district in Rhode Island-Massachusetts: Geol. Soc. America Bull., v. 25, p. 435–476

Webber, G. R., Hurley, P. M., and Fairbairn, H. W., 1956, Relative ages of Eastern Massachusetts granites by total lead ratios in zircon: Am. Jour. Sci., v. 254, p. 574–583

Williams, C. R., and Billings, M. P., 1938, Petrology and structure of the Franconia quadrangle, New Hampshire: Geol. Soc. America Bull., v. 49, p. 1011–1044

U.S. Geological Survey, Washington 25, D. C.
Manuscript Received by the Secretary of the Society, July 19, 1960
Publication Authorized by the Director, U.S. Geological Survey

E. J. ZELLER
E. E. ANGINO
M. D. TURNER

BASAL SEDIMENTARY SECTION AT WINDY GULLY, TAYLOR GLACIER, VICTORIA LAND, ANTARCTICA

Abstract: The contact between the basement complex and the sedimentary sequence in the Royal Society Range is well exposed on both sides of Windy Gully along the main valley of the Taylor Glacier. The basal beds, consisting of cross-bedded sandstones, are overlain by 110 feet of alternating sandstones and dark fissile shales. Overlying these beds are massive sandstones of "normal" Beacon lithology. A 960-foot diabase sill has been injected 255 feet above the base of the massive sandstone unit. The section was measured for 390 feet above the top of the sill and probably overlaps with the lower portion of the Beacon section recently described by McKelvey and Webb.

Stewart (1934), Crohn (1959), and others refer to the Beacon sandstone as a formation. On the basis of field studies made during the 1959–1960 Antarctic field season, the present authors agree with Harrington (1958) and urge that the Beacon sandstone and associated sills be raised to group status and that formational names be used to identify smaller easily separable, identifiable, and widespread units within the group. The sediments described in this paper are, therefore, considered part of the "normal" Beacon sandstone formation. Accordingly, a

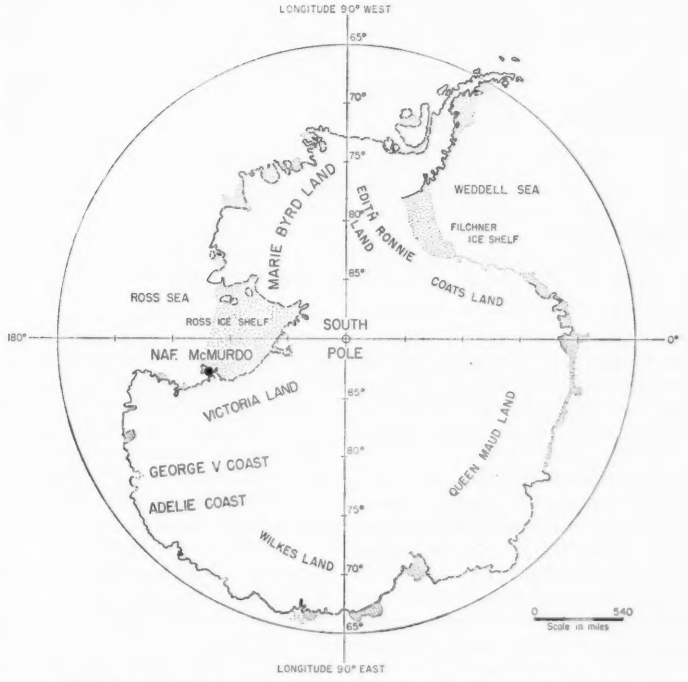

Figure 1. Map of Antarctic continent showing major land areas

Geological Society of America Bulletin, v. 72, p. 781–786, 3 figs., 1 pl., May 1961

composite section near Windy Gully, Upper Taylor Valley, Victoria Land, Antarctica, is described, and two new member names are proposed.

The Beacon group, one of the most widespread stratigraphic units known in the Antarctic, extends almost 2000 miles from the Adelie coast through George V and South Victoria Land into Marie Byrd Land (Stewart, uncertain. Stratigraphically, the Beacon is considered late Paleozoic–early Mesozoic in age (Fairbridge, 1952, p. 66). Fish scales of Late Devonian age have been described from lower units of the Beacon sandstone, near Granite Harbor, McMurdo Sound, Antarctica (Woodward, 1921), and fossil wood (*Antarctorylon*), winged spores (*Pityosporites*), and *Glossopteris* flora all of Permo-Carboniferous age have been

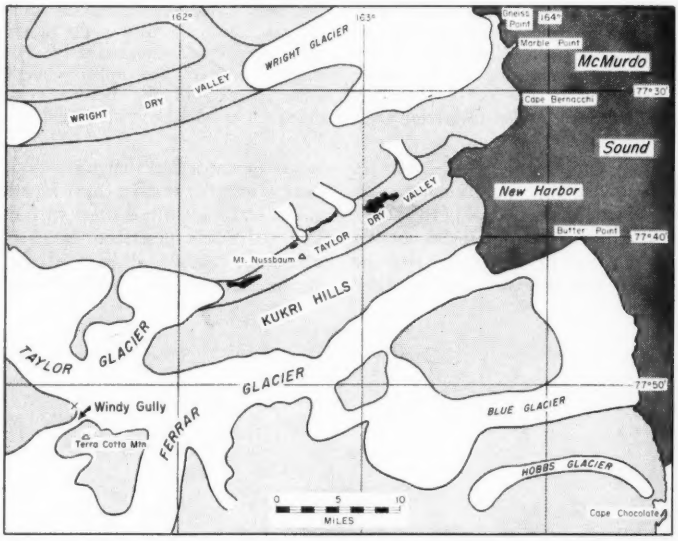

Figure 2. Index map of part of western coast of McMurdo Sound, South Victoria Land, Antarctica. The location of the section described is indicated by an X. The dark patches in Taylor Dry Valley are lakes.

1934) (Fig. 1). Along the length of its outcrop, this unit ranges from 2000 feet thick (Ferrar, 1907) in the Ferrar Glacier district of South Victoria Land to 7000 feet in the Mt. Fritdjof Nansen area of Marie Byrd Land (Gould, 1931).

The Beacon sandstone has been described primarily as a fine-grained, arkosic, quartz sandstone with thin interbedded shales, coals, conglomerates, and scattered thin limestones (Ferrar, 1907; and others). The presence of coal beds, cross-bedding, ripple marks, sun cracks, and similar structures strongly suggests a continental and/or shallow-water origin for the Beacon (Fairbridge, 1952, p. 66).

The Beacon group is everywhere intruded by massive diabase sills ranging up to 1000 feet or more in thickness. The age of these sills is reported from the upper units (Seward, 1914). This evidence is the basis for assigning a Devono-Triassic? age to the Beacon.

The section examined (Figs. 2, 3), located about 25 miles west of the coastal metasedimentary belt, rests on a granitic basement complex. Dark, coarse-grained gneissic rocks are exposed at several points along the basement sedimentary contact.

An Ar^{40}/K^{40} date of 520 m.y. (Goldich, Nier, Washburn, 1958) was obtained from paragneiss bedrock samples collected at Gneiss Point, McMurdo Sound, Antarctica, 45 miles northeast of Windy Gully. Too much confidence should not be placed in this figure, for as Goldich *et al.* (1958, p. 956) point out: "Gneiss Point is situated on a great fault zone and also is in close proximity to the volcanic islands of

TABLE 1. DETAILED STRATIGRAPHIC SECTION

Bed no.	Thickness (feet)	Remarks
31	245	Top of section, top of Member A1. Alternating soft and hard, thin to massively bedded, buff sandstone
30	10	Soft sandstone with vertical concretionary forms
29	5	Soft, light-colored sandstone
28	123	Hard, massive buff sandstone. Lower 40 feet thin-bedded with some thick beds. Many of the thin beds are green
27	2	Thin diabase sill
26	5	Quartzite bed
25	960	Massive diabase sill
24	255	White to buff fine-grained sandstone with occasional bands of conglomerate. Upper 6 inches altered to quartzite. Abundant fucoids 10–16 feet above base, cross-bedding 75 feet above base. Thin sill at 111 feet and a 20-inch sill at 114 feet
23	3.8	Dark-reddish purple silty shale, laminated at base and blocky at top
22	12.5	Thinly laminated siltstone and shale, with occassional thinly laminated gray dolomitic limestones. Color varies from dark purple at bottom to greenish gray at top
21	6.7	Thinly laminated, dark-greenish-gray siltstones with white nodules of calcite
20	7.2	Greenish-gray, hard laminated shale. Lower 1.3 feet is nodular and irregularly bedded; prominent mud cracks are visible
19	19.5	Dark purplish silty shales interbedded with greenish-gray bands of silty shale
18	6.5	Thin-bedded, dark-purplish shale, the lower 10 inches wavy-bedded greenish siltstone with mud cracks
17	4.5	Dark-greenish to purple clayey sandstone interbedded with light-pinkish siltstones
16	3.6	Purplish to dark-green shale, 4 inches greenish-brown sandstone at the base
15	3.3	Reddish-purple thin-bedded shale
14	1.8	Green to brown, very thin-bedded sandstone
13	0.7	Purple shale and sandstone
12	0.7	Brownish sandstone
11	1.7	Purple shale
10	1.4	Greenish, silty very thinly cross-bedded sandstone
9	2.4	Thin interbedded purple shale and white sandstone
8	9	Light-pink, thinly bedded kaolinitic sandstone; abundant fucoids in top 4 feet
7	3.6	Alternating thin-bedded reddish-purple shale and white sandstone
6	3.7	Light-pink, very thin-bedded sandstone with a few dark-green shale partings
5	3.4	Light- to dark-green sandy and silty, finely laminated shale, occasional thin stringers of white sandstone
4	12	White to very light-buff, fine-grained kaolinitic sandstone. Lower 3 feet contains glauconitic pellets; upper 9 feet coarse-grained and cross-bedded
3	1.9	Dark-greenish-gray sandstone, thin-bedded at base
2	5–100	Lower 75 feet is a brownish to light-tan sandstone; upper 20 feet, where present, is a light-buff sandstone with fucoids
1	0–5	Thin discontinuous conglomerate, grading to sandstone at top

the Ross Sea of which Ross Island is active. For these reasons geologic interpretations of the 520 m.y. age must be cautious." It seems reasonable, however, to assume that the Windy Gully metamorphic complex may be of comparable age, possibly older. The coastal metasedimentary rocks are probably of late Proterozoic (Eocambrian) age.

An erosional surface, presumably of late Precambrian age, truncates the basement complex. In places, other small igneous intrusions have been injected directly along the sedimentary igneous contact. Over a broad extent of South Victoria Land, the basement rocks are also intruded by large diabase sills, some of which are 1500 feet thick (McKelvey and Webb, 1959).

A thin conglomerate in the lowest part of the basal member (here named the Windy Gully member after a notch between New Mountain and Terra Cotta Mountain) provides ample evidence that the decidedly nonconformable contact is sedimentary. Relief on the erosional surface ranges from 80 to 100 feet (Pl. 1, fig. 1), suggesting a substantial period of erosion before sandstone deposition.

The section begins with a very thin discontinuous conglomerate, which grades into a sandstone ranging in thickness from 5 to 100

feet in outcrops west of Windy Gully. In most places the basal beds are somewhat darker than the overlying units (Pl. 1, fig. 2). The lower unit is a brownish to light-tan sandstone, cross-bedded, with subrounded grains ranging from 1 mm to very fine. Quartz pebbles are scattered throughout the basal beds. Above the base are

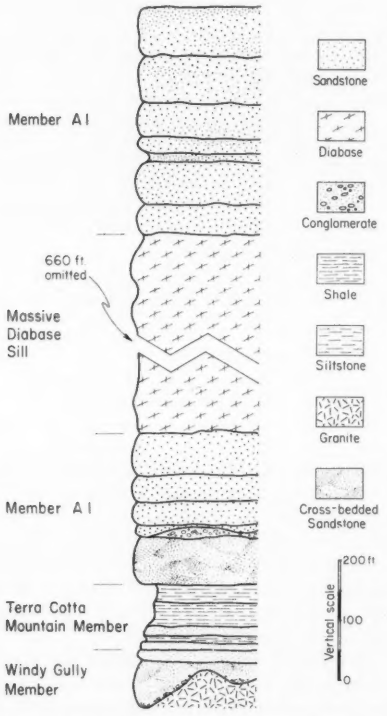

Figure 3. Composite stratigraphic section near Windy Gully, Upper Taylor Valley, South Victoria Land, Antarctica

discontinuous cobble and boulder beds. Boulders range up to 18 inches in length; one boulder 6 feet long was noted. These beds, most of which are not more than 3 feet thick, are greenish and show cross-bedding.

Three thin cobble and boulder bands 5–10 feet apart were noted. The boulders, originally a medium crystalline, dark igneous rock, show considerable alteration by weathering. The uppermost 20 feet of the Windy Gully member is a light-buff sandstone containing beds with fucoidal structures. A lithologic change occurs at the top of the Windy Gully formation.

Above this break in lithology, there is 110 feet of alternating sandstone and shale beds of different color and thickness (Pl. 2, figs. 1, 2), here designated the Terra Cotta Mountain member (Table 1). The north flank of Terra Cotta Mountain shows excellent outcrops of this member. A decided break in the sedimentation occurs at the top of this sequence.

Overlying the alternating sandstones and shales of the Terra Cotta Mountain member is a 255-foot white to buff, very fine-grained sandstone with occasional lenses of conglomerate. Presumably it is the lower part of Member A of McKelvey and Webb (1959). We refer to this and the section above the diabase sill as Member A1. Cavernous weathering with abundant fucoids occurs 10–16 feet above the base of Member A1. Scattered throughout are occasional ferruginous bands. Cross-bedding is present 75 feet above the base of the unit. At 80 feet occurs a lens of greenish conglomerate, overlain by two thin sills at 110 and 115 feet respectively above the base of Member A1. The lowest part of Member A1 is capped by a massive 960-foot diabase sill (Pl. 2, fig. 3), which has altered the upper 6 inches of the sandstone to quartzite.

The diabase sill is topped by 390 feet of alternating soft and hard, thin to massively bedded, white to buff sandstone of "normal" Beacon lithology (also similar to Member A of McKelvey and Webb). The 1815-foot section described here extends above for several hundred more feet, probably merging with the lower part (Member A) of the section reported by McKelvey and Webb (1959). All the Beacon sediments in the area under discussion dip gently to the west.

Acknowledgments

The authors express their thanks to all Naval personnel of Task Force 43, Deep Freeze 60, who aided in the completion of the field work described in this paper. Financial assistance from the U. S. Antarctic Research Program of National Science Foundation is gratefully acknowledged.

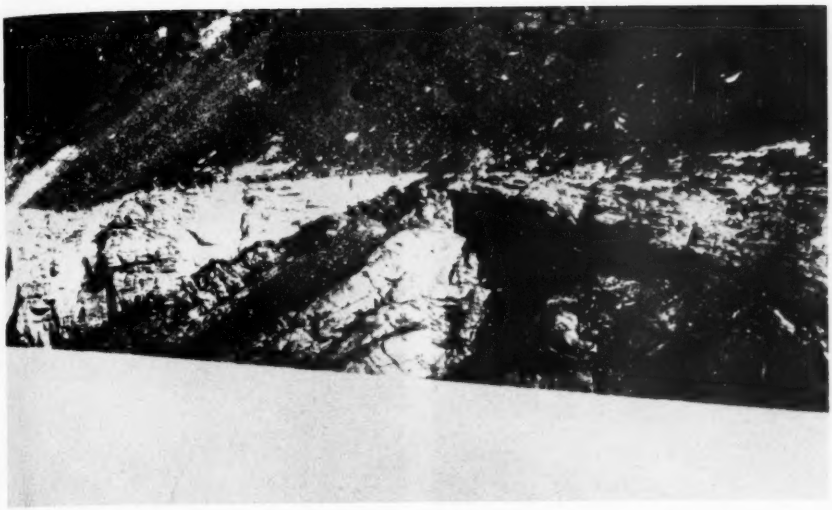

Figure 1. Contact between basement rock and sedimentary sequence, exposed just west of Windy Gully. Note thinning of Windy Gully member over basement high. White area in foreground is part of Taylor Glacier.

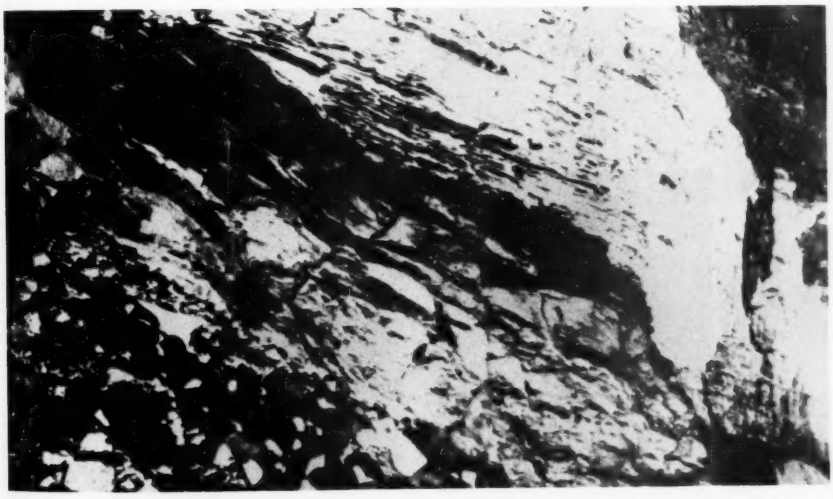

Figure 2. Lower part of Windy Gully member. Man in lower left provides scale.

EXPOSURES OF WINDY GULLY MEMBER

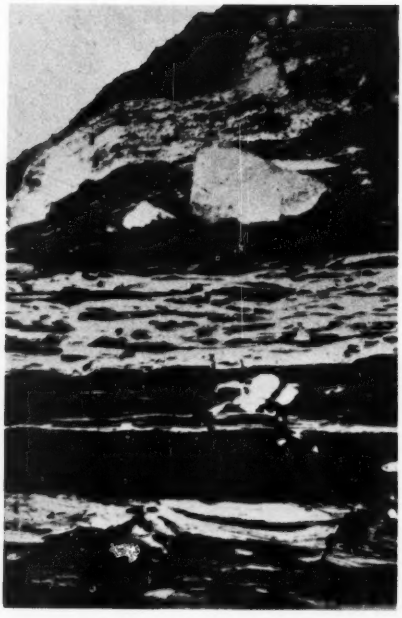

Figure 1. Beds 7 through 10 (Table 1) of Terra Cotta Mountain member overlain by 9-foot white sandstone bed which contains fucoidal structures

Figure 2. Terra Cotta Mountain member and lower part of Member A1. Contact at base of white sandstone cliff. Black shale below white sandstone cliff is 25 feet thick. Base of diabase sill visible above lower part of Member A1. Taylor Glacier at right

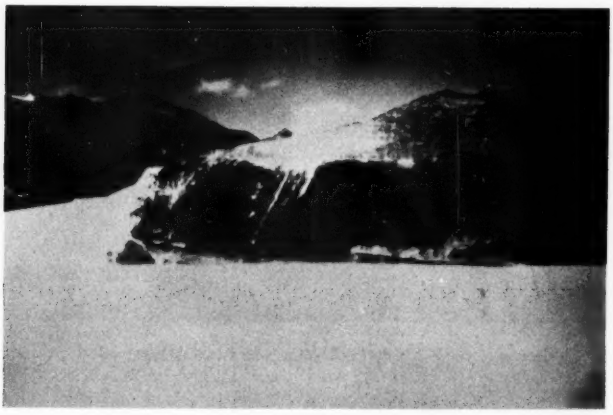

Figure 3. Panorama of Windy Gully area; notch on extreme left is Windy Gully. Black band in center of view is a massive 960-foot diabase sill. Taylor Glacier in foreground

EXPOSURES OF TERRA COTTA MOUNTAIN MEMBER AND WINDY GULLY AREA

ZELLER *ET AL.*, PLATE 2
Geological Society of America Bulletin, volume 72

References Cited

Crohn, P. W., 1959, A contribution to the geology and glaciology of the western part of Australian Antarctic Territory: Dept. Nat. Development, Commonwealth of Australia Buil. 52, 103 p.

Fairbridge, R. W., 1952, The geology of the Antarctic, p. 56–101 *in* Simpson, F. A., *Editor*, The Antarctic today: New Zealand Antarctic Society, 389 p.

Ferrar, H. T., 1907, Geology—Field geology: Nat. Antarctic Expedition, 1901–1904, Natural History, v. 1, p. 1–100

Goldich, S. S., Nier, A. O., Washburn, A. L., 1958, A^{40}/K^{40} age of gneiss from McMurdo Sound, Antarctica: Am. Geophys. Union Trans., v. 39, p. 956–958

Gould, L. M., 1931, Some geographical results of the Byrd Antarctic Expedition: Geog. Rev., v. 21, p. 177–200

Harrington, H. J., 1958, Nomenclature of rock units in Ross Sea region of Antarctica: Nature, v. 182. p. 290

McKelvey, B. C., and Webb, P. N., 1959, Geological investigations in South Victoria Land, Antarctica, Pt. II, Geology of Upper Taylor Glacier region: New Zealand Jour. Geology & Geophysics, v. 2, p. 718–728

Seward, A. C., 1914, Antarctic fossil plants: British Antarctic ("Terra Nova"), Expedition, 1910, Natural History Rept., Geology, v. 1, no. 1, p. 1–49

Stewart, Duncan, Jr., 1934, The petrography of the Beacon sandstone of South Victoria Land; Am. Mineralogist, v. 19, p. 351–359

Woodward, A. S., 1921, Fish remains from Upper Old Red Sandstone of Granite Harbor, Antarctica: British Antarctic ("Terra Nova") Expedition, 1910, Natural History Rept., Geology, v. 1, no. 2, p. 51–62

Dept. Geology, University of Kansas, Lawrence, Kans.; Dept. Geology, University of Kansas, Lawrence, Kans.; National Science Foundation, Washington, D. C.

Manuscript Received by the Secretary of the Society, August 15, 1960

MARIE

A. P. CRARY

MARINE-SEDIMENT THICKNESS IN THE EASTERN ROSS SEA AREA, ANTARCTICA

Abstract: Thickness of ocean sediments was obtained at two locations in the eastern Ross Sea area, Antarctica, during the International Geophysical Year. Sediment thickness in the vicinity of the Little America Station is about 1325 m. Cores from the upper meter of these sediments are composed mainly of a mixture of coarse and fine glacial till.

During the International Geophysical Year operations in Antarctica, the thickness of ocean sediments was obtained at the Little America Station (lat. 78°10′ S., long. 162°13′W.) by seismic-refraction and reflection methods. Figure 1 shows the Ross Sea and floating Ross Ice Shelf areas; bottom contours are taken from Crary and van der Hoeven (In press). Bentley *et al.* (1960) published the first outline of the configuration of West Antarctica under its ice layers. A large channel with rock surface well below sea level was found between the

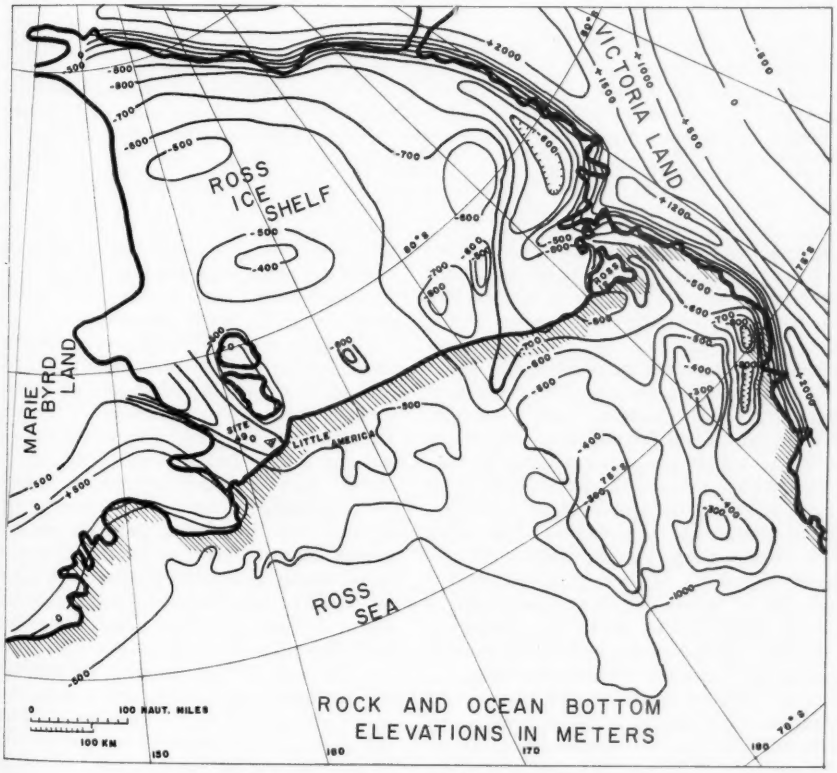

Figure 1. Ross Sea and Ross Ice Shelf area, Antarctica

Geological Society of America Bulletin, v. 72, p. 787–790, 3 figs., May 1961

Ross Sea and the Bellingshausen Sea. Depths to rock surfaces in most areas of the channel are considerably below the floor depths found under the Ross Ice Shelf (Fig. 1).

Information on the seismic velocities in the sediments was obtained by taking a profile on the thin ice of Kainan Bay near the Little America Station. The distances involved were limited to the confines of the bay, about 3 km. Though this profile was not reversed, nor instant of firing obtained at the longer distance shots, the reflections from the ocean floor were good, and the multiple reflections received made possible the determination of firing times and the amount of slope of the bottom under the line of profile. The water in Kainan Bay was 606 m deep at the recording site in the inner part of the bay, and the ocean floor sloped upward toward the northwest by about half a degree. Refraction signals were obtained only on the record from the shot 3 km from the detectors. Over the instrument separation of 300 m, a slight increase in velocity was obtained, with values of 2400 and 2444 m/sec for the two sides of the spread. After correction for an assumed dip equal to that of the ocean floor, these values become 2428 and 2473 m/sec; the depth to these velocities was 109 and 205 m below the ocean floor, using a velocity of 2000 m/sec for the top sediments.

Further information on the sediment velocity is obtained from the sub-bottom seismic reflections received on the records with shorter distances from shot to recorder. Sub-bottom reflections that could be identified were limited to those arriving before the second ocean-floor reflection, after which they were masked. From the variation of the reflection times with distances over the 300-meter geophone spread, the average velocity for the entire path can be obtained. These values of average velocity were then corrected for the known travel time and distance in the water to obtain sediment velocity. The errors involved in the assumption of a straight-line path were estimated from theoretical calculations by using the known depth and velocity of water with various sediment depths and velocities. The results of this reflection study are listed in Table 1.

These velocity values and the refraction values obtained are plotted in Figure 2. The results fall between Nafe and Drake's (1957) values for shallow- and deep-water marine sediments. The discrepancy between refraction and reflection velocities may be due to anisotropic conditions in the upper sediments.

Table 1. Calculation of Sediment Depths

Distance	Time X=O (sec)	Average velocity (km/sec)	Sediment velocity uncorrected (km/sec)	Correction (km/sec)	Sediment velocity (km/sec)	Sediment depth (meters)
0 −350 m	.934	1.53	2.33	−.26	2.07	98
0 −350	1.255	1.69	2.20	−.13	2.07	430
500–800	1.170	1.66	2.20	−.17	2.03	335
500–800	1.237	1.72	2.32	−.19	2.13	423
500–800	1.347	1.90	2.65	−.25	2.40	609
500–800	1.504	2.05	2.83	−.20	2.63	873
500–800	1.545	2.05	2.77	−.18	2.59	913
500–800	1.666	1.93	2.42	−.12	2.30	950

The main seismic reversed profile was made on the floating shelf ice in the vicinity of Little America Station, with surface elevations above sea level about 39 m and average ice thickness 238 m (Crary, in press). The seismic line was laid out with a deep crevassed valley in the center, which successfully eliminated the direct ice waves except on a few of the shorter recording distances. This seismic work on the shelf ice was limited by the high-velocity ice layer to seismic waves with velocities greater than 3.80 km/sec. The time-distance graph is shown in Figure 3. Two high-speed signals from below the sediments were received: one with velocities 4.21 and 4.27 km/sec from the southeast and northwest respectively; and a deeper one with velocities 6.08 and 6.74 km/sec, also from the southeast and northwest respectively. The returns received on the northwest side of the line were not so clear as on the other side, because they were masked somewhat by the direct ice waves with 3.75 to 3.80 km/sec

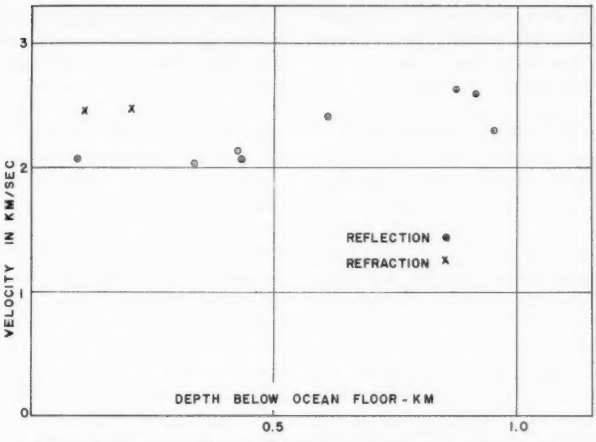

Figure 2. Seismic velocity of sediments, Kainan Bay, Antarctica

velocities. Interpolation was made by conventional seismic computing methods, using an ice thickness of 238 m with an average velocity of 3.45 km/sec, a water layer 409 m thick with a velocity of 1.44 km/sec, and sediments below this with an average velocity of 2.40 km/sec. The results (Fig. 3) show a sediment thickness of 1325 m, which thins at a low rate, about 1 m in 200 m distance, toward the southeast. The thickness of the 4.24 km/sec layer is not so well defined but is about 645 m in the center of the profile. It is underlain by a layer with an average velocity of 6.38 km/sec and a slope of 2.6° down toward the northwest.

At site 49 of the inland traverse, about 35 km southeast of the Little America Station, at lat. 78°25′ S. and long. 161°20′ W., a single unreversed refraction shot was fired, with pertinent data as follows: distance: 9.87 km; travel time: 2.630 sec; refraction velocity: 4.51 km/sec. The reflection survey indicated 363 m ice, 293 m water, and negligible slope

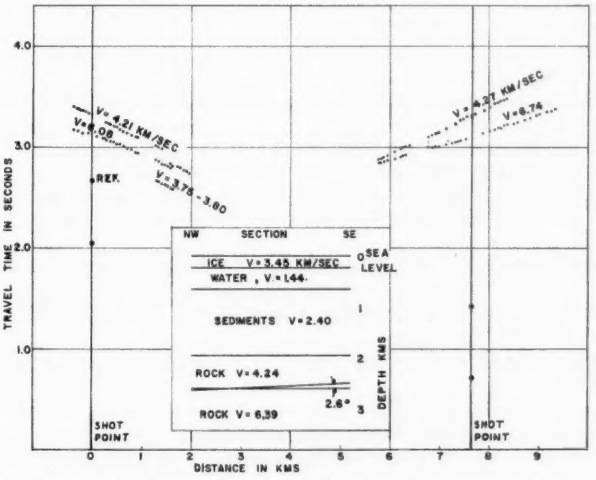

Figure 3. Time-distance curve of seismic-refraction profile, Little America Station, Antarctica

of the ocean floor at this site. If sediment velocity of 2.40 km/sec is used, the thickness of the sediments here would be 754 m.

Preliminary refraction velocities of 4.30, 5.43, and 6.54 km/sec have been obtained by the Little America Station traverse party in the upper Skelton Glacier area south of McMurdo Sound on the western side of the Ross Ice Shelf (Crary, 1959). From the known geological section in the McMurdo Sound area these values are tentatively associated with the Beacon sandstone, granitic or gneissic rock, and gabbro, respectively. Though no intermediate velocity was obtained on the profile at Little America, the same general type of Beacon series rocks appears to underlie the marine sediments. The Beacon series thickness obtained at the top of the Skelton Glacier by the seismic refraction was about 870 m, comparable to the 645 m deduced from the Little America Station study. At the Byrd Station, Bentley *et al.* (1960) report a similar velocity immediately under the ice.

It would be logical to expect similar thick sediments in most of the Ross Sea and Ross Ice Shelf areas. If depths to bed rock are compared with those in the Ross Sea—Bellingshausen Sea channel (Bentley *et al.*, 1960), the depths below sea level at the Little America Station and site 49 are 1933 and 1354 m respectively.

Cores from the upper meter of these sediments are composed mainly of a mixture of coarse and fine glacial till and have been examined by various investigators, including Stetson and Upson (1937), Thomas (1960), and personnel of the U. S. Navy Hydrographic Office (1956, p. E1–E23). Though there is no reason to believe that the total sediment column was deposited by ice, most of it may have been. Many factors will complicate sedimentation by rafting from shelf ice. Eventually, sediments will build up to ground the ice which will then redeposit them farther north. This continuing process will be aided by lowered sea level and land uplift. Rafted material brought down from glaciers of the Amundsen and Bellingshausen seas will also be carried west to the Ross Sea by prevailing surface currents. Sediment thicknesses in other parts of the Ross Sea should be determined and long piston cores obtained.

Acknowledgments

The assistance of Lyle McGinnis and Stephen den Hartog in the field work of the refraction profiles is acknowledged. The author is also indebted to Edward Thiel and Ned Ostenso for completing the refraction profile in Kainan Bay.

References Cited

Bentley, C. R., Crary, A. P., Ostenson, N. A., and Thiel, E. C., 1960, Structure of West Antarctica: Science, v. 131, no. 3394, p. 131–136 in press

Crary, A. P., 1959, Oversnow traverses from IGY Little America Station: IGY Bull. 27; Am. Geophys. Union Trans., v. 40, p. 311–315

—— in press, Glaciological studies at the Little America Station, Antarctica; IGY World Data Center A. Glaciology: Am. Geog. Soc.

Crary, A. P., and van der Hoevan, F., in press, Sub-ice topography of Antarctica, 160° W. to 130° E.: Internat. Assoc. Hydrology Rept., Helsinki Assembly of IUGG

Nafe, John E., and Drake, Charles L., 1957, Variation with depth in shallow and deep water marine sediments of porosity, density and the velocity of compressional and shear waves: Geophysics, v. 22, p. 523–553

Stetson, H. C., and Upson, J. E., 1937, Bottom deposits of the Ross Sea: Jour. Sed. Petrology, v. 7, p. 55–56

Thomas, Charles W., 1960, Late Pleistocene and Recent limits of the Ross Ice Shelf: Jour. Geophys. Research, v. 65, p. 1784–1792

U. S. Navy Hydrographic Office, 1956, Report on Operation Deep Freeze 1, TR-33: Washington, D.C., 81 p., appendices

Arctic Institute of North America, 1530 P Street, N.W., Washington 5, D.C.
Manuscript Received by the Secretary of the Society, December 8, 1960

W. U. AULT
J. P. EATON
D. H. RICHTER

LAVA TEMPERATURES IN THE 1959 KILAUEA ERUPTION AND COOLING LAKE

Abstract: The 1959 summit eruption of Kilauea Volcano, Hawaii, filled the crater of Kilauea Iki with a lake of lava 365 feet deep. Temperatures of the erupting basalt ranged between 1060° and 1190°C. Temperatures down a 12.7-foot-deep hole, drilled into the crust of the lake 5 months after cessation of eruptive activity, agree with calculated temperatures based on the heat equation. The cooling effect of rainfall is pronounced only in the upper 3½ feet of the crust.

The 1959 summit eruption of Kilauea Volcano, Hawaii, between November 14 and December 21 consisted of 17 eruptive phases, each characterized by vigorous fountaining and extrusion of lava from a common vent in the side of Kilauea Iki Crater (Eaton and Richter, 1960). During the first phase of activity, lava filled the crater to the level of the vent; and as each succeeding phase raised the level of lava in the lake, cessation of fountaining was immediately followed by backflow of lava down the vent. The final period of backflow and crustal foundering, which ceased on December 23, 1959, left a lake of lava 365 feet deep and 135 acres in extent, which contains nearly 50,000,000 cubic yards of fresh tholeiitic olivine basalt. This lake of lava is readily accessible and offers an unparalleled opportunity for studying a vast quantity of slowly crystallizing basaltic lava.

In March 1960, after the lake surface had cooled sufficiently, a reference level line was surveyed across the lake floor. In April 1960, two holes were drilled into the crust over the deepest portion of the lake. The holes, 13.5 feet apart and 6 and 12.7 feet deep, were drilled with an ordinary carbide-tip hollow masonry bit, 1⅛ inch diameter, in a ½ h.p. electric hand drill, powered by a small portable generator. The deeper of the two holes was drilled dry to a depth of 7 feet; below that level, water was used sparingly to cool the bottom of the hole. The shallower hole was drilled with water throughout its length.

The holes were drilled in an attempt to gain information on the rate of cooling in a large, semienclosed body and to determine what effects rainfall, convection, and the latent heat of crystallization have on the cooling. A knowledge of the temperature within the cooling crust is also necessary to supplement contraction studies and to aid in the interpretation of magnetic data on the lake's surface. Petrographic studies and chemical analyses of cores from the drill holes should yield information on the differentiation processes taking place within the lake.

Temperatures of the lava in the fountain, river, and lake during the eruption were measured by two Leeds and Northrup optical pyrometers of incandescent-filament type; temperatures in the cooling crust of the lake were obtained by a chromel-alumel thermocouple and potentiometer assembly. Comparison of readings between the two optical pyrometers and between the pyrometers and thermocouple-potentiometer at the fusion point of NaCl and up to 1000°C, under black-body conditions in the laboratory, indicates an accuracy of ±2°C at 800°C and ±5°C at 1000°C and above, for the optical pyrometer measurements. Even closer agreement has been obtained between the optical pyrometer and thermocouple-potentiometer in the field, where comparison measurements in the deep drill hole agreed within 1°C at 910°C.

Lava temperatures, obtained on various forms of fluid lava, during the 1959 eruption are listed in Table 1.

Most of the lava-fountain temperature measurements, taken at night from an observation point on the crater rim, and about 600 feet from the fountain, were obtained when bursts of fountain activity or shifting fountain direction bared the bright incandescent core of the jetting lava. The dense screen of intensely

Geological Society of America Bulletin, v. 72, p. 791–794, 2 figs., May 1961

radiating fragments of lava surrounding the fountain core minimized heat loss by radiation from the core, so that the interior of the fountain approximated a cavity type of artificial black body. Temperatures in the range 1180° to 1190°C were measured during a number of eruptive phases and probably closely approach the true temperature of the erupting lava. Moreover, recent laboratory crystal-melt investigations of natural Hawaiian basalts (Yoder and Tilley, 1957) strongly corroborate the temperatures cited above. Microscopic examination of pumice produced in the lava fountain shows that the 1959 lavas, which averaged about 49 per cent silica, were within the temperature range of olivine crystallization when extruded from the vent. A comparable tholeiitic basalt (1921 Kilauea flow) studied by Yoder and Tilley has an olivine crystallization temperature range between 1235° and 1185°C, in excellent agreement with the maximum temperatures observed in the 1959 lava fountain.

TABLE 1. LAVA TEMPERATURES, 1959 ERUPTION OF KILAUEA

Nature of lava	Temperature (°C)
Lava fountain	1060–1190
Lava river flowing into lake and lava flows on lake	1050–1127
Lava cascading back down vent	1120

Temperature measurements in the cooling lake crust were begun immediately after completion of the drill holes and have been continued periodically up to the present. Recovery of bottom-hole temperature after drilling was very rapid. Based on the final high temperature (910°C in the deep hole) on the day following

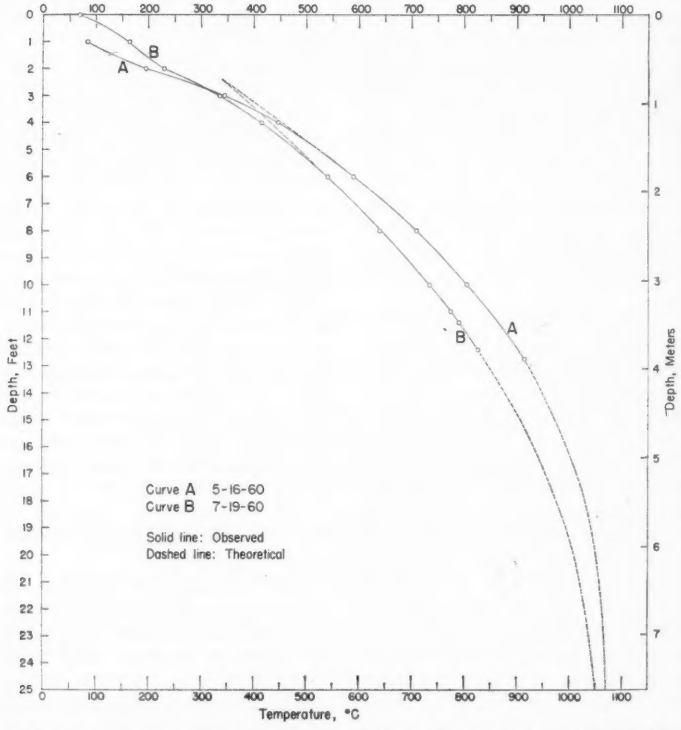

Figure 1. Temperature profiles in the 12.7-foot-deep drill hole in Kilauea Iki lava lake as measured in May and July of 1960. The observed data coincide with the theoretical at depths greater than 5 feet.

drilling, recovery was 80 per cent after 17 minutes, 90 per cent after 47 minutes, and 98 per cent after 3 hours. Equalization of temperature within the deep hole, by convection of air in the hole or by radiation from the glowing bottom, appears to have made little headway, since temperatures at comparable depths in the shallow 6-foot hole agree within 3°C.

Figure 1 shows two temperature curves obtained in the deep drill hole on May 16 and July 19, 1960. Superposed on the graph of observed temperatures are two theoretical comparison curves which represent solutions of the heat equation,

$$\frac{\partial T}{\partial t} = h^2 \frac{\partial^2 T}{\partial x^2}$$

with the initial condition $T_o = 1075°C$ for all depths $x \geq 2.39$ feet (73 cm), at time $t = 0$, and with the boundary condition $T = 340°C$ at $x = 2.39$ feet for all $t > 0$. To fit both sets of observed points using a common value of diffusivity it was necessary to consider time, $t = 0$, as beginning 33 days after the end of the eruption. Convection in the lake beneath the cooling crust is perhaps responsible for the necessary shift in time scale. The value of diffusivity determined by fitting the theoretical curves to the observations is $h^2 = 0.0033$ cm^2 sec^{-1}.

The two measured temperature profiles (Fig. 1, curves A and B) taken 64 days apart, plus six other profiles obtained in that interval, reveal a considerable and consistent cooling of the lake's crust. Extension of the theoretical curves downward indicates that the top of the partially fluid zone of crystallization, with temperatures of about 1050°C, would have been 20 feet below the surface on May 16 and 25 feet on July 19. These theoretical curves, however, do not take into consideration the effects of the latent heat of crystallization or the increase in heat capacity (decrease in diffusivity) that should be expected as the zone of crystallization is approached. Jaeger (1957), considering the cooling of an intrusive sheet, concludes that the latent heat supplied to the cooling mass signifi-

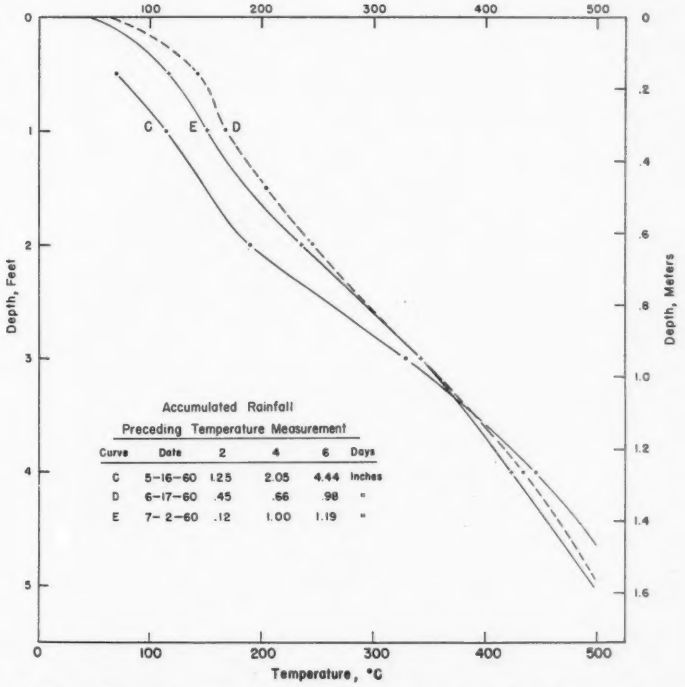

Figure 2. Three temperature profiles in upper layer of crust of Kilauea Iki lava lake, showing the cooling effect of rainfall

cantly increases the time required for complete solidification. Although the cooling history of a lake of lava will undoubtedly be very different from that of the sill-like body considered by Jaeger, the over-all effect of latent heat should be similar. On this basis the depth to the zone of crystallization may be less than that predicted by the theoretical cooling curves, and temperatures higher than 1075°C, the initial temperature (T_o) of the lava used in calculating the theoretical curves, may occur at depth in the lake.

The effect of rainfall on the surface of the lake is seen in the erratic nature of the temperature profiles in the upper portion of the crust. Figure 2 shows three temperature profiles for the shallow portion of the deep drill hole and the accumulated inches of rainfall in the 2-, 4-, and 6-day periods immediately preceding the measurements. The separation of the curves above a depth of 3½ feet demonstrates the effectiveness of various amounts of rainfall in cooling the lava within this zone. The change in slope of the profiles above a depth of 1½ feet, showing relatively high temperatures in the extreme upper portions of the hole, is caused by escaping superheated steam.

Maximum lava temperatures of 1180° to 1190° C measured during the 1959 eruption are compatible with recent laboratory data on crystal-melt relations for similar basaltic rocks and probably closely approach the true temperatures of the erupting lavas. Temperature profiles to depths of almost 13 feet in the cooling crust of the lake indicate a solid crystalline layer only 25 feet thick on July 19, 1960. The writers plan to obtain additional data on the cooling of the lake by continuing temperature measurements and by periodically extending the drill holes.

Acknowledgments

The authors gratefully acknowledge the continued support of the National Park Service in this and other geological investigations within Hawaii National Park. Special thanks are due the many Park Service personnel for their encouragement and active participation in these studies.

Addendum

On August 24, 1960, using a drill powered by a 2½ h. p. gas engine, the authors drilled the 12.7-foot hole to 22.8 feet, where it penetrated pasty, still crystallizing lava. During the period August 25 to September 9, 1960, a fluid phase filled the bottom 5 inches of the hole, and bottom-hole temperatures of 1057° to 1065°C were measured.

References Cited

Eaton, J. P., and Richter, D. H., 1960, The 1959 eruption of Kilauea: Geotimes, v. 4, no. 5, p. 24–27, 45

Jaeger, J. C., 1957, The temperature in the neighborhood of a cooling intrusive sheet: Am. Jour. Sci., v. 255, p. 306–318

Yoder, H. S., and Tilley, C. E., 1957, Basalt magmas, p. 156–161 *in* Annual Report to the Director: Geophys. Lab., Carnegie Inst. Washington, p. 150–252

U. S. Geological Survey, Volcano Observatory, Hawaii
Manuscript Received by the Secretary of the Society, September 6, 1960
Publication Authorized by the Director, U. S. Geological Survey